UNIVERSITEIT VAN PRETORIA
UNIVERSITY OF PRETORIA
YUNIBESITHI YA PRETORIA

The synthesis of immobilised reagents based on a polymerised Triphenylphosphine scaffold for use in flow chemistry applications

by

Gakanego Valerie Ramaotsoa

Submitted in partial fulfilment of the requirements for the degree of Doctor of Philosophy
in the Faculty of Natural & Agricultural Sciences
University of Pretoria
Pretoria

February 2020

Supervised by Dr J-L. Panayides

Co-supervised by Dr D.L. Riley

© University of Pretoria

DECLARATION

I, Gakanego Valerie Ramaotsoa declare that the thesis, which I hereby submit for the degree of Doctor of Philosophy at the University of Pretoria, is my own work and has not previously been submitted by me for a degree at this or any other tertiary institution.

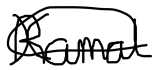

Gakanego Valerie Ramaotsoa

February 2020

© University of Pretoria

ACKNOWLEDGEMENTS

I would like to acknowledge the following people and institutions for their support throughout this project:

My supervisor Dr Jenny-Lee Panayides and co-supervisor Dr Darren Riley for the dedication and hard work you have contributed and ensuring that I complete this thesis without lacking anything. Thank you for believing in me, you have really made a difference in my life.

My parents for their support and the sacrifices they have done for me to be where I am. I love you very much.

To the Riley research group: thank you for patiently availing yourselves to help me no matter how small the task may have been.

The Council for Scientific and Industrial Research for generously funding my studies and the staff members for your wonderful help.

The financial assistance of the National Research Foundation (NRF) towards this research is hereby acknowledged. Opinions expressed and conclusions arrived at, are those of the author and are not necessarily to be attributed to the NRF.

Most importantly, I would like to thank my husband, Willan Maswanganyi. You have been my rock and strength, a friend to offload my troubles and my sunshine. Thank you, I love you very much.

All this was possible because of His omnipotence, omniscience and omnipresence, Jesus Christ.

© University of Pretoria

RESEARCH OUTPUTS

Journal articles

Immobilized tetrakis(triphenylphosphine)palladium(0) for Suzuki-Miyaura coupling reactions under flow conditions, V. Ramaotsoa, I. Strydom, J-L. Panayides and D. Riley, *React. Chem. Eng.*, 2019, **4**, 372-382.

Draft article: Reduction of alkenes using a novel ozonolysis flow reactor

Poster presentations

Synthesis of an immobilized palladium catalyst for Suzuki-Miyaura coupling reactions under flow conditions, V. G. Ramaotsoa, I. Strydom, D. Riley, J-L. Panayides, *43rd SACI National Convention,* 2018, CSIR ICC, Pretoria. Received best poster prize.

Synthesis of monolith supported reagents with application to flow based API product, V. G. Ramaotsoa, D. Riley, J-L. Panayides, *CSIR Emerging Researcher Symposium,* 2018, CSIR ICC, Pretoria. Received best PhD poster prize.

Towards the Synthesis of Monolith-Supported Catalysts, V. G. Ramaotsoa, D. Riley, J-L. Panayides, *SACI North Young Chemists Symposium,* 2017, Tshwane University of Technology, Pretoria.

Progress Towards the Synthesis of Microsphere-Supported Catalysts, G. V. Ramaotsoa, D. Riley, J-L. Panayides, *14th Frank Warren conference,* 2016, Rhodes University, Grahamstown. Received best poster prize.

© University of Pretoria

ABSTRACT

Throughout the years, there have been challenges associated with the purification of some critical reactions which have proved to be time consuming and tedious. However, these difficulties have been grandly simplified by the use of immobilized reagents which can be readily removed by filtration and thus decreasing the purification time. An added advantage, is the incorporation of the solid-supported reagents onto flow reactors to facilitate in-line purification thus minimizing exposure to hazardous chemicals, waste and reaction time for some protocols.

In this thesis the application of polymer-bound triphenylphosphine was compared using commercial unsupported, commercial polystyrene-supported and in-house modified polymer-supported triphenylphosphine reagents in the ozonolysis, Wittig and Suzuki-Miyaura coupling reactions. Validation of the supports was compared under both batch and flow conditions in each case.

Our in-house polymer-supported triphenylphosphine reagent, formed by precipitation polymerisation of diphenyl (4-vinylphenyl)phosphine, showed a phosphorus loading of 1.85 mmol/g and was benchmarked against commercial polystyrene-supported triphenyl-phosphine which had a phosphorus loading of 3.00 mmol/g.

Firstly, we demonstrated the application of polymer-bound triphenylphosphine as a reductant in ozonolysis reactions under batch-flow hybrid conditions. The transformations were conducted using our newly developed ozonolysis flow setup which allowed reactions to be performed at ambient temperatures. Aldehydes were formed in moderate to high yields of 52-70% at room temperature, with cooled temperatures favouring the formation of the analogous acids. Of key importance was that the in-house polymer-supported triphenylphosphine reagent showed an improvement in yields after 48 hours relative to the commercial polystyrene reagent, with a four-fold reduction in the amount of reductant used.

Secondly, we demonstrated the conversion of commercial polystyrene-supported triphenylphosphine and in-house polymer-supported triphenylphosphine to Wittig benzyl phosphonium salts which gave a phosphorous elemental loading of 0.818 mmol/g and 1.614 mmol/g respectively. The formation of alkene products was observed at 30 °C when

© University of Pretoria

using in-house polymer-supported phosphonium salt but product formation was only observed at 60 °C for the analogous commercial polystyrene support. The Wittig reactions under batch and flow conditions gave high yields for the unsupported phosphonium salt. In contrast, the commercial and in-house polymer-supported phosphonium salts gave varying yields, which were substrate dependant.

Lastly, we transformed in-house polymer-supported triphenylphosphine reagent into polymer-supported tetrakis(triphenylphosphine)palladium catalysts under batch and flow conditions affording palladium loadings of 0.460 mmol/g and 0.689 mmol/g respectively. The prepared catalysts were benchmarked against commercial polystyrene-supported tetrakis(triphenylphosphine)palladium catalyst which has a reported palladium loading of 0.500 mmol/g. Demonstrating their use in Suzuki-Miyaura coupling reactions under batch and flow conditions showed comparative results. We observed an increase in yield for both the commercial and in-house catalysts under flow conditions compared to batch use with varying yields achieved with a single reaction. We were also able to readily recycle the substrates across the catalyst house in a packed-bed reactor affording close to quantitative conversion.

Overall, our in-house polymer-supported reagent and catalyst were an improvement to the commercially available polymer-supported counterparts. For the ozonolysis reactions, four-fold less reductant was used, reaction activity was observed at lower temperatures for the Wittig reaction and our catalyst offered an economical alternative to expensive reagent in Suzuki-Miyaura reactions. Although the unsupported reagents gave higher yields, the approach suffered from complicated purification protocols to remove unreacted triphenylphosphine and spent triphenylphosphine oxide. When employing flow conditions using solid-supported reagents/catalysts this was greatly simplified as these reagents remained in the packed-bed reactor.

© University of Pretoria

LIST OF ABBREVIATIONS

ACHN	1,1'-Azobis(cyanocyclohexane)
AIBN	2,2'-Azobis(isobutyronitrile)
API	Active pharmaceutical ingredient
Ar	Aromatic
BBN	Borabicyclo[3.3.1]nonane
BEMP	2-*tert*-Butylimino-2-diethylamino-1,3-dimethylperhydro-1,3,2-diazaphosphorine
BET	Brunauer–Emmett–Teller
BINOL	1,1'-Bi-2-naphthol
Bn	Benzyl
BPR	Back pressure regulator
bpy	Bipyridine
BZA	Benzylamine
cat	Catalyst
CHD	Cyclohexane-1,3-dione
DAST	Diethylaminosulfur trifluoride
DBU	Diazabicycloundecene
DCM	Dichloromethane
DIPEA	Diisopropylethylamine
DMA	Dimethylamine
DMAP	4-Dimethylaminopyridine

© University of Pretoria

DMF	*N,N*-Dimethylformamide
DMSO	Dimethyl sulfoxide
dpca	1,4-Dihydrophenonthrolin-4-one-3-carboxylic acid
dppf	1,1'-Bis(diphenylphosphino)ferrocene
DVB	Divinylbenzene
EDX	Energy dispersive x-ray
eq	Equivalents
FTIR	Fourier transform infrared spectroscopy
GC	Gas chromatography
h	Hour
HPLC	High performance liquid chromatography
HRMS	High-resolution mass spectroscopy
mp	Melting point
mw	Microwave
m/z	Mass-to-charge ratio
Nb	Norbornene
NMR	Nuclear magnetic resonance
PBR	Packed-bed reactor
PDI	Polydispersity index
PIFA	[Bis-(trifluoroacetoxy)iodo]benzene
PS	Polymer-supported

© University of Pretoria

PSTA	Polymer-supported siloxane transfer agent
PTFE	Polytetrafluoroethylene
PXRD	Powder x-ray diffraction
QP	Quadrapure
RAFT	Reversible addition-fragmentation chain transfer
ROMP	Ring-opening metathesis polymerisation
rt	Room temperature
salen	Salicylaldehyde and ethylenediamine
SEM	Scanning electron microscopy
SPE	Solid phase extraction
TBAA	*tert*-Butyl acetoacetate
TEM	Transmission electron microscopy
TEMPO	2,2,6,6-Tetramethylpiperidine-1-oxyl radical
THF	Tetrahydrofuran
TLC	Thin layer chromatography
TMS	Trimethylsilyl
TOF	Time-of-flight
Tol	Toluene
TON	Turnover number
T_R	Residence time
TsOH	*p*-Toluenesulfonic acid

© University of Pretoria

TU	Thiourea
UV	Ultraviolet

© University of Pretoria

DIAGRAM KEY FOR FLOW COMPONENTS

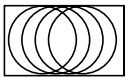

Coil

Pump

T-piece

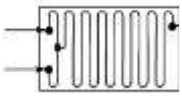

Dual entry microchip

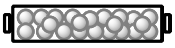

Packed column

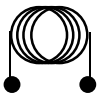

sample loop

Single entry microchip

Gas cylinder

Capillary column

© University of Pretoria

TABLE OF CONTENTS

Acknowledgements i

Research outputs ii

Abstract iii

List of abbreviations v

Diagram key for flow components ix

Chapter 1: Introduction 1

1.1. Background of solid-supported in batch chemistry 1

1.2. Application of solid-supported reagents in batch 4

1.3. Application of solid-supported catalysts in batch 11

1.4. Background on flow chemistry 14

1.5. Application of solid-supported reagents in flow 17

1.6. Application of solid-supported catalysts in flow 25

1.7. Monolith-supported reagents 29

1.7.1. Thermally triggered free radical polymerization 31

1.7.2. RAFT polymerisation 38

Chapter 2: Project overview, aims and objectives 43

2.1 Project overview 43

2.1.1. Ozonolysis 43

2.1.2. Wittig olefination reactions 46

2.1.3. Suzuki-Miyaura coupling 47

2.2 Aims and objectives 49

Chapter 3: Preparation of immobilized triphenylphosphine reagents 50

3.1. Introduction 50

3.2. Batch synthesis 51

3.2.1. Polystyrene-supported triphenylphosphine prepared from 4-bromopolystryrene 51

3.2.2. In-house polymer-supported triphenylphosphine prepared using precipitation polymerization 55

© University of Pretoria

3.3 Flow synthesis 58

3.3.1. In-house polymer-supported triphenylphosphine using precipitation polymerization 58

Chapter 4: Application of triphenylphosphine reagents to ozonolysis Reaction 61

4.1. Introduction 61

4.2. Batch Synthesis 62

4.2.1. Model Study 62

4.2.2. Optimisation of reaction concentration and reaction time 63

4.2.3. Optimisation of reaction temperature 65

4.3. Flow synthesis 68

4.4. Conclusion 70

Chapter 5: Preparation of immobilized phosphonium salts and their use in the Wittig reaction 72

5.1. Introduction 72

5.2. Batch Synthesis 73

5.2.1. Synthesis of unsupported and polystyrene-supported phosphonium salts 73

5.2.2. Synthesis of in-house solid-supported phosphonium salt 209 74

5.3. Flow synthesis 77

5.3.1. Unsupported triphenylphosphine 77

5.3.2. Polystyrene-supported triphenylphosphine 78

5.3.3. In-house polymer-supported phosphonium salt 209 80

5.4. Overall application to Wittig reactions in batch and flow 81

5.5. Conclusion 84

Chapter 6: Preparation of immobilized palladium catalysts and their use in the Suzuki-Miyaura coupling reaction 86

6.1. Introduction 86

6.2. Batch Synthesis 87

© University of Pretoria

6.2.1. Synthesis and characterization of in-house polymer-supported tetrakis(triphenylphosphine)palladium(0) 87

6.2.2. Optimization studies of catalyst 215a for Suzuki-Miyaura coupling reactions 95

6.3. Flow Synthesis 98

6.3.1. Synthesis of catalyst 215c 98

6.3.2. Suzuki-Miyaura coupling reactions using catalyst 215a and 215c 100

6.4. Conclusion 105

Chapter 7: Overall conclusion and future work 107

7.1. Overall conclusion 107

7.2. Future work 108

Chapter 8: Experimental 110

8.1. General procedures 110

8.2. Synthesis and characterization of immobilized triphenylphosphine reagent 113

a. Batch synthesis of in-house polystyrene-supported triphenylphosphine 201 113

b. Synthesis of in-house polymer-supported triphenylphosphine 146 114

8.3. Synthesis and characterization for batch ozonolysis reaction 115

8.4. Synthesis and characterization for flow ozonolysis reaction 115

a. General procedure 1: Ozonolysis reactions using commercial unsupported triphenylphosphine 115

b. General procedure 2: Ozonolysis reactions using commercial polystyrene-supported triphenylphosphine 201a 116

c. General procedure 3: Ozonolysis reactions using in-house polymer-supported triphenylphosphine 146 116

8.5. Synthesis and characterization for batch Wittig reaction 119

a. Synthesis of benzyltriphenylphosphonium bromide 206 119

© University of Pretoria

b. Synthesis of polystyrene-supported benzyltriphenylphosphonium bromide 208 119
c. Synthesis of in-house polymer-supported benzyltriphenyl-phosphonium bromide 209 119
d. General batch procedure 1: Wittig reactions using unsupported benzyl salt 206 120
e. General batch procedure 2: Wittig reactions using polystyrene-supported benzyl salt 208 120
f. General batch procedure 3: Wittig reactions using in-house polymer-supported benzyl salt 209 120

8.6. Synthesis and characterization for flow Wittig reaction 121
a. Synthesis of polystyrene-supported benzyl salt 208a 121
b. Synthesis of in-house polymer-supported benzyl salt 209a 121
c. General flow procedure 1: Wittig reactions using unsupported benzyl salt 206 121
d. General flow procedure 2: Wittig reactions using polystyrene- or in-house polymer-supported benzyl salt 122

8.7. Synthesis and characterization for batch Suzuki-Miyaura coupling reaction 125
a. Synthesis of in-house polymer-supported tetrakis(triphenyl-phosphine)palladium 215a 125
b. Synthesis of in-house polymer-supported tetrakis(triphenyl-phosphine)palladium 215b 126
c. General batch procedure 4: Suzuki-Miyaura coupling reactions using commercial unsupported tetrakis(triphenylphosphine)palladium 126
d. General batch procedure 5: Suzuki-Miyaura coupling reactions using commercial polystyrene-supported tetrakis(triphenylphosphine)-palladium 128
e. General batch procedure 6: Suzuki-Miyaura coupling reactions using polymer-supported tetrakis(triphenylphosphine)palladium 215a 128

© University of Pretoria

8.8. Synthesis and characterization for flow Suzuki-Miyaura coupling reaction 128

a. Synthesis of in-house polymer-supported tetrakis(triphenyl-phosphine)palladium 215c 128

b. General flow procedure 3: Suzuki-Miyaura coupling reactions using commercial polystyrene-supported tetrakis(triphenylphosphine)-palladium 129

c. General flow procedure 4: Suzuki-Miyaura coupling reactions using in-house polymer-supported tetrakis(triphenylphosphine)palladium 215c 130

8.9. Synthesis of the 2-bromo-3-methoxynaphthalene (219) starting material for Suzuki-Miyaura coupling reactions 130

Chapter 9: References 136

Chapter 10: Appendices 144

10.1. Appendix A: Supporting Information 144

10.1.1. Synthesis of solid-supported triphenylphosphine 201 144

10.1.2. Ozonolysis selected examples from model study 145

10.1.3. Wittig selected examples from model study 151

10.1.4. Suzuki-Miyaura selected examples from model study 160

© University of Pretoria

Introduction

© University of Pretoria

Chapter 1

Introduction

1.1. Background of solid-supported batch chemistry

The last two decades have seen researchers becoming more focused on the idea of "green chemistry" in synthetic processes, and although there is no general method to follow there are some cleaner, more environmentally friendly protocols that have been implemented. These methods include using less electricity and flowing water, reducing the use of toxic chemicals, using catalysts versus stoichiometric additions, using mild solvents, biodegradable material and the reduction of chemical waste. Column chromatography is arguably one of the most widely used means of purification at bench scale, however, the method is inherently inefficient, being associated with the production of high quantities of chemical solvent waste and poor scalability. The wastage is further exacerbated in instances where complex matrices exist, where the separation of several compounds often requires multiple chromatographic separations. This insight has in part directed an on-going focus on the use of solid-supported reagents, catalysts (reagents used in sub-stoichiometric quantities to transform substrates into new compounds and/or to control stereochemistry outcomes) and scavengers (reagents used for quenching by-products or removing excess/unreacted starting materials). A further use of scavengers is the ability to selectively catch the required product away from any contaminating impurities, filter and then re-release the desired product in a pure form (commonly known as "catch and release").

Solid-supported reagents are insoluble solids (usually polymers) containing active/ functionalised sites on the surface of the support, with which reagents can interact in order to undergo a chemical reaction. This concept was brought to light in 1963 by Bruce Merrifield who published his work on solid phase peptide synthesis of a tetrapeptide which would ease the formidable purification of long chain polypeptides.[1] This was executed by attaching the first amino acid to a solid polymer by a covalent bond, followed by the addition of successive amino acids in a stepwise manner until the desired chain length was assembled. Conveniently, the intermediate peptides were purified by dissolving away the impurities through filtration and not by the usual recrystallization procedures. The final step was the removal of the peptide from the insoluble solid support. The chosen resin was a polystyrene resin cross-

© University of Pretoria

linked with a small percentage of divinylbenzene (DVB) with chloromethyl functional groups as the active species. In 1963, Merrifield and Wang reported the synthesis of protected peptide hydrazides using a resin with *t*-alkyloxycarbonylhydrazide functional groups.[2] Although Merrifield was credited for this insight, solid-supported reagents could be traced back to 1935 where industrial chemists, Adams and Holmes described phenol-formaldehyde based spherical particles for ion-exchange chemistry and in 1946 Hohenstein and Mark introduced the use of styrene and divinylbenzene to produce sulfonic acid resins.[3]

Resin scaffolds such as glass beads, silica, cellulose and monoliths have been used with the reactive species remaining accessible (Figure 1).[4] Due to the nature of the scaffolds, analysis methods differ from homogeneous reagents. Therefore, detection of elements and percentage loading is determined by elemental analysis, functional groups are monitored using fourier transform infrared (FTIR) spectroscopy, solid state nuclear magnetic resolution (NMR) spectroscopy and the morphology of the polymer can be determined by scanning electron microscopy (SEM).

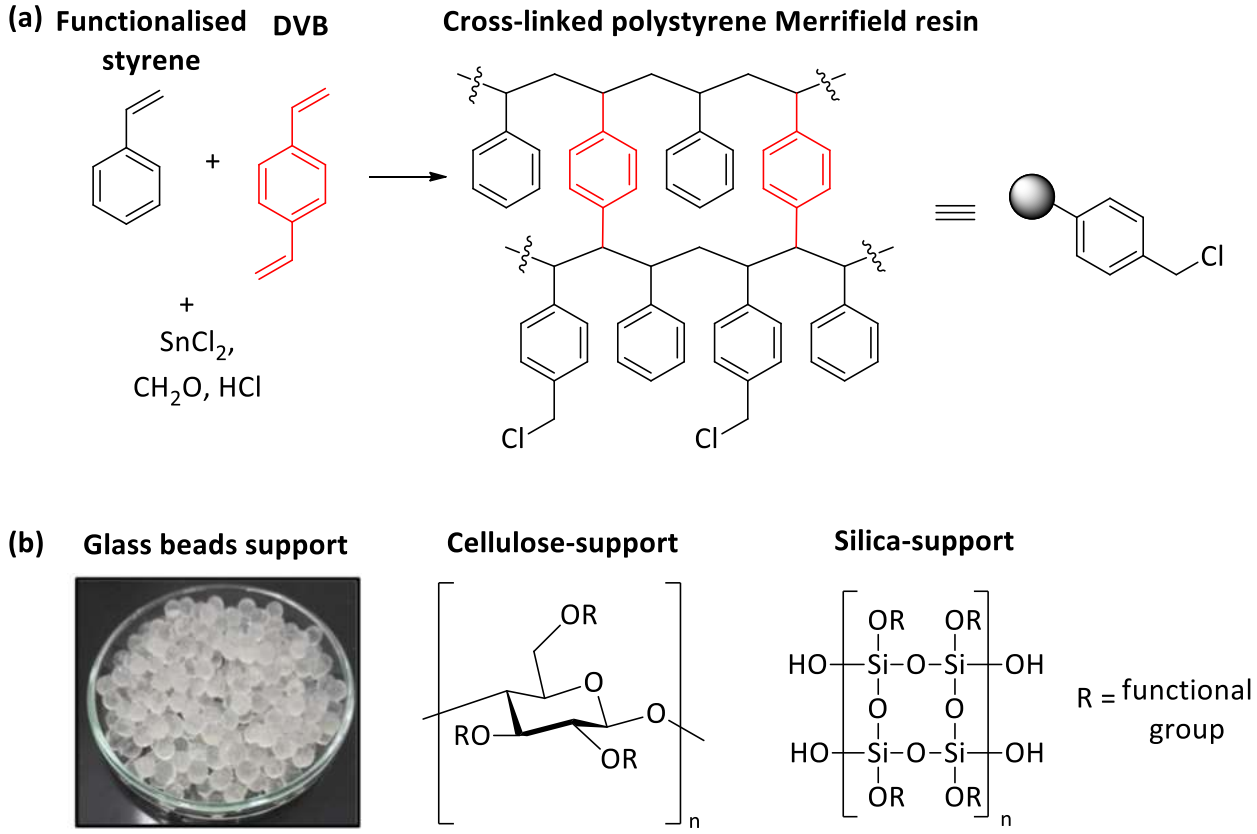

Figure 1: Examples of immobilisation supports: (a) Merrifield resin, (b) different types of solid supports

© University of Pretoria

The advantages of using solid-supported reagents are: (i) the convenient separation from the desired product by simple filtration; (ii) using excess reagents to drive complete conversion of a starting material; (iii) safe handling of toxic and explosive reagents; (iv) reagents that are incompatible in a homogeneous solution can be used simultaneously; (v) recovered reagent can be recycled thus reducing costs; and (vi) if by-products form a scavenging reagent can be incorporated to purify the product. Several shortcomings are involved when using resins due to the heterogeneous nature of the reaction conditions and these include: (i) prolonged reaction times; (ii) part of the resin may be found in the final product; (iii) difficulties of resin swelling which is linked with the degree of cross-linking; (iv) difficulty in monitoring progress by thin layer chromatography (TLC); (v) temperature conditions can be limited by stability of the polymer; and (vi) side reactions with the polymer may occur.[5,6,7] Numerous solid-supported reagents are available for commercial purchase with different functional groups and uses, examples of select solid-supported reagents are given in Table 1.

Table 1: Examples of commercially available immobilised reagents

Active functionality	Use	Active functionality	Use
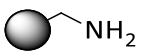	Acid scavenger	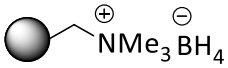	Reducing agent
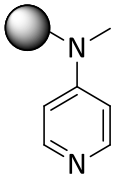	Base	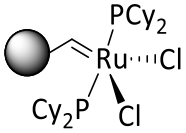	Metathesis catalyst
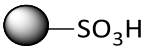	Amine scavenger, deprotection	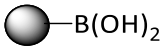	Boronic acid
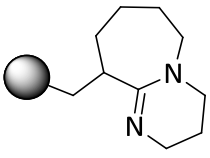	Base	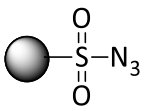	Diazo transfer agent
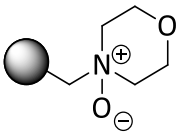	Oxidizing agent	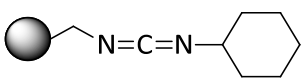	Coupling agent

© University of Pretoria

1.2. Application of solid-supported reagents in batch

An overview highlighting several processes using different types of solid-supported reagents are described in the following sections, but for a more comprehensive overview the reader is directed to the review by Ley and co-workers.[8]

In 2002 Ley and co-workers introduced a synthesis of the natural product carpanone using solid-supported reagents (Scheme 1). The synthesis began by allylating sesamol **1** in the presence of a supported phosphazene base and allyl bromide. The formed aryl ether **2** was then subjected to a Claisen rearrangement in an ionic liquid, which was removed by filtration through a plug of silica. Isomerisation was then enabled by using polymer-supported Felkin's iridium catalyst. Carpanone **5** was then formed via tandem oxidative coupling Diels Alder reaction sequence by reaction with solid-supported Co(salen) catalyst. The unreacted phenol was removed using solid-supported sodium bicarbonate, the aldehyde by-product was removed by a solid-supported scavenger, trisamine, and the desired compound was obtained in 70% yield across the four steps with no chromatogrphy.[9]

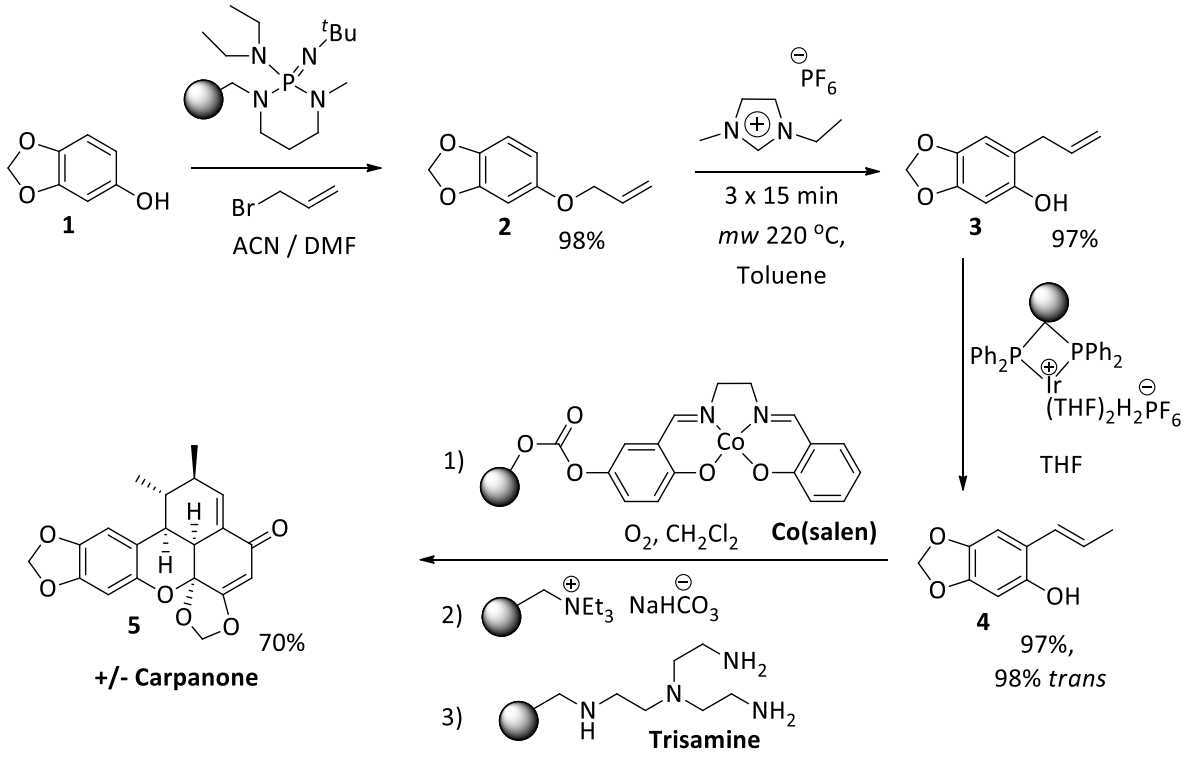

Scheme 1: Solid-supported synthesis of carpanone[9]

A "catch and release" synthesis of amides using polymer-supported cyclohexane-1,3-dione (PS-CHD) **10** was demonstrated by Turner and co-workers.[10] Synthesis of PS-CHD **10** was

© University of Pretoria

achieved by reacting 1-ethyl-3,5-dimethoxy-cyclohexa-2,5-dienecarboxylic acid **7** with solid-supported *N*-methylaminomethyl **6** to form a bis-enol ether **8**. This was then transformed into PS-CHD, first by a mono hydrolysis with TFA to produce vinyl ether **9**, followed by using microwave heating and the addition of butylamine to completely hydrolyse the methoxy groups in two steps. The "catch and release" potential of the polymer was demonstrated by reacting PS-CHD with benzoyl chloride **11** as the catched and released agent to form an enol ester **12**, followed by a reaction with benzylamine **13** to give benzamide **14** in a high yield of 95%. The product was then readily separated from PS-CHD by filtration (Scheme 2).

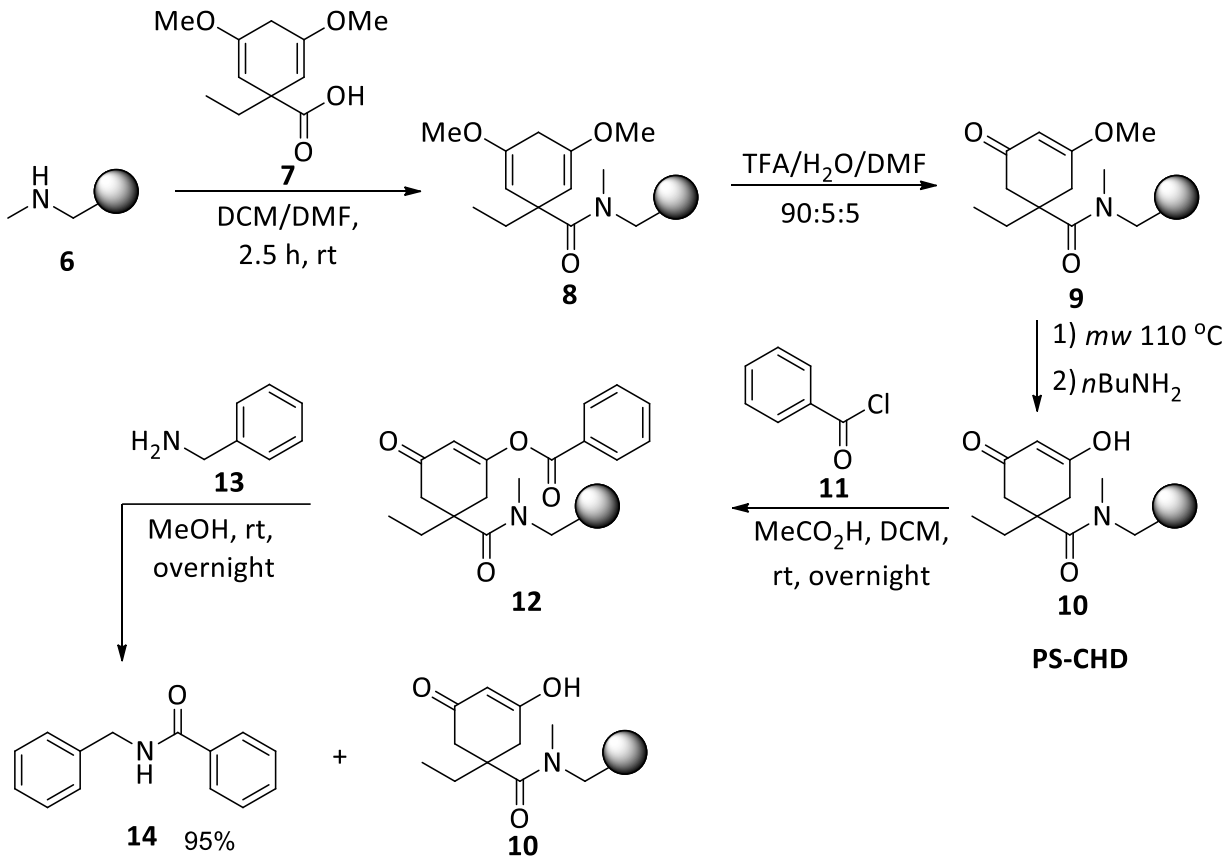

Scheme 2: Synthesis of PS-CHD and demonstration of "catch and release" to give amide 14[10]

Diaz, Yang and Gendre used aryl halides grafted onto commercially available polystyrene SynPhase lanterns **15** to synthesise diaryl sulphides (Scheme 3).[11] SynPhase lanterns are modular solid substrates with low cross-linked surfaces that hold discrete quantities of single compound and are able to be optimized for the synthesis of small organic molecules or peptides.[12] The lanterns functionalized with long-chain hydroxymethylphenoxyvaleric amide linker were coupled with aryl halides using N,N'-Diisopropylcarbodiimide in the presence of

© University of Pretoria

DMAP. A number of supported aryl systems were reacted with thiols **16** in the presence of solid-supported borohydride, with cross coupling preceding cleavage by the borohydride, and nickel bipyridine (bpy) dibromide catalyst to give thio ethers **17** in high yields (91-100%).

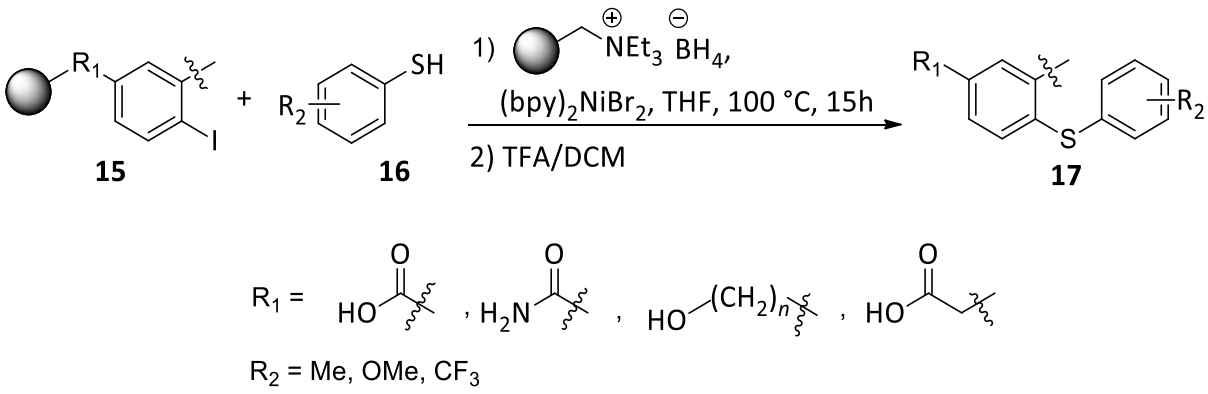

Scheme 3: Synthesis of diaryl thiols via solid-supported aryls[11]

Polymer-supported *p*-toluenesulfonic acid (PS-TsOH) has proved to be a good reagent for the cleavage of aromatic ethers **18** as reported by Ruchirawat and co-workers (Scheme 4).[13] Vanillin was O-alkylated with varying protecting groups (benzyl, isopropyl and *tert*-butyl). The vanillin derivatives were then subjected to deprotection using PS-TsOH to afford the corresponding phenols **19** in moderate to high yields (62-95%). The polymer-supported scaffold was formed on silica or cross-linked polystyrene, with deprotection using the former giving faster conversions due to the larger surface area. Upon deprotection, R formed a carbocation which either experienced a Friedel-Crafts C-alkylation reaction with vanillin and toluene or became deprotonated on the carbon adjacent to the carbocation to form olefin by-products.

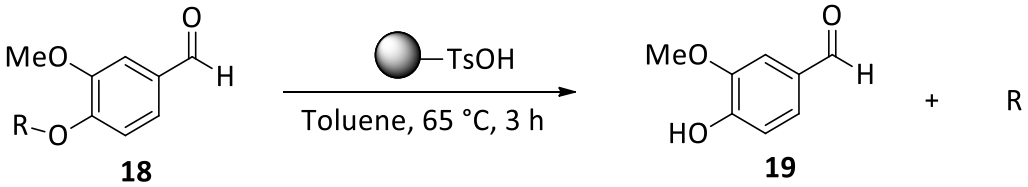

Scheme 4: Deprotection of aromatic ethers using PS-TsOH[13]

The epoxidation of alkenes was reported by Asensio and co-workers with the use of a solid-supported percarboxyethyl (peroxyacid) **21** (Scheme 5).[14] The supported reagent was prepared from a silica scaffold obtained by the acid hydrolysis of cyanoethyl functionalised

© University of Pretoria

silica **20**, followed by treatment with 30% hydrogen peroxide in sulfuric acid. Epoxidations to form the epoxides **23** were carried out at room temperature using excess amount of the supported reagent and alkene **22**, achieving high conversion of 94-99%. The epoxide product was readily recovered by removing the spent solid supported reagent by filtration, the support was then easily regenerated by treatment with 30% hydrogen peroxide in an acidic medium.

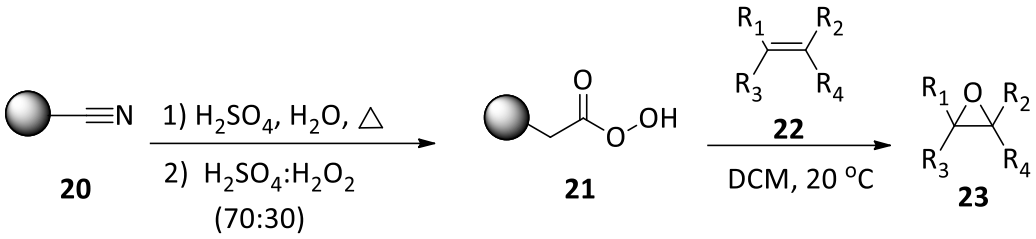

Scheme 5: Synthesis of silica-supported peracid[14]

In 2014, Bräse and co-workers developed a polymer-supported reagent **27** for the dithioacetalisation of aldehydes **28** into dithioacetals and ketones into dithioketals in the presence of the Lewis acid boron trifluoride (Scheme 6).[15] An upside to this reagent was that it did not exhibit the notorious odour of thiols. The polymer was synthesized by reacting adipoyl dichloride **25** with polymer-supported amine **24** to form an acyl chloride polymer **26** in the presence of 4-Dimethylaminopyridine (DMAP), which was then reacted with either ethanedithiol or propanedithiol and tetrafluoroboric acid diethyl ether complex. The aldehyde substrate was converted into thioacetal **29** upon reaction with the thionium supported reagent **27**. The results of the dithionisation gave a range of yield for **29** from low (aliphatic compounds) (22-49%) to moderate to high (aromatic compounds) (55-97%).

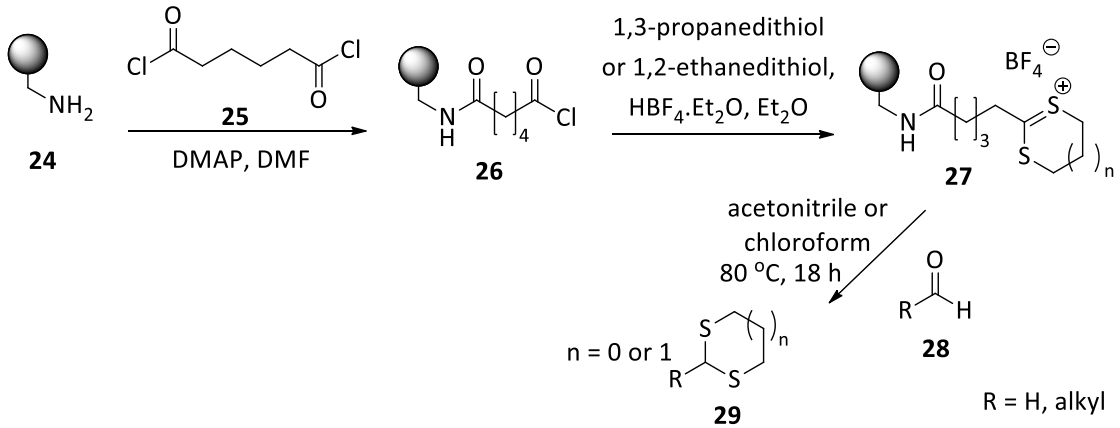

Scheme 6: Dithioacetalisation of aldehydes using polymer-supported reagent[15]

© University of Pretoria

In the same year, Smith and Nguyen reported the synthesis of a polymer-supported siloxane transfer agent (PSTA) **36** that was used in cross-coupling catalysed reactions of lithiated species **37** with aryl halides **38** (Scheme 7).[16] Synthesis of the polymer was initiated by treating 2-bromobenzaldehyde **30** with allylmagnesium chloride **31** to form a benzylic alcohol **32**. Further reaction of benzylic alcohol **32** with chlorodimethylsilane led to siloxane **33**, which was then subjected to hydroboration to form **34**, followed by cross coupling via Suzuki-Miyaura to afford the *p*-silylsubstituted vinylbenzene monomer **35**, which was polymerized under radical conditions to afford the polymer-supported reagent PSTA **36**. The PSTA **36** was validated in cross-coupling reactions to form biaryls **39** in high yields with no homocoupling of the reagents. The 1-oxa-2-silacyclopentene moiety of **36** reacted with the aryl lithium substrate to form an alkoxide intermediate. The subsequent addition of the aryl halide furnishes a brook-like rearrangement to yield the product.[17] Advantageously, simple filtration was used to remove the polymer and recycling of the supported reagent was possible after use without a decrease in the reaction efficiency. (Scheme 8).

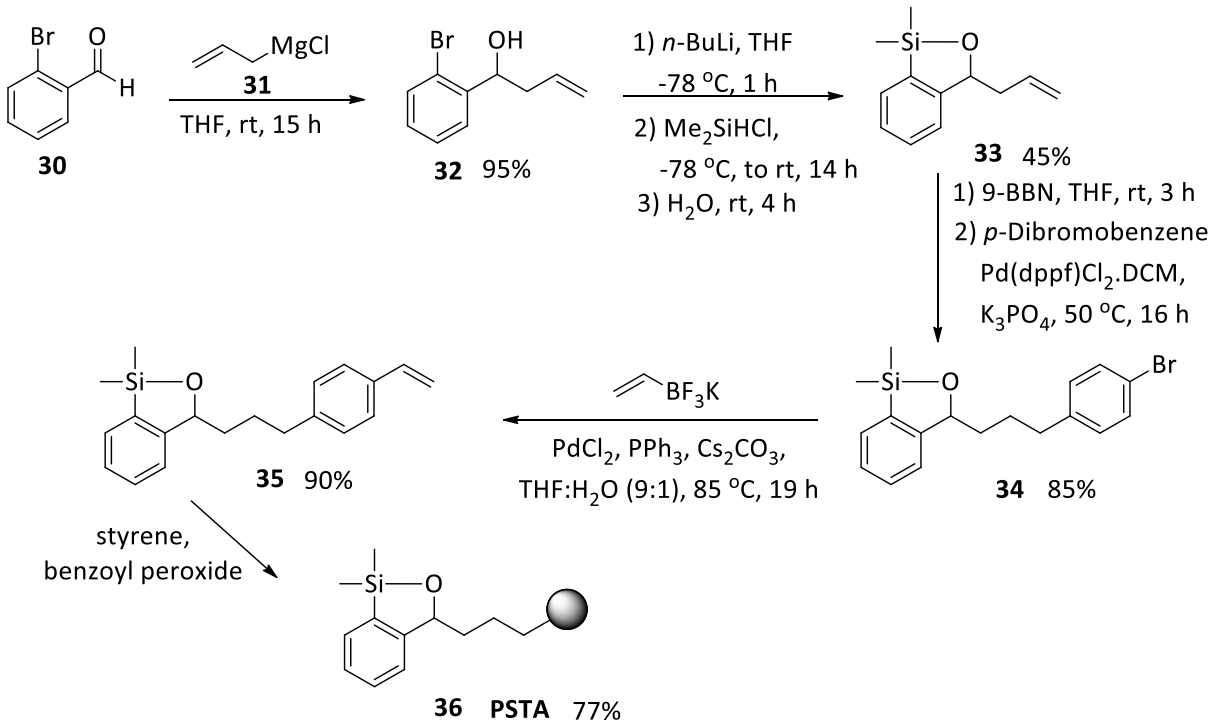

Scheme 7: Synthesis of siloxane transfer agent[16]

© University of Pretoria

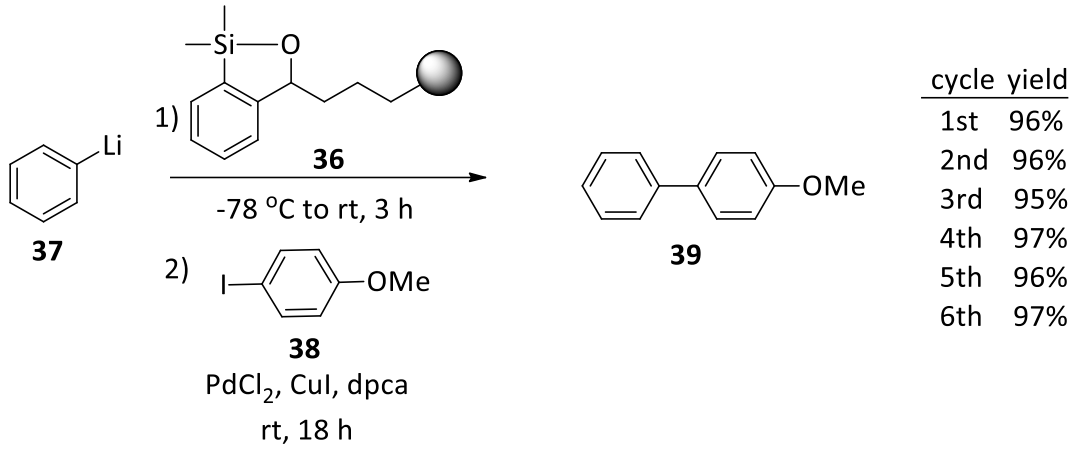

Scheme 8: Cross-coupling reaction in the presence of PSTA and recycling evidence[16]

In 2015, Hanson and co-workers prepared silica-based supports containing an oligomeric benzyl or triazole phosphate **43** functionality for use as alkylating reagents (Scheme 9).[18] The benzyl reagent was formed from activated silica **40** by using ring-opening metathesis polymerisation (ROMP) conditions onto norbornene silyl tagged silica (Si-Nb) **41** in two steps, followed by addition of norbornene-tagged benzyl phosphate **42**. A range of compounds containing alcohol, thiol and amine functional groups were alkylated to form benzylated compounds **44** in high yields of 95-99% (Scheme 10) and the silica phosphate scaffold was removed by filtration through celite using solid phase extraction (SPE).

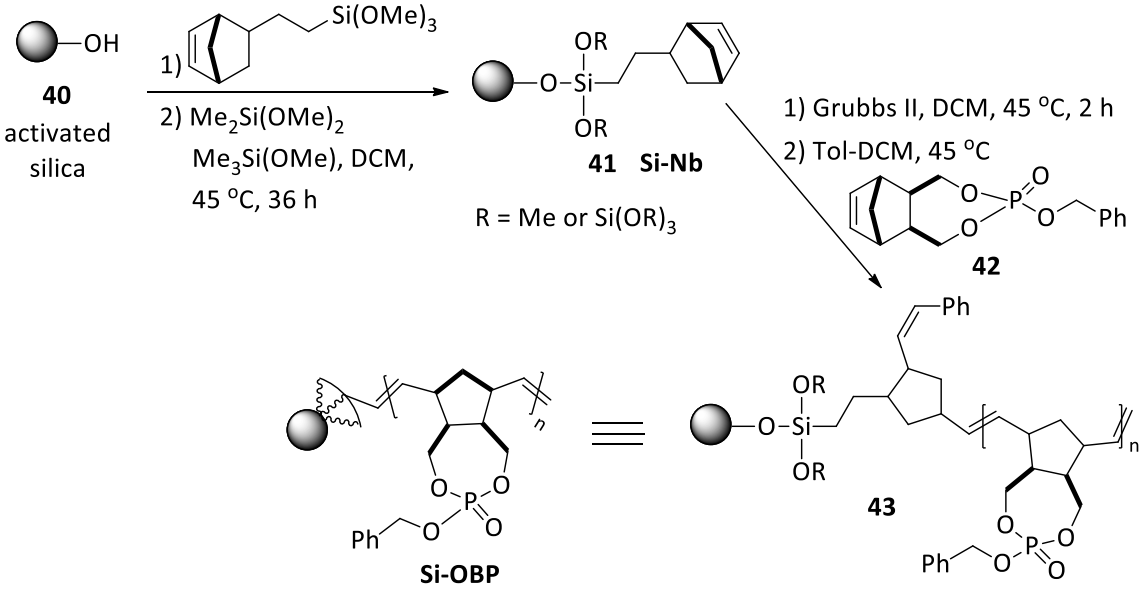

Scheme 9: Synthesis of silica-supported benzyl phosphate reagent[18]

© University of Pretoria

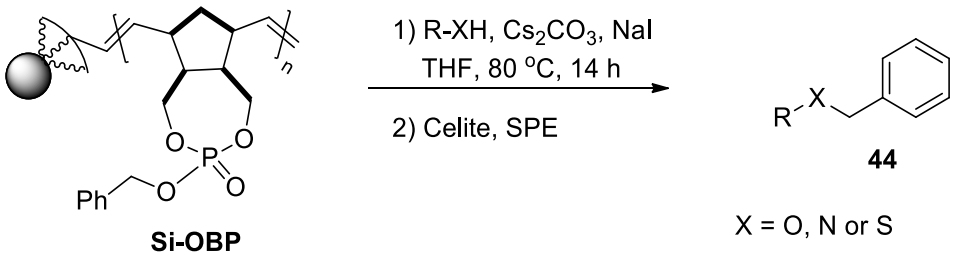

Scheme 10: Alkylation of compounds using benzyl phosphate polymer[18]

In 2016, Bräse and co-workers further introduced the synthesis of six-membered heterocycles using an immobilised oxazolone **49**, which was synthesized by reacting Merrifield polymer **45** with an acrylic acid **46** linker to form polymer **47**, followed by reaction with the oxazolone **48** via Michael addition. The immobilized oxazolone **49** was then reacted with difunctional nucleophiles **50** causing a cyclisation and cleavage of the polymeric scaffold (Scheme 11).[19] The synthesis gave quinoxalinones, pyrazin-2-ones, benzoxazoles and dihydrooxazinones **51** in moderate to high yields (51-86%).

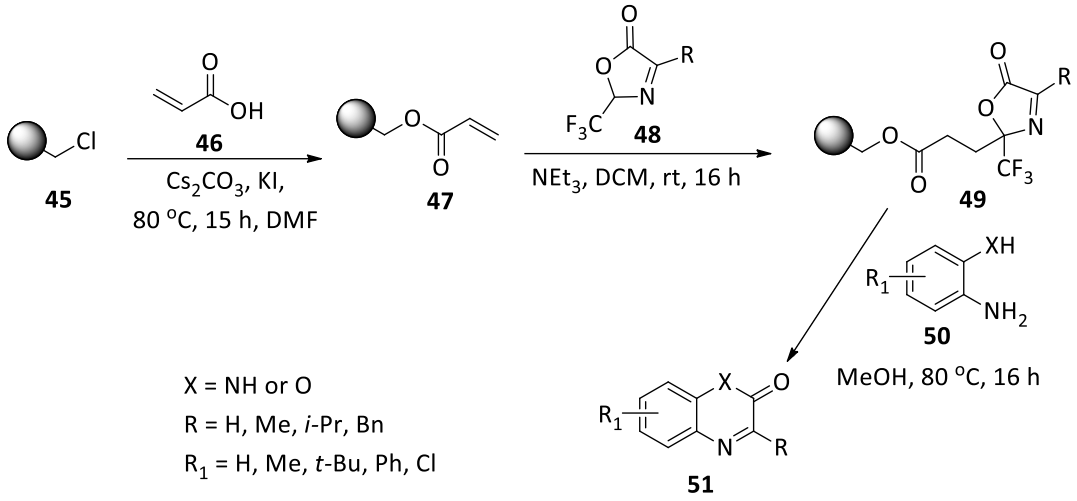

Scheme 11: Synthesis of polymer-supported oxazolone and heterocyclic compounds[19]

In the same year, Bräse and co-workers developed another sulfur containing polymer-supported reagent which was used to synthesise diaziridines and diazirines **55** in moderate to high yields (63-97%) (Scheme 12).[20] The immobilized sulfonyl oxime **54** was synthesized by reacting an oxime having different phenyl substituents **53** with polymer-bound sulfonyl chloride **52**. The cleavage of the immobilized sulfonyl group to form the diaziridines was facilitated by reaction with ammonia.

© University of Pretoria

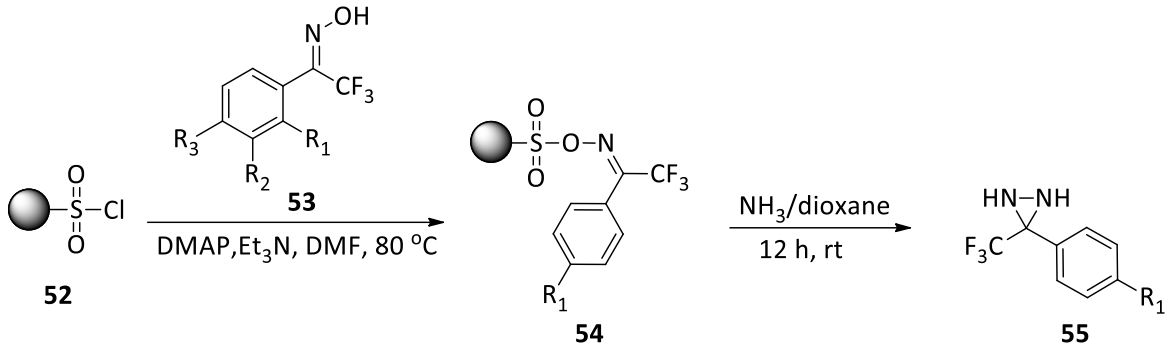

R_1 = H, OMe, Cl, Br, 4-bromophenyl or 4-ethinylphenyl

Scheme 12: Synthesis of polymer-bound sulfonyl oxime and cleavage to form diaziridines[20]

1.3. Application of solid-supported catalysts in batch

The use of solid supports have not only been demonstrated as stoichiometric reagents and scavengers but also as catalysts. These compounds are used to introduce chemical transformations at an increased rate using less energy, at times reducing the number of synthesis steps. Normally reactions are controlled by optimization of temperature, concentration and pressure to increase reagent-substrate interaction. However, the use of catalysts pushes reactions towards a desired product and in most cases without unwanted by-products.[21] Homogeneous catalysts have the same phase as the reactants, i.e. soluble in the matrix (reaction solvent) thereby making all active sites accessible. Added advantages of homogeneous catalysts include distinct chemical composition, reproducible synthesis at mild conditions, and catalyst structures can be easily determined by spectroscopic analysis. The main disadvantage arises during separation of products from the catalyst. When distillation of the product is used; however, the elevated temperatures usually decompose the catalyst and other conventional methods like chromatography and extraction lead to loss of catalyst.[22]

As previously mentioned, the simple purification of polymer-supported reagents is a key advantage, especially so in the case of catalysts based on transition metals, which are expensive to purchase and prepare, so it is important to be able to recover, regenerate and reuse them. This recyclability is especially useful in the synthesis of compound libraries.[23] In addition, some catalysts are sensitive to handle outside of inert conditions, but when immobilized they often become more stable and the leaching of their metals into the final products reduced. The main disadvantage in using heterogeneous catalysts is the necessity to use complex characterisation methods, in addition it has been observed that some

© University of Pretoria

catalysts cannot be recycled. Solid-supported catalysts can either be porous with site interaction available throughout the inert surface or impenetrable where reactions occur only with the active sites on the surface. There is a plethora of literature on the rapid synthesis and application of polymer-supported catalysts. An overview highlighting several processes using solid supported catalysts are described in the following sections, for a more comprehensive analysis the reader is directed to the reviews by Kann; Janda and co-workers; and Marco and co-workers.[23,24,25]

In 2016, Watts and co-workers described the synthesis of *para*-methane diesters **59** using a solid-supported scandium triflate catalyst **58** under solvent-free conditions (Scheme 13).[26] *Para*-methane-3,8-diol **56** was acylated with various acid anhydrides **57** (acetic, pentanoic and hexanoic) in the presence of polymer-supported scandium acid catalyst in moderate to high yields (85-97%).

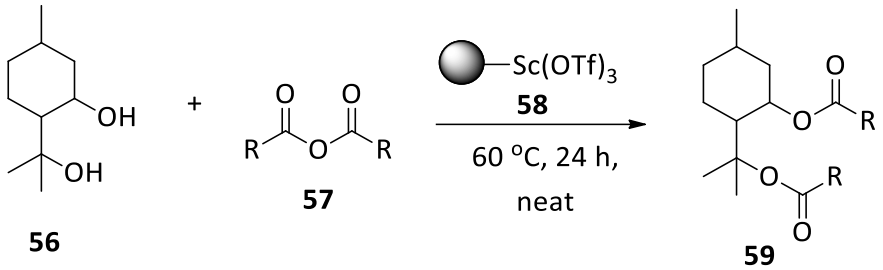

R = Me, ethyl, butyl or pentyl

Scheme 13: Polymer-supported acylation[26]

Polymer-supported organocatalysts (catalysts lacking a metal element) in the form of chiral bifunctional squaramides **63** were developed by Pedrosa and co-workers in 2017. These catalysts were used in stereoselective Michael addition reactions between alkenes and different nucleophiles.[27] The organocatalyst was prepared in a two-step synthesis via condensation of a diamine **60** and diethyl squarate **61** to form **62**, followed by reaction with polystyrene resins having either a methylamine, ethylamine or butylamine linker (Scheme 14). The different catalysts were tested on the reaction of nitrostyrene **64** with acetylacetone **65**, affording **66** in good yields (70-97%) and enantiomeric ratios (81:19 to 99:1) (Scheme 15).

© University of Pretoria

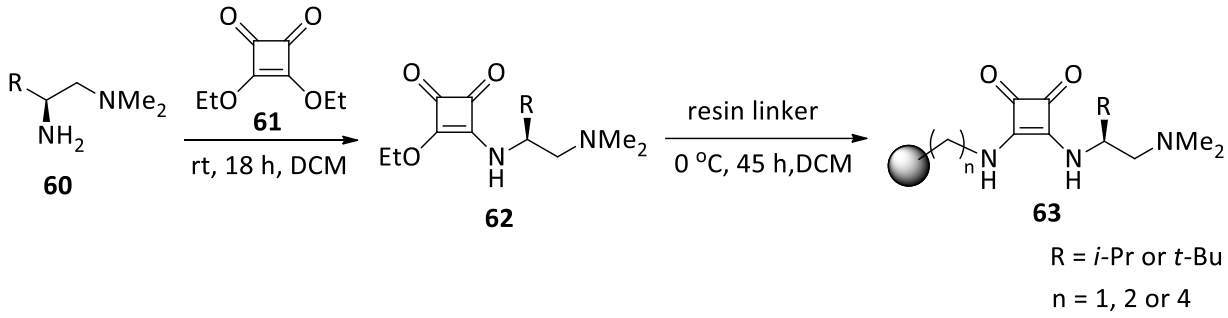

Scheme 14: Synthesis of polymer-supported organocatalysts[27]

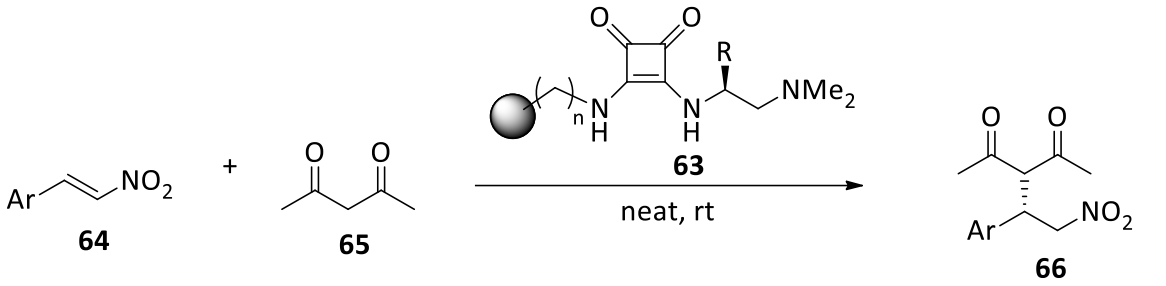

Scheme 15: Michael addition reaction of nitroolefins and acetylacetone[27]

Similarly, in 2018, Harada and co-workers reported a silica-supported chiral catalyst for use in the arylation of aldehydes.[28] The catalyst **68**, had a Bi-naphthol (BINOL) scaffold and was synthesised by grafting hydrosilane precursor **67** onto the surface of silica particles with tris(pentafluorophenyl)borane as a catalyst followed by capping the free silanol groups with $EtMe_2SiH$ (Scheme 16). This catalyst was used in conjunction with a titanium reagent to facilitate the arylation of aldehyde **69** with aryl Grignard reagent **70** to give compounds **71** in high yields, 83-92% and enantiomeric excess of 83-94% (Scheme 17).

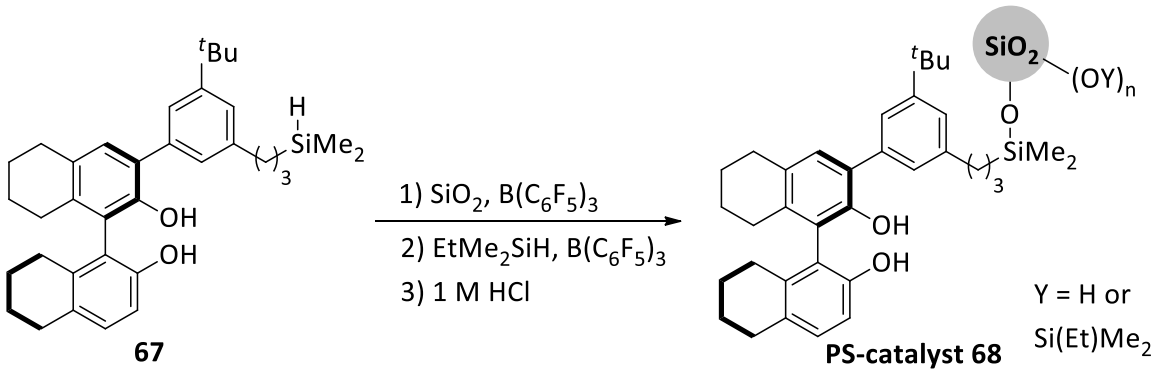

Scheme 16: Synthesis of BINOL catalyst[28]

© University of Pretoria

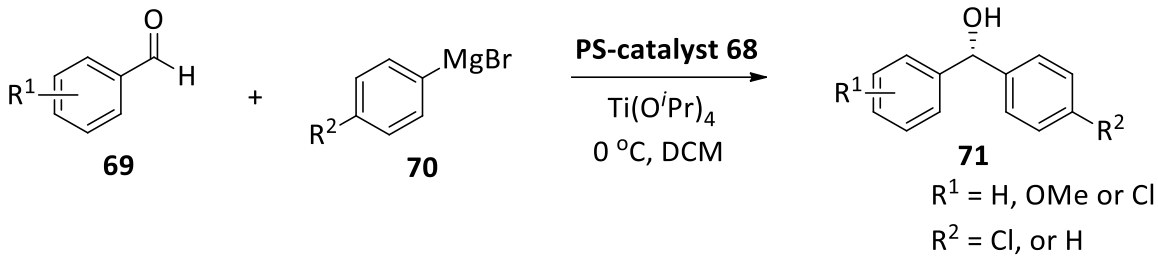

Scheme 17: Aldehyde arylation using BINOL catalyst[28]

This section has demonstrated how solid-supported reagents have improved the synthesis and purification of organic compounds. In addition, the active sites can be tailored for specific transformation such as epoxidation, deprotection, cross-coupling and alkylation. The easy filtration of solid-supported reagents expanded the thinking of researchers on how to reduce the manual handling of the reagents by incorporating them into the concept of automated flow chemistry. In the next section the introduction of flow chemistry will be outlined and the integration of solid-supported reagents thereof.

1.4. Background on flow chemistry

Flow chemistry is a process wherein reactions are performed in continuous flowing streams, often coupling multiple steps together in an effort to improve productivity and efficiency from those of existing batch protocols.[29] The approach replaces traditional glassware (round-bottomed flasks, test tubes or closed vessels) with columns, mixing chips and coil reactors that may be subjected to various process protocols including heating/cooling, oscillation, ultrasound and microwave irradiation, with in-line monitoring possible at any stage using a variety of analytical techniques including ultraviolet (UV), FTIR, NMR spectroscopy and high performance liquid chromatography (HPLC). In addition, rapid optimisation and quality control (flow rates, reactant concentration, temperatures and pressures) can be enabled to ensure reproducibility through the incorporation of automated and real-time analysis.[30] Continuous flow is not only limited to chemical transformations and separations but can also incorporate crystallization and drying.[31] In contrast most traditional batch syntheses require manual work-up and purification before continuing to next step, under ideal conditions this can be avoided with flow approaches allowing the isolation of pure material without interruption (Scheme 18).

© University of Pretoria

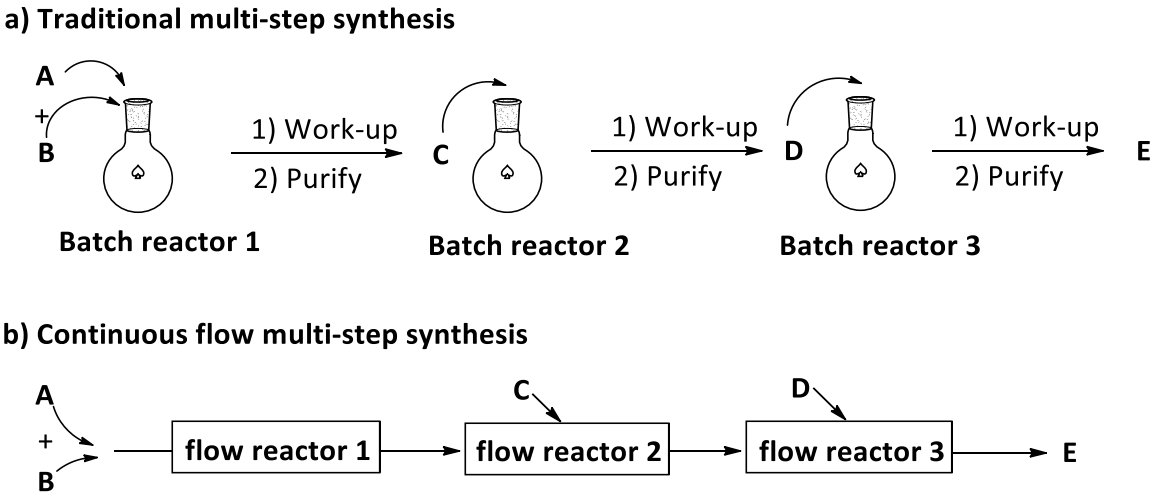

Scheme 18: Batch vs Flow synthesis

The main disadvantage of using flow synthesis rather than traditional batch synthesis, apart from the high instrument cost versus relatively cheap standard glassware, arises when blockages occur in the microreactors and small internal diameter tubing due to the formation of precipitates resulting from inorganic salts and insoluble products separating from the reaction mixture. Air bubbles in the tubing can also create a disturbance in the system pressure causing the reaction to abort. Another concern is choice of solvent, as high viscosity promotes the challenge of pressure building up in the microreactors and in general the use of corrosive reagents in the flow streams is not advised as these will damage the reactor components. Overall a change in the mindset of the chemist is required to adapt to the new technology, for example instead of reaction time the chemist now needs to consider residence time (the time it takes for reagents to be in contact with a reactor, governed by reactor volume and reaction flow rate). Despite the many challenges associated with flow synthesis, the opportunities for reduced purification time, inclusion of in-line monitoring and reduced solvent wastage generally outweighs them.[32,33,34] This revolution does not decrease the purpose of chemists, but rather increases the development skills of the chemist to overcome the challenges.

A few flow reactor designs are available on the market, each one custom designed for specific synthetic applications. These include the Uniqsis FlowSyn,[35] Syrris Asia series,[36] Chemtrix Labtrix,[37] Vapourtec R-series,[38] ThalesNano H-Cube[39] and YMC KeyChem-integral[40] systems to name a few. Some are equipped with syringe pumps, while others have HPLC pumps and

© University of Pretoria

the computer operated systems allow the user to run multiple flow reactions with scheduling and experiment recording (Figure 2).

Uniqsis: FlowSyn

Syrris: Asia series

Chemtrix: Labtrix

Vapourtec: R-Series

ThalesNano: H-Cube

YMC: KeyChem-Integral

Figure 2: Selected examples of commercially available flow reactors

Several different flow arrangements exist that can be adopted depending on one's synthetic needs. The simplest setup comprised of a linear series of reactors which allows for multi-step synthesis of material can be produced by aligning reactors in series (Scheme 19a). In instances where the synthesis of a library of compounds is required, the use of divergent or convergent setups can be more applicable (Scheme 19b and c). Finally, a recirculating setup can be used if the reaction transformation requires a longer reaction time that cannot be achieved by simple modification of flow rates or increasing the rector module size (Scheme 19d).[41]

© University of Pretoria

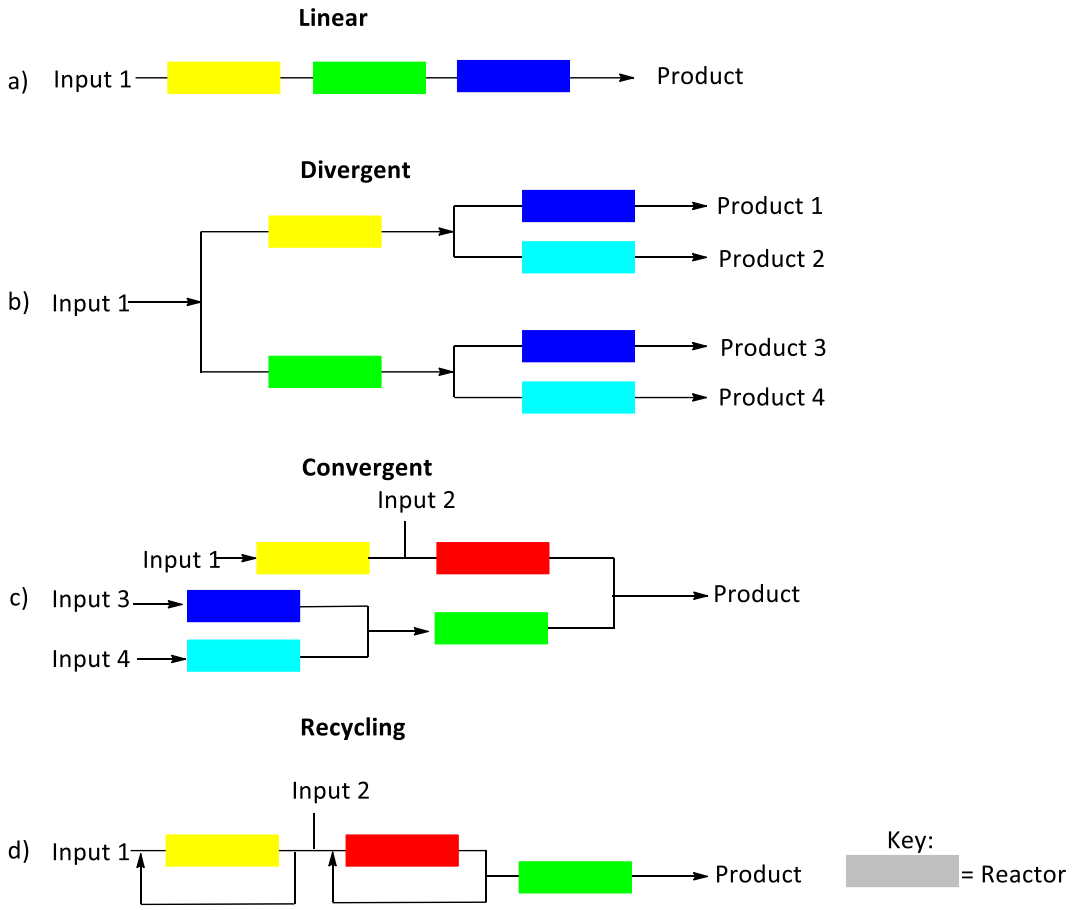

Scheme 19: Types of continuous flow setups[41]

1.5. Application of solid-supported reagents in flow

Flow technology lends itself to the use of solid-supported reagents and scavengers which can readily be incorporated into columns and packed-bed reactors, therefore eliminating the need for filtration.[30,41] The large surface area of the packed material allows for improvements in efficiency and as the reagents continuously flow through the reactor the residence times and subsequently the contact time the reagents have can be precisely controlled, a situation which cannot be mimicked in a standard batch reactor. Applying the linear setup of reactors described above (Scheme 19a, two reagent streams, A and B) various combinations can be developed, three examples of packed-bed arrangements are highlighted here (Scheme 20). Type 1 has the reagents pumped into the system, mixed together at a T-piece connector followed by reaction in a mixing chip, to allow for adequate contact time, and flowing through a packed column with solid-supported reagent to yield product C (Scheme 20a). Type 2 has the reagents first reacting in a coil reactor before passing through a packed column with solid-supported catalyst followed by a solid-supported scavenger reagent which reacts with

© University of Pretoria

impurities such as unreacted started material or by-products leaving the product to flow out clean (Scheme 20b). Type 3 has a similar setup as type 2, with the use of a "catch and release" scavenger which reacts with the product and traps it allowing the impurities to flow out into waste collection. When all the impurities have been removed, an introduction of a third reagent C then reacts with the "caught" product causing it to be released cleanly (Scheme 20c). The caution of using "catch and release" scavengers is determining the right reagent to selectively remove impurities leaving the product untouched and vice-versa.

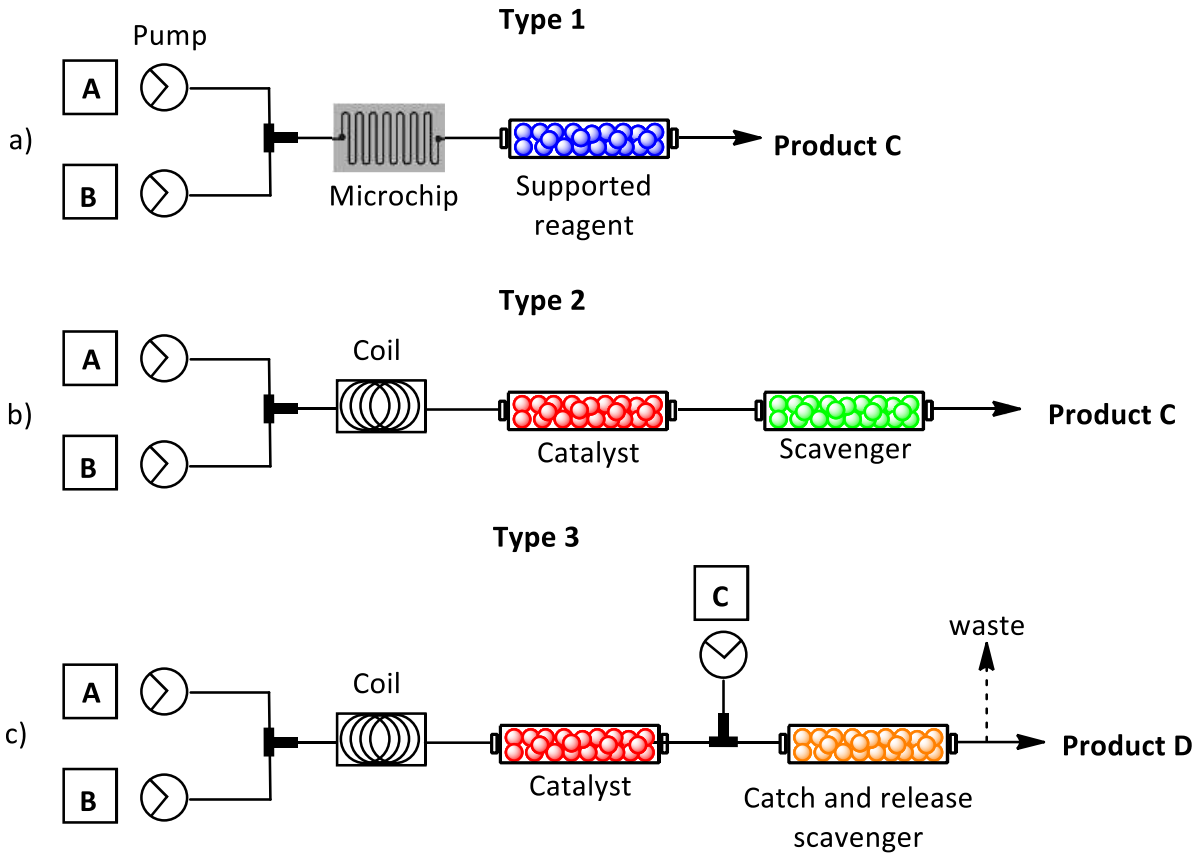

Scheme 20: Schematic example showing the different types of flow setups with packed beds

There are numerous examples of the use of supported reagents in flow chemistry. An overview highlighting selected processes using solid supported reagents are described in the following sections, for a more comprehensive analysis the reader is directed to the reviews by Ley, and Baxendale and co-workers.[42,43]

In 2006, ley and co-workers developed a method for regioselectively synthesizing oxazoles which are substituted at the 4 and 5 positions (Scheme 21).[44] Isocyanides containing electron

© University of Pretoria

withdrawing groups were used and as such isocyanoacetates **73** were coupled with various acyl chlorides **72** in a mixing chip to form intermediate **74** which was then immediately passed through a column packed with a polymer-supported base, 2-*tert*-butylimino-2-diethylamino-1,3-dimethyl- perhydro-1,3,2-diazaphosphorine (PS-BEMP). This then facilitated an intramolecular cyclisation thereafter, passage through a column housing a nucleophilic scavenger quadrapure benzylamine (QP-BZA) removed impurities and facilitated the desired oxazoles **75** in >80 % yields with a 30 minute residence time.

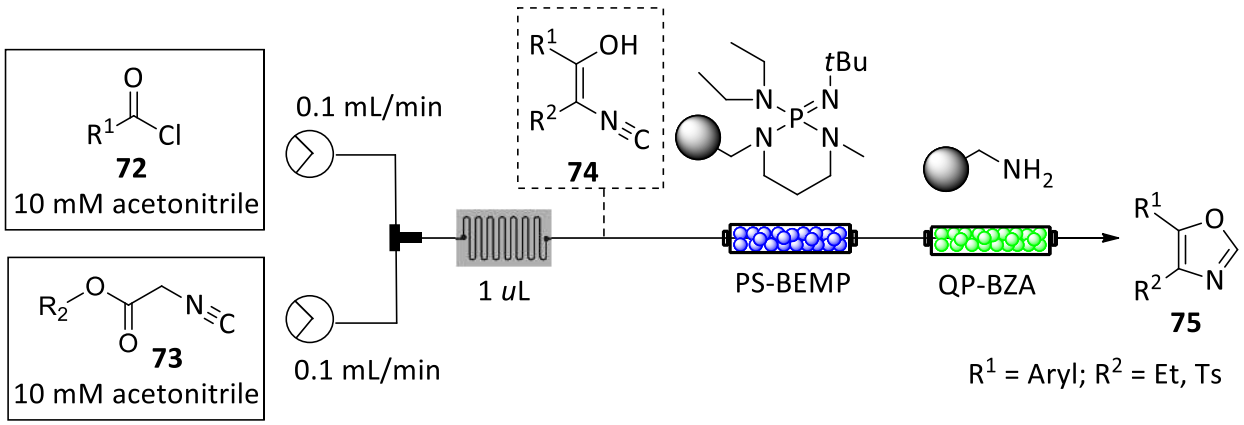

Scheme 21: Flow synthesis of oxazoles[44]

In the same year the group reported the synthesis of a cytotoxic alkaloid natural product oxomaritidine, **85**, (Scheme 22).[45] In the first step 4-(2-bromoethyl)phenol **76** is converted to the corresponding azide **78** by passage through polymer-supported azide (PS-NMe_3N_3). Simultaneously, the oxidation of 3,4-dimethoxybenzyl alcohol **77** to aldehyde **79** was facilitated by passage through polymer-supported tetra-*N*-alkylammonium perruthenate (PS-NMe_3RuO_4). The intermediates were then passed through a polymer-supported phosphine to facilitate an Aza-Wittig reaction to form imine intermediate **80**. Hydrogenation was then conducted by passing the reagent through an H-cube hydrogenation reactor fitted with a column packed with palladium on carbon (Pd/C) to form intermediate **81**, followed by trifluoroacetylation of the amine using **82** to afford amide intermediate **83**. Thereafter, oxidative phenolic coupling was enabled by a polymer-supported [bis-(trifluoroacetoxy)-iodo]benzene (PS-PIFA) to generate tricyclic intermediate **84**. The stream was then passed through polymer-supported base (PS-NMe_3OH) prompting the cleavage of the amide bond and 1,4-conjugate addition to form the product **85** in 50% overall yield.

© University of Pretoria

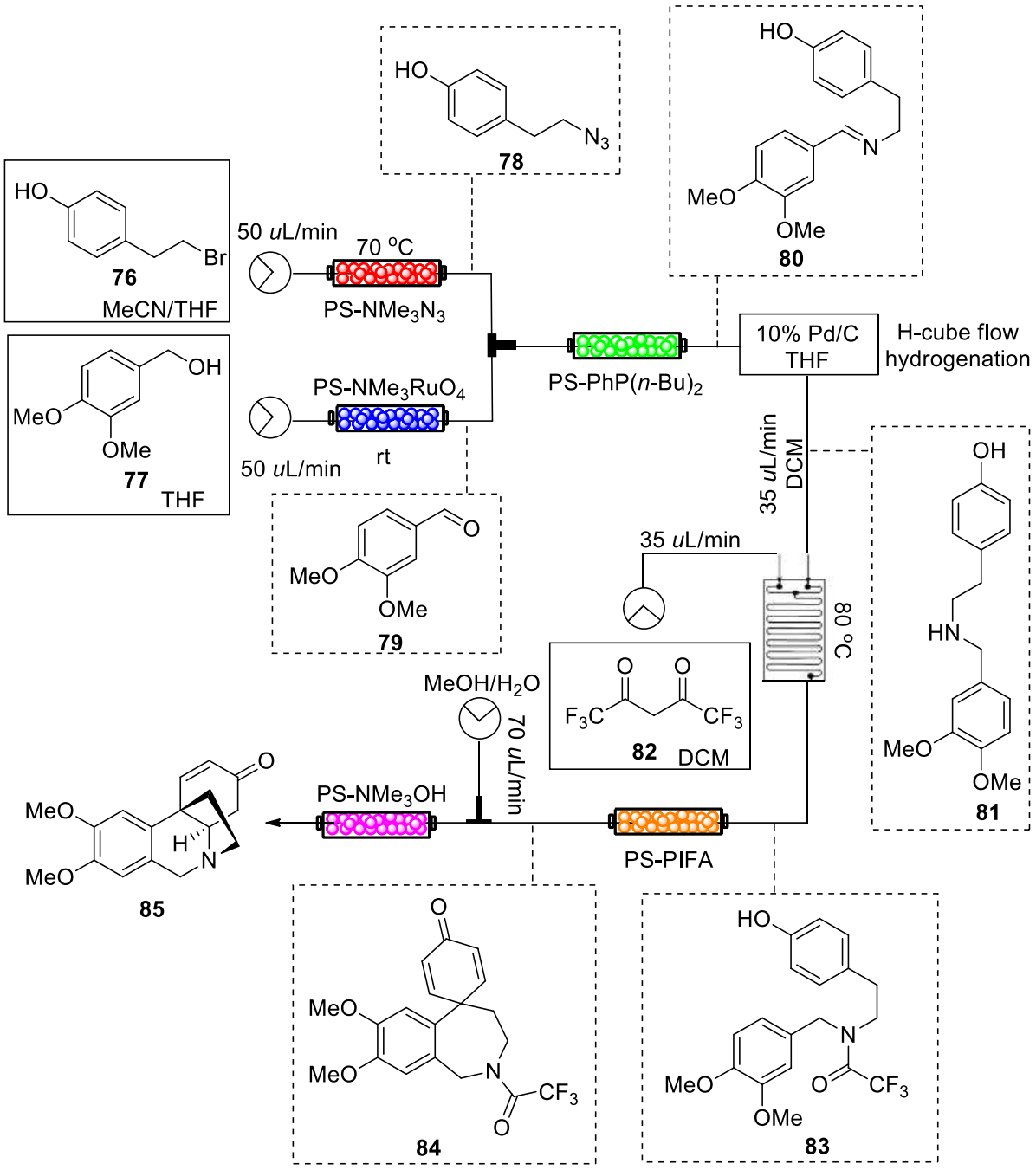

Scheme 22: Flow synthesis of oxomaritidine[45]

Baxendale and co-workers reported the synthesis of diazoketones **88** from aliphatic and aromatic acyl chlorides in 2010 (Scheme 23).[46] The reaction proceeded by mixing an acyl chloride **86** and a diazo compound **87** in a T-piece mixer followed by incubation in a 10 mL coil reactor. Trimethylsilyldiazomethane **87** was used instead of diazomethane due to its stability and because it did not form diazonium salts. The reagent stream was initially passed through a polymer-supported amine base but this resulted in unreacted acyl chloride and trimethylsilyl-protected diazoketone side products. The authors swapped to a polymer-

© University of Pretoria

supported tetraalkylammonium fluoride salt which reacted with the trimethylsilyl thus deprotecting any trimethylsilyl-protected diazoketone and gave conversion to the desired products **88**, in isolated yields of 78-98% for alkyl and 46-83% for aryl systems.

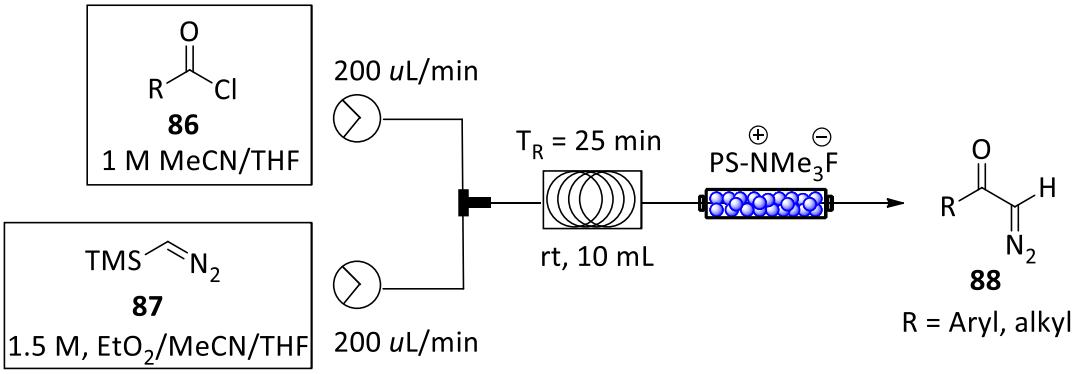

Scheme 23: Flow synthesis of diazoketones[46]

In 2010, Ley, Baxendale and Hopkin reported the synthesis of an active pharmaceutical ingredient (API), Imatinib **95**, which is used for the treatment of chronic myeloid leukaemia and gastrointestinal stromal tumours (Scheme 24).[47] The synthesis began with an amide coupling between acid chloride **89** and aniline **90** facilitated by passage through a polymer-supported base (PS-DMAP) and polymer-supported dimethylamine (PS-NMe_2), which acted as an acid scavenger to form **91**. Intermediate **91** was collected in a fraction collector housing *N*-methylpiperazine **92** where S_N2 reaction occurred allowing the displacement of the chloride, thereafter passage through a column packed with calcium carbonate. This was followed by passage through polymer-supported isocyanate (PS-NCO) to scavenge any unreacted *N*-methylpiperazine resulting in intermediate **93** which was sequentially passed through silica-supported sulfonic acid (SS-SO_3H) which acted as a "catch and release" scavenger of **93** allowing any unreacted **91** to pass through to waste. A stream of 1,8-Diazabicyclo[5.4.0]undec-7-ene (DBU) was then passed through the column to release intermediate **93**. The final step was a Buchwald-Hartwig coupling reaction between intermediate **93** and **94** in the presence of a palladium catalyst which reacted in coil at 150 °C for thirty minutes. The resulting crude mixture was washed with water before being purified with in-line chromatography, as chemical differentiation between the species was not possible using scavengers, giving Imatinib **95** in 69% overall yield.

© University of Pretoria

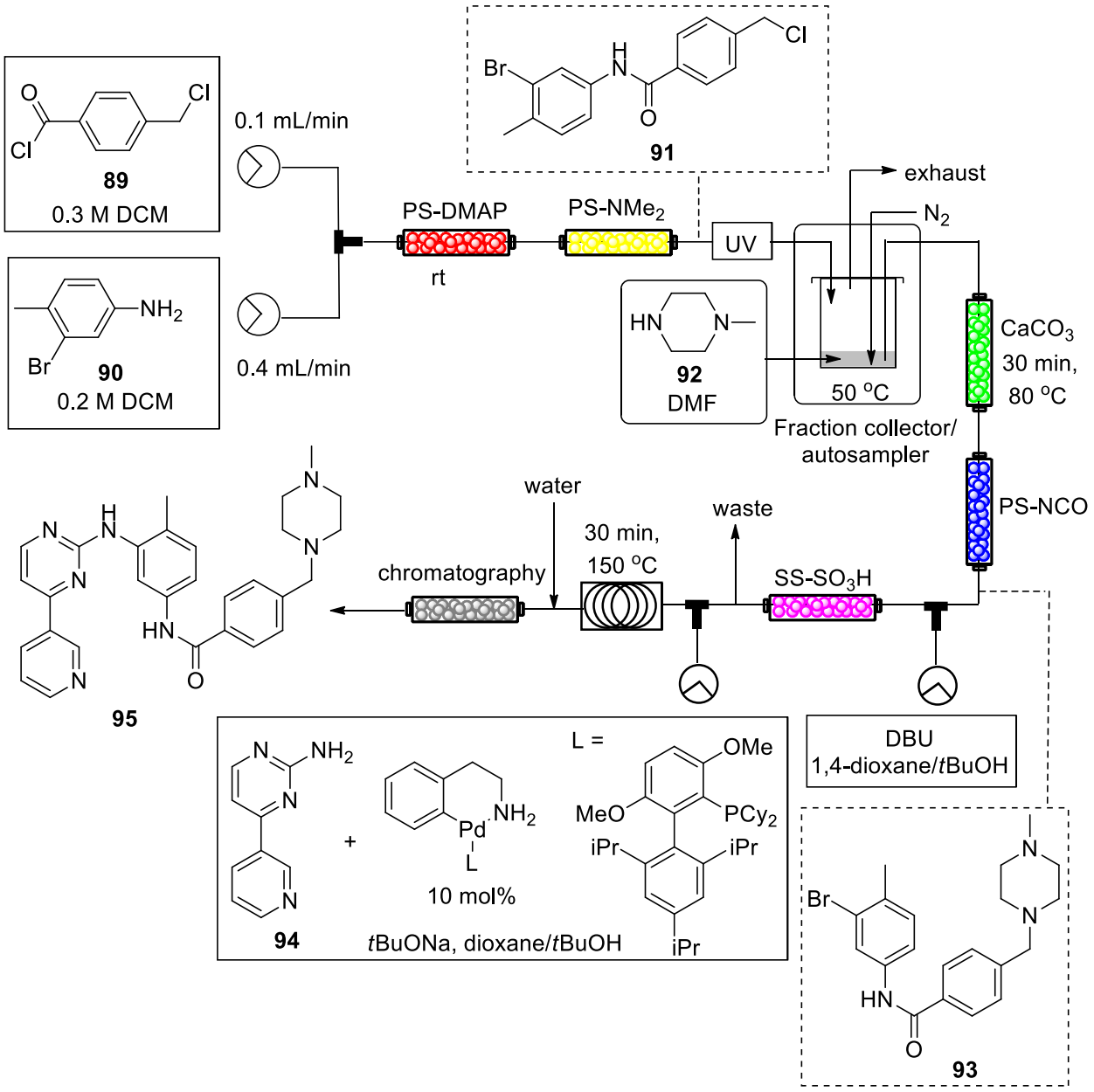

Scheme 24: Flow synthesis of Imatinib[47]

In 2012, Baxendale described the synthesis of 7-hydroxycoumarin-8-carbaldehyde **104** (Scheme 25).[48] The synthesis was initiated by reacting ethyl acetoacetate **96** with phenol **97** via a Pechmann condensation reaction to form intermediate **98**, which was immediately subjected to the Mannich reaction with pyrrolidine **99** and formaldehyde **100**, resulting in intermediate **101**. Addition of peracetic acid **102** caused *N*-oxidation of the pyrrolidine to produce intermediate **103** and passage through quadropure dimethylamine (QP-DMA) removed the excess acid. The final step was achieved by the Polonovski rearrangement which is an elimination reaction using trifluoroacetic anhydride **82** which formed an iminium species

© University of Pretoria

and hydrolysis to the aldehyde which was achieved in the presence of aqueous hydrochloric acid resulting a 59% yield of the desired product **104**.

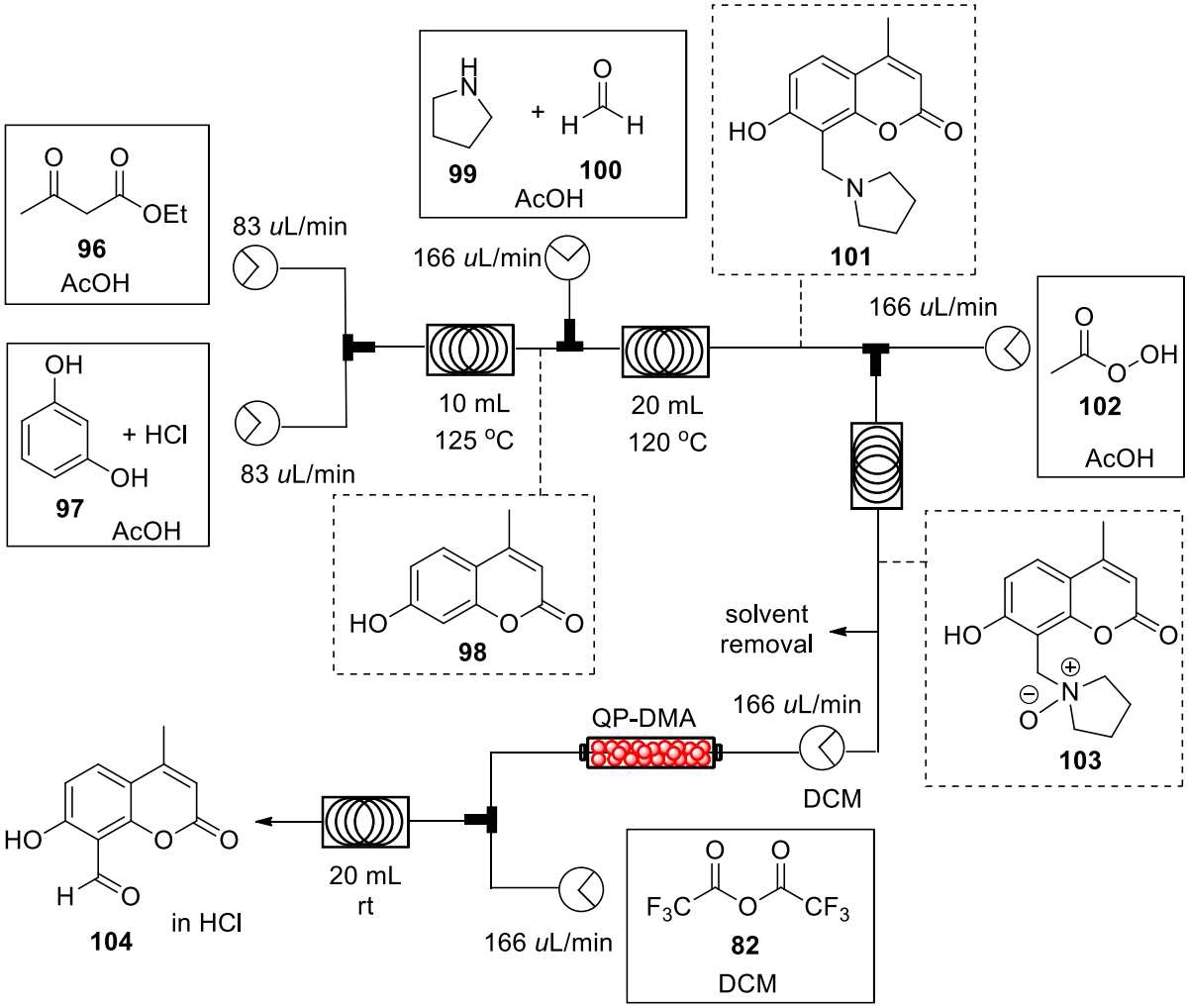

Scheme 25: Flow synthesis of 7-hydroxycoumarin-8-carbaldehyde[48]

In 2013, Ley and co-workers reported the synthesis of a key intermediate oxazole carboxylic acid **108** of *O*-methylsiphonazole (Scheme 26).[49] The synthesis commenced with the formation of an amide from the reaction between dimethoxycinnamic acid **105** and threonine *tert*-butyl ester hydrochloride **106**, which was then converted into intermediate **107** using diethylaminosulfur trifluoride (DAST) and a series of columns packed with solid-supported reagents set-up to scavenge and quench excess reagents. Firstly polymer-supported sulfonic acid (PS-SO_3H) was used to scavenge unreacted triethylamine, imidazole and residual threonine *tert*-butyl ester, then polymer-supported dimethylamine (PS-NMe_2) to scavenge unreacted hydrochloric acid, followed by calcium carbonate and finally a column filled with silica to quench and trap DAST and hydrogen fluoride affording the oxazoline **107** in 90% yield.

© University of Pretoria

This oxazoline intermediate **107** was then subjected to oxidation using bromotrichloromethane and cleavage of the *tert*-butyl ester was enabled by polymer-supported sulfonic acid and purification using a silica column. This resulted in isolation of the pure product **108** in overall yield of 90%.

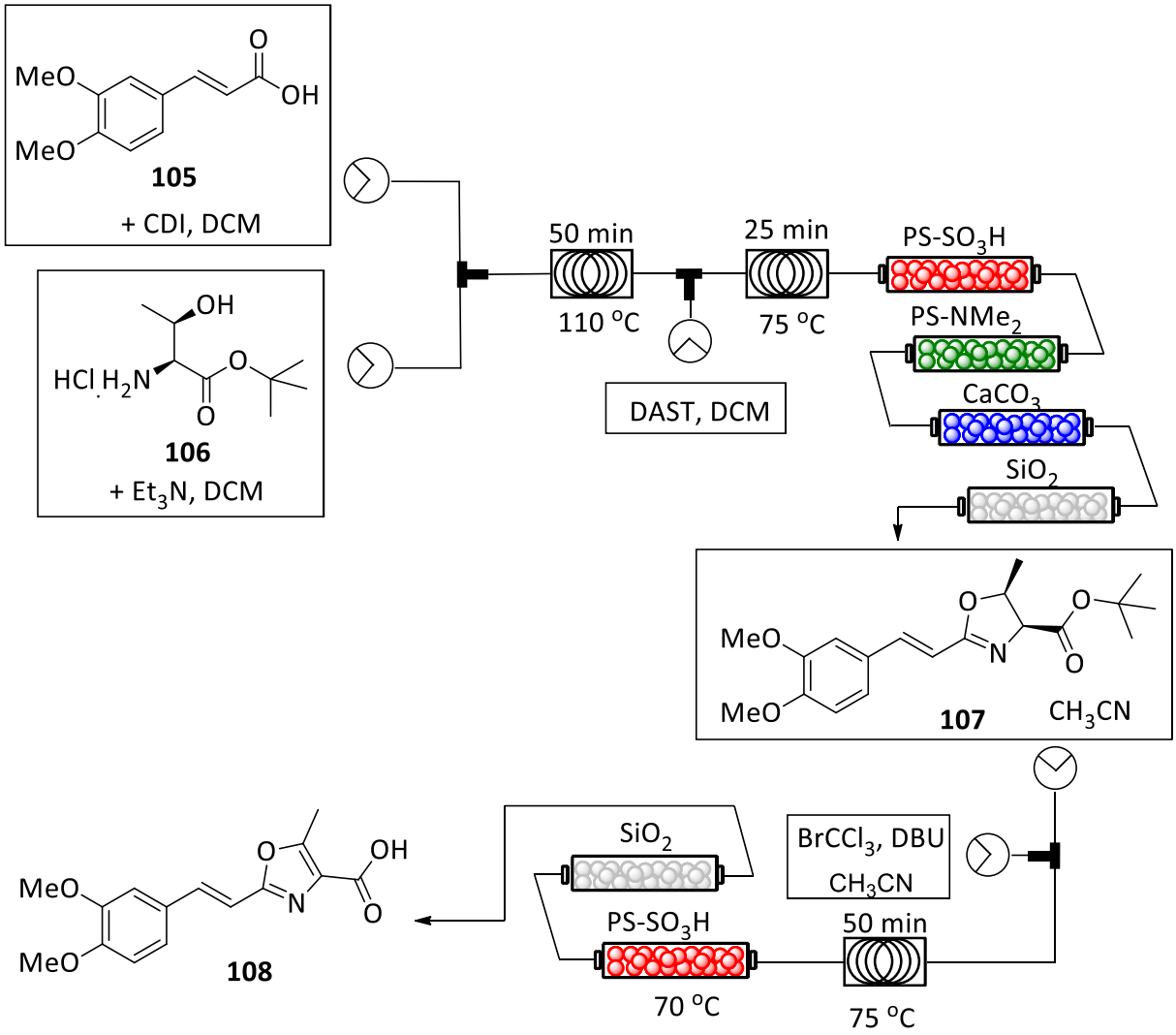

Scheme 26: Flow synthesis of a key intermediate of *O*-methylsiphonazole[49]

Recently, Palmieri and co-workers published the synthesis of thiophene-2-carboxylates **113** from β-nitroacrylates (Scheme 27).[50] The synthesis began with the formation of intermediate **111** via Michael addition of nitroacylate **109** and thioacetic acid **110** at 100 °C in a coil reactor. This was followed by the elimination of nitrous acid by passage through basic PS-carbonate to form intermediate **112**. The stream was then passed through acidic Amberlyst-15 facilitating the cleavage of the dioxolane ring and thioacetate ester, resulting in an

© University of Pretoria

intramolecular cyclisation via the Paal-Knorr thiophene synthesis to form the thiophene products **113** which were isolated after chromatography in low to good yields (38-88%).

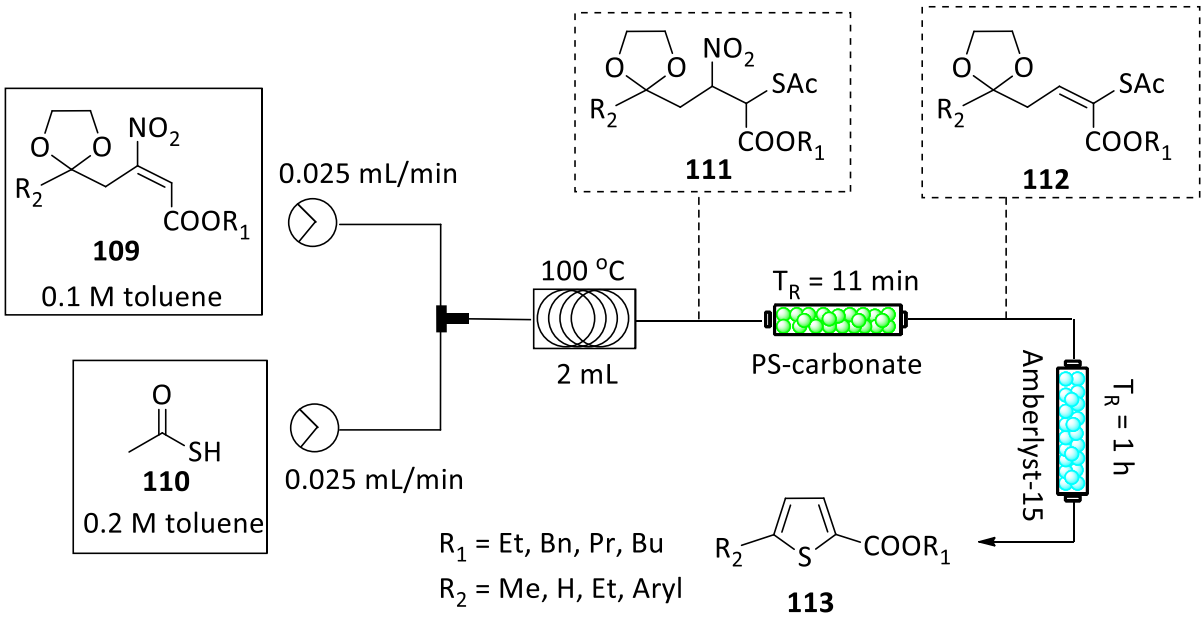

Scheme 27: Flow-synthesis of thiophene-2-carboxylates[50]

1.6. Application of solid-supported catalysts in flow

Catalysis plays a major role in many chemical transformations for the production of key intermediates and a plethora of catalysts have been made to overcome the challenges of metal leaching and high cost by immobilizing them onto solid supports. The advantages of incorporating solid-supported catalysts with flow chemistry include low reagent and catalyst consumption, less waste and increased efficiency, less manual handling as excess of the catalyst can be packed in a column to run multiple reactions, and in some cases repeated use of packed catalysts in multiple reactions. In addition, in a flow reactor, harsher conditions can be considered due to high pressure and faster heat transfer. Of key importance, mechanical stirring or agitation is eliminated in a flow reactor which evades the mechanical degradation of the solid-support material and shortened lifetimes of the catalysts.[51] Particularly, challenges arise when considering asymmetric catalysis, as development of an immobilization approach that maintains both good stereoselectivity and catalyst activity is not easy. At times it is possible to simply react existing homogeneous catalysts with solid support scaffold rather than synthesizing from monomers.[52]

© University of Pretoria

Described here is an overview highlighting selected examples using solid supported catalysts in continuous flow, for a more comprehensive review the reader is directed to the article by Verboom and co-workers.[53]

Darvas and co-workers demonstrated the incorporation of carbon monoxide gas using a X-cube reactor to facilitate aminocarbonylation reactions between *p*-iodobenzoic acid **114** and amine **99** using pre-packed cartilages with an immobilised palladium(0) or palladium(II) catalyst (PS-Pdcat.) from ThalesNano.[54] The monoamides **115** were collected in 30-81% yield in just two minutes with no by-products observed, with an example of iodobenzoic acid and pyrrolidine shown schematically (Scheme 28).

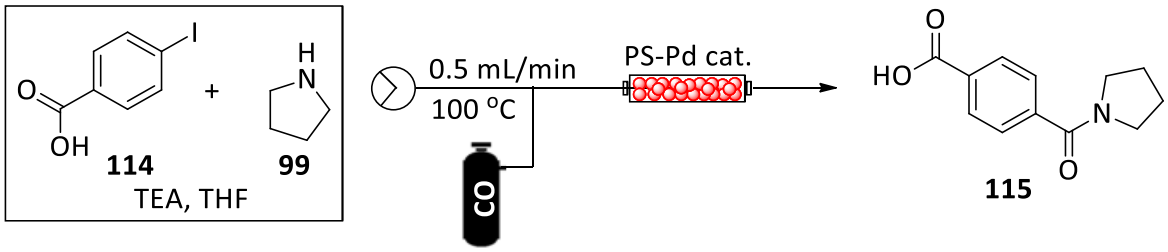

Scheme 28: Flow synthesis of monoamides[54]

Baxendale and co-workers converted diazoketones **88** into quinoxalines **117** using a supported copper(II) triflate catalyst (Scheme 29).[46] These compounds have exhibited therapeutic properties such as kinase inhibition, anti-tumor, anti-viral and anti-inflammatory activity. The diazoketone **88** was reacted with diamine **116** and passed through a column housing a plug of supported copper(II) triflate catalyst (PS-Cu cat.), followed by a plug of immobilised thiourea (QP-TU) to capture any dissolved metal salts. The stream was then passed through polymer-bound tosylchloride (PS-TsCl) to remove any unreacted diamine and reduced quinoxaline derivatives. Finally, the reaction stream was passed through a column filled with polymer-supported-tosylhydrazine (PS-TsNHNH$_2$) to scavenge unreacted diazoketone, giving the desired products in 40-95% yield without the need for further purification.

© University of Pretoria

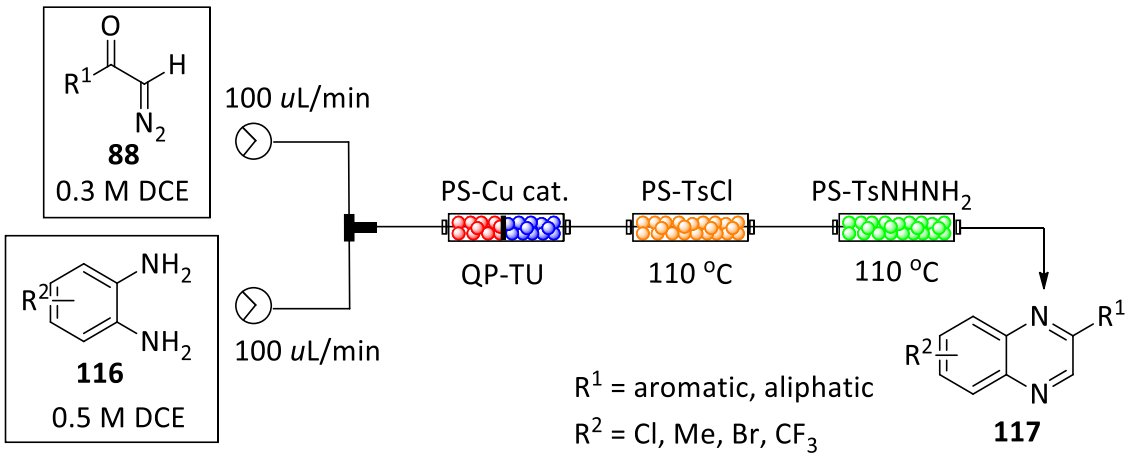

Scheme 29: Flow synthesis of quinoxalines[46]

In 2014 Pericàs and co-workers demonstrated a three component intermolecular *anti*-diastereoselective Mannich reaction using an immobilised organocatalyst **121** derived from threonine (Scheme 30).[55] Although, proline catalyses reactions of hydroxyacetone to form *syn* adducts, the use of primary amino acids affords the *anti* adducts, through formation of the (*Z*)-enamine intermediate which results from a hydrogen bonding interaction between the NH group and the oxygen atom of the hydroxy group of the enamine. Since amino acid organocatalysts and Mannich adducts are highly polar, immobilizing the catalyst eliminates the tedious process of purification. Hydroxyacetone **118**, aniline **119** and an aldehyde **120** were passed through the catalyst with in-line IR monitoring to determine the optimal flow rate for complete conversion, giving *anti*-β-amino-α-hydroxycarbonyl compounds **122** in 69-94% yield with moderate to good diastereoselectivities (up to 8:92 *syn:anti*) and enantioselectivities (80-96% ee). A recycling study showed that after three runs the activity and selectivity of the catalyst decreased.

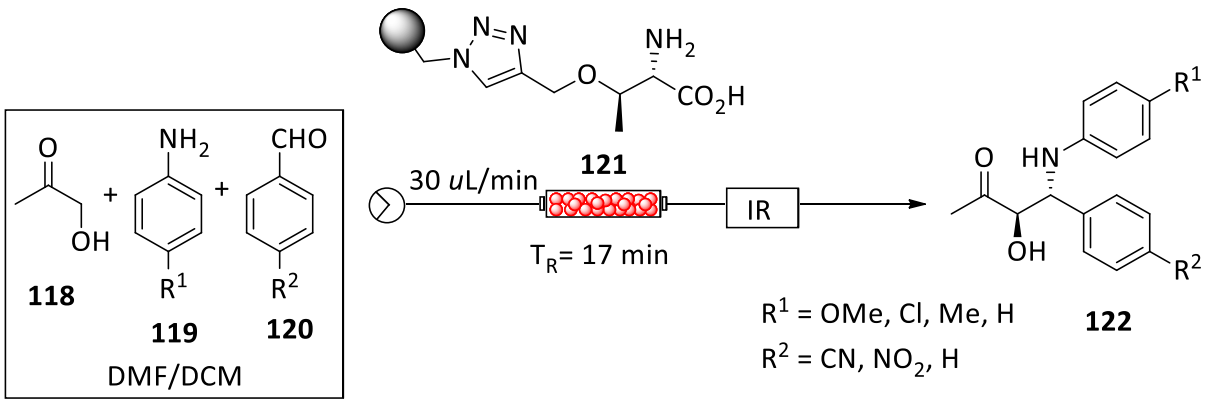

Scheme 30: Flow enantioselective *anti*-Mannich synthesis[55]

© University of Pretoria

The dehydrogenation of cyclohexanol **123** using a copper catalyst immobilised via incipient wetness impregnation onto silica using copper(II) nitrate trihydrate was demonstrated by Iwanek, Ulkowska and Glinski in 2016 (Scheme 31).[56] Interestingly, the liquid cyclohexanol **123** was converted into a gas which was then passed through the supported catalyst to form cyclohexanone **124**, thereafter the product was condensed into a liquid phase and collected in 82% yield, with analysis of products done by gas chromatography (GC). The high temperatures were chosen based on the boiling points of the reagents.

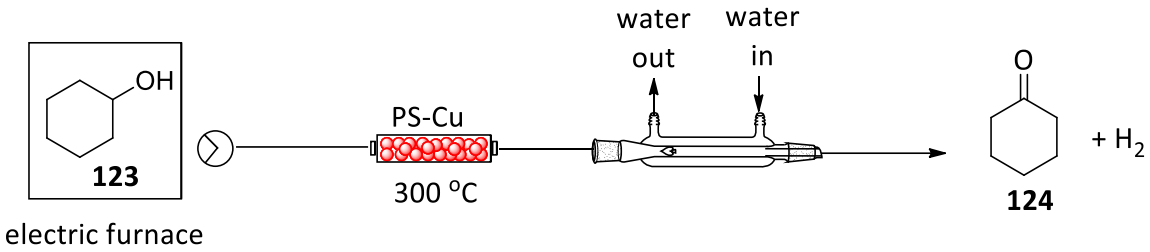

Scheme 31: Flow dehydrogenation of cyclohexanol[56]

In the same year Pericàs and co-workers showed the enantioselective cyclopropanation reaction using a chiral immobilised catalyst **128** synthesized from grafting hydroxyproline derivative onto polystyrene through benzyl linkers.[57] The dual reactivity of bromomalonates as an electrophile and a nucleophile, via the iminium ion-enamine intermediate, results in a Michael reaction which produces enantioenriched cyclopropanes. However, the presence of the *gem*-diester moiety on the cyclopropane generates a base- mediated ring opening progression.[58] The group sought to eliminate this process by minimizing the contact between the base and product. The synthesis involved a reaction between *α,β*-unsaturated aldehydes **125** and bromomalonate **126** with a base, *N*-methylimidazole **127** (Scheme 32). Passage through a column packed with the catalyst **128**, followed by addition of ammonium chloride and reaction in a coil reactor prior to downstream phase separation to remove excess base afforded the products **129** in low to moderate yields of 26-71%, with 91-96% enantiomeric excess and greater than 95:5 diastereoselectivity.

© University of Pretoria

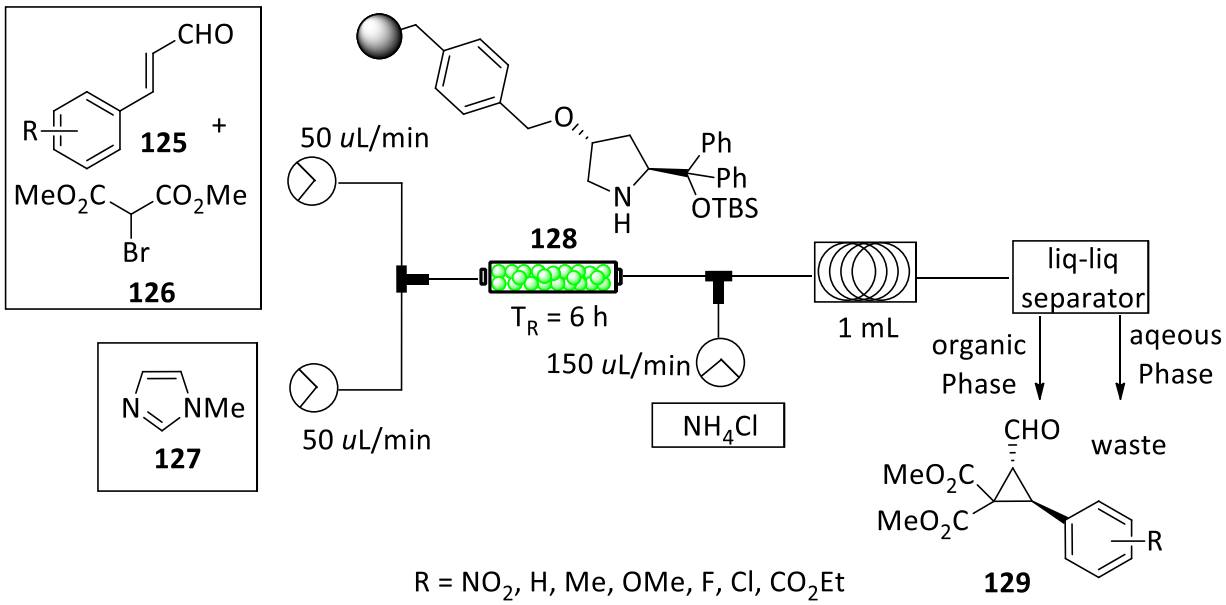

Scheme 32: Flow cyclopropanation reaction[57]

The use of solid-supported reagents to perform various chemical transformations in flow synthesis has been described. The advantages of having packed columns in series has also shown to be the solution for in line purification of by-products or unreacted starting materials. There also exists a sub-class of solid-supported reagents, monoliths, which have added advantages of having an internal structure consisting of a combination of large macropores for flow through passage together with a network of smaller mesopores to allow diffusion towards the active sites.[59]

1.7. Monolith-supported reagents

The evolution of monoliths and monolith-supported reagents began in the late 1960's when Kubìn and co-workers were investigating the preparation of alternative solid supports, which at the time were based on beaded polymers and inorganic oxides. They developed methacrylate-based hydrogel-type materials with low degrees of cross-linking that were compressible, allowing for low flow rates. A breakthrough began when these materials were used for the separation of small analytes in HPLC by means of open-pore poly(urethane)-based materials.[60,61] The road to monoliths continued when challenges were encountered using bead packed columns which had large void volumes and as a result a significant portion of the column volume was not used for separation. When a mobile phase was pumped through the column, the liquid flowed through the interstitial voids between the particles, which afforded the smallest resistance to its flow, leaving the liquid in the pores stationery.

© University of Pretoria

As a result, if a sample was injected into the stream, the compounds were also carried through the voids and only flowed through the pores by diffusion. The process worked well for small organics, however, the transfer of proteins, nucleic acids and synthetic polymers was significantly slower. The obvious solution for the poor mass transfer was to reduce the size of the porous particles which subsequently would reduce the diffusion lengths, however, the interstitial spaces diminished as well, decreasing the permeability and increasing the back pressure in the column. This then led to the introduction of slightly cross-linked, gel-type co-polymers that required swelling to become porous, thereby allowing all the sites to be accessible. Nevertheless, this limited the choice of solvents and the swollen polymer proved challenging to handle and tended to break down with rapid change of solvent strength. Thus, the idea of monolithic columns arose wherein the pores could be independently optimized, simultaneously allowing the permeability and mass transfer to be maximized (Figure 3).[62,59]

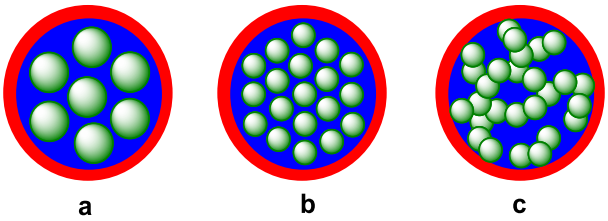

Figure 3: Evolution of columns: (a) highly permeable and less-efficient packed column, (b) less-permeable and highly efficient packed column, (c) highly permeable and highly efficient monolithic column[59]

Monoliths, initially termed “continuous rods” by Svec and Fréchet in the early 1990’s, are therefore, a single continuous piece of uniformly porous material prepared by precipitation polymerisation in a column. Initially they were to be used for chromatography, acting as an alternative to the standard columns packed with particles.[61] Monolithic columns have been prepared from either organic or inorganic material such as silica. Silica-based monoliths are prepared using a sol-gel process of hydrolysis and polycondensation of tetramethoxysilane in the presence of polyethylene oxide which is used as a soft template. During the polycondensation step, phase separation occurs, and the post-synthesis heat treatment affords silica monolithic materials with well-defined macro- and meso-pores.[63] There are several different approaches to prepare monoliths: thermally, UV or electron-beam triggered free radical polymerization, reversible addition-fragmentation chain transfer (RAFT)

© University of Pretoria

polymerization, ROMP, controlled tetramethylpiperidinyloxyl (TEMPO)-mediated radical polymerization, polyaddition and polycondensation. Selected examples of monolith preparation using thermally triggered free radical polymerization and RAFT polymerization will be discussed here as these are widely applied in flow chemistry.

1.7.1. Thermally triggered free radical polymerization

These monoliths are synthesized by co-polymerizing a functionalized monomer and cross-linker in the presence of a porogenic solvent (to create pores) and radical initiator. The reagents are first heated until homogeneous, followed by transfer into a column (glass or stainless steel), heated until polymerized and finally washed to remove the porogen and expose the interconnected pores (Scheme 33).

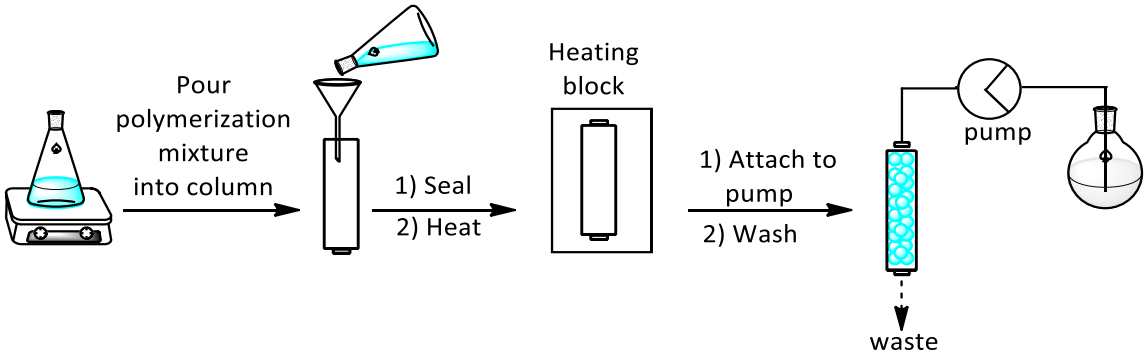

Scheme 33: Schematic preparation of monolith by thermally triggered free radical polymerization

Under these conditions, the synthesis of an effective monolith is governed by the following parameters: (i) polymerization temperature, where the higher the temperature, the faster the rate of polymerization; (ii) mole fraction of the initiator, where more or less of the initiator will determine the rigidity of the monolith; (iii) chemical nature of the monomer and cross-linker; as well as (iv) the polarity of the porogen, where the choice of solvent is dependent on the polarity of the monomer and cross-linker. Ideally a good solvent acts as a macroporogen and is easily removed after polymerization. The addition of another monomer helps control the porous structure.[64,65]

Svec and Fréchet developed monolith **132** from a mixture of glycidyl methacrylate **130** and ethylene dimethacrylate **131** monomers, dodecanol and cyclohexanol as porogens and polymerization with 2,2'-azobis(isobutyronitrile) (AIBN) radical initiator, followed by a methanol wash. The epoxide end groups were then functionalized by filling the column with

© University of Pretoria

sulfuric acid and heating it to form a hydrolysed monolith **133** or by filling the column with diethylamine to form an aminated monolith **134** (Scheme 34).[61]

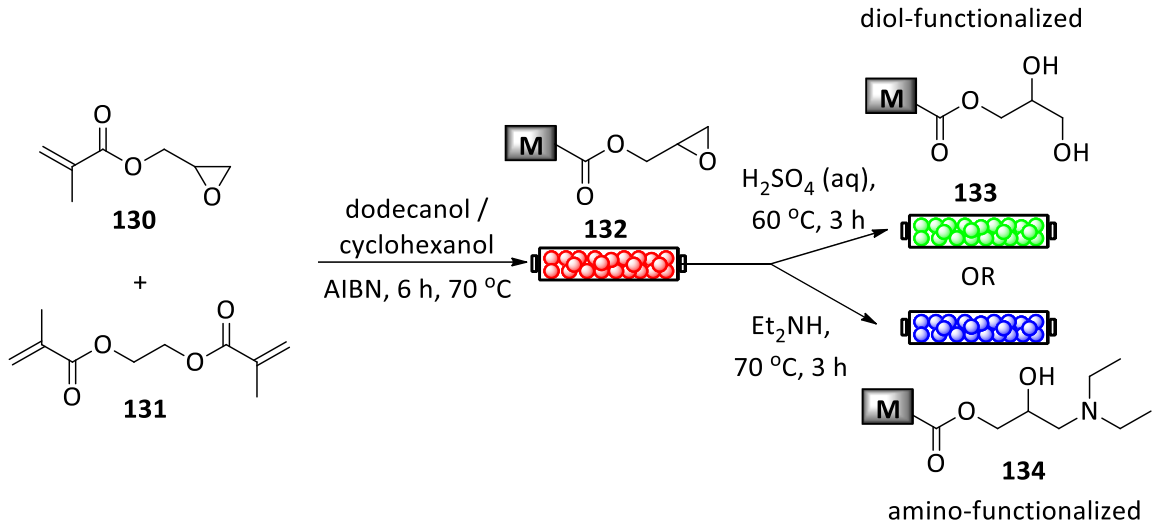

Scheme 34: Synthesis of epoxide monolith **132**[61]

Ley and co-workers converted *N*-(*tert*-butyl)phenylsulfinimidoyl chloride, which was initially reported by Mukaiyama in early 2000 for conducting oxidation reactions, into a monolithic support. Monomeric *S*-4-vinylphenyl ethanethioate, synthesized from *p*-bromostyrene **135**, was polymerised using 1,4-divinylbenzene (DVB) as cross-linker, dodecanol and AIBN to yield a thioacetate monolith **136** (Scheme 35).[66]

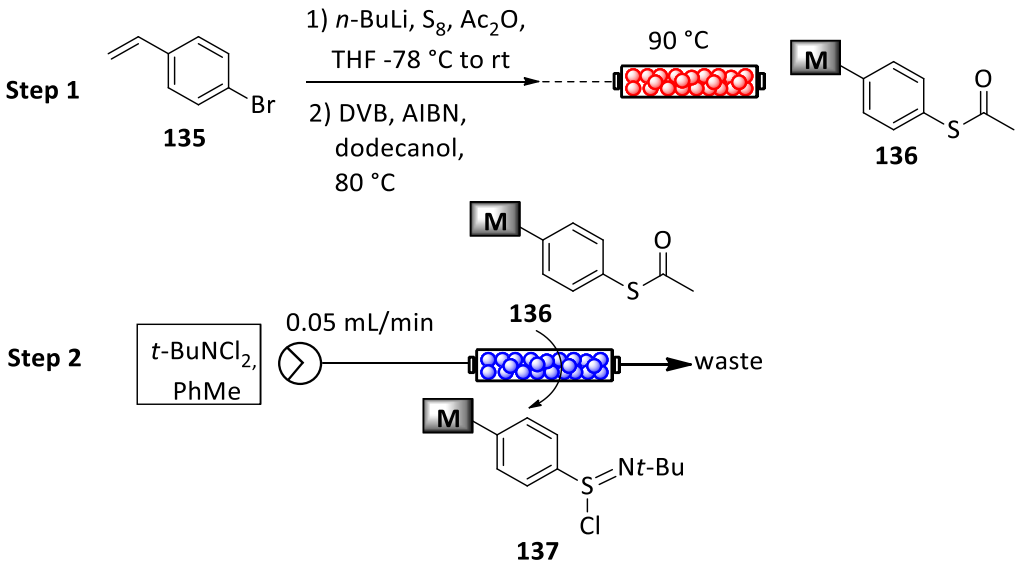

Scheme 35: Synthesis of *N*-(*tert*-butyl)phenylsulfinimidoyl chloride monolith[66]

© University of Pretoria

This was then functionalized with *N*-*tert*-butyl-*N*,*N*-dichloroamine, which was observed with a colour change from off-white to bright yellow forming the desired monolith reagent **137** (Figure 4). Oxidation of alcohols **138** in the presence of diisopropylethylamine (DIPEA) gave ketones and aldehyde products **140** in low to excellent conversions of 34-95% (Scheme 36), with an observed colour change from bright yellow to light brown indicating a reduction to the *N*-*tert*-butylphenylsulfenamide monolith **139** (Figure 4).

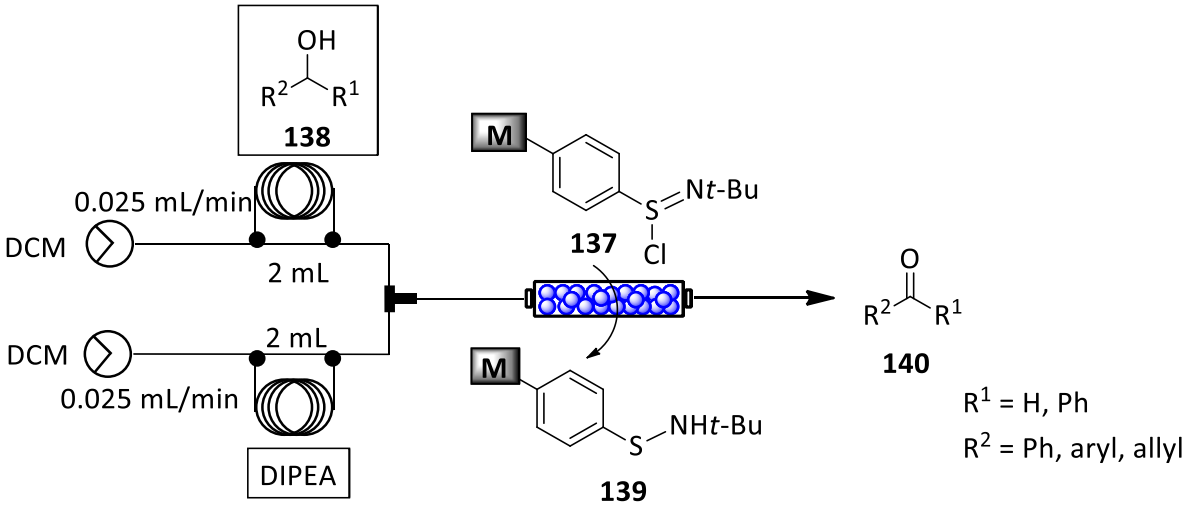

Scheme 36: Oxidation using *N*-(*tert*-butyl)phenylsulfinimidoyl chloride monolith[66]

Figure 4: Colour changes from left to right: thioacetate monolith **136** (white); *N*-(*tert*butyl)-phenylsulfinimidoyl chloride monolith **137** (bright yellow); *N*-(*tert*butyl)phenylsulfenamide reduced monolith **139** (light brown)[66]

Triphenylphosphine is a commonly used reagent with a wide range of applications, however, the reagent notoriously causes purification difficulties, usually requiring expensive and time-consuming column chromatography to remove triphenylphosphine oxide by-product from the final product. Monolith-supported triphenylphosphine **146** has been prepared thermally

© University of Pretoria

using diphenyl(4-vinylphenyl)phosphine **141**, divinylbenzene **142**, styrene **143**, dodecanol **144** with variation of the radical initiator which could be dibenzoyl peroxide **145**, AIBN or azobis-(4-cyanovaleric acid) (Scheme 37).[67] Dibenzoyl peroxide has a slower initiation rate compared to azo-based initiators, which ensures the entire polymerization mixture is at the target temperature before precipitation of polymer chains occurs, thus forming a more homogeneous polymerization.[68]

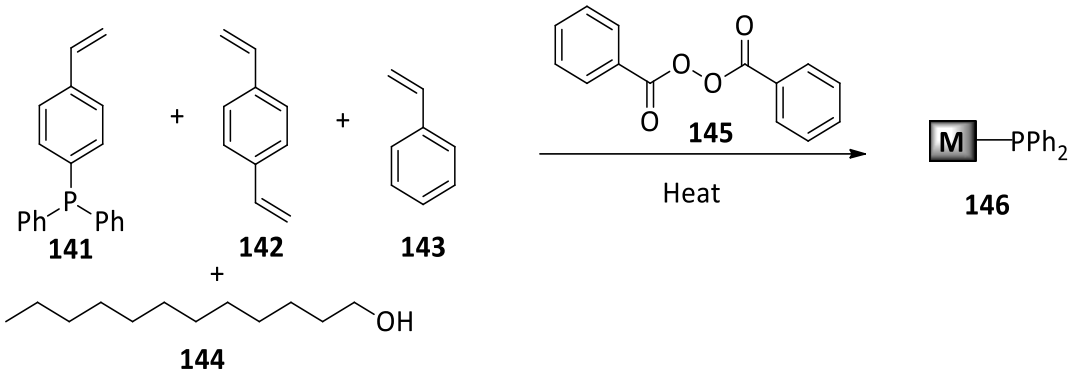

Scheme 37: Synthesis of monolith-supported triphenylphosphine[67]

In 2011, the Ley research group developed a number of monolithic-triphenylphosphine reagents, the first being applied to the Staudinger aza-Wittig reaction for the synthesis of alkyl and aryl azides in flow (Scheme 38).[67] The monolithic triphenylphosphine **146** was first loaded with an azide reagent **147** via the Staudinger reaction, followed by washing with a solvent to remove any impurities and any unreacted reagent to yield an iminophosphorane monolith **148**. Thereafter, aza-Wittig reactions were carried out by passing a solution of aldehyde or ketone through the monolith to form products **149** in moderate to high yields (62-98%).

© University of Pretoria

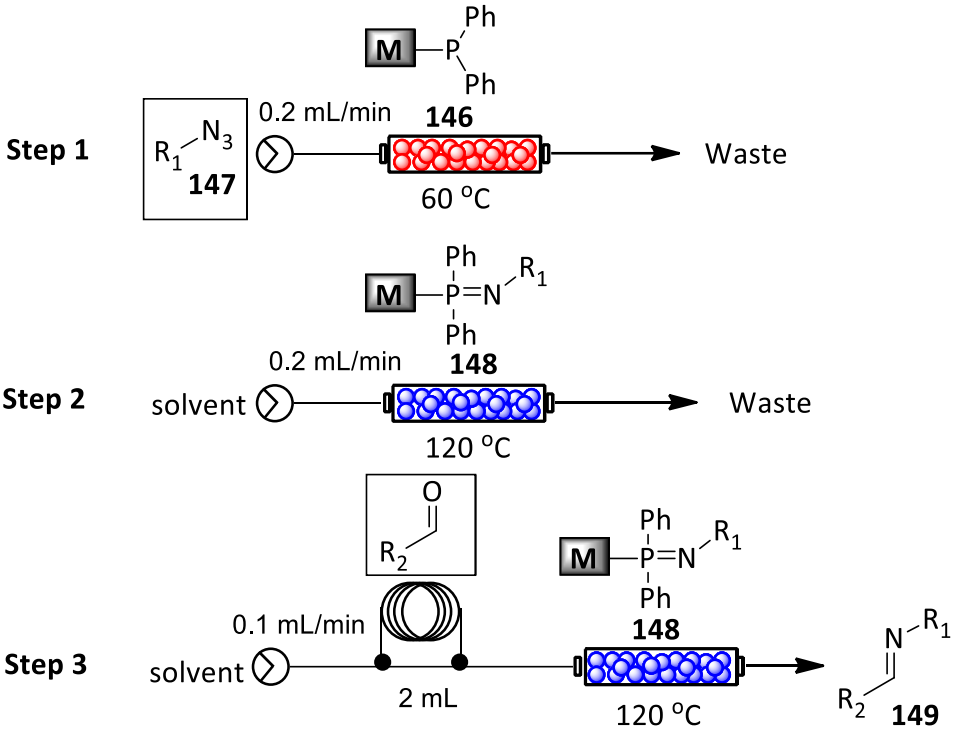

R_1 = Bn, PhOMe, aryl or Allyl; R_2 = Ph, PhOMe or aryl

Scheme 38: Overall reaction sequence for Staudinger aza-Wittig reactions in flow[67]

The research group then applied the triphenylphosphine-monolith to Appel reactions by loading the triphenylphosphine-monolith with carbon tetrabromide, yielding a light brown monolith **150** with elemental analysis indicating 27.6% bromine content. This was evidence that the loading had taken place and that there was less than one molecule of carbon tetrabromide per phosphorus atom. This was then used to transform alcohols into brominated products **151** in a flow synthesis with high yields of 68-95% (Scheme 39). The group also observed that the loaded monolith could be reused for multiple reactions before being completely spent without any detectable cross-contamination when monitoring the colour change (Figure 5).[69]

© University of Pretoria

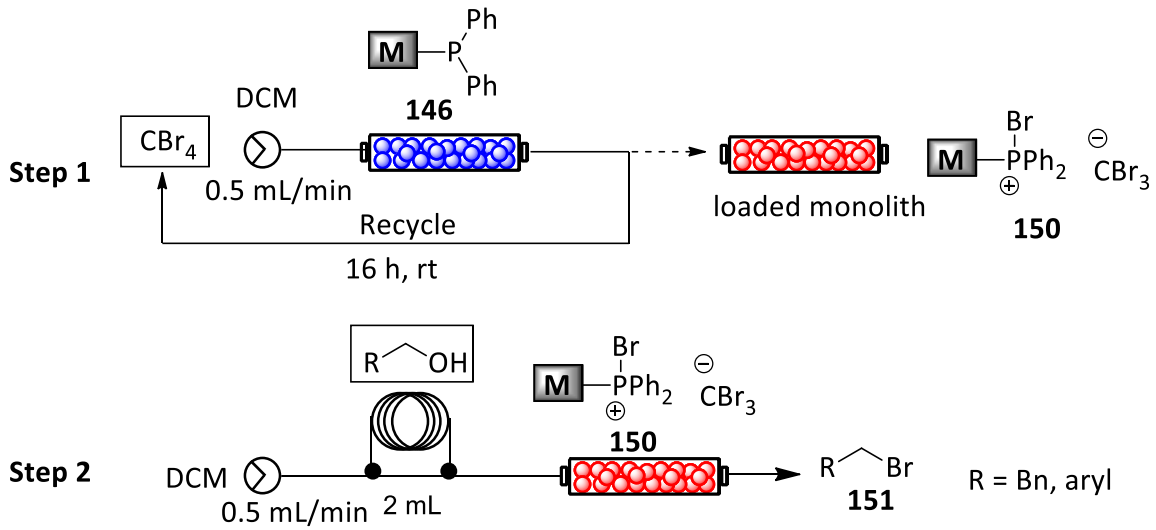

Scheme 39: Appel reaction: (a) Loading of triphenylphosphine-monolith; (b) alcohol conversion into bromide[69]

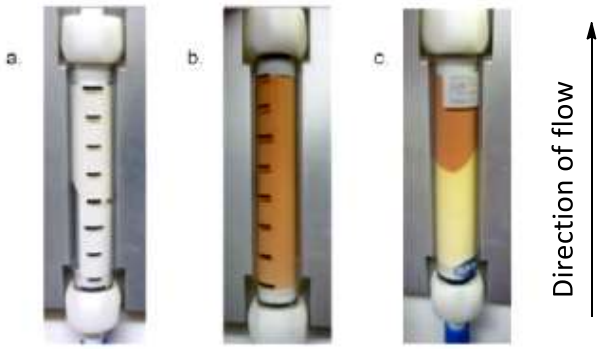

Figure 5: Observed colour change during Appel reactions: (a) unloaded triphenylphosphine monolith; (b) monolith functionalized with CBr_4; (c) monolith after partial consumption of active brominating species[69]

In 2013, Ley and co-workers then further applied the monolithic-triphenylphosphine to form Ramirez *gem*-dibromo-olefination products **153** in flow from aldehydes (Scheme 40). Preparation of the monolith reagent, (dibromomethylene)triphenylphosphorane **152**, is similar to the Appel reagent, except preparation was done at 0 °C vs room temperature. However, they found that Appel reactions could be conducted on the Ramirez monolith intermediate. Again, a single monolith reagent, with a single flow pass of the aldehyde, could be used for multiple reactions without cross-contamination of reactants.[70] It was observed that benzylic and alkyl aldehydes containing electron withdrawing groups on the phenyl ring gave high yields (78-98%) whereas, aldehydes having a phenol group gave little or no yield as

© University of Pretoria

the hydroxy groups were found to be reacting with triphenylphosphine sites within the monolith.

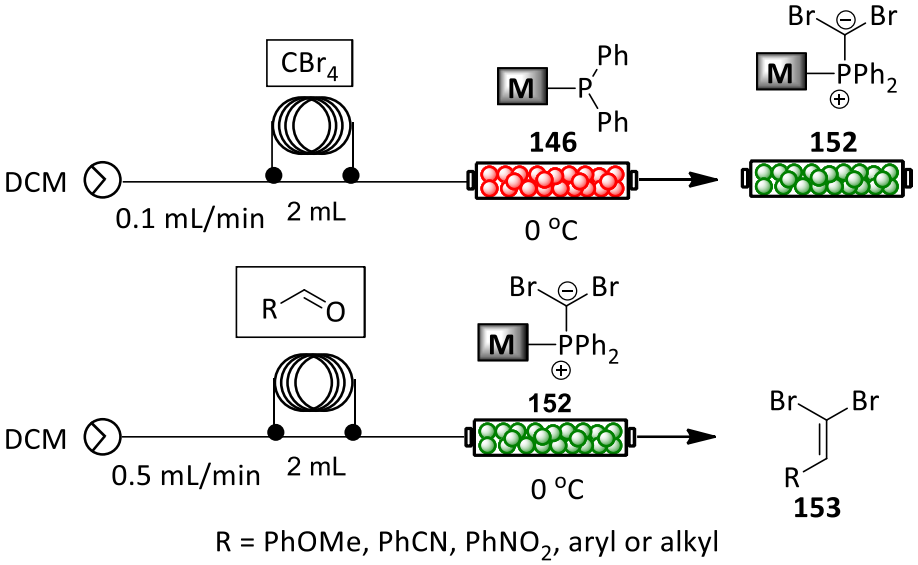

Scheme 40: Transformation of aldehydes into dibromo-olefins[70]

In 2014, Ley and co-workers prepared a monolith ylide **155** by recycling methyl 2-bromopropionate **154**, followed by recycling diazabicycloundecene (DBU) through monolith **146**. A Wittig reaction was then demonstrated converting 2,3-butane diacetal protected aldehyde **156** to α,β-unsaturated methyl ester **157** in 95% yield by passing through **155** followed by polymer-supported benzylamine (PS-BZA) scavenger (Scheme 41).[71]

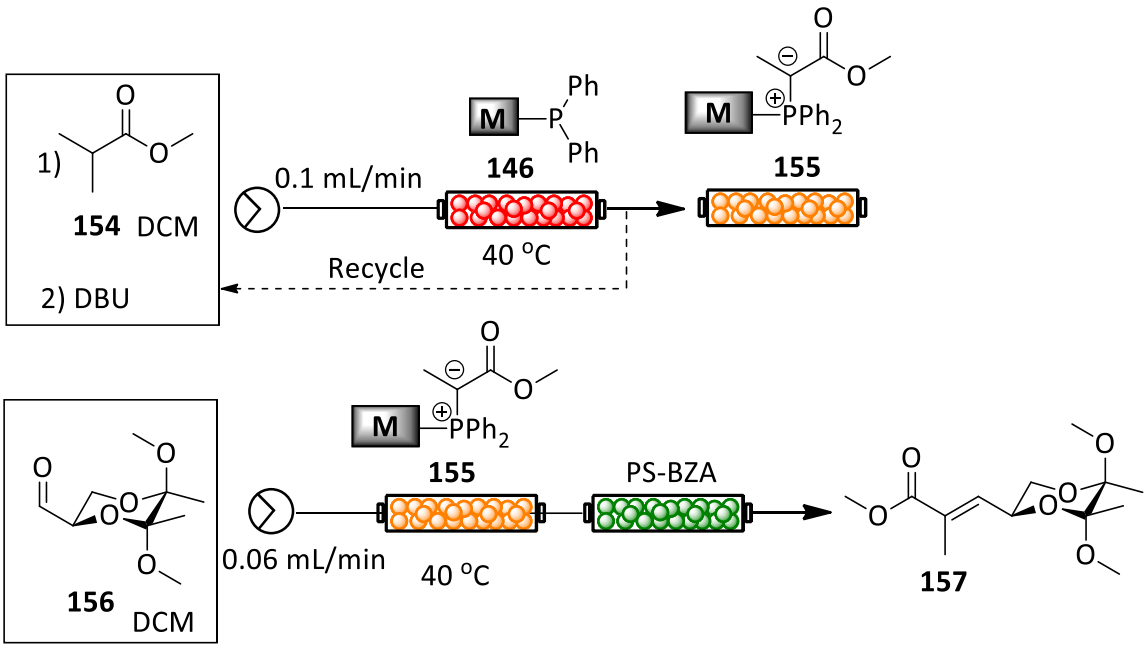

Scheme 41: Application of monolith ylide to Wittig reaction[71]

© University of Pretoria

1.7.2. RAFT polymerisation

RAFT polymerisation uses a chain transfer agent usually in the form of a thiocarbonylthio compound to control the molecular weight during conventional free-radical polymerisation. The advantage of using RAFT polymerization over conventional radical polymerization is that a single optimization of the polymerization process provides a generic monolith with accessible RAFT end groups to enable grafting of functionality. In other words, multiple functional moieties can be attached to each reactive site on the monolithic substrate, whereas co-polymerization requires re-optimization of the polymerization conditions for each new set of functional monomers and crosslinkers in order to obtain monoliths with the desired properties.[72,73] Moad and co-workers described a method where styrene and divinylbenzene were used as monomers, dodecanol as a porogen, AIBN as a radical initiator and 2-cyano-2-propyl dodecyl trithiocarbonate **158** as the RAFT agent to form monolith **159** (Scheme 42).[72]

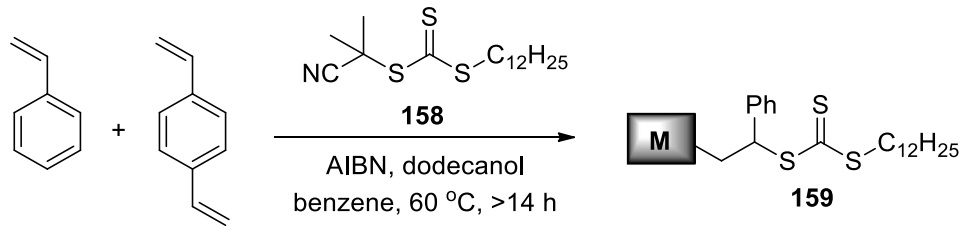

Scheme 42: RAFT synthesis of polystyrene-based monolith[72]

The group then functionalized monolith **159** with 4-styryldiphenylphosphine **141** to form triphenylphosphine monolith **160** and utilized as a catalyst in a Michael addition reaction of acetyl acetone **161** and diethyl azodicarboxylate (DEAD) to give **162** with a conversion of 77% (Scheme 43).[73] The catalysis is initiated by an attack triphenylphosphine on the *β*-position of the electronically poor alkene of acetyl acetone. This generates an *α*-carbanion which reacts as a nucleophile and attacks the electrophilic reagent, DEAD, and because the phosphine is a good leaving group, this yields the product and thus affords triphenylphosphine as a catalyst.[74] The addition of another RAFT agent **158** to the polymerisation mixture was needed as low dispersity was formed, in the absence of the reagent, which indicated that the trithiocarbonate effected good control over the polymerisation of **141**. The grafting process was repeated five times to increase the loading content of phosphorus onto the monolith.

© University of Pretoria

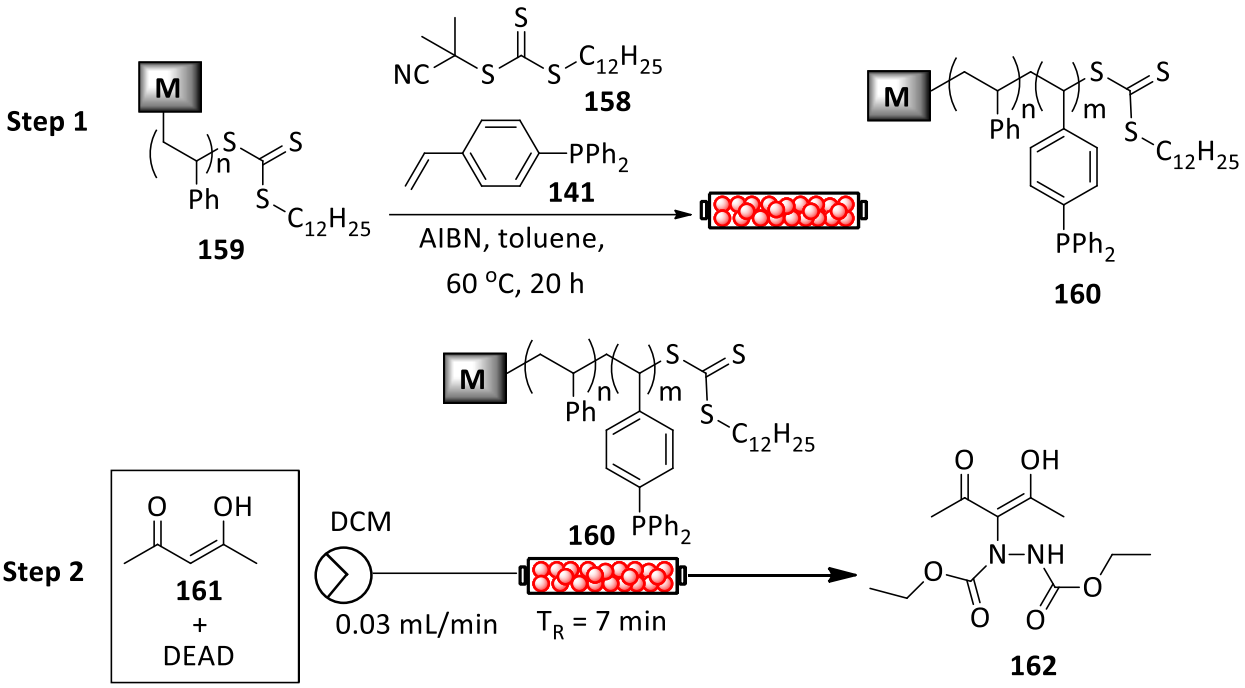

Scheme 43: Michael addition using a surface-grafted RAFT monolith[73]

The Moad group further functionalized RAFT monolith **159** by attaching (4-vinylphenyl)boronic acid **163** to give monolith **164** (Scheme 44) which could potentially be used for catalysed amide formation.[72,75]

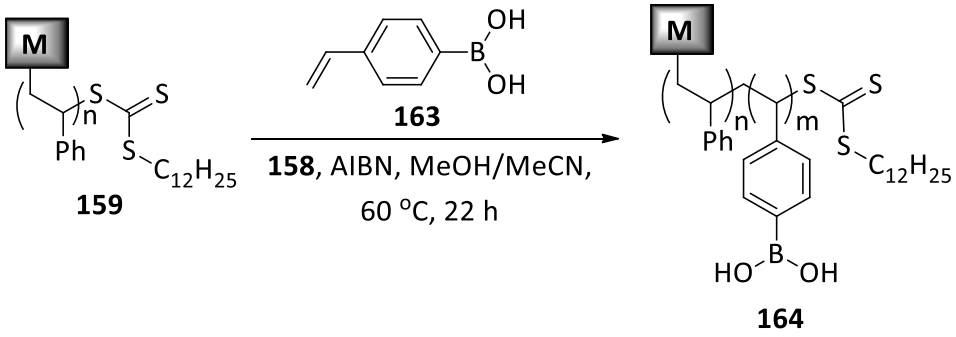

Scheme 44: Synthesis of monolith-supported boronic acid[72]

Dong and co-workers developed a novel imprinted monolithic material with the capacity of protein exclusion for the selective extraction of clenbuterol from biological samples (Scheme 45).[76] The monolith was prepared in a two-step procedure comprised of an inner structure which housed a clenbuterol imprinted monolithic trithioester polymer **169**, which was synthesized by polymerising ethylene dimethacrylate **165**, methacrylic acid **166** and clenbuterol **167** with chain transfer agent **168**. The second step which was synthesized by grafting glycerol monomethacrylate **170** to the end groups and these created barriers for

© University of Pretoria

protein diffusion **171**, created the hydrophilic outer layer which created barriers for protein diffusion that allowed more than 90% of bovine serum albumin to be excluded. Therefore, when the imprinted monolith was used as a solid-phase extraction pre-column, the percentage (87-97%) of clenbuterol in human serum could be determination through HPLC.

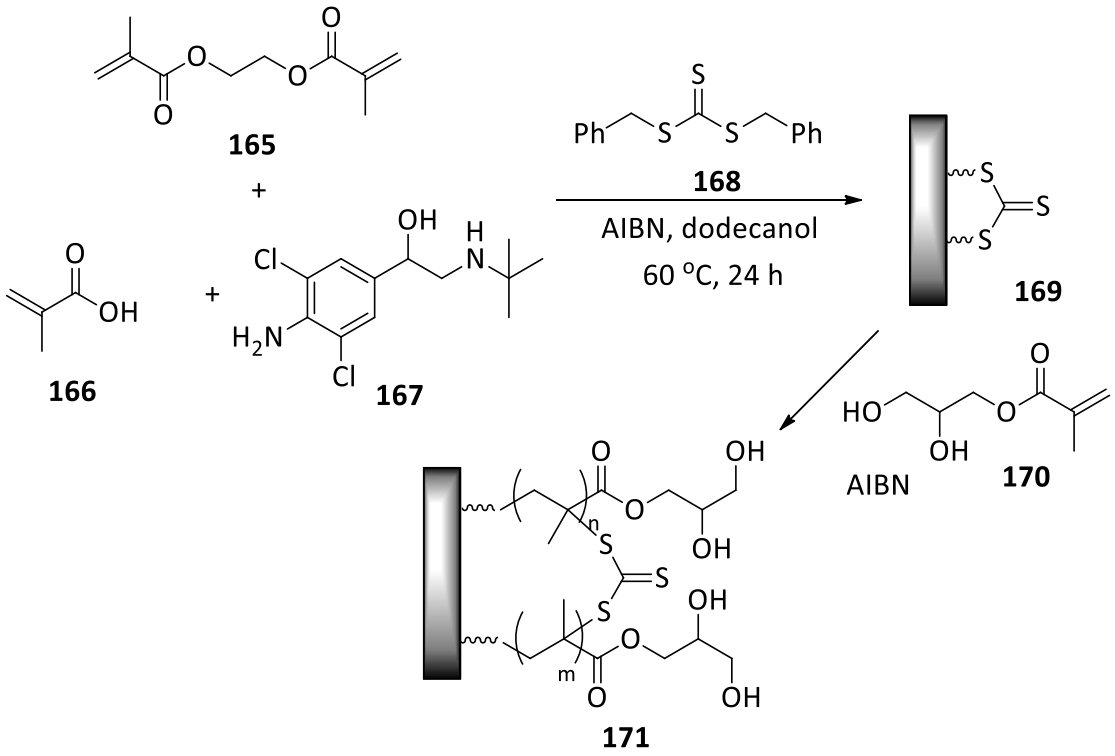

Scheme 45: Grafting of glycerol monomethacrylate on the imprinted monolith[76]

Recently there have been more examples of monolith-supported catalysts emerging in flow. Baxendale and co-workers reported an immobilised iridium catalyst **174** used for transfer hydrogenation reactions in flow (Scheme 46).[77] Monolith **173** which was synthesized via a Suzuki-Miyaura reaction of bromopyridine and vinylphenylboronic acid, followed by polymerisation of the product with styrene and divinylbenzene. The iridium dimer complex, pentamethylcyclopenta-dienyliridium(III)chloride **172** was then loaded onto monolith **173** by passing the complex solution together with *tert*-Butyl acetoacetate (TBAA) through the column. The monolith was then used to reduce aldehydes and ketones affording products in low to high conversions (18-100%).

© University of Pretoria

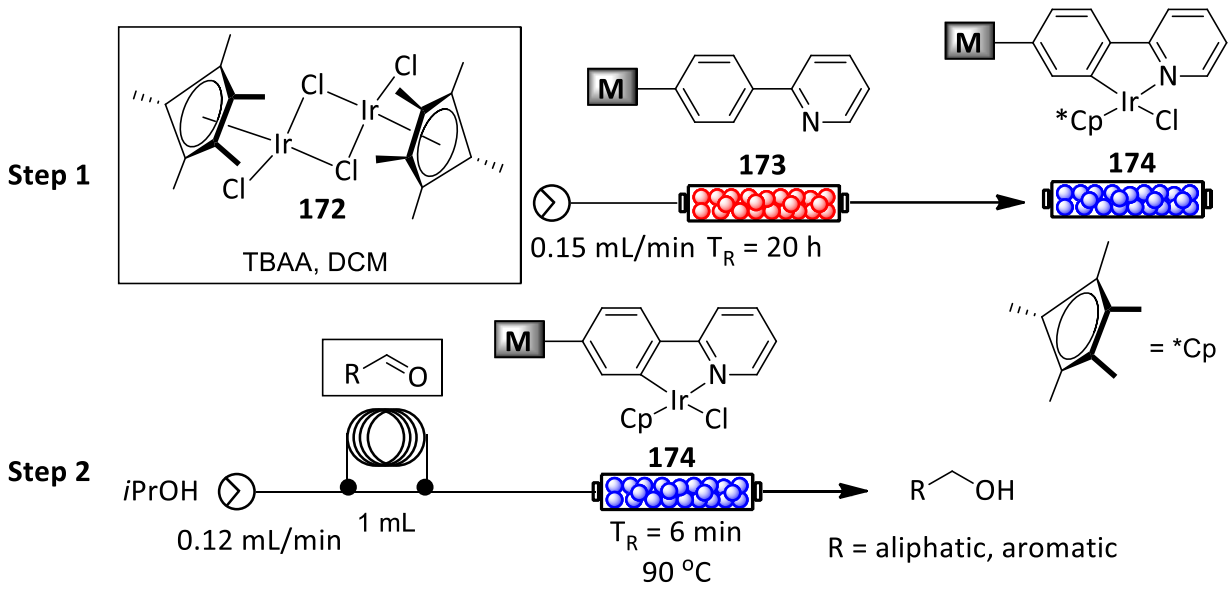

Scheme 46: Synthesis of Iridium monolith and transfer reductions of aldehydes and ketones[77]

There have been some monoliths that have been prepared on a miniaturised scale, in a twenty-two centimetre glass capillary, rather than the typical 10 mL glass column, as demonstrated by Ghanem and Adly, to line-up with the vision of producing efficient synthetic routes which lead to less waste.[78] The immobilised dirhodium catalyst **176**, synthesized by reacting a pyridine-derived monolith with diirhorium(II) catalyst, was used for an asymmetric cyclopropanation reaction of styrene **143** and dimethyl α-diazobenzylphosphonate **175** giving **177** in 44% yield and diastereoselectivity greater than 20:1 *E:Z* (Scheme 47).

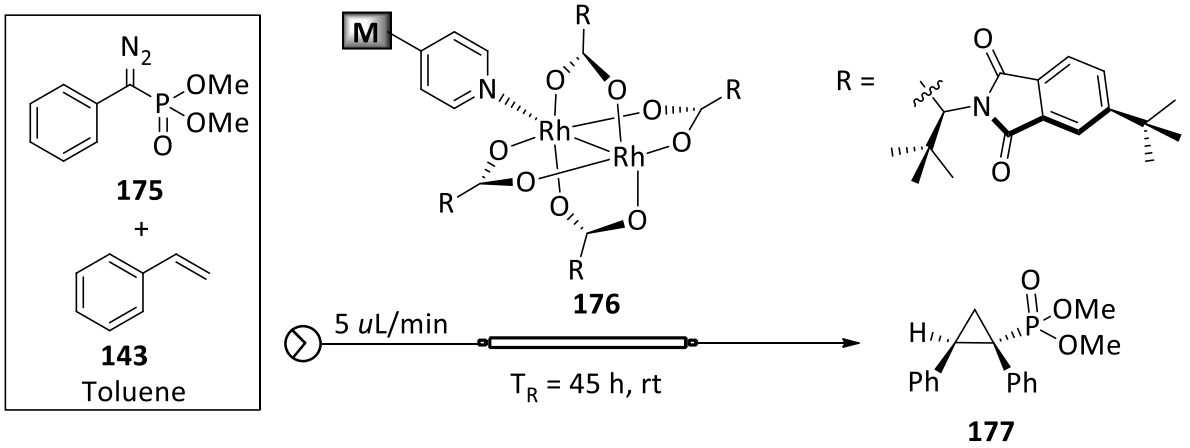

Scheme 47: Flow catalysed cyclopropanation reaction[78]

© University of Pretoria

This mini review has indicated the plethora of polymer-supported reagents and their use in batch and flow processes. As synthesis continues to move towards flow technology with incorporation of monolith-supported reagents and catalysts there, however, lacks adequate examples. We wish to explore these supports and solve some of the existing problems in the laboratory.

© University of Pretoria

Project Overview, Aims and Objectives

© University of Pretoria

Chapter 2

Project overview, aims and objectives

2.1 Project overview

In the preceding chapter the concept of applying solid-supported reagents to avoid the purification difficulties associated with traditional solution-phase synthesis was outlined. It was revealed that an added benefit of supported reagents is the ability to drive reactions to completion through the addition of excess reagents, without the complications associated with work-ups and purifications. Separation of the insoluble polymeric support can readily be achieved by simple filtration, however, bead-type solid supported reagents can suffer from poor mass transfer as well as problems associated with swelling. Therefore, other supports such as monoliths (which are a single continuous piece of uniformly porous material prepared by precipitation polymerisation of a functionalised monomer) have been developed as replacements for bead-type supports for use in continuous-flow synthesis to avoid some of these issues.

In this thesis we focused on three reaction classes, namely: i) ozonolysis, ii) Wittig and iii) Suzuki-Miyaura coupling, where the use of solid-supported triphenylphosphine as both a reagent and a scaffold for other solid-supported reagents and catalysts was investigated. In all instances, the approaches developed are contrasted against existing reported examples reported under both batch and flow conditions.

2.1.1. Ozonolysis

Ozone is a well-known oxidizing agent with a broad range of industrial applications from chemical synthesis to waste treatment and water purification. It has a minimal environmental impact and low cost, but suffers from safety issues relating to the generation of unstable and highly energetic ozonide intermediates.[79] The reagent is most commonly used to oxidise double bonds to reactive ozonide species, which can, through treatment with a suitable reductant, afford aldehydes and/or ketones. Studies have already demonstrated the feasibility of conducting flow-based ozonolysis procedures to expedite chemical processing and improve safety.[80] Unfortunately, many of these systems are not suited to direct scale-up or scale-out parallel application. Consequently, there is a need to develop a simple, high-performing and safe system for the processing of larger quantities of substrate.[81]

© University of Pretoria

In the process of synthesizing formylacetic esters **179**, Larsson and co-workers used the ozonolysis of trans-β-hydromuconic esters **178** utilizing polystyrene-bound triphenylphosphine (PS-PPh_3) as a reductant (Scheme 48).[82] The reduction was initially performed using unsupported triphenylphosphine in solution and was accomplished overnight using 1.5 equivalents, however purification of the product by distillation led to decomposition. When using these identical conditions with the PS-PPh_3 a large amount of the ozonide was left unreacted. The reaction was driven to completion by stirring for 48 hours, but that resulted in increased decomposition of the product. Running the reaction in deuterated chloroform enabled the group to follow the decay using NMR. Therefore, employing two equivalents of the reducing agent for 24 hours finally led to full conversion (90-100% yield) into the aldehyde without any detectable decomposition givin.[82]

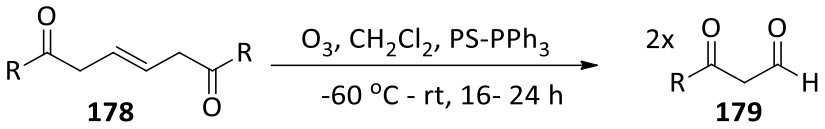

R = OMe, OEt, O*i*Pr, O*t*Bu, OBn or NH*i*Pr

Scheme 48: Ozonolysis of trans-β-hydromuconic esters[82]

In 2010, Ley and co-workers developed a flow-based ozonolysis process using a commercial semi-permeable membrane, Teflon AF-2400, which selectively allows gases (but not liquids) to permeate the membrane.[83] They constructed a chamber in which the membrane tubing was housed and supplied it with a flow of ozone from an ozone generator (Figure 6).

Figure 6: Ozonolysis membrane chamber[83]

© University of Pretoria

A 0.1 M solution of alkenes **180** as a substrate in methanol, spiked with Sudan red 7B dye, an ozone indicator which turns colourless when alkene is used up, was pumped through the membrane using syringe pumps, exposed to ozone, followed by quenching the product with triphenylphosphine to form ketones **181** (Scheme 49). It was found that one hour of exposure to the supplied ozone was sufficient to give complete conversion to benzophenone. In order to facilitate rapid purification and simplify the analysis of products, the reaction streams were quenched by dropping into a flask containing a four-fold excess of polymer-supported triphenylphosphine suspended in methanol, followed by filtration. In total eleven examples of different alkenes were demonstrated using this approach giving yields in 57-95%.[83]

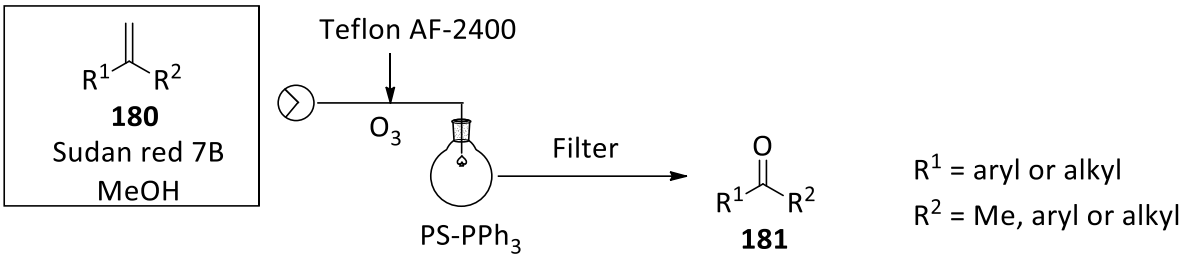

Scheme 49: Synthesis of ketones by ozonolysis using Teflon AF-2400 membrane

Later Ley and co-workers used an alternative method to transform a homoallylic alcohol, **182**, into an aldehyde (Scheme 50). The reaction commenced first with a silylation reaction, where a stream of triethylsilyl trifluoromethanesulfonate **183** and diisopropylethylamine were reacted in a 1 mL mixing chip. The reaction stream was then diluted with methanol and subjected to a rapid flow of ozone, with the resulting ozonide collected by instantaneous quenching in a flask containing solid-supported triphenylphosphine to generate the aldehyde **184** in 84% yield.[71]

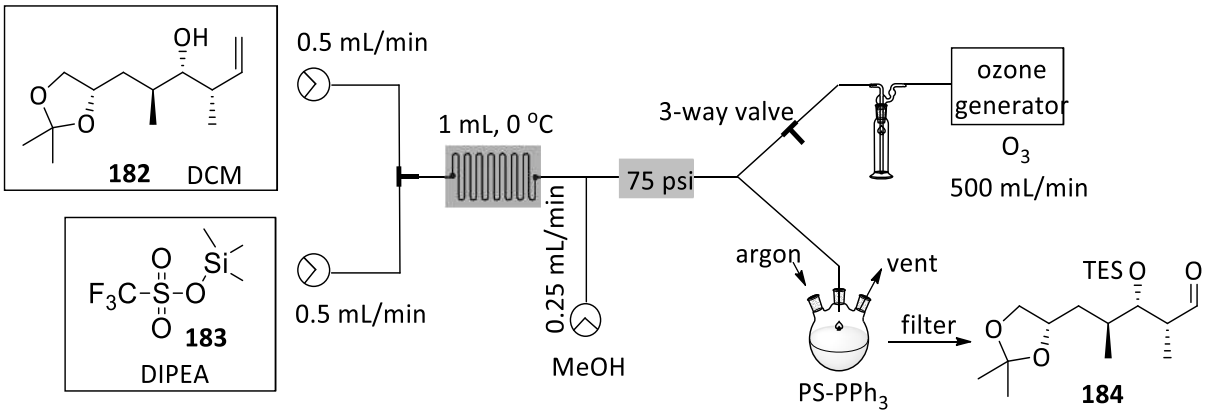

Scheme 50: Flow ozonolysis of homoallylic alcohol[71]

© University of Pretoria

2.1.2. Wittig olefination reactions

The Wittig reaction has been widely used to transform aldehydes into alkenes and is performed using phosphonium salts, which under basic conditions forms analogous ylides *in situ*. The drawback with this reaction in solution phase is the formation of stoichiometric amounts of phosphine oxides as a by-product. These phosphine oxides, in particular triphenylphosphine oxide, complicate downstream processing and purification for polar compounds. To avoid this, the use of solid-supported triphenylphosphine can be used to prepare solid-supported ylides.

As described in Chapter 1, Ley and co-workers demonstrated this principle in their flow synthesis of the spirocyclic polyketide natural product, spirangien A methyl ester, through the use of a solid-supported phosphonium ylide **155**, functionalized from solid-supported triphenylphosphine. The reagent was used to transform 2,3-butane diacetal **156**, a protected aldehyde, into α,β-unsaturated methyl ester **157** without further purification, as the resultant triphenylphosphine oxide by-product remained immobilized on the solid-support (Scheme 41).[71]

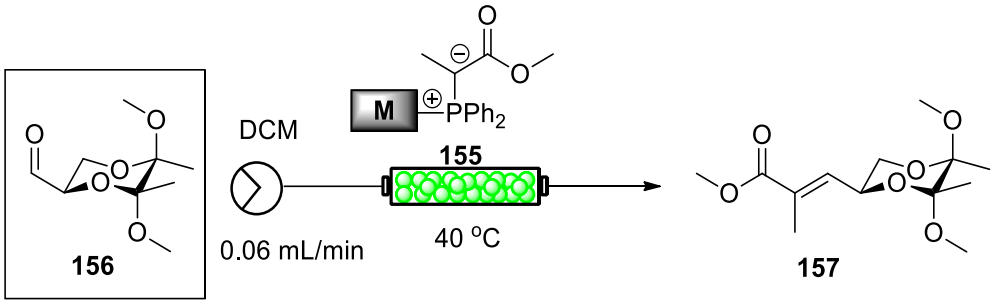

Scheme 41: Wittig flow synthesis of α,β-unsaturated methyl ester[71]

In 2001, Westman developed a protocol which integrated the use of microwave heating to reduce the time taken to functionalize the polymer (~48 hours to 7 days with traditional heating) (Scheme 51). The polymer-supported triphenylphosphine was first treated with methyl bromoacetate **185** in toluene at 150 °C for three minutes in the microwave, to yield the phosphonium salt **186**. The polymer was then treated with aqueous potassium carbonate at 125 °C for five minutes in order to form the corresponding ylide **187** prior to washing and treatment with pyridine 3-carboxaldehyde **188** in DMF at 180 °C for five minutes. The desired product **189** was obtained in >95% conversion (81% yield) as monitored by liquid chromatography mass spectrometry (LC-MS). A one pot synthesis was then developed using

© University of Pretoria

one equivalent of aldehyde, three equivalents of solid-supported triphenylphosphine, four equivalents of alkyl halide and four equivalents of potassium carbonate in 2 mL of methanol heated to 150 °C for 5 minutes, this did not change the yields obtained in the two-step synthesis.[84]

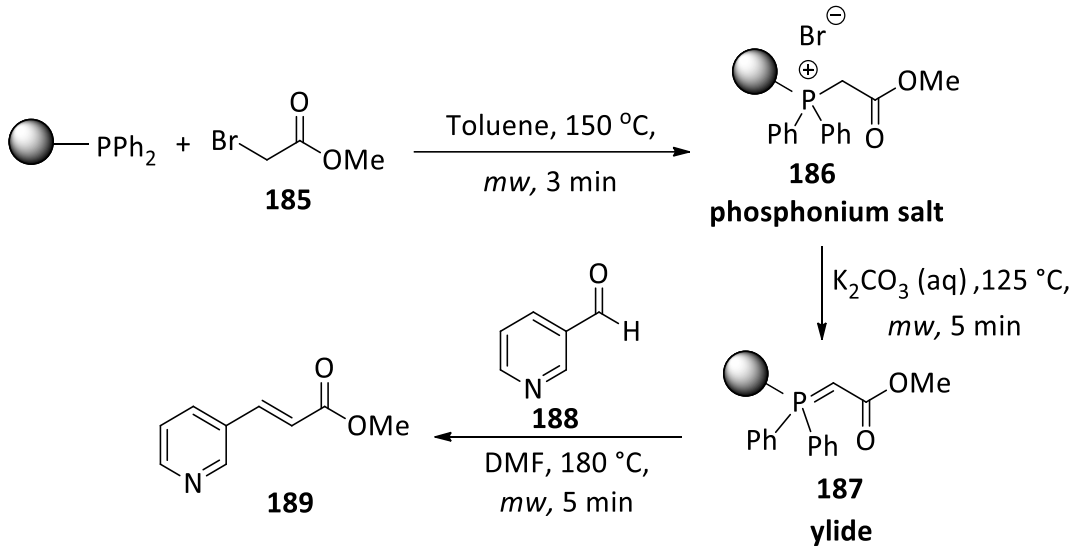

Scheme 51: Microwave assisted Wittig reaction[84]

2.1.3. Suzuki-Miyaura coupling

The Suzuki-Miyaura coupling reaction, which affords the coupling of boronic acids to aryl halides and is typically catalysed by palladium or nickel catalysts, is an essential and widely utilised carbon-carbon bond forming reaction. The reaction typically requires high catalyst loadings of expensive catalysts with difficult purification procedures, often leaving metal traces in the final product.[85] In addition, high temperatures are also required for complete substrate conversion, which decreases the lifespan of the catalyst and can lead to the formation of degradation by-products. The use of solid-supported catalysts ultimately reduces the purification problems,[32] however there are limited examples that incorporate triphenylphosphine as a solid support for the catalyst.

Merrifield polymer **45** was transformed into a catalyst by Le Drian and Fenger by simply substituting the chlorine with diphenylphosphine to form polymer **190**, followed by reaction with different palladium sources such as palladium(II) chloride, tetrakis(triphenylphosphine)palladium, and bis(dibenzylideneacetone)dipalladium(0) to give catalyst group **191** (Scheme 52).[86] These catalysts were then validated using the Suzuki cross-coupling reaction between phenyl boronic acid **192** and 4-bromopyridine **193** to give 4-phenyl

© University of Pretoria

pyridine **194** in yields of 76-90%. Results showed that the palladium to phosphorus ratio had no influence on the activity of the catalyst. [86]

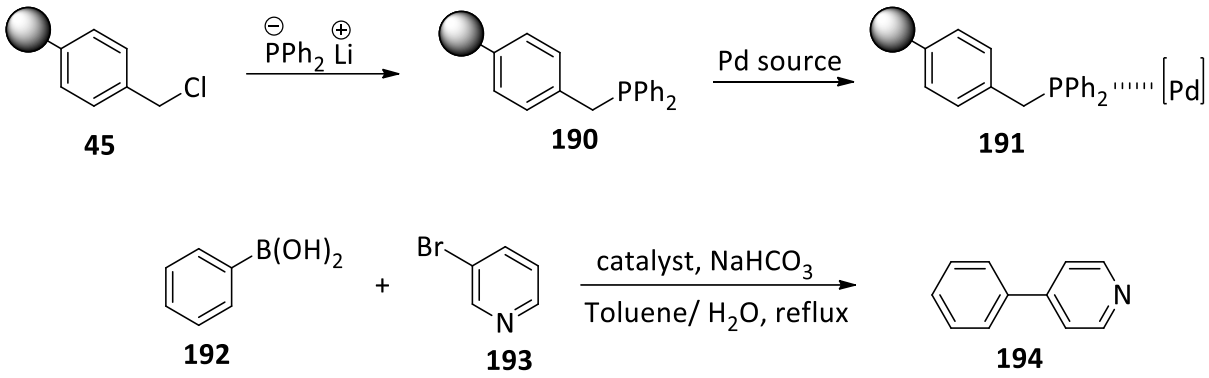

Scheme 52: Synthesis of Merrifield derived palladium catalyst and use in the Suzuki coupling reaction[86]

The use of SilicaCat DPP-Pd **196**, a silica-based supported diphenylphosphine palladium catalyst developed by Pagliaro and co-workers, has been reported in continuous flow synthesis (Scheme 53). The catalyst was packed in a column and streams of aryl halide **195** (0.83 M, 0.055 mL/min) in tetrahydrofuran (THF), and phenyl boronic acid (0.45 M) and potassium carbonate (0.55 M) in a mixture of H_2O-EtOH (1:1), were then pumped through the column heated at 80 °C. Under these conditions, 78-100% conversion was obtained in less than 20 minutes and almost quantitative yield (97%) of the biaryl target compound **197** was reported.[87]

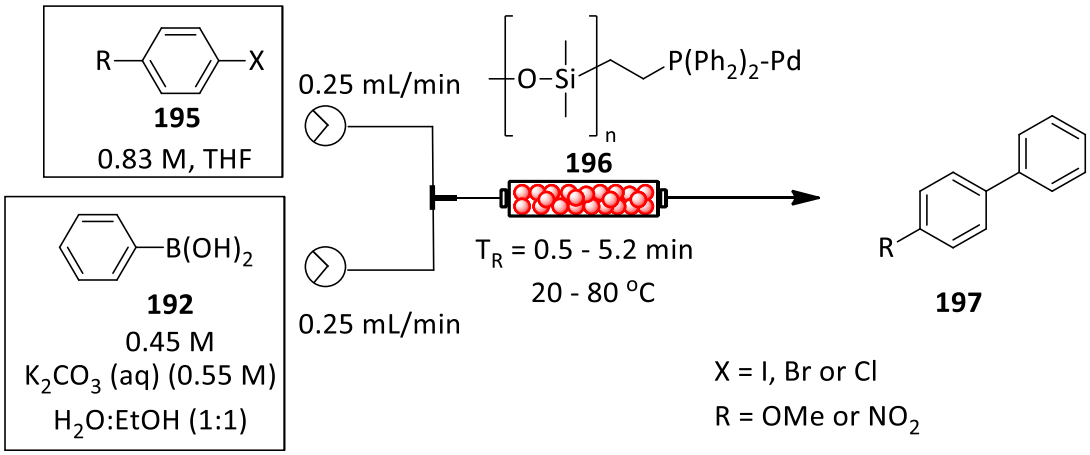

Scheme 53: Suzuki coupling using SilicaCat DPP-Pd[87]

© University of Pretoria

2.2 Aims and objectives

The aims of this doctoral research project were to (Scheme 54):

a) Synthesize solid-supported triphenylphosphine in a bead and monolithic form, and show its efficacy as a solid-supported reagent by contrasting it with commercial unsupported and polystyrene-supported triphenylphosphine.

b) Demonstrate the application of solid-supported triphenylphosphine as a reductant in ozonolysis reactions under batch and flow conditions.

c) Prepare solid-supported ylides and demonstrate their use in Wittig reactions under batch and flow conditions.

d) Prepare solid-supported tetrakis(triphenylphosphine)palladium and demonstrate its use in Suzuki-Miyaura coupling reactions under batch and flow conditions.

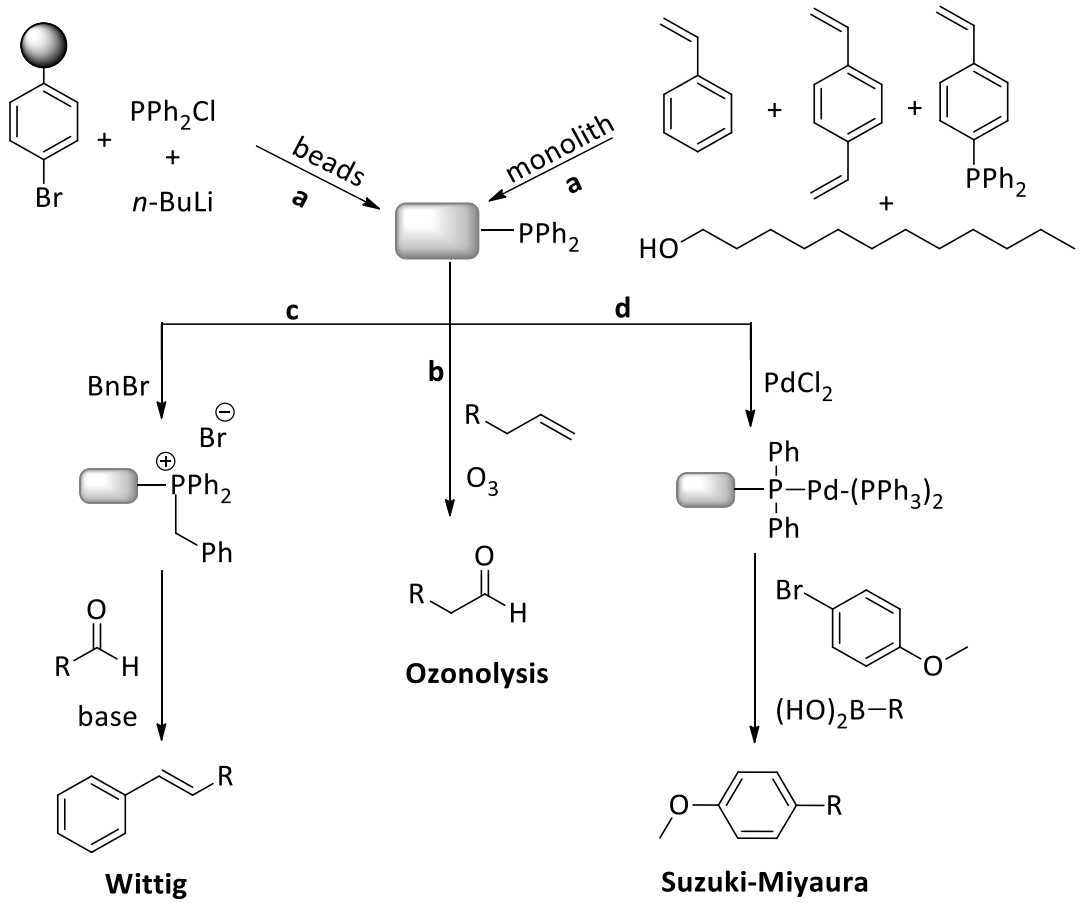

Scheme 54: Summary of the desired applications of the developed forms of immobilized triphenylphosphine in various syntheses

Ultimately, we aimed to synthesize a convenient solid-supported reagent that is cheaper than current commercial reagents.

© University of Pretoria

Results and Discussion

© University of Pretoria

Chapter 3

Preparation of immobilized triphenylphosphine reagents

3.1. Introduction

There are two known methods for functionalising polystyrene to form solid-supported triphenylphosphine: (i) by direct lithiation of the polystyrene and (ii) by halogen–metal exchange, followed in both cases by reaction with a phosphine reagent such as chlorodiphenyl phosphine (Scheme 55).

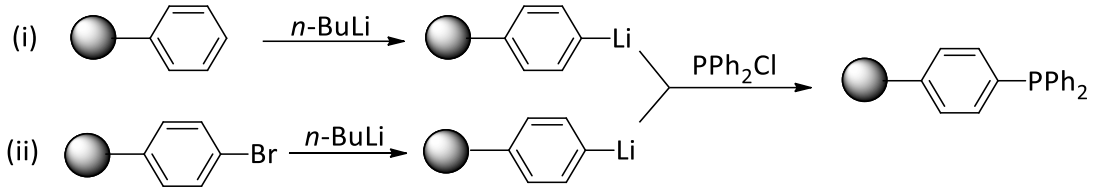

Scheme 55: Approaches for the synthesis of polymerized triphenylphosphine

These procedures suffer in that the polystyrene backbone typically contains carbon-carbon double bonds (derived from divinylbenzene crosslinking) and reaction with *n*-butyllithium often leads to unwanted side reactions with these bonds. As a result, the polymer formed becomes contaminated and has poor swelling properties, reducing the number of exposed active sites. In addition, relatively small diameter (<75 µm) polystyrene beads are produced instead of larger beads (>150 µm) which are required for optimal handling properties. In general, larger diameter polymers are free flowing and greatly reduce the problem of static often associated with smaller diameter polymers. An added advantage is that when removing the reagent, the rate of filtration of larger diameter beads is faster and less of the polymer support can pass through the filter.[6,88]

In this chapter we report on the use of a cost-effective metal-halogen exchange method of derivatising 4-bromopolystyrene into polystyrene-supported triphenylphosphine, as well as the synthesis of an in-house form of solid-supported triphenylphosphine. In addition, we report on their use as reductants in ozonolysis reactions with comparison to commercial solid-supported and solution phase triphenylphosphine.

© University of Pretoria

3.2. Batch synthesis

3.2.1. Polystyrene-supported triphenylphosphine prepared from 4-bromopolystryrene

The study was initiated by synthesizing low-cost polystyrene-supported triphenylphosphine **201** using the method reported by Spring and co-workers[89] and comparing it to an analogous commercial polystyrene-supported triphenylphosphine reagent (Sigma Aldrich 366455). The synthesis began with the formation of a highly active Grignard species (arylmagnesium nucleophile) **199** through the reaction of commercial 4-bromopolystyrene **198** with *i*-Pr(*n*-Bu)$_2$MgLi (Oshima's trialkylmagnesate complex).[90] This complex is used for halogen-magnesium exchange reactions and is prepared by the reaction of *iso*-propyl magnesium chloride with two equivalents of *n*-butyllithium (Scheme 56). Titration of the *n*-butyllithium reagent to get an exact concentration was crucial before every reaction as the process was highly sensitive to the stoichiometric equivalents of the *n*-butyllithium. Thereafter, a Grignard alkylation reaction proceeded, wherein **199** substituted the chloride atom of chlorodiphenylphosphine **200** to yield polystyrene-supported triphenylphosphine **201** as yellow beads. It was crucial to (i) swell the 4-bromopolystyrene beads **198** overnight in anhydrous tetrahydrofuran before use to ensure optimal surface area exposure and (ii) avoid vigorous stirring which typically results in the physical break down of the polystyrene beads.

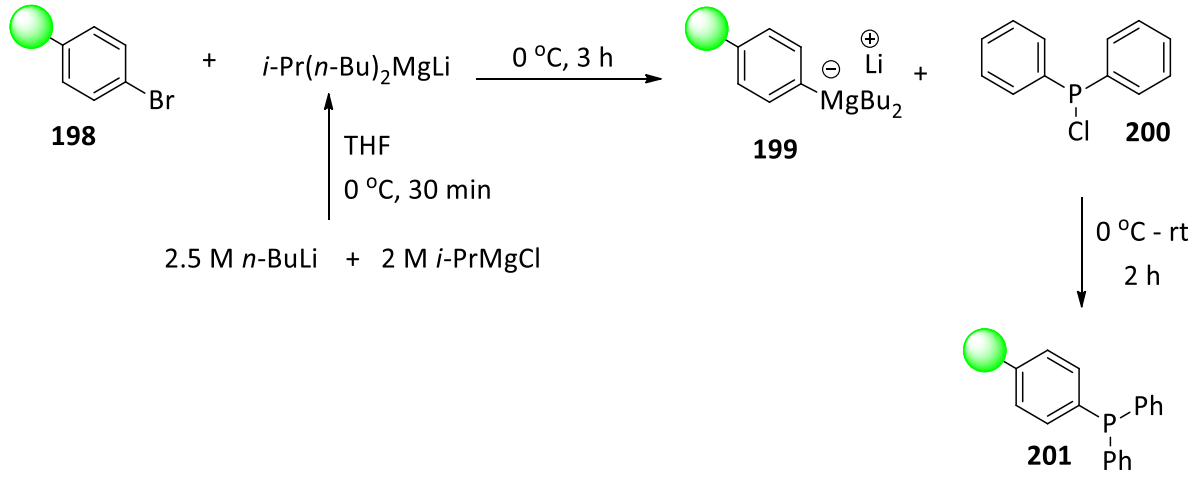

Scheme 56: Synthesis of polystyrene-supported triphenylphosphine[89]

Analysis of the insoluble supported triphenylphosphine **201** was conducted by swelling the beads in deuterated solvent and running the material as a gel using ^{31}P NMR spectroscopy, with comparison to commercially available unsupported and polystyrene-supported triphenylphosphine. The commercial unsupported and supported triphenylphosphine

© University of Pretoria

exhibited broad singlet peaks in the negative region at -5.28 ppm and -6.59 ppm respectively. In contrast, our in-house synthesized polystyrene-supported triphenylphosphine showed a singlet peak in the positive region at 28.8187 ppm which is characteristic of triphenylphosphine oxide, suggesting that oxidation was taking place during synthesis of **201** (Figure 7).

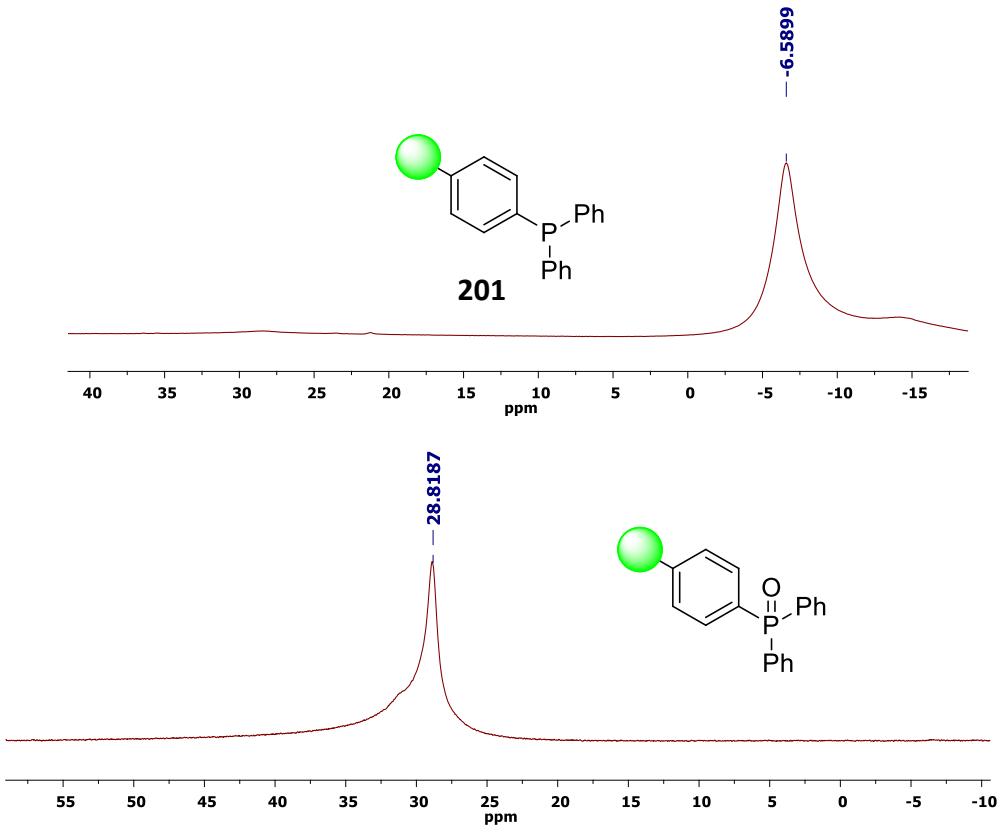

Figure 7: ^{31}P NMR spectra comparison between commercial polystyrene-supported triphenylphosphine (top) and in-house synthesized polystyrene-supported triphenylphosphine (bottom)

In order to try to prevent the oxidation through human error, the reaction was repeated using freshly prepared Oshima's trialkylmagnesate complex using both 1.6 and 2.5 M *n*-butyllithium, but in both cases the same result was observed. We then optimized the reaction conditions by either using *n*-butyllithium only, to form lithyl species **199a**, or *iso*-propyl magnesium chloride, to form the Grignard reagent **199b** (Scheme 57), but again the formation of the unwanted oxide persisted (Table 2, entries 1-3). Reactions were then conducted in flame-dried Schlenk vessels, with additional bubbling of argon through the pre-dried solvents for an hour prior to reaction to ensure the complete elimination of oxygen from

© University of Pretoria

the reaction vessel. Under these oxygen exclusive conditions, using freshly prepared Oshima's trialkylmagnesate complex, the correct product **201** was obtained (Table 2, entries 6-7) with 100% conversion.

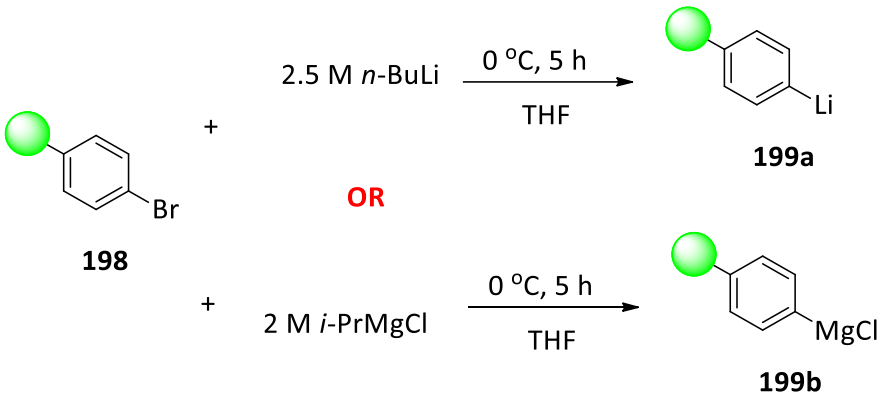

Scheme 57: Optimization of step 1

Table 2: Optimisation for synthesis of in-house PS-triphenylphosphine

Entry	Base	*n*-BuLi (M)	*i*-PrMgCl (M)	Product
1	*n*-BuLi	1.6	-	Oxide
2		2.5	-	Oxide
3	*i*-PrMgCl	-	2.0	Oxide
4[a]	Oshima's reagent	1.6	-	Oxide
5[a]		2.5	-	Oxide
6[b]	Oshima's reagent	1.6	2.0	**201**
7[b]		2.5	2.0	**201**

Reactions conditions: [a] non-degassed solvents or [b] degassed solvents under Schlenk conditions

The product was confirmed by ^{31}P NMR analysis which showed a single peak at -6.31 ppm (Figure 8). SEM scans were then run to compare the morphology of the beads of the in-house synthesized polystyrene-supported triphenylphosphine **201** and commercial polystyrene-supported triphenylphosphine **201a** (Figure 9), which revealed spherical shaped ten micro molar sized particles at three hundred times magnification (Figure 9A and C) and irregular shaped one micro meter sized particles at ten thousand times magnification (Figure 9B and D) for both reagents. The uniformity of the particle shapes of **201** was due to the reaction being shaken and not stirred. Although synthesizing our own polystyrene-supported

© University of Pretoria

triphenylphosphine seemed cost-effective it was decided to use the commercial polystyrene-supported triphenylphosphine **201a** for all following reactions in the thesis.

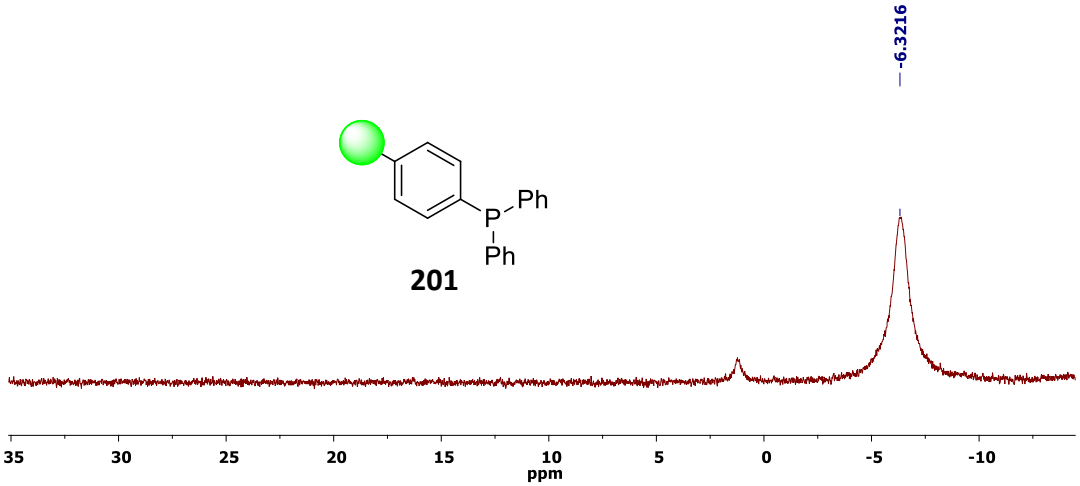

Figure 8: ^{31}P NMR analysis of polystyrene-supported triphenylphosphine synthesized using Schlenk conditions

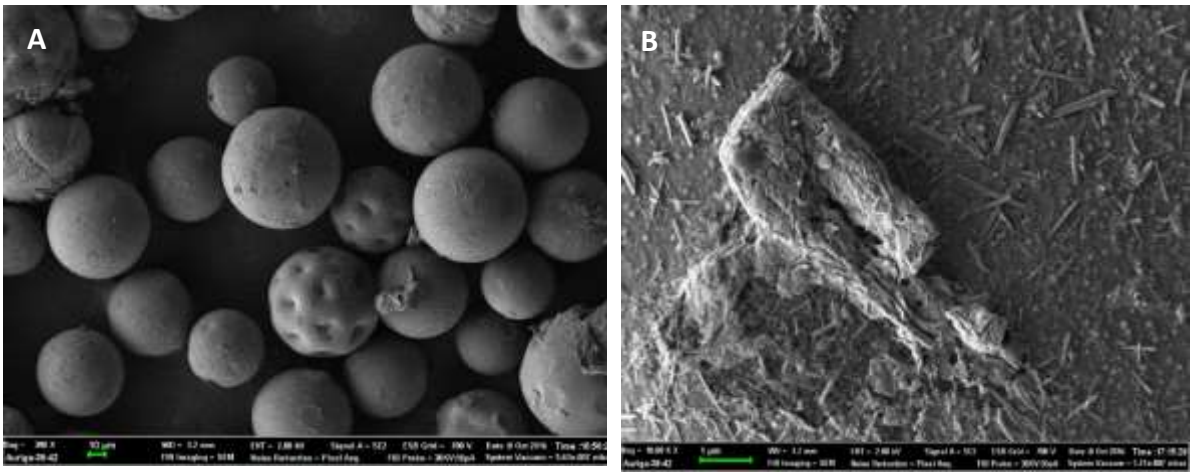

Figure 9: SEM scans comparing in-house prepared polystyrene-supported triphenylphosphine **201** (**A**: 300 X, 10 µm, 2.00 kV; **B**: 10.00 K X, 1 µm, 2.00 kV) with commercial polystyrene-supported triphenylphosphine **201a** (**C**: 300 X, 10 µm, 2.00 kV; **D**: 10.00 K X, 1 µm, 5.00 kV)

© University of Pretoria

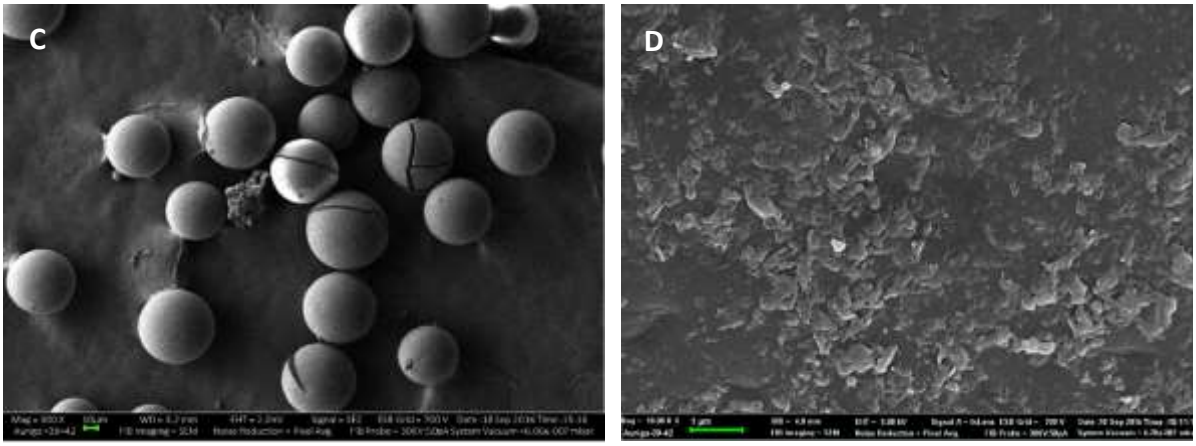

Figure 9 continued: SEM scans comparing in-house prepared polystyrene-supported triphenylphosphine **201** (**A**: 300 X, 10 µm, 2.00 kV; **B**: 10.00 K X, 1 µm, 2.00 kV) with commercial polystyrene-supported triphenylphosphine **201a** (**C**: 300 X, 10 µm, 2.00 kV; **D**: 10.00 K X, 1 µm, 5.00 kV)

3.2.2. In-house polymer-supported triphenylphosphine prepared using precipitation polymerization

We next attempted the synthesis of solid-supported triphenylphosphine reagent. These are usually synthesized via precipitation polymerisation on flow reactors in glass columns, however, we were interested in using the material both in monolithic form (flow) and as a finely ground powder (batch and flow). As a result, we adapted the procedure of Ley and co-workers[70] where diphenyl (4-vinylphenyl)phosphine (monomer) **141**, divinylbenzene (cross-linker) **142**, styrene (monomer) **143** and dodecanol (porogen) **144** were heated at 50 °C in a glass vial until dissolution. Thereafter dibenzoyl peroxide (radical initiator) was added and the solution was heated for a further five minutes before being allowed to polymerise in a standard convection oven at 92 °C for 48 hours, resulting in the formation of a white solid polymer **146** (Scheme 58).

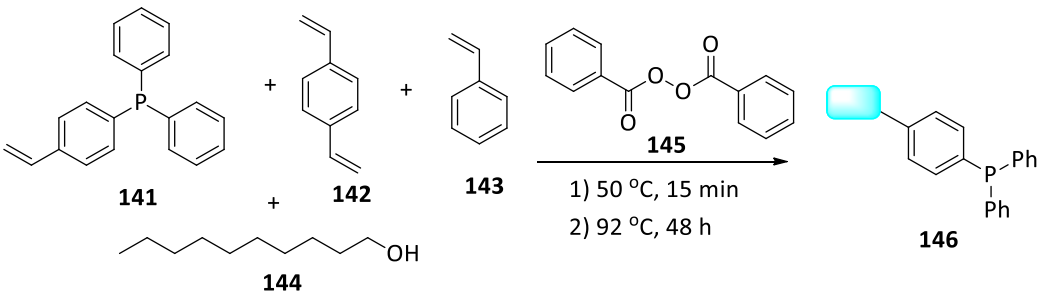

Scheme 58: Synthesis of monolith-supported triphenylphosphine[70]

© University of Pretoria

The vial was then broken to release the polymer-supported reagent which was crushed with a mortar and pestle before being washed with hot anhydrous dichloromethane (DCM) to remove the dodecanol, allowing all the various active sites of the solid-supported reagent to be exposed. The material was collected by filtration and dried under argon to ensure no exposure to oxygen, yielding polymer-supported triphenylphosphine as a white powder. SEM analysis of the polymerised material revealed a largely uniform morphology of particles in the size range of 0.5-1 µM (Figure 10). Infrared spectroscopy revealed comparable spectra for the commercial unsupported-, commercial polystyrene-supported- and in-house prepared solid-supported-triphenylphosphine **146** (Figure 11). Elemental analysis was determined using energy dispersive x-ray spectroscopy (EDX) of the in-house polymer-supported triphenylphosphine **146** and compared to the commercial polystyrene-supported triphenylphosphine, which revealed a phosphorus loading of 1.85 mmol/g for **146** vs 3.00 mmol/g for polystyrene-supported triphenylphosphine.

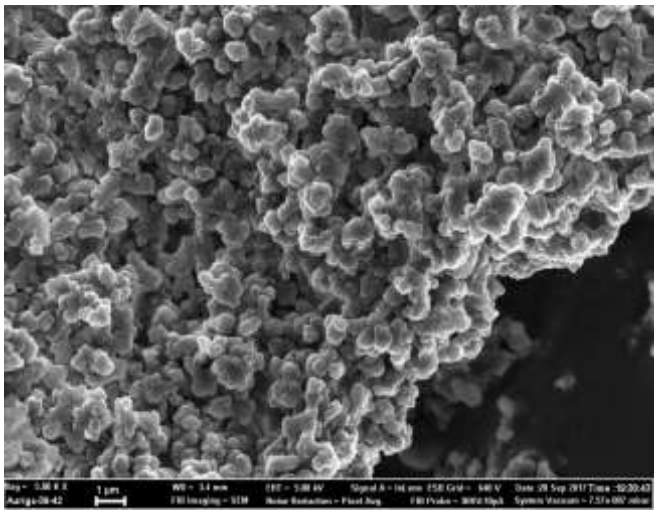

Figure 10: SEM surface analysis of in-house polymer-supported triphenylphosphine at 5.00 K X, 1 µm, 5.00 kV

© University of Pretoria

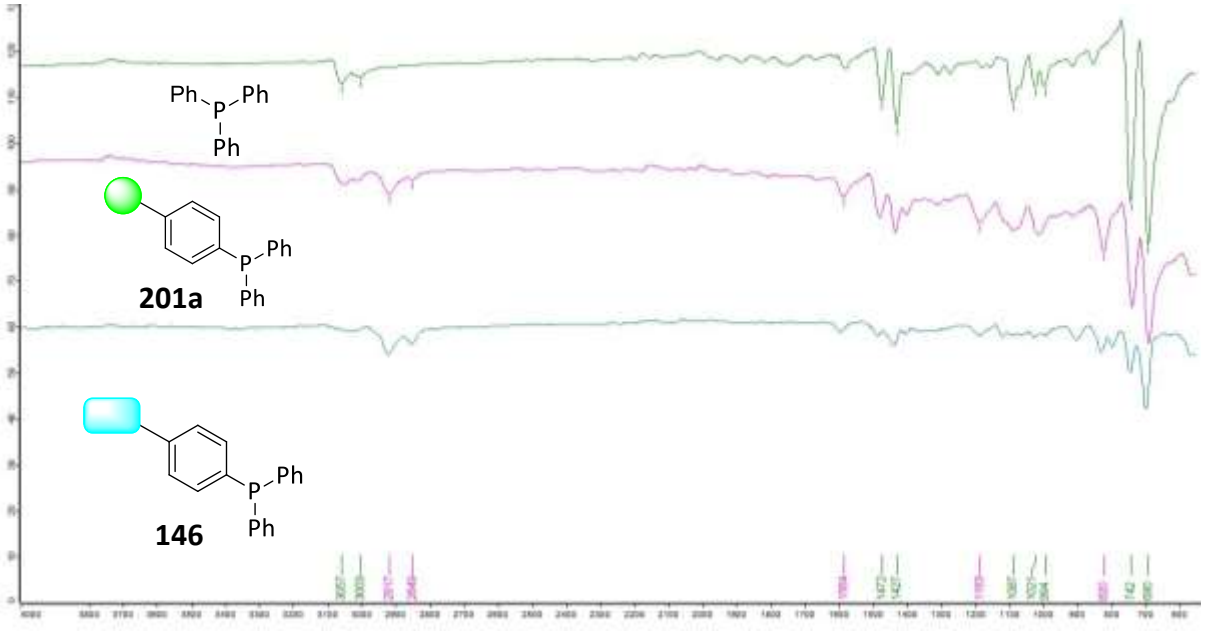

Figure 11: FTIR spectra comparison of unsupported- (top), polystyrene-supported- (middle) and in-house polymer-supported triphenylphosphine (bottom)

Cost analysis was conducted for the synthesis of the in-house prepared polymer-supported triphenylphosphine **146** and was compared with commercial reagents. The synthesis of one gram of polymer-supported **146** reagent was R195.43, Table 3. A price comparison with commercial reagents revealed our polymer to be cheaper than reagents from Sigma Aldrich (R187.57 and R197.57 cheaper) but slightly pricier than Fluorochem (R47.43 excess) and Rapp polymere (R17.03 excess), Table 4.

Table 3: Cost of making 1 g of in-house polymer-supported triphenylphosphine **146**

Entry	Reagent	Mass needed (g)	Price/g[a]
1	diphenyl-(4-vinylphenyl)phosphine	0.668	R191
2	Divinylbenzene	0.404	R2
3	Styrene	0.092	R0.06
4	Dodecanol	0.90	R2.24
5	Dibenzoyl peroxide	0.0014	R0.13
			R195.43

[a] Calculated using prices from Sigma Aldrich

© University of Pretoria

Table 4: Cost comparison of commercial polymer-supported triphenylphosphine with in-house prepared polymer **146**

Entry	Company	Loading (mmol/g)	Price/g	Price/5g
1	Sigma Aldrich	3.0	R383	R1915
2	Sigma Aldrich	1.6	R393	R1965
3	Fluorochem[a]	1.4-2.0	R148.10	R740
4	Rapp polymere[b]	1.0-1.5	R178.40	R892.06
5	In-house polymer	1.85	R195.43	R977.15

[a] Pound exchange rate = R21.16, [b] Euro exchange rate = R18,98

3.3. Flow synthesis

3.3.1. In-house polymer-supported triphenylphosphine using precipitation polymerization

To afford a monolithic form of the reagent, using the same stoichiometric quantities as in batch,[70] the polymerisation was carried out in a 10 mL glass Omnifit™ column which was sealed at both ends and allowed to polymerize upright in a standard convection oven at 92 °C over 48 hours. Upon cooling, the column was mounted to a heating block on a Uniqsis FlowSyn SS reactor (Figure 12).

© University of Pretoria

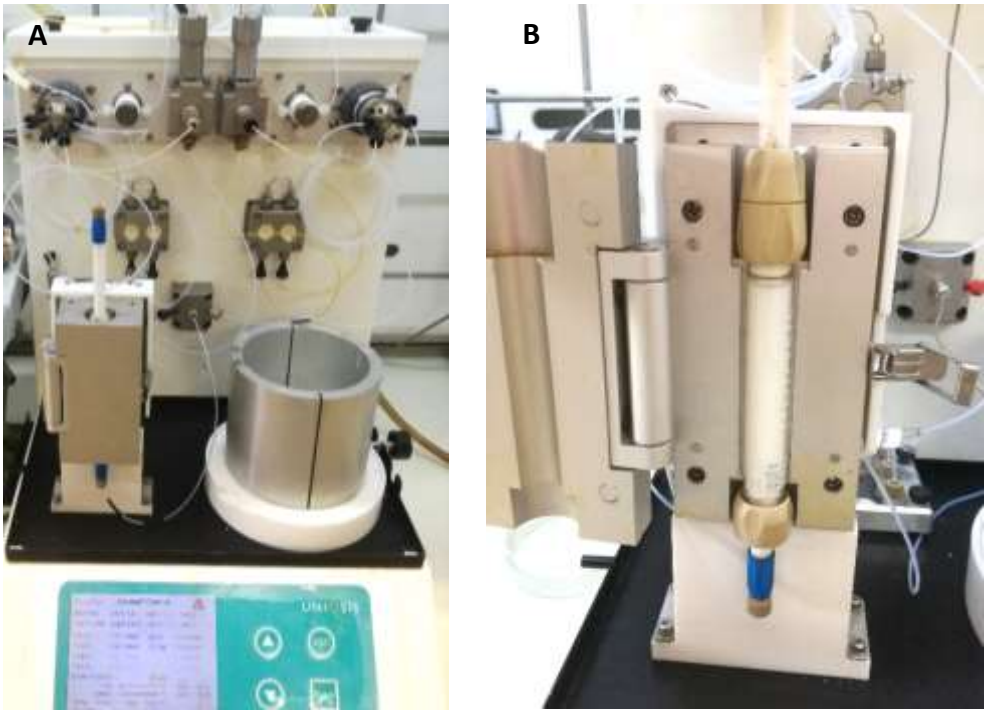

Figure 12: Uniqsis FlowSyn SS reactor (**A**), 10 mL glass Omnifit™ on heating block (**B**)

Attempts were then undertaken to remove the porogen by pumping a stream of heated dichloromethane (60 ˚C) through the monolith. Unfortunately, even in the absence of a back pressure regulator (BPR) and at low flow rates (~0.01 mL/min) we were unable to reproducibly wash the monolith (Table 5, entry 1). Furthermore, in our hands we found the approach to be undesirable, as in order to achieve workable flow rates (up to 1.0 mL/min) the approach required washing over a period of three days with constant change in the solvent direction of flow to avoid pressure build up. The process was repeated using 1,1'-azobis(cyanocyclohexane) (ACHN) as a radical initiator, however, this resulted in a solid monolith that could also not be washed with dichloromethane at 0.01 mL/min (Table 5, entry 2). Optimizations were attempted to study the influence polymerisation time had on the flow rate. A decrease of the time by half to 24 hours (Table 5, entry 3) improved the flow rate to 0.1 mL/min and a second decrease by half to 12 hours (Table 5, entry 4) further improved the flow rate to 0.25 mL/min, but this was still not adequate. As such we reverted to using benzoyl peroxide and again reduced the polymerisation time by half to 24 hrs (Table 5, entry 5), which showed no improvement from 48 hours (Table 5, entry 1). Further reduction of the time to 12 hours gave a maximum flow rate of 0.25 mL/min (Table 5, entry 6). At 6 hours polymerization time (Table 5, entry 7) a gel-like monolith was observed. In an attempt to increase the number of pores in the monolith, we opted to double the amount of porogen

© University of Pretoria

with heating for 48 hours, but this also resulted in the formation of a unpolymerized gel-like monolith (Table 5, entry 8). Formation of a monolith in the absence of the porogen gave a clear crystalline monolith which could not be washed (Table 5, entry 9).

Table 5: Monolith optimisation on Flow

Entry	Radical initiator	Polymerisation time (hrs)	Maximum washing flow rate achieved (mL/min)
1	Benzoyl peroxide	48	0.01
2	ACHN	48	0
3	ACHN	24	0.1
4	ACHN	12	0.25
5	Benzoyl peroxide	24	0.01
6	Benzoyl peroxide	12	0.25
7	Benzoyl peroxide	6	0
8	Benzoyl peroxide	48 [a]	0
9	Benzoyl peroxide	48 [b]	0

Reaction conditions: [a] Double volume of porogen used; [b] absence of porogen

Considering these inconsistencies and reproducibility issues, we made a decision to rather polymerise the monolith using the conditions outlined in entry 1 and grind the resultant monolith into small particles in order to employ a packed-bed reactor (PBR) approach. All flow reactions would then be conducted using a batch synthesized, crushed, in-house polymer-supported triphenylphosphine reagent **146**. We further felt that the latter approach, although not achieving the high surface contact typical of a monolithic support, is more easily implemented and if required, is more amenable to scale-up, as traditional monoliths cause a build-up of pressure and are difficult to synthesise without specialized internal supports on large-scale.

© University of Pretoria

Chapter 4

Application of triphenylphosphine reagents to ozonolysis reaction

4.1. Introduction

Ozonolysis is the cleavage of an alkene by ozone to either produce two carbonyl compounds or, in the case of cyclic alkenes, to form dicarbonyl compounds The mechanism begins with a 1,3-dipolar cycloaddition, a one-step five-membered ring-forming reaction between two conjugated compounds in which two new single bonds are formed joining the two reagents at each end, between the alkene and ozone to form an unstable molozonide intermediate. In an aprotic solvent such as dichloromethane, the unstable intermediate then undergoes a cycloreversion, reaction to form a carbonyl and carbonyl oxide intermediates, re-orientation of the resulting species and a second cycloaddition affording the more stable ozonide. However, in the presence of a protic solvent such as methanol, the molozonide forms hydroperoxide and carbonyl intermediates. This is then followed by a reduction, typically mediated by triphenylphosphine or dimethyl sulfide, to yield the aldehyde/ketone products (Scheme 59).

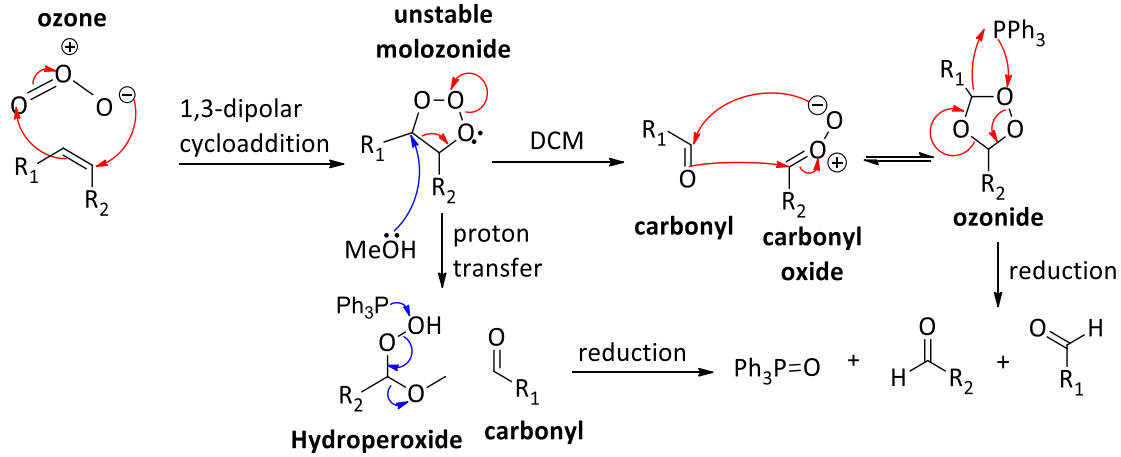

Scheme 59: Ozonolysis reaction mechanism

There are a few difficulties associated with ozonolysis: (i) the safety risks associated with handling explosive ozonide species; (ii) the work-up with both triphenylphosphine and dimethyl sulfide is challenging, as triphenylphosphine is difficult to separate from the products it requires complex column chromatography purification and to remove dimethyl sulfide requires large quantities of aqueous washing, and (iii) the need for low temperatures

© University of Pretoria

is problematic as industrial processes rarely go below -30 °C due to the costs associated with cooling on scale.

We have developed a novel means of conducting ozonolysis in flow which allows the reactions to be performed safely at higher temperatures and this approach forms part of the PhD research of Ms Nicole Neyt (UP) and will be disclosed in detail in her thesis (currently under preparation). Herewith we investigated the use of solid-supported reagents to further improve the reductive workup to access aldehydes and ketones. The conventional used triphenylphosphine reductant is often not used due to difficulties associated with downstream separation from the desired products. Our approach improves purification by employing an easier clean-up through simple removal of the spent immobilised triphenylphosphine by filtration and is cheaper with respect to solvent usage.

4.2. Batch Synthesis

4.2.1. Model Study

Initially a model study was conducted in batch looking at the conversion of styrene **143** into benzaldehyde **143a** (Scheme 60), in order to determine the following conditions: (i) optimal concentration of the substrate stock solution (ii) optimal reaction temperature.

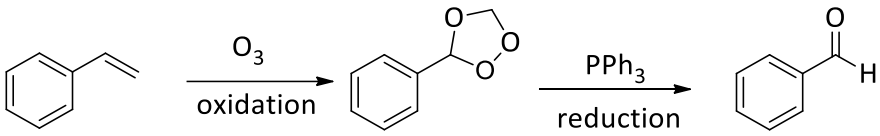

143 **143a**

Scheme 60: Ozonolysis of styrene

The ozonolysis reaction is usually conducted at a low temperature (-78 °C) in order to stabilize the ozonide formed. In addition, the use of mixtures of protic and aprotic solvents have been reported to increase solubility and maximize the yield of the aldehydes, while minimizing the production of carboxylic acids. As a result, mixed solvent systems comprised of dichloromethane and alcoholic solvents are commonly used.[91]

We elected to proceed with a 1:1 dichloromethane and methanol solvent system for reduction of styrene to benzaldehyde. The first step transforms the alkene to the ozonide and is usually evidenced by the appearance of a blue colour in the reaction mixture, which is an indication of excess ozone in the solution after all the alkene has reacted. However, as this

© University of Pretoria

colour is very faint at low solution concentrations and could easily be missed, we opted to use Sudan Red dye which turns the solution from red to colourless when all of the alkene has been consumed. The batch setup involves bubbling ozone gas through a polytetrafluoroethylene (PTFE) tube into a flask containing the coloured solution. The amount of ozone bubbling into the alkene solution was carefully controlled through a needle valve to prevent splashing and evaporation of the solvent. Once the reaction was complete, it was necessary for oxygen to be bubbled through the ozonide solution in order to remove any unreacted ozone still in solution that could complicate the subsequent reduction step. This was then followed by addition of triphenylphosphine to obtain the aldehyde product (Scheme 61).

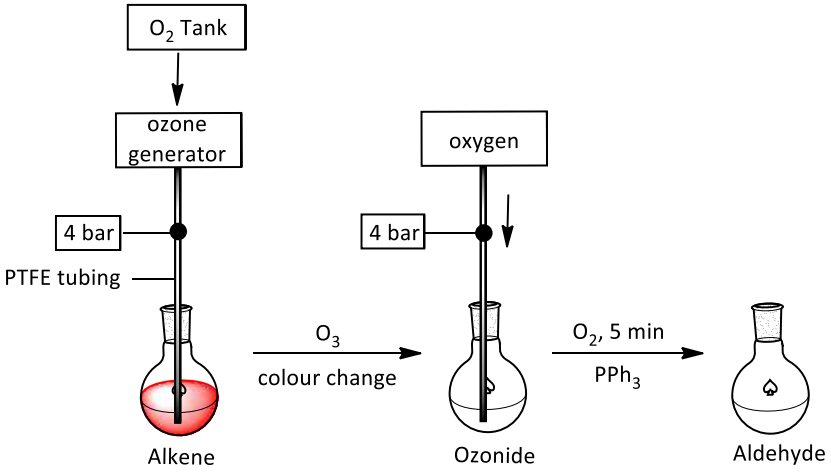

Scheme 61: Representation of ozonolysis batch reaction on model substrate

4.2.2. Optimisation of reaction concentration and reaction time

We began by studying the relationship between the reaction concentration and the time taken to form the ozonide. Using the setup described in Scheme 61, the reaction was conducted in a dichloromethane:methanol mixture and was monitored by observing the colour change from red to colourless. This was followed by treatment with triphenylphosphine to obtain the desired aldehyde. The reaction was first conducted at room temperature using a 0.5 M solution (10 mL) to find out if the ozonide was stable at this concentration. After reduction, work-up and chromatography to remove triphenylphosphine oxide and formaldehyde by-products, the results were obtained and indicated 76% yield of the aldehyde, suggesting that in the case on hand that the hydroperoxide was stable at ambient temperature. Completion of the reduction step was monitored by dipping peroxide

© University of Pretoria

strips into the solution. The strips turned blue when there was still peroxide in the solution and cream colour upon consumption of the hydroperoxide intermediate. The reduction step was completed after 5 minutes to form the aldehyde. Evidence of the product was determined using ^{1}H NMR spectroscopy, which revealed a singlet at 10 ppm (red spectrum) and shift of the aromatic peaks from between 6.5 and 7.5 ppm to between 7.5 and 8 ppm, due to the presence of a carbonyl functional group as well as the absence of the alkene peaks of styrene between 5 and 6 ppm (blue spectrum) (Figure 13).

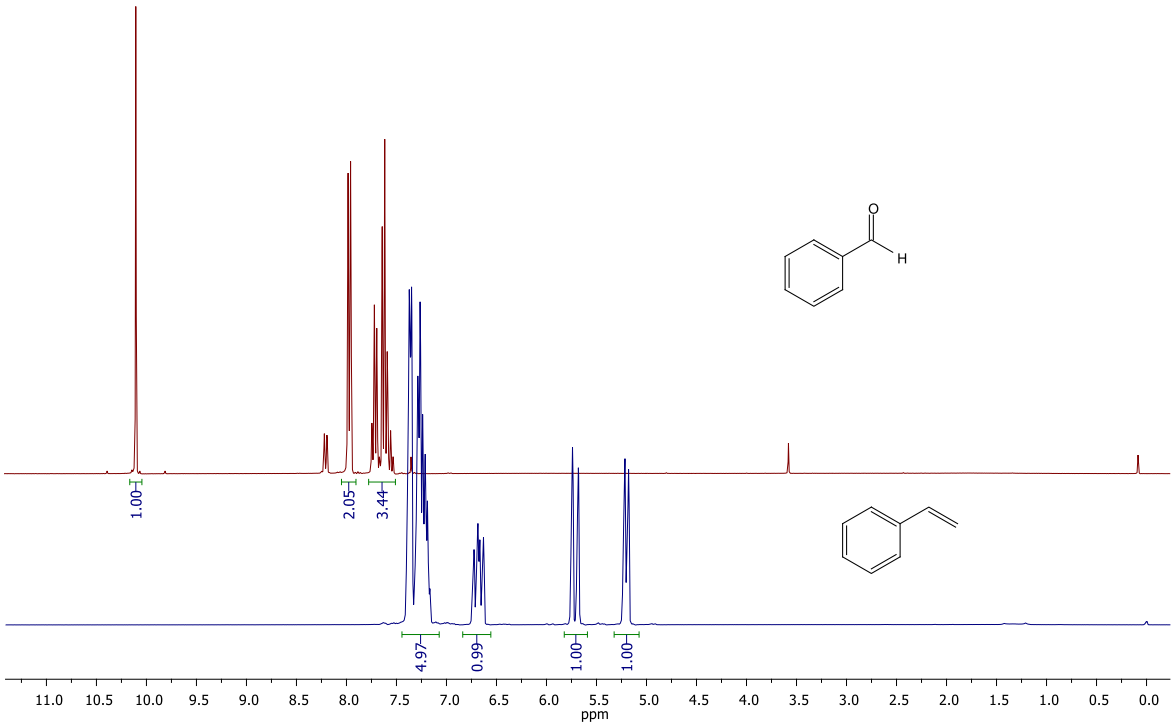

Figure 13: ^{1}H NMR spectra comparison between styrene (blue) and benzaldehyde (red)

The concentration study continued at room temperature but now using 0.1 M solution of styrene in which the taken time for the reaction to complete was reduced, with complete ozonolysis (monitored by colour change from red to colourless) occurring at 86 minutes for 5.76 mmol of starting material (Table 6, entry 4). Therefore, in this example the lower the concentration of the solution the faster the ozonolysis reaction occurs because the amount of ozone relative to starting material increases with decreasing concentration, for example 0.1 M running for 86 minutes vs 0.5 M running for 121 minutes.

© University of Pretoria

Table 6: Optimization of concentration vs reaction time

Entry	Concentration (M)	Hydroperoxide formation time (min)	% Yield[a]
1	0.5	121	76
2	0.3	94	74
3	0.25	90	75
4	0.1	86	76

Reaction conditions: [a] Isolated yield after reduction

4.2.3. Optimisation of reaction temperature

We then proceeded to do a study to determine what effect the temperature had on product formation, using a 0.1 M solution of styrene in a dichloromethane:methanol mixture. Interestingly, at lower temperatures (Table 7, entries 2-4) the formation of the desired benzaldehyde was not observed, as evidenced by absence of the distinct aldehyde singlet at 10 ppm. We then tested whether forming the hydroperoxide at a cold temperature, then warming the solution to room temperature before reduction, had any effect on the outcome. The aldehyde was indeed observed, and the product was collected in 75% yield (Table 7, entry 5), which was similar to the 76% yield observed at room temperature (Table 7, entry 1).

Table 7: Optimization of temperature vs reaction time

Entry	Temperature (°C)	Hydroperoxide formation time (min)	% Yield[a]
1	25	86	76
2	0	70	-
3	-10	75	-
4	-40	80	-
5	-10[b]	75	75

Reaction conditions: [a] Isolated yield after reduction; [b] solution warmed to room temperature before reduction

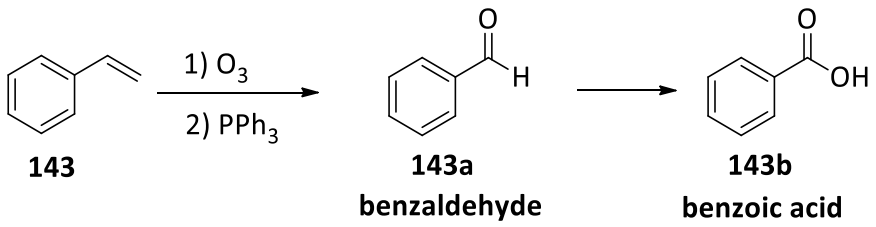

143 **143a benzaldehyde** **143b benzoic acid**

Scheme 62: Oxidation to benzoic acid

© University of Pretoria

From the spectra (Figure 14, orange and green spectra) it was evident that reduction using triphenylphosphine favoured warmer temperature conditions. Analysis of the spectra suggested that at cold temperatures, after reduction to benzaldehyde the oxidation occurred to form benzoic acid **143b** (Scheme 62). Figure 15 shows a spectral comparison between commercial benzoic acid and the formed carboxylic acid by ozonolysis of styrene at cold temperatures.

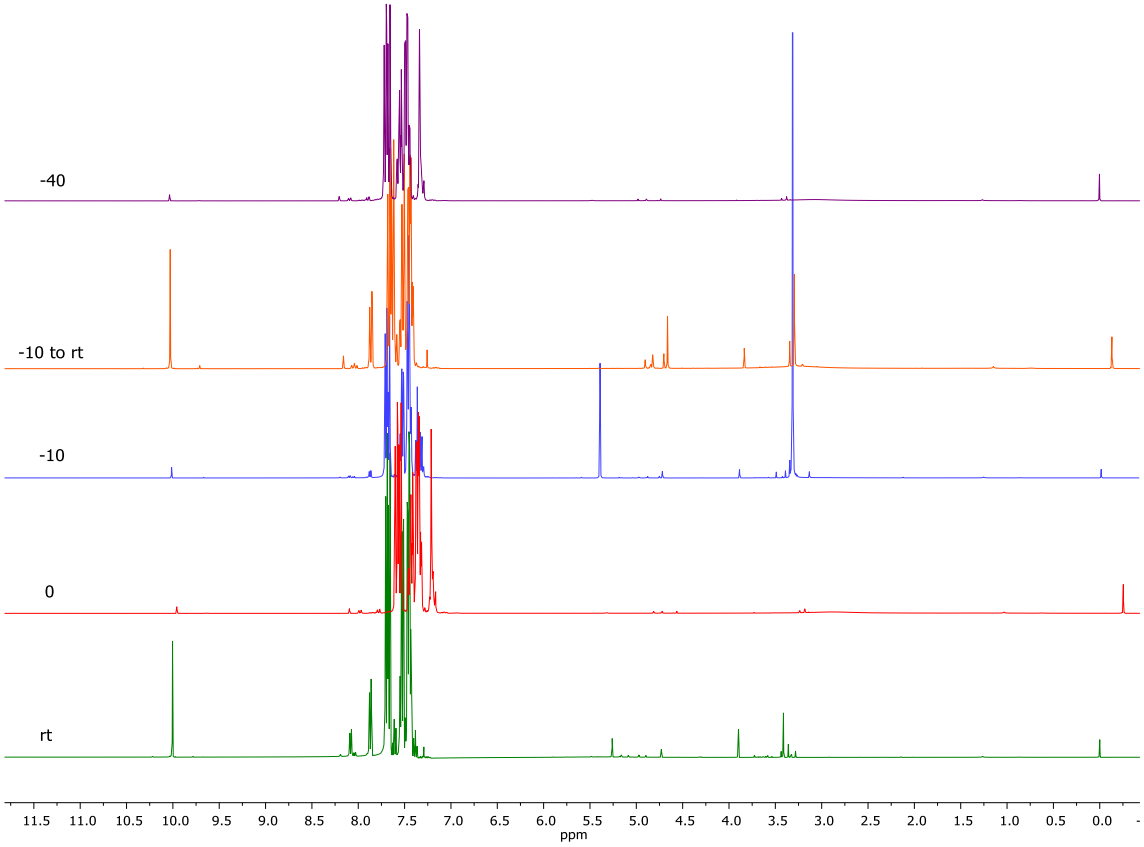

Figure 14: ^{1}H NMR spectra showing temperature comparison for the ozonolysis of styrene; benzaldehyde (orange and green) and benzoic acid (purple, blue and red)

© University of Pretoria

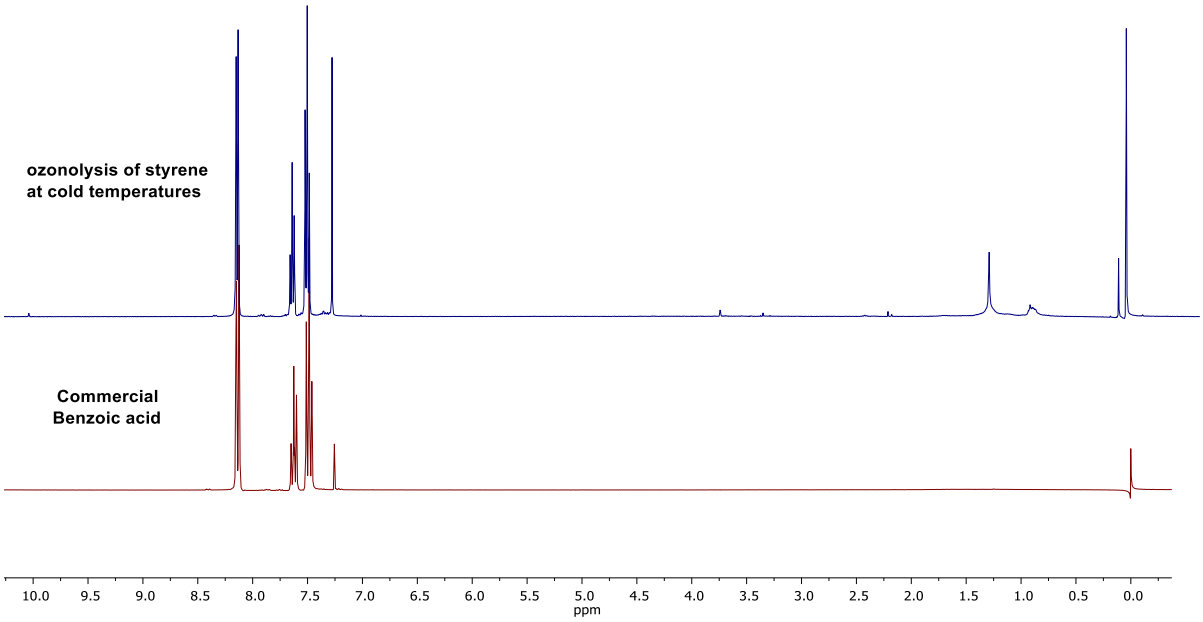

Figure 15: ^{1}H NMR spectra comparison of commercial benzoic acid (red) and ozonolysis of styrene at cold temperatures (blue)

To verify that the reduction step requiring room temperature was not substrate dependant, the conditions were applied to cyclohexene **202** and *n*-hexene **203** (Scheme 63). Results of the proton spectra (Figure 16) indicated that at room temperature, ozonolysis was favoured for aromatic (from before), cyclic and alkyl substrates.

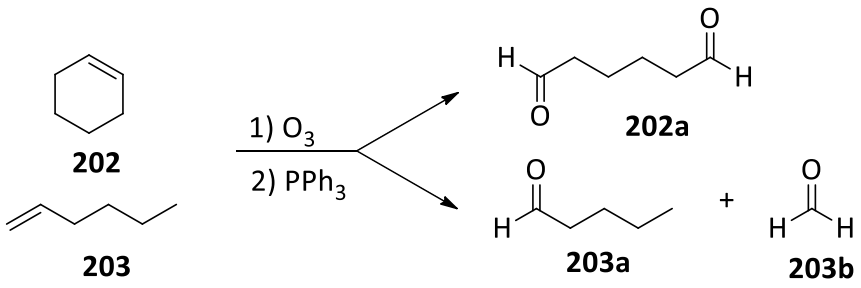

Scheme 63: Ozonolysis of cyclohexene and hexene

© University of Pretoria

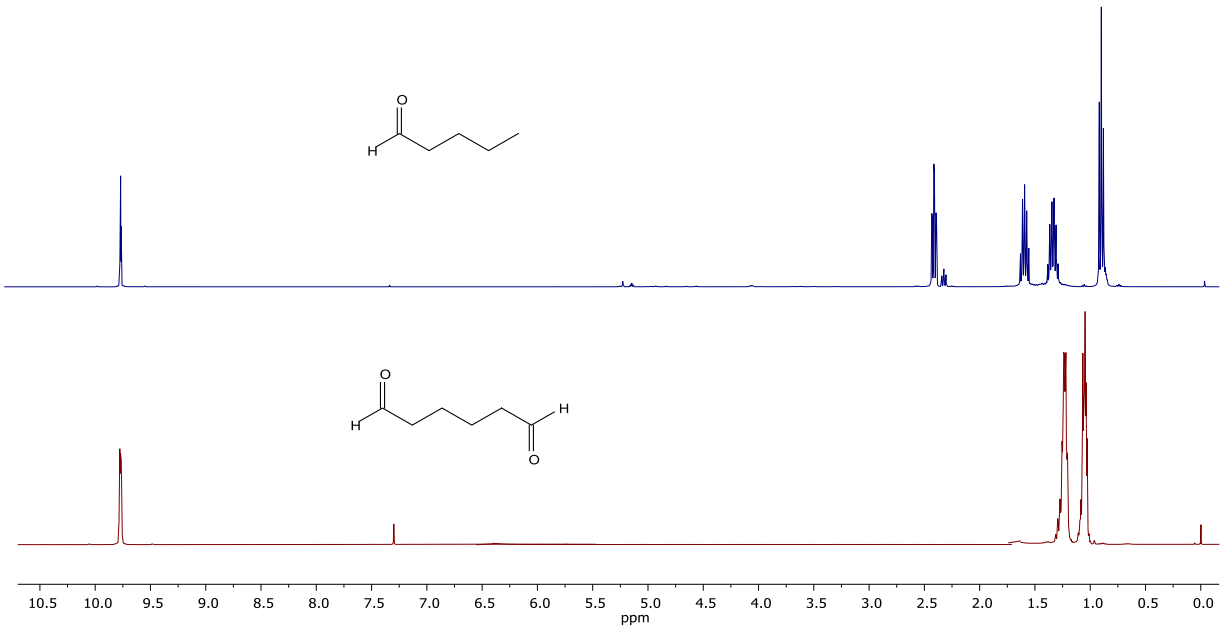

Figure 16: ^{1}H NMR spectra of pentanal (blue) and hexanedial (red)

4.3. Flow synthesis

Our group has developed an ozonolysis continuous flow system made up of an inner solvent tube housed inside an outer tube where gas flows through wherein reactions can be performed at higher temperatures, faster and with continuous removal of ozone gas (Figure 17).

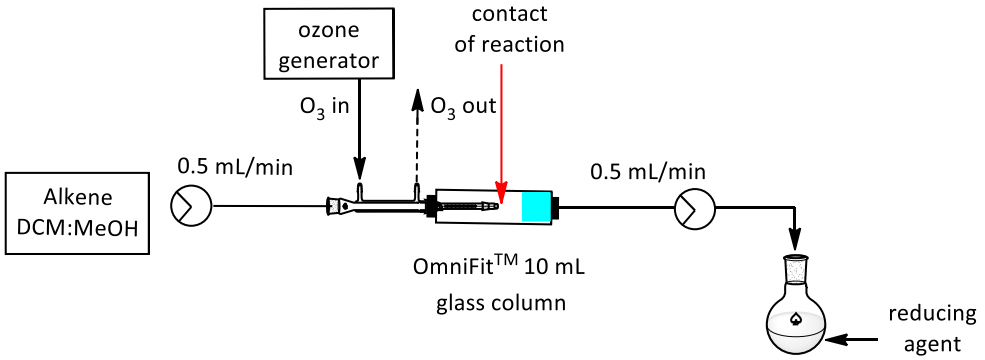

Figure 17: Schematic representation of ozonolysis flow setup*

The newly developed ozone flow system was used to test the scope of our in-house polymer-supported triphenylphosphine and its efficacy relative to the commercial reagents. The alkene substrates were pumped into the column where reaction with the ozone occurred at

* Reactor design reported herein developed and prototyped by Ms Nicole Neyt (PhD) candidate) and forms part of her PhD research (thesis under preparation). Operational details will be discussed there.

© University of Pretoria

room temperature. The hydroperoxide stream then pumped into a flask at room temperature housing the reducing agent. The overall results using the commercial unsupported triphenylphosphine reagents, commercial supported triphenylphosphine **201a** and in-house prepared polymer-supported triphenylphosphine **146**, and alkene substrates are shown in Table 6. Reactions were conducted using 1.0 equivalent of the alkene with 2.5 equivalents of triphenylphosphine reagent at an overall flow rate of 1.0 mL/min. It was noted that higher flow rates resulted in the reactions not reaching completion. It took only five to ten minutes for each reduction to occur, monitored by peroxide strips, when using unsupported triphenylphosphine but there was a significant increase in reaction times when using the supported triphenylphosphine reagents which were filtered after 48 hours for yields greater that 50%. Only one equivalent of polymer-supported reagent **146** was needed to reduce the hydroperoxide in contrast to the four-fold excess of commercial supported triphenylphosphine needed for conversions greater than 50%. From Table 8 it is noted that product yields decreased slightly when using supported triphenylphosphine in comparison to the unsupported triphenylphosphine. This was thought to be due to incomplete conversion of what appeared to be hydroperoxide even after 48 hours. We could however, conclude that the in-house polymer-supported reagent was an improvement over the commercial supported reagent as higher yields were obtained with only one equivalent of reagent. The observed lower product yield for alkyl alkenes was due to the formation of formamide co-products (Table 8, entries 4 and 5).

© University of Pretoria

Table 8: Ozonolysis flow results comparison between commercial unsupported, commercial supported **201a** and in-house prepared polymer-supported triphenylphosphine **146**

Entry	Alkene	Aldehyde	% Yield[a]		
			PPh_3	201a	146
1	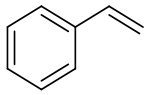 **143**	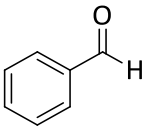 **143a**	76	67	70
2	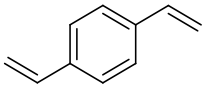 **142**	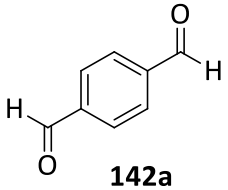 **142a**	74	67	69
3	**202**	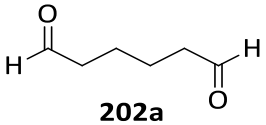 **202a**	73	66	68
4	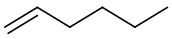 **203**	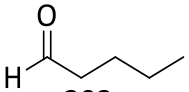 **203a**	65	55	58
5	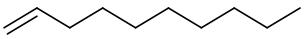 **204**	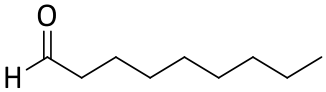 **204a**	63	52	55
6	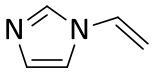 **205**	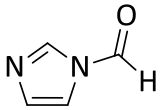 **205a**	68	62	64

Reaction conditions: 0.1 M alkene solution, 2.5 equivalents of reducing agent, [a] isolated yield

4.4. Conclusion

In conclusion, we have demonstrated the conversion of alkenes to aldehydes using unsupported-, polystyrene-supported and in-house synthesized polymer-supported triphenylphosphine **146** using our newly developed in-house ozonolysis flow setup achieving moderate to high yields (55-70%) using in-house polymer-supported reagent **146**. Reactions were conducted using a concentration of 0.1 M to promote faster conversion of the alkene into the hydroperoxide and carried out at room temperature, as cooled temperatures favoured the formation of benzoic acid. Furthermore, we have shown that the in-house polymer-supported reagent **146** gives an improvement relative to the commercial

© University of Pretoria

polystyrene reagent, with the advantage of one-fold versus four-fold of material used when reducing the ozonide to the aldehyde and also giving higher yields than the commercial polystyrene-supported reagent. However, the disadvantage of our in-house polymer-supported reagent is the difficulties of large scale production where crushing and washing the reagent would require much effort.

© University of Pretoria

Chapter 5

Preparation of immobilized phosphonium salts and their use in the Wittig reaction

5.1. Introduction

The mechanism of the Wittig reaction begins with the formation of a phosphonium salt by the reaction of an alkyl/benzyl halide with triphenylphosphine via an S_N2 reaction, which is followed by treatment with a base to form the ylide. The ylide then reacts with an aldehyde via a [2 + 2] cycloaddition setup which forms a four-membered intermediate, oxaphosphetane. This intermediate then undergoes a reverse [2 + 2] cycloreversion, resulting in the formation of an alkene and a triphenylphosphine oxide by-product (Scheme 64).[92]

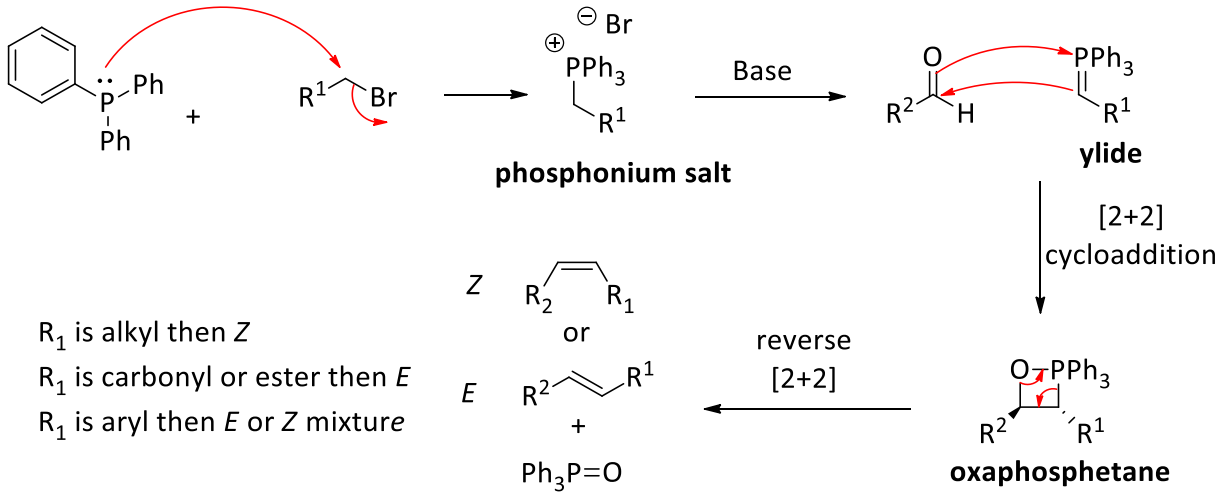

Scheme 64: Wittig reaction mechanism

The stereoselectivity of the alkene is dependent on the nature of the ylide and is readily predicted. If the substituent on the carbon atom of the ylide is one that is conjugated or anion stabilizing such as carbonyl groups, the ylide is termed as stabilised and will highly produce a *E* selective alkene.[93] The stabilized ylides are really stable but not very reactive, and as such the phosphonate ester is often used instead. This modification is called the Horner–Wadsworth–Emmons and the phosphonate esters are deprotonated using strong to give enolate- type anions that react with the aldehydes to give the *E*-alkenes. If the substituent is not conjugated it is termed unstabilised and will highly produce a *Z* isomer. However, if the ylide is semi-stabilised such as aryls then the *E/Z* selectivity is often poor.[94]

© University of Pretoria

Chapter 5 Preparation of immobilized phosphonium salts and their use in the Wittig reaction

In this chapter we describe the conversion of commercial unsupported-, commercial polystyrene- and in-house polymer-supported triphenylphosphine into phosphonium salts. These reagents were then used in the Wittig reaction to transform various aldehydes to form alkenes and comparison of the results were obtained for both batch and flow applications.

5.2. Batch Synthesis

5.2.1. Synthesis of unsupported and polystyrene-supported phosphonium salts

A specific selectivity was not a target and thus we chose to use the semi-stabilised aryl ylide. Thus, we initiated the study by first synthesizing the unsupported phosphonium salt **206** from benzyl bromide and triphenylphosphine, followed by treatment with a base to form the ylide **207** (Scheme 65). Since under basic Wittig conditions the ylide can form *in situ*, it was only necessary to synthesize the supported phosphonium salts. Thus, synthesis of polystyrene-supported phosphonium salt **208** was achieved by reacting commercial polystyrene-supported triphenylphosphine with benzyl bromide for 48 hours (Scheme 66). It was necessary to leave the reaction for a longer time to ensure a 100% conversion to the phosphonium salt and the solvent was changed, as dimethylformamide was a better swelling solvent than dichloromethane.

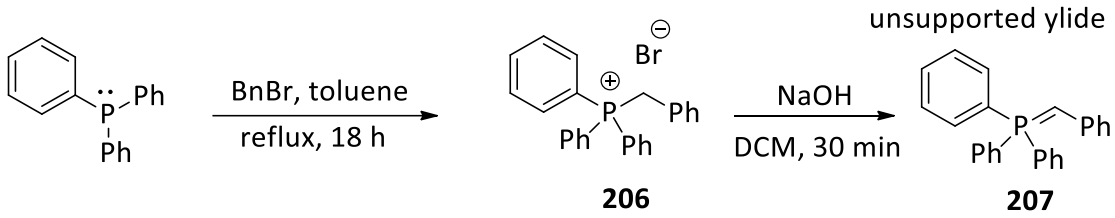

Scheme 65: Synthesis of unsupported ylide

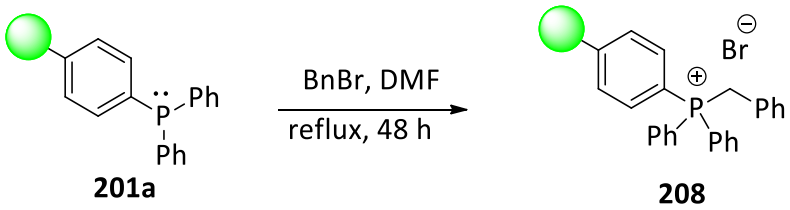

Scheme 66: Synthesis of polystyrene-supported benzyl phosphonium salt

Analysis using ^{31}P NMR was conducted and compared to the analogous unsupported phosphonium salt **207**, which revealed a comparable broad singlet peak at 23.19 ppm (Figure

© University of Pretoria

18). The downfield shift from -6.31 to 23.19 ppm was indicative of the transition from a free triphenylphosphine to a quaternary phosphine reagent.

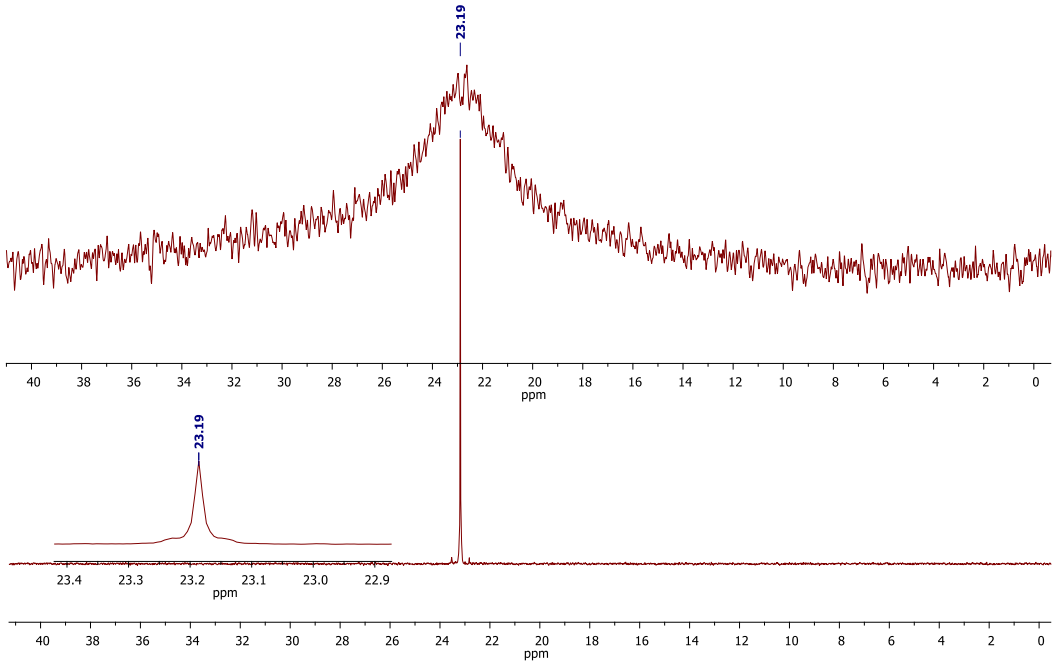

Figure 18: ^{31}P NMR comparison between in-house polystyrene-supported (top) and unsupported (bottom) benzyl salt

5.2.2. Synthesis of in-house polymer-supported phosphonium salt 209

Thereafter, the synthesis of in-house polymer-supported phosphonium salt **209** was achieved by reacting in-house polymer-supported triphenylphosphine **146** with benzyl bromide (Scheme 67). Unlike the polystyrene-supported phosphonium salt, the in-house polymer-supported reagent would not swell in the deuterated solvent to perform the desired NMR analysis. Therefore, IR spectroscopy was used which revealed comparable P-C peaks for all three reagents (Figure 19).

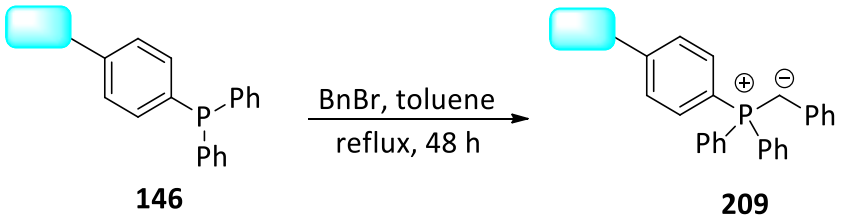

146 **209**

Scheme 67: Synthesis of in-house polymer-supported phosphonium salt

© University of Pretoria

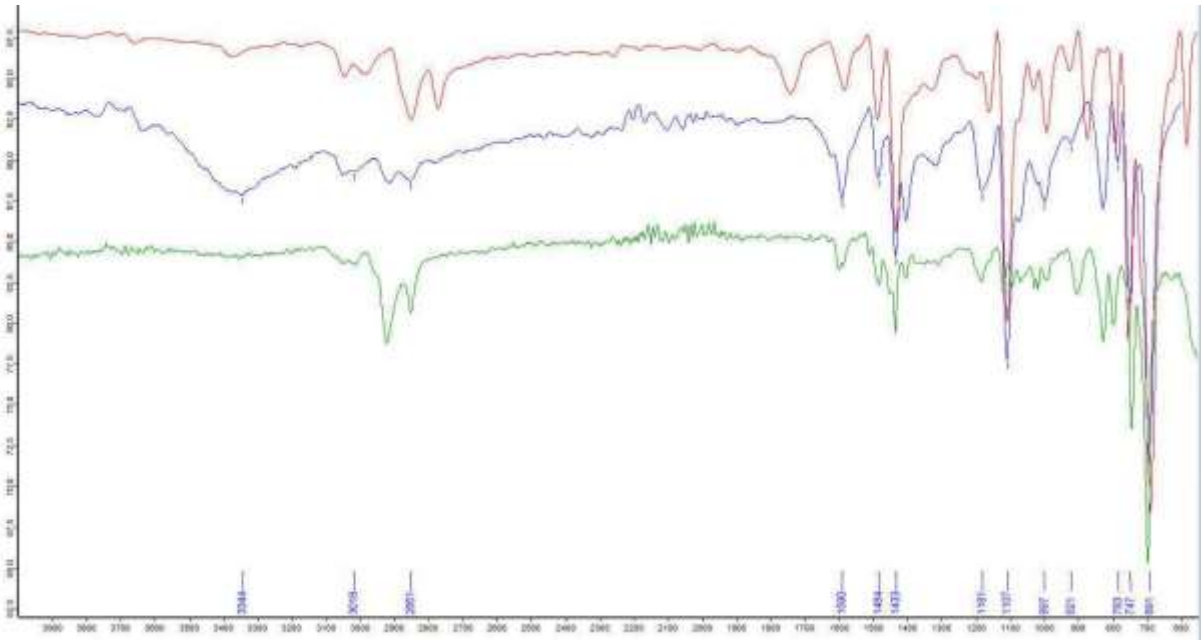

Figure 19: FTIR spectra of unsupported- (red), polystyrene-supported- (blue) and in-house polymer-supported (green) phosphonium ylide

In addition, phosphorus and bromide elemental loadings were calculated using EDX spectroscopy for each benzyl salt (Table 9). The unsupported and in-house polymer-supported salts, **209**, revealed double the amount of phosphorus loading than the polystyrene-supported salt, **208**. Similarly, the bromide loading of the unsupported salts was double that of the in-house polymer-supported salt **209** and six times that of the polystyrene salt. This was not an issue as the bromide did not play a role in the Wittig reaction, but double the stoichiometric amount of polystyrene-supported salt would have to be used for comparable results.

Table 9: Elemental loading of the benzyl phosphonium salts

	Phosphonium salt		
Elements	**Unsupported 206** (mmol/g)	**Polystyrene-supported 208** (mmol/g)	**In-house solid-supported 209** (mmol/g)
Phosphorus	1,969	0.8179	1.614
Bromide	2,073	0.3170	1.042

© University of Pretoria

The SEM analysis of the samples at five thousand times magnification revealed trapezoid shaped crystals for the unsupported-benzyl salt, Figure 20A, a sub-micromolar particle size for in-house polymer-supported benzyl salt **209** (due to the polymeric backbone) Figure 20B and irregular shaped beads polystyrene-supported salts **208** due to breakdown caused by stirring, Figure 20C.

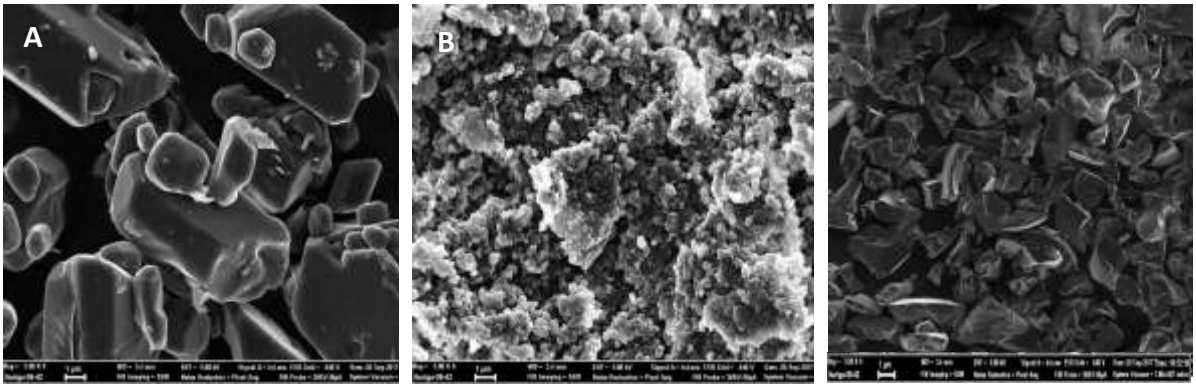

Figure 20: SEM surface analysis of unsupported benzyl salt **A**, in-house polymer-supported benzyl salt **B** and polystyrene-supported salt **C** at 5.00 K X, 1 µm, 5.00 kV

Batch Wittig reactions using benzaldehyde **143a** as a substrate were conducted to find the optimal temperature. Initially a solution of 50% aqueous sodium hydroxide at room temperature was used as a base, but due to the high viscosity of the solution it would not be ideal for flow synthesis. Hence, the base solution was changed to 1.0 M sodium ethoxide (Scheme 68). It was important to prepare fresh sodium ethoxide and store it under argon for a maximum of two days to prevent degradation. Reactions were carried out in ethanol at room temperature using unsupported phosphonium salt. It was observed that increasing the phosphonium salt equivalents from 1.2 to 2.0 gave full conversion of starting material after thirty minutes, as monitored by TLC. When using supported phosphonium salts there was incomplete conversion of starting material (~30% yield), even after 18 hours of reaction time. Increasing the temperature to 60 °C improved the yield slightly to 40% while higher temperatures (90 °C) degraded the polymers (Table 10).

© University of Pretoria

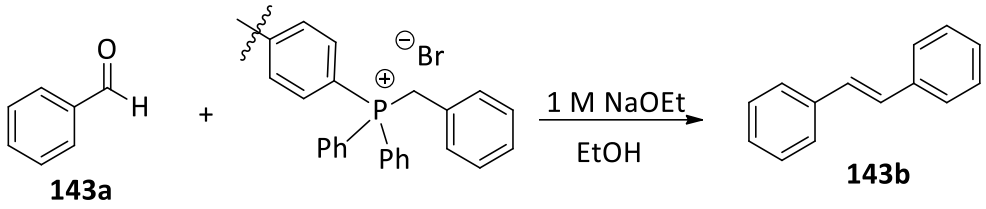

Scheme 68: Batch Wittig reactions

Table 10: Temperature optimisation of phosphonium salts

Entry	Temperature (°C)	% Yield from 143a		
		Unsupported salt 206	Polystyrene-supported salt 208	In-house polymer-supported salt 209
1	25	97	30	32
2	60	-	40	43
3	90	-	-	-

Reaction conditions: 1.0 eq. of aldehyde, 2.0 eq. of benzyl salt and 3.0 eq. NaOEt

5.3. Flow synthesis

5.3.1. Unsupported triphenylphosphine

The unsupported phosphonium salt could not be synthesized in flow due to formation of the oxaphosphetane precipitate which would result in blockage of the flow reactor tubes. Therefore, benzyl salt **206** prepared in batch was used and reaction optimizations were carried out on benzaldehyde as a model substrate using the Uniqsis FlowSyn SS reactor. The Wittig reaction proceeded with a stock solution of aldehyde (1.0 eq) and benzyl salt (2.0 eq) in ethanol (1.0 M), which were combined with a stock solution of sodium ethoxide (1.0 M) (1:3) at a T-piece mixer. Thereafter, the reaction stream was passed through a 14 mL coil, to allow enough contact time between the two reagents, followed by a 100 psi back pressure regulator (Scheme 69). The crude mixture was worked-up followed by column purification.

© University of Pretoria

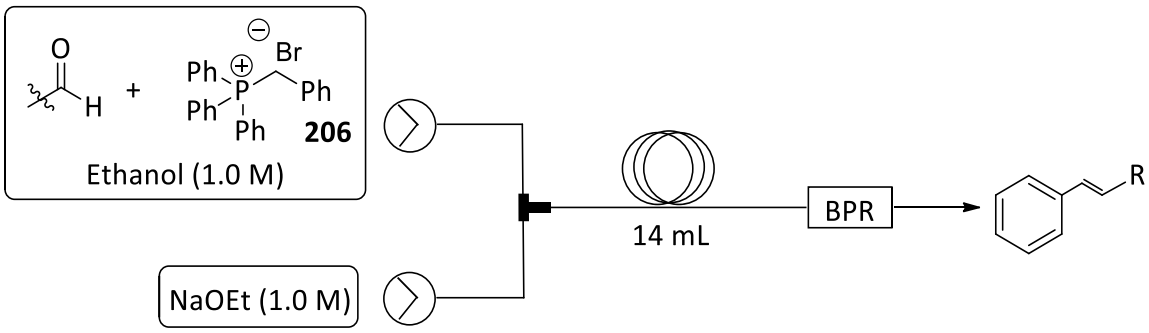

Scheme 69: Schematic flow setup for unsupported Wittig reactions

Reactions ran over an extended period of time at room temperature without reaching completion. Optimization of reaction conditions revealed that increasing the residence time and temperature improved the yield (Table 11, entries 2 to 4). Increasing the temperature to 60 °C with a 30 minutes residence time gave the optimum results, affording the product with a 100% yield (Table 11, Entry 6).

Table 11: Optimization of residence time using benzaldehyde

Entry	Temperature (°C)	Residence time (min)	% Yield
1	rt	15	23
2	rt	30	30
3	50	15	56
4	50	30	70
5	60	15	95
6	60	30	100

Reaction conditions: 1.0 eq. of aldehyde, 2.0 eq. of benzyl salt and 3.0 eq. NaOEt

5.3.2. Polystyrene-supported triphenylphosphine

A glass OmniFit™ column containing commercial polystyrene-supported triphenylphosphine **201a** was mounted into a Uniqsis FlowSyn SS column heating block and washed with dry toluene at 70 ˚C for five minutes. Thereafter, the system was loaded with benzyl bromide solution (0.2 M) at 0.2 mL/min (70 °C) with the output stream passed through a back pressure regulator and fed back into the reagent stock vessel to afford a simple recycling system

© University of Pretoria

(Scheme 70). This recycling process was to ensure maximum loading of benzyl bromide onto the support. The resulting loaded polymer-salt was then washed with dry toluene (0.2 mL/min, 70 °C) for one hour to wash off any unreacted benzyl bromide before yielding the phosphonium salt, **208a**.

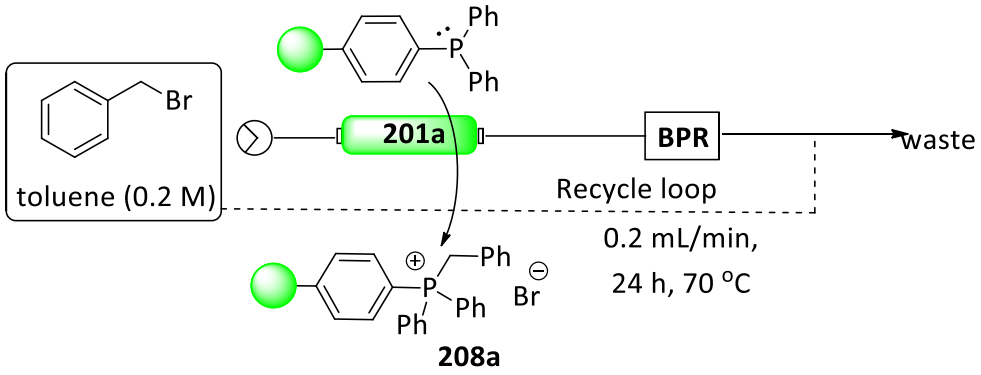

Scheme 70: Schematic flow setup for synthesis of polystyrene-supported phosphonium salt

The Wittig reaction setup was analogous to that used for the unsupported reagent, except that the coil reactor was replaced with a 10 mL glass OmniFit™ column housing **208a** (Scheme 71).

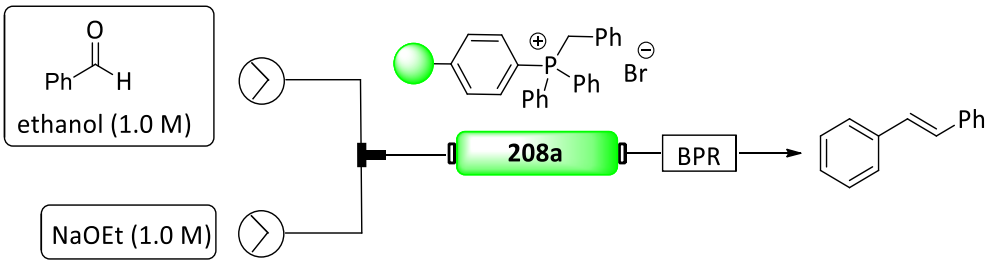

Scheme 71: Schematic flow setup for polystyrene-supported Wittig reactions.

A temperature versus residence time optimization was again conducted using benzaldehyde, as the model system (Table 12). No conversion was observed with reactions conducted at 30 °C, but doubling the temperature to 60 °C showed some improvement (Table 12, entries 1 to 4). After extending the residence time to 60 minutes the yield improved to 50% (Table 12, Entry 6). The flow rate could not be decreased further (due to residence time and amount of packed reagent in the column) to explore longer reaction times and at higher temperatures the polystyrene support degraded. As such, we selected to use the condition outlined in Table 12, Entry 6 as the standard conditions moving forward.

© University of Pretoria

Table 12: Optimisation of polystyrene-supported Wittig reaction using benzaldehyde

Entry	Column temp. (°C)	Residence time (min)	Flow rate (mL/min)	% Yield
1	30	15	0.133	0
2	30	30	0.092	0
3	30	60	0.052	0
4	60	15	0.133	30
5	60	30	0.092	42
6	60	60	0.052	50

Reaction conditions: 1.0 eq. of aldehyde, 3.0 eq. NaOEt and 200 mg of benzyl salt

5.3.3. In-house polymer-supported phosphonium salt 209

A PBR containing finely ground in-house polymer-supported triphenylphosphine **146** was mounted into a Uniqsis FlowSyn SS column heating block and washed with dry toluene. Thereafter, the system was loaded with benzyl bromide solution (0.2 M, 0.2 mL/min, 70 °C), with the output stream passed through a backpressure regulator and fed back into the reagent stock vessel to afford a recycling system for 24 hours (Scheme 72). The loaded column was then washed with dry toluene (0.2 mL/min, 70 °C) for one hour to collect any unreacted benzyl bromide before yielding the phosphonium salt **209a**.

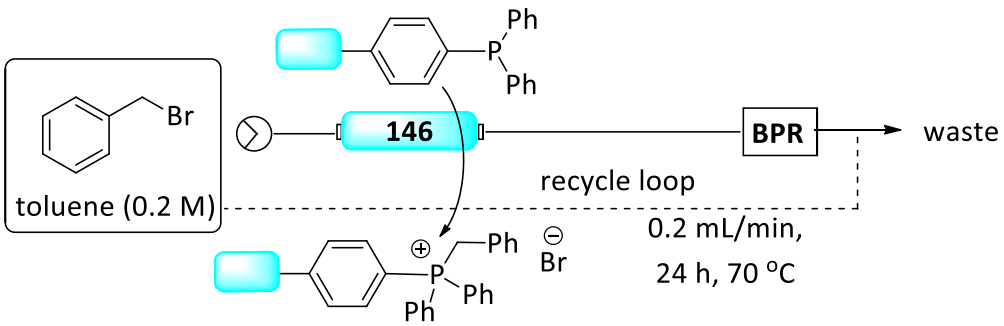

209a

Scheme 72: Schematic flow setup for synthesis of in-house polymer-supported phosphonium salt

© University of Pretoria

The in-house polymer-supported Wittig reaction setup was a replica of the polystyrene-supported approach (Scheme 73). Optimization of temperature versus residence time of benzaldehyde showed conversion at 30 °C, unlike the polystyrene-supported salt (Table 12, entries 1 to 3 vs Table 13, entries 1 to 3). Doubling the temperature had a positive influence on the yield (Table 13, entry 4) and leaving the reaction at an hour residence time gave 51% yield (Table 13, Entry 6). We again selected to use these conditions outlined as the standard conditions moving forward.

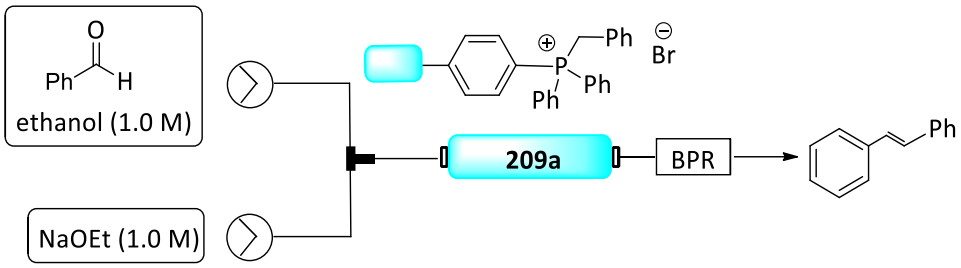

Scheme 73: Schematic flow setup for solid-supported Wittig reactions

Table 13: Optimization of solid-supported Wittig reaction using benzaldehyde in flow

Entry	Column Temp. (°C)	Residence time (min)	Flow rate mL/min	% Yield
1	30	15	0.133	10
2	30	30	0.092	15
3	30	60	0.052	24
4	60	15	0.133	38
5	60	30	0.092	42
6	60	60	0.052	51

Reaction conditions: 1.0 eq. of aldehyde, 3.0 eq. NaOEt and 200 mg of benzyl salt

5.4. Overall application to Wittig reactions in batch and flow

The overall results using the different benzyl phosphonium salts and aldehyde substrates in batch and flow optimised conditions are shown in Table 14. Reactions were conducted using 1.0 equivalent of aldehyde, 2.0 equivalents (proportion of phosphorus) of benzyl salt by and 3.0 equivalents of base. For flow synthesis, the supported phosphonium ylide was washed

© University of Pretoria

with ethanol for thirty minutes after each run (one hour residence time), to collect any product remaining on the column.

Table 14: Batch and flow comparison of Wittig reactions using unsupported-, polystyrene-supported- and in-house polymer-supported benzyl salt.

Entry	Aldehyde	Alkene	% Yield[a]					
			Batch			Flow		
			206	208	209	206	208a	209a
1	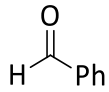 **143a**	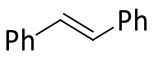 **143b**	97	40	43	95	50	51
2	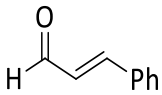 **210**	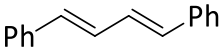 **210a**	88	32	44	82	28	49
3	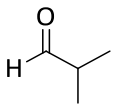 **211**	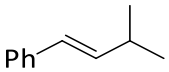 **211a**	96	38	23	84	42	25
4	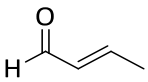 **212**	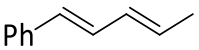 **212a**	98	42	24	91	40	27
5	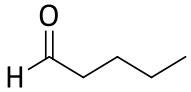 **213**	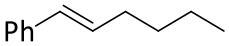 **213a**	98	35	20	83	51	22
6	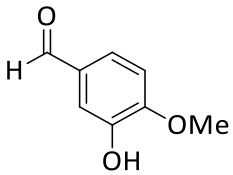 **214**	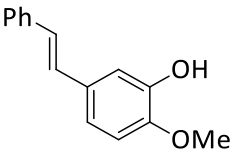 **214a**	83	40	24	61	35	27

Reaction conditions: [a] Isolated yield, unsupported (**206**), polystyrene- (**208**) and in-house polymer-supported (**209**)

From the table it is noted that product yields decreased significantly when using supported phosphonium salts in comparison to the unsupported salt. This was due to incomplete conversion of starting materials even after 18 hours of batch reaction time. It was observed

© University of Pretoria

that passage across a heated packed-bed reactor housing the phosphonium salts **208a** and **209a** afforded comparable yields to those obtained under batch conditions, but in a largely reduced reaction time (1 hour vs 18 hours) with only a single pass across the phosphonium salt bed. From our results, it appears that flow is an improvement on the traditional batch synthesis, with evidence of yield improvements for some reactions. Since the solid-supported reagents gave fluctuating yields, we could not conclude whether the in-house polymer-supported salt **209** and **209a** an improvement upon the polystyrene salt. We however, observed a lower product yield for alkyl aldehydes when using either solid-supported salt (Table 12, entries 3 to 5) but a higher product yield for aromatic aldehydes (Table 12, entries 1 and 2), with entry 6 being the exception which may be influenced by the substituents. Figure 21 reveals the proton NMR spectra transformation of pentanal (green) and *iso*-butanal (red). Evidence of successful Wittig transformation is seen by the presence of proton signals in the aromatic region of the ^{1}H NMR spectrum, as well as alkene proton signals observed between 6 and 6.5 ppm. From the spectra of **211a** (red) the *E:Z* ratio was approximately 2:1 as evidenced by the presence a minor doublet at 1.04 ppm and a triplet at 5.47 ppm. However, a mixture of isomers was not observed for all substrates but coupling constants suggested that the *E* isomer was favoured irrespective of which benzyl salt was used.

© University of Pretoria

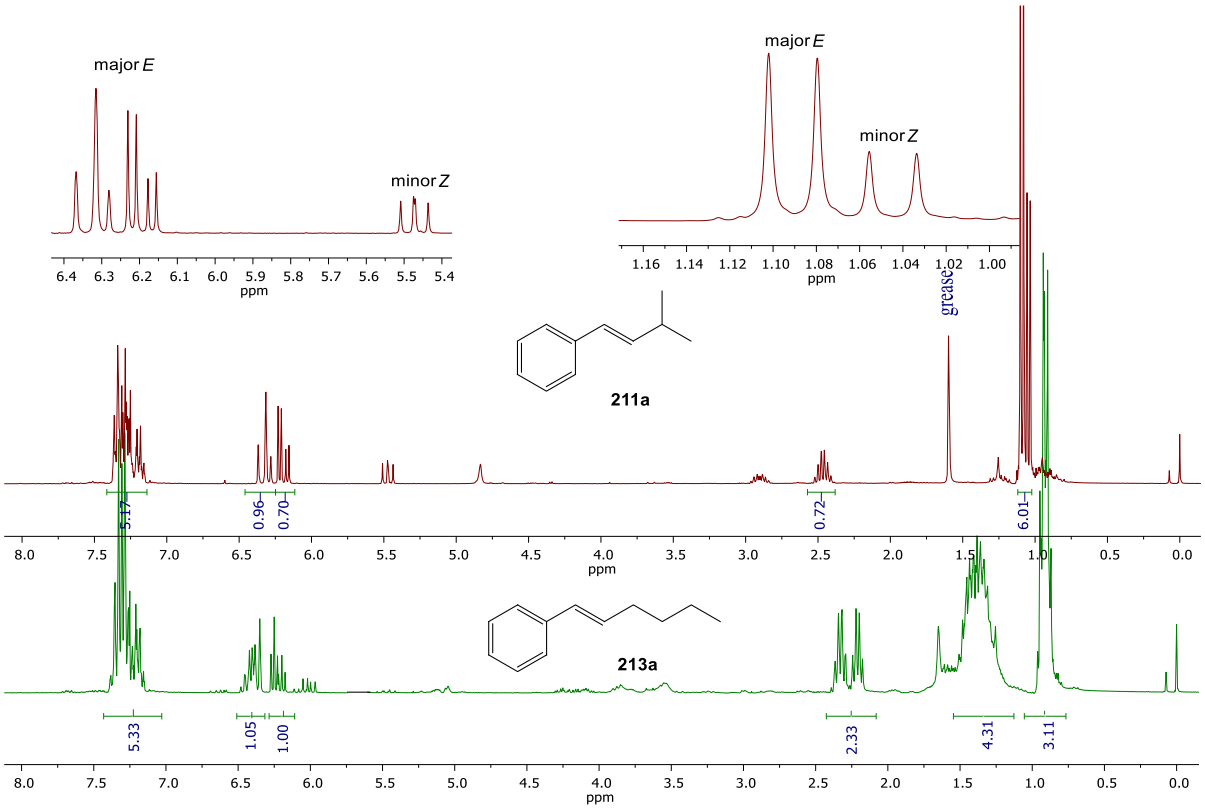

Figure 21: ^{1}H NMR spectra comparison of **213a** (green) and **211a** (red)

5.5. Conclusion

We have demonstrated the conversion of commercial unsupported-, commercial polystyrene- and in-house polymer-supported triphenylphosphine to phosphonium salts **206**, **208** and **209**. The efficacy of these salts was shown for Wittig reactions under batch and flow conditions, with the flow translation requiring the use of a base with low viscosity (50% sodium hydroxide vs 1 M sodium ethoxide). The phosphorous elemental loading of **208** was 0.8179 mmol/g whereas that of **209** was 1.614 mmol/g (Table 9), making the in-house polymer-supported phosphonium salt an improvement on the polystyrene-supported reagent (due to the presence of more phosphorus sites) as evidenced by formation of the product at 30 °C, (Table 12, entries 1 to 3 vs Table 13, entries 1 to 3). In-house polymer-supported salt **209** gave a phosphorous loading that was closely comparable to unsupported salt **206** (1.614 versus 1.969 mmol/g) however the yields were not comparable 32-40% vs 83-97% respectively but rather the yields were comparable with **208** (23-44%). Under flow conditions, preparation of phosphonium salts **208a** and **209a** was conveniently achieved by recycling benzyl bromide across the PBR. Passage across a heated packed-bed reactor housing the phosphonium salts **208a** and **209a** afforded comparable yields of 35-51% and

© University of Pretoria

22-49% respectively to those obtained under batch conditions, but in a largely reduced reaction time (1 hour vs 18 hours) with only a single pass across the phosphonium salt bed. From our results, it appears that flow is an improvement on the traditional batch synthesis, with evidence of yield improvements for some reactions (Table 14).

© University of Pretoria

Chapter 6

Preparation of immobilized palladium catalysts and their use in the Suzuki-Miyaura coupling reaction

6.1. Introduction

The Suzuki-Miyaura coupling reaction is a carbon-carbon bond forming reaction via the catalysed coupling of boronic acids to aryl/alkyl halides. The Suzuki-Miyaura catalytic cycle is initiated by the dissociation of the catalysts to a coordinatively unsaturated complex **A**, followed by an oxidative addition of an aryl/alkyl halide to Pd(0) complex **A** to give a Pd(II) complex intermediate **B**. Participation of a base allows the organoborane reagent to react with intermediate **B** via transmetalation to afford intermediate **C**. This is then followed by reductive elimination to give the desired product and regenerate the original Pd(0) complex **A** (Scheme 74).

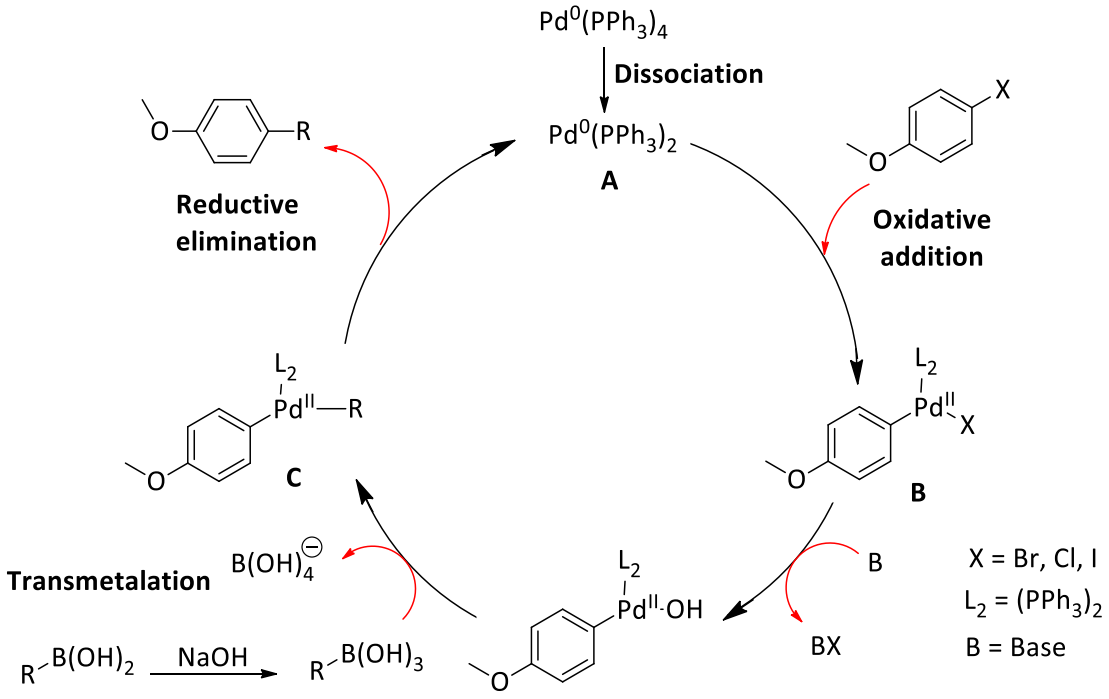

Scheme 74: Mechanism of the Suzuki-Miyaura coupling catalytic cycle.

In this chapter we transformed our in-house polymer-supported triphenylphosphine into a palladium catalyst, tetrakis(triphenylphosphine)palladium. We then carried out Suzuki-Miyaura coupling reactions with various boronic acids and two different aryl halides,

© University of Pretoria

comparing the results for batch and flow synthesis against the commercial unsupported and polystyrene-supported catalysts.

6.2. Batch Synthesis

6.2.1. Synthesis and characterization of in-house polymer-supported tetrakis-(triphenylphosphine)palladium(0)

Like the Wittig solid-supported salts, the catalyst was prepared as a finely ground solid-supported version for use under batch conditions. Following the steps to synthesize polymer-supported triphenylphosphine **146** (Chapter 3, Scheme 58), the washed and ground reagent was then suspended in degassed dimethyl sulfoxide (DMSO) and treated with palladium chloride to produce supported bis(triphenylphosphine)palladium chloride **215**, which is formed by binding two triphenylphosphine sites of the polymer. Treatment with hydrazine hydrate aided the reduction of palladium (II) to palladium (0) yielding polymer supported tetrakis(triphenylphosphine)palladium(0) **215a**, which is formed by binding four triphenyl-phosphine sites of the polymer, as a green solid (Scheme 75).

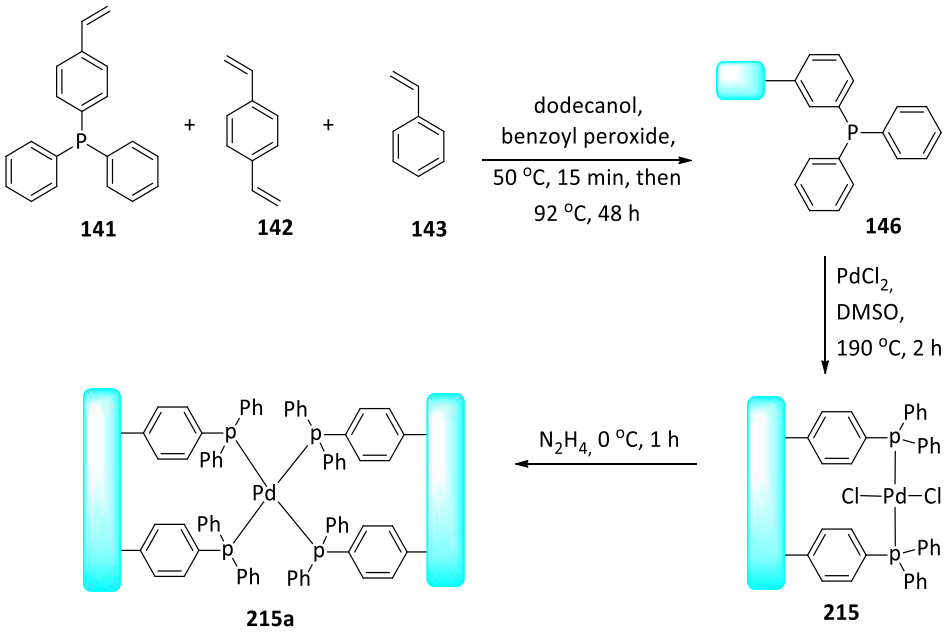

Scheme 75: Preparation of solid-supported tetrakis(triphenylphosphine)palladium **215a**

Since the tetrakis(triphenylphosphine)palladium catalyst requires four triphenylphosphine groups coordinating to a single palladium metal centre, there was a concern of inadequate spatial availability of triphenylphosphine, and as such an alternative catalyst **215b** was

© University of Pretoria

prepared by adding excess triphenylphosphine (2.0 eq.) after the polymer had been refluxed for 2 hours with palladium chloride prior to reduction with hydrazine hydrate (Scheme 76).

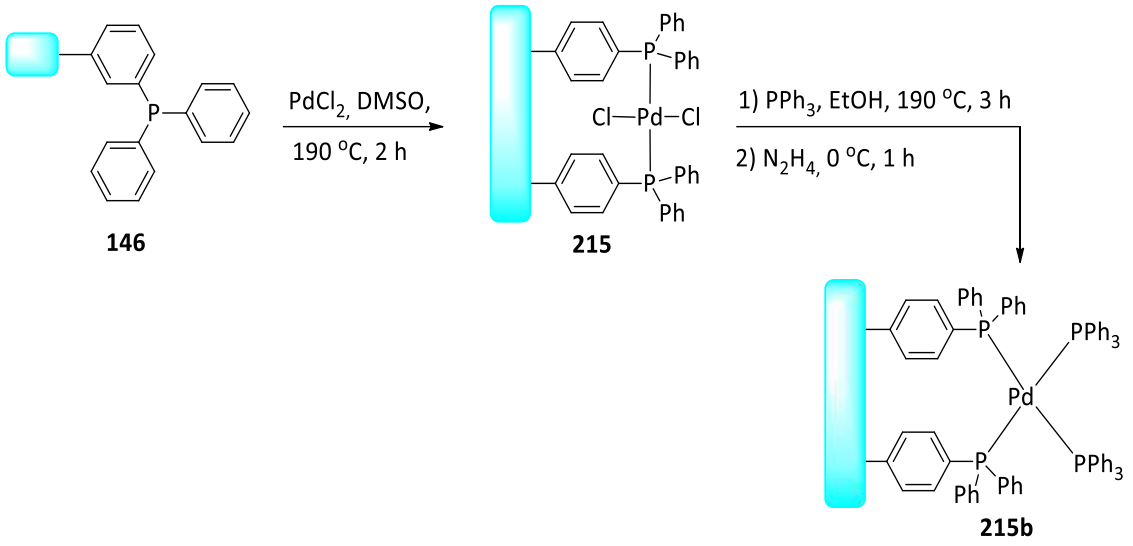

Scheme 76: Preparation of solid-supported tetrakis(triphenylphosphine)palladium **215b** prepared with excess triphenylphosphine

The morphology and loading of the catalysts were characterised using EDX, SEM and transmission electron microscopy (TEM) and compared to the commercial polystyrene-supported tetrakis(triphenylphosphine)palladium catalyst (Sigma Aldrich, 511579). The EDX data revealed a palladium loading of 0.460 and 0.909 mmol/g for **215a** and **215b** respectively, which were within the loading range of 0.500-0.900 mmol/g of the commercial catalyst. The palladium loading of **215a** (0.46 mmol/g) to phosphine loading of **146** (1.85 mmol/g) gave a 1:4 ratio and was evidence that four phosphine ligands were coordinated to the palladium metal. In addition, SEM scans revealed a largely uniform sub-micromolar particle size for both the immobilized triphenylphosphine **146** and the catalyst **215a** (Figure 22A and B). Interestingly, catalyst **215b** showed larger particle sizes ranging from 1-4 micromolar (Figure 22C). The high palladium loading observed in **215b** was accompanied by a reduced surface area which was not ideal. In comparison, commercial polymer-supported tetrakis(triphenyl-phosphine)palladium showed particle sizes >40 micromolar in diameter (Figure 22D). The TEM scans of catalyst **215a** and commercial polymer-supported tetrakis(triphenyl-phosphine)palladium (Sigma Aldrich, 511579) are shown at resolutions of 50 and 5 nm (Figure

© University of Pretoria

23). The corresponding d-spacing plots confirmed the presence of palladium, and in both instances **215a** and the commercial catalyst were comparable.

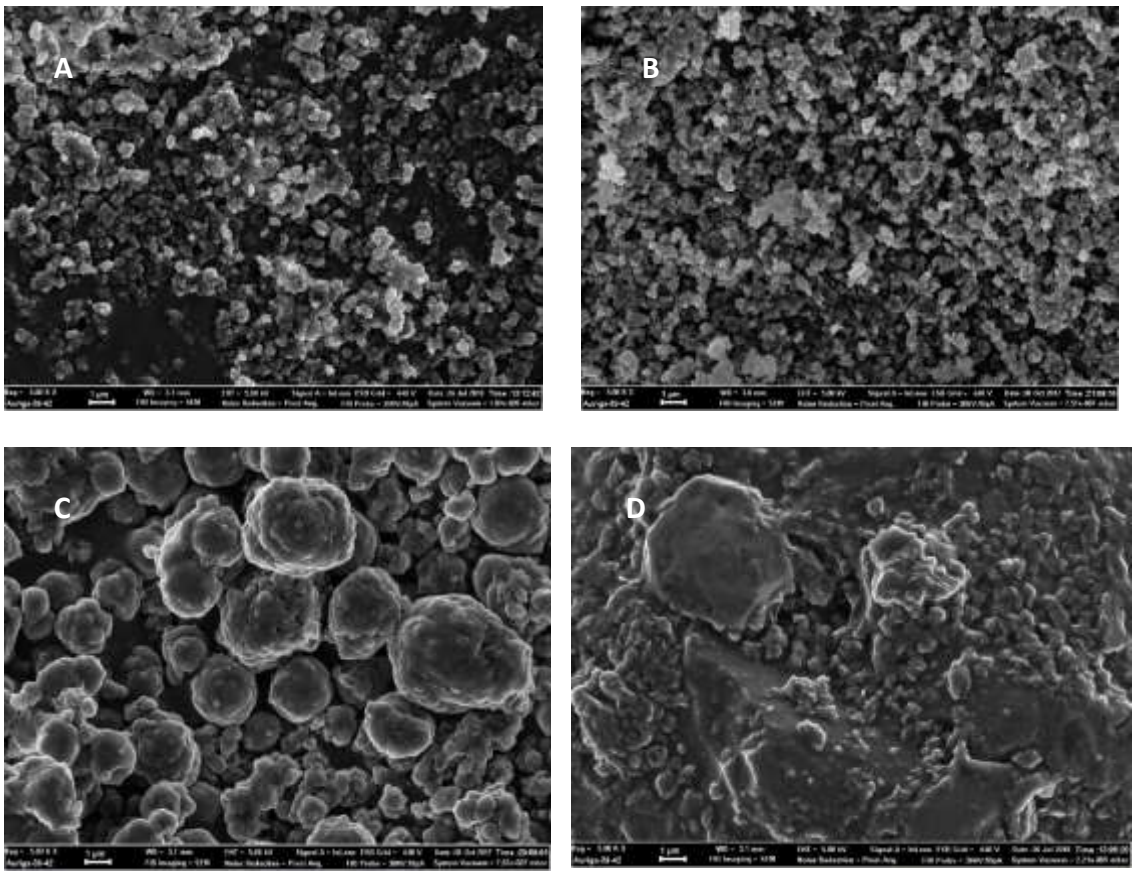

Figure 22: SEM scans (5.00 K X magnification, FIB probe = 30 kV:10 pA, voltage = 640 V) of immobilized triphenylphosphine **146** (A), catalyst **215a** (B), catalyst **215b** (C) and commercial polystyrene-supported tetrakis(triphenylphosphine)palladium (Sigma Aldrich 511579) (D)

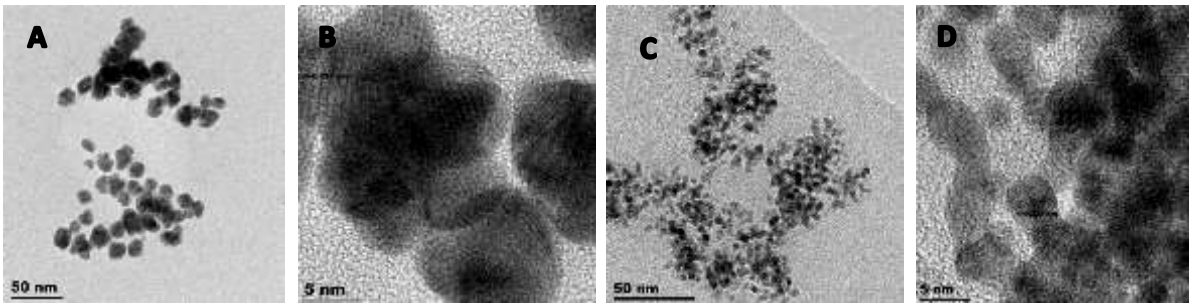

Figure 23: TEM scans of catalyst **215a** (A and B) at a resolution of 50 nm and 5 nm respectively, and commercial polystyrene-supported catalyst (Sigma Aldrich 511579) (C and D) at a resolution of 50 nm and 5 nm respectively

© University of Pretoria

Further characterisation was evidenced by comparison of **215a** and the commercial catalyst using ^{31}P solid-state NMR, FTIR spectroscopy and powder x-ray diffraction (PXRD), Figure 24, 25 and 26 respectively. In all instances **215a** showed close correlation with the commercial sample and PXRD suggested that both catalysts possess an amorphous morphology, with **215a** having some crystalline material present.

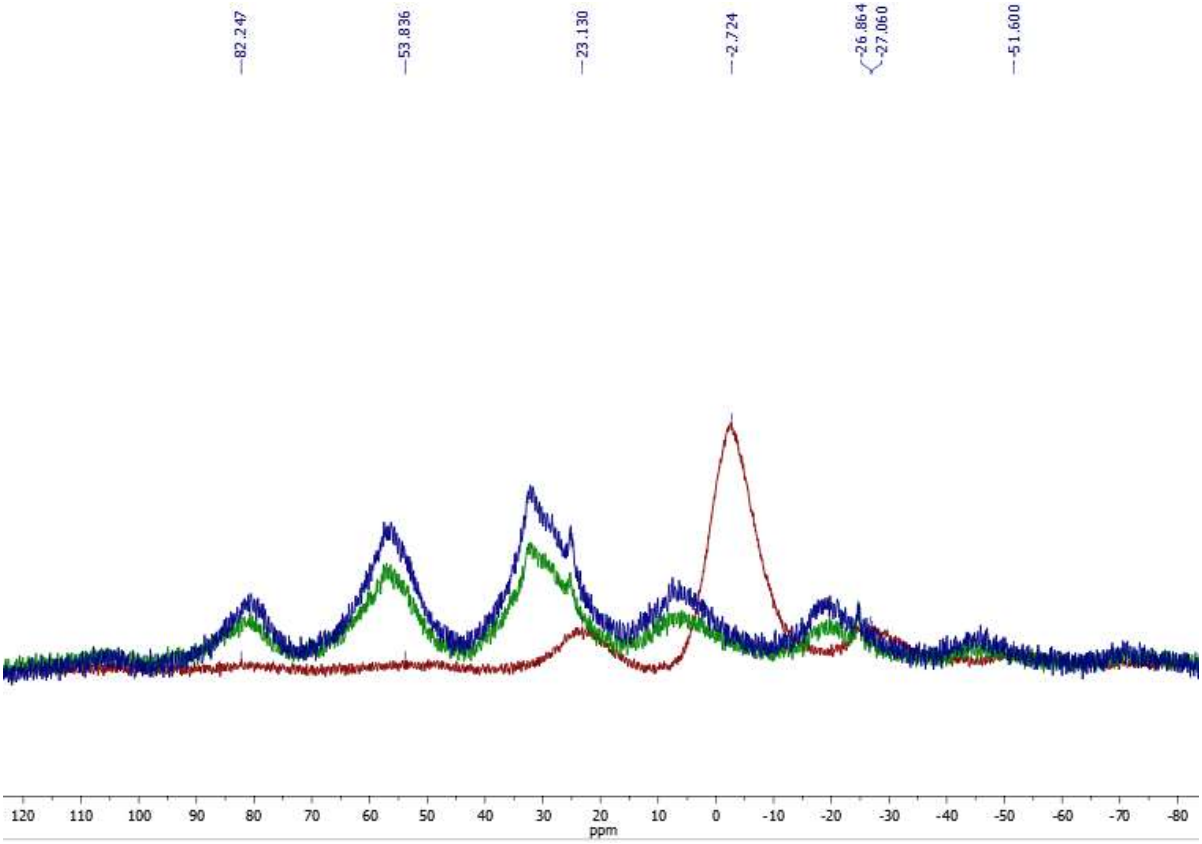

Figure 24: Solid-state ^{31}P NMR of **215a** (blue), commercial polystyrene-supported tetrakis(triphenylphosphine)palladium (Sigma Aldrich 511 579) (green) and triphenylphosphine scaffold **146** (red)

© University of Pretoria

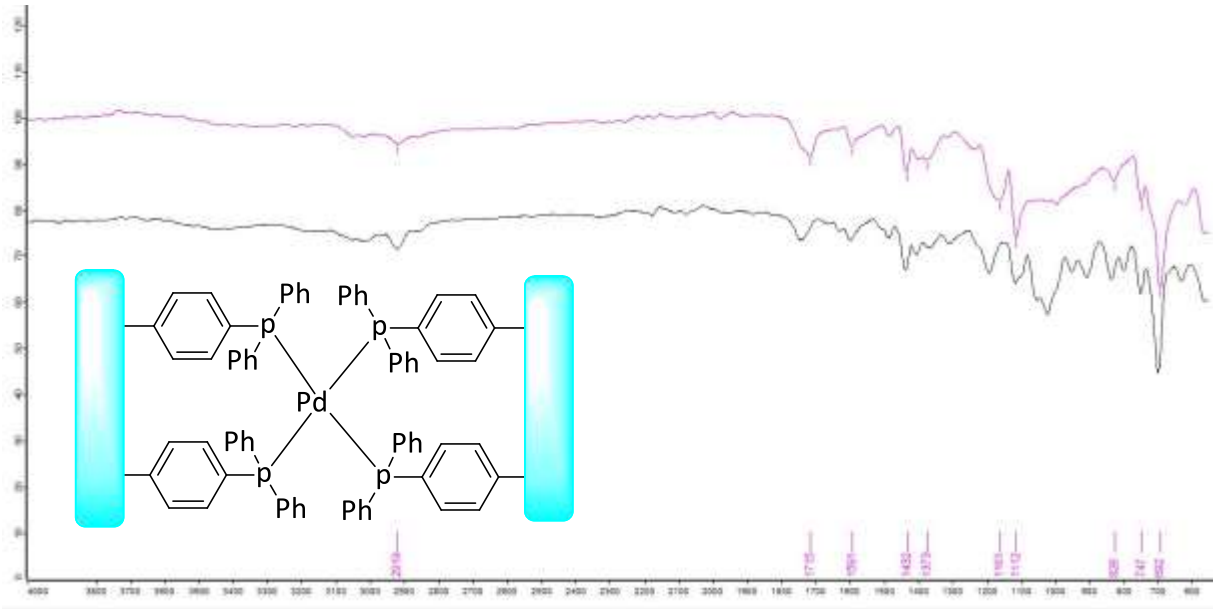

Figure 25: FTIR of commercial polystyrene-supported tetrakis(triphenylphosphine)palladium (Sigma Aldrich 511 579) (pink) and **215a** (black)

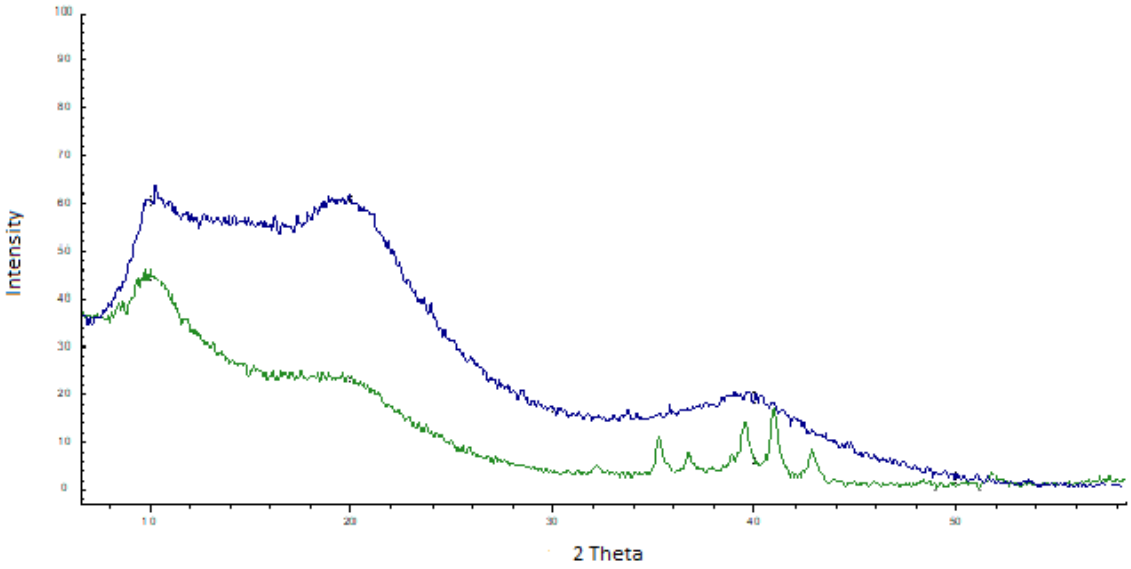

Figure 26: PXRD of commercial polystyrene-supported tetrakis(triphenyl-phosphine)palladium (blue) (Sigma Aldrich 511 579) and **215a** (green)

Brunauer–Emmett–Teller (BET) analysis revealed a type II nitrogen adsorption–desorption isotherm for **215a** indicating multi-layer adsorption (Figure 27A), with a sharp uptake of the gas at the relative pressure of 0.90 due to capillary condensation. Pore size distribution was indicative of a wide range of pore-sizes (Figure 27B). Interestingly a negative isotherm was

© University of Pretoria

obtained for the commercial polystyrene-supported catalyst suggesting low surface area and/or low pore volume (Figure 27C).

Finally, particle size distribution was analysed with the particles dispersed in water. The polydispersity index (PDI) of **215a** (0.348) indicated that the particles follow a mid-range value to almost monodispersed pattern with an average particle size diameter of 321 nm (Figure 28A). The presence of ~10% larger particles was observed and likely due to precatalyst **146** being manually ground by hand prior to functionalisation to afford **215a**. In contrast, the commercial catalyst showed a very broad distribution (PDI = 1) with an average particle size diameter of 895 nm (Figure 28B). The textural properties of catalyst **215a** are summarized against the commercial polystyrene-supported catalyst, Table 15.

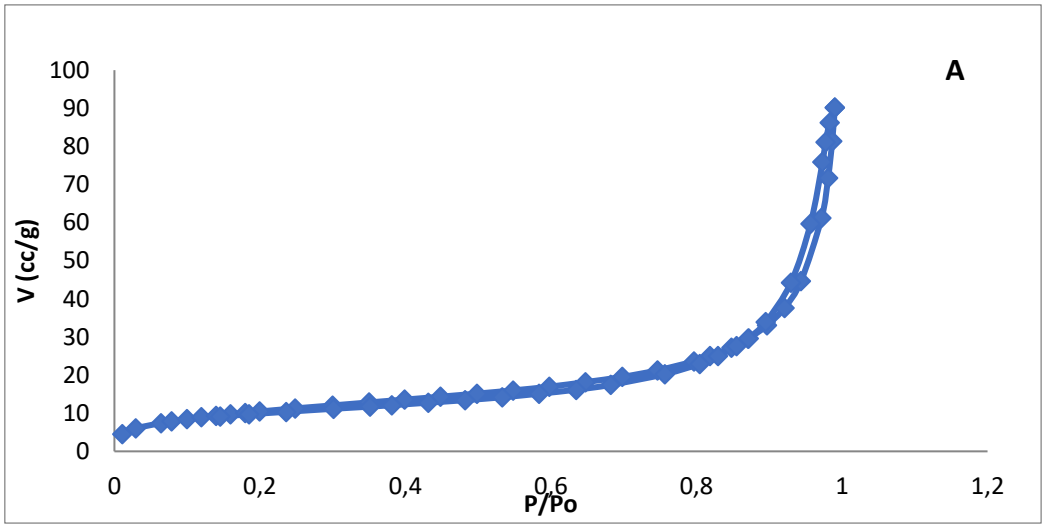

Figure 27: Nitrogen adsorption/desorption isotherms of catalyst **215a** at 77 K (A) and pore size distribution of catalyst **215a** (B), negative nitrogen adsorption/desorption isotherms of commercial polystyrene-supported catalyst (C)

© University of Pretoria

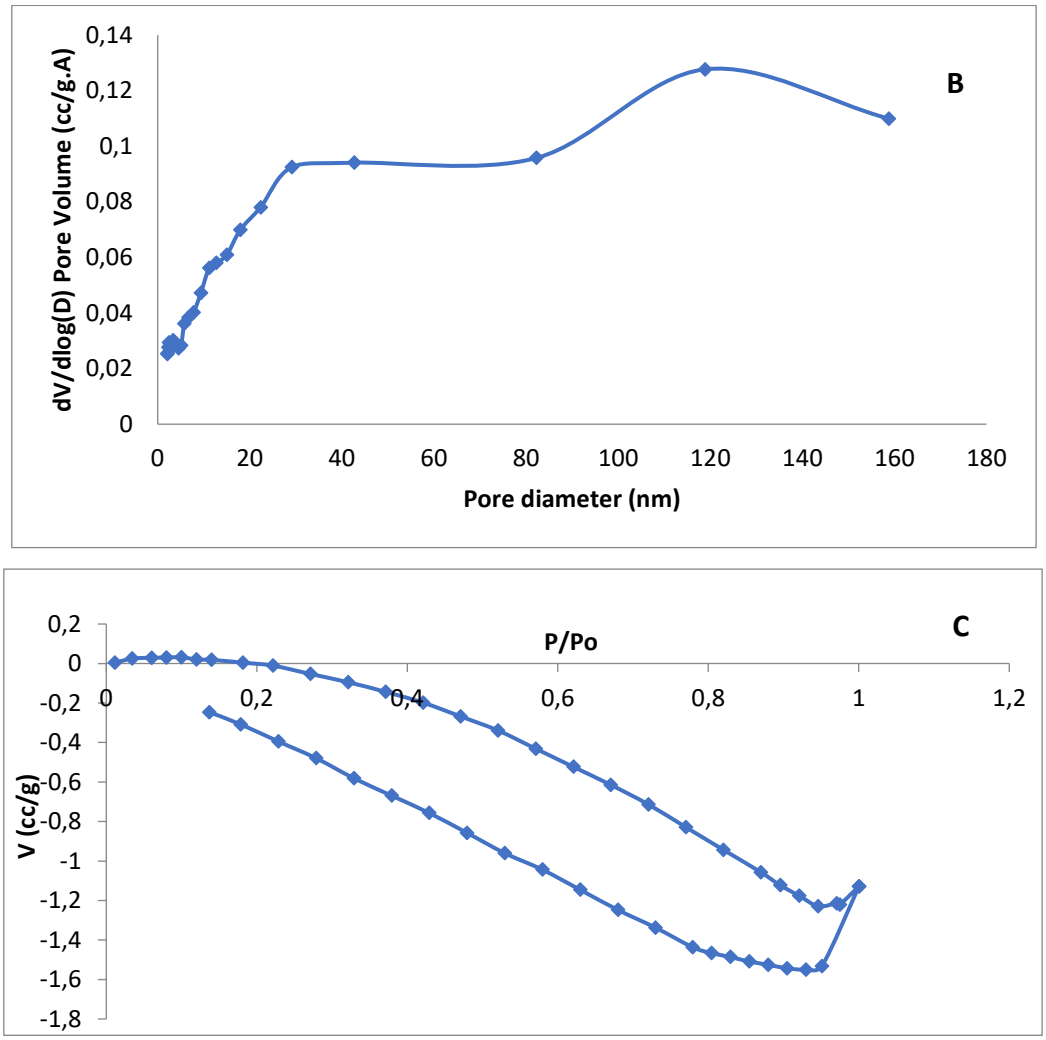

Figure 27 continued: Nitrogen adsorption/desorption isotherms of catalyst **215a** at 77 K (B) and pore size distribution of catalyst **215a** (B), negative nitrogen adsorption/desorption isotherms of commercial polystyrene-supported catalyst (C)

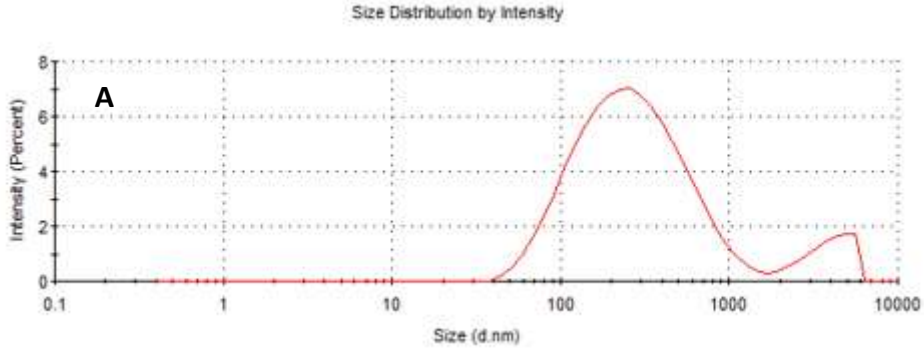

Figure 28: Particle size distribution **215a** with PDI = 0.348 (A) and commercial polystyrene-supported tetrakis(triphenylphosphine)palladium (Sigma Aldrich 511 579) with PDI = 1.000 (B)

© University of Pretoria

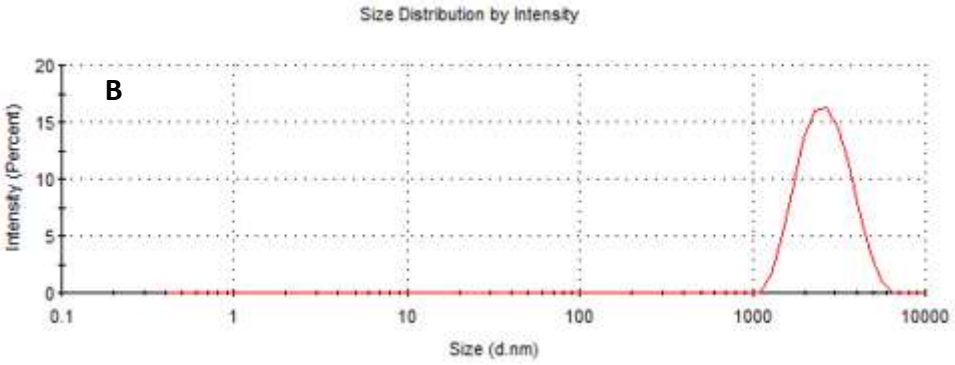

Figure 28 continued: Particle size distribution **215a** with PDI = 0.348 (A) and commercial polystyrene-supported tetrakis(triphenylphosphine)palladium (Sigma Aldrich 511 579) with PDI = 1.000 (B)

Table 15: Properties summary for catalyst **215a** vs commercial polystyrene-supported tetrakis(triphenylphosphine)palladium

Property	215a	Sigma Aldrich 511579
BET surface area (m2/g)	35.2	0.0128
Mesopore volume (cm3/g)	0.143	N/A
Pore diameter (nm)	16.2	N/A
Average particle size diameter (nm)	321	895
Palladium loading (mmol/g)	0.460	0.500-0.900

Cost analysis was conducted for the synthesis of the in-house prepared polymer-supported tetrakis(triphenylphosphine)palladium catalyst **215a** and was compared with Sigma Aldrich commercial reagent (511 579). The synthesis of one gram of polymer-supported catalyst **215a** was R422.25, Table 16. A price comparison with the commercial catalyst revealed our polymer to be R521.75 cheaper than the catalyst from Sigma Aldrich, Table 17.

Table 16: Cost of in-house polymer-supported tetrakis(triphenylphosphine)palladium

Entry	Reagent	Mass needed (g)	Price/g
1	In-house PPh_3	1.00	R195.43
2	Palladium chloride	0.246	R226.32
3	Hydrazine hydrate	0.255	R0.5
			R422.25

© University of Pretoria

Table 17: Cost comparison of commercial polymer-supported tetrakis(triphenylphosphine)palladium with in-house prepared polymer catalyst **215a**

Entry	Company	Loading (mmol/g)	Price/g	Price/5g
1	Sigma Aldrich	0.4-0.9	R944	R3642
2	In-house polymer catalyst	0.46	R422.25	R2111.25

6.2.2. Optimization studies of catalyst 215a for Suzuki-Miyaura coupling reactions†

The Suzuki-Miyaura coupling reaction was optimized using catalyst **215a**, boronic acid **192** and iodoanisole **216** to produce biaryl anisole **217** (Scheme 77). Screening began by using typical Suzuki-Miyaura solvent systems and potassium phosphate tribasic (Table 18, entries 1 to 3). These afforded high yields of 75-85% and only trace amounts of the unwanted biaryl product **218**. The potassium phosphate tribasic was unfortunately insoluble in these solvents and as a homogeneous solvent system was needed for flow translation, a biphasic solvent system (1:1) was adopted (Table 18, entries 4 to 8). A 1:1 mixture of tetrahydrofuran:water gave the best yield for **217** of 92% and only 3% of **218** (Table 18, entry 8). In the presence of other bases (Table 18, entries 5 to 7) the isolated yields were significantly lower, in the range of 63-69% than when using potassium phosphate tribasic.

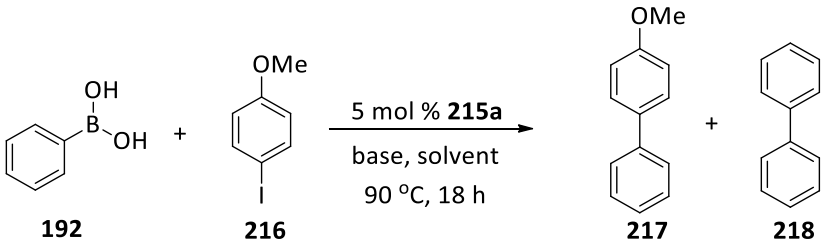

192 216 217 218

Scheme 77: Model study for Suzuki-Miyaura reaction

† Experimental work reported in section 6.2.2 conducted by Mr Ian Strydom (PhD candidate) and forms part of his PhD research (thesis under preparation). The results are reported here for comparative analysis.

© University of Pretoria

Table 18: Solvent and base optimization of model Suzuki-Miyaura batch reactions

Entry	Solvent	Base	% Conversion	% Yield Biaryl 218	% Yield Product 217
1	Toluene	K_3PO_4	84	3	79
2	Dioxane	K_3PO_4	87	3	75
3	THF	K_3PO_4	99	2	85
4	Dioxane:H_2O	K_3PO_4	88	2	85
5	THF:H_2O	K_2CO_3	89	3	69
6	THF:H_2O	NEt_3	74	7	54
7	THF:H_2O	KOH	87	3	63
8	THF:H_2O	K_3PO_4	95	3	92

Reaction conditions: **192** (3.0 eq), **216** (1.0 eq), base (3.0 eq), 5 mol % of **215a**. Conversions and yields determined by GC-FID as the average of two experiments, with anisole as internal standard. [Note: results reported in this table were generated by Mr Ian Strydom]

The effect of how temperature and stoichiometric ratios of the reactants affected the outcome of the reaction were then investigated. The reaction was initially screened between 70 to 90 °C using one equivalent of **192** and potassium phosphate tribasic (Table 19, entries 1 to 3) with 5 mol % catalyst **215a**. The temperature range did not affect the conversion significantly, but a slight improvement was observed at 90 °C (Table 19, entry 3). Increasing the stoichiometric amount of **192** incrementally while keeping the base constant at one equivalent resulted in an increase in yield from 65 to 90% (Table 19, entries 3-5), while increasing the stoichiometric amount of base and keeping **192** at one equivalent afforded an increase from 65 to 76% (Table 19, entries 3 and 6). Furthermore, when increasing the stoichiometric equivalents of **192** and the base to three equivalents no significant change in yield was afforded (Table 19, entry 5 and 7). When 1.2 equivalents of **192** and 1.5 equivalents of the base were used, only 85% conversion and 72% yield were observed (Table 19, entry 8). A moderate increase in yield to 87% and none of product **218** was observed with 1.2 equivalents of **192** and 3.0 equivalents of base (Table 15, entry 9, turnover number (TON) of 17.4 in 18 h, time-of-flight (TOF) of 2.69 × 10−4 s^{-1}). We selected to continue all Suzuki-

© University of Pretoria

Miyaura reaction using these conditions (Table 19, entry 9). Although not as efficient as when using large excesses of the boronic acid, the decision was determined by a desire to minimize the amount of waste and purification complications produced by the boronic acid. In addition, it was the largest cost contributor to the process.

Table 19: Temperature and stoichiometric equivalents of reagents optimization of model Suzuki-Miyaura batch reactions

Entry	Equivalents of boronic acid 192	Equivalents of base	Temp (°C)	% Conversion	% Yield biaryl 218	% Yield product 217
1	1	1	70	64	2	62
2	1	1	80	61	2	57
3	1	1	90	67	2	65
4	2	1	90	69	2	67
5	3	1	90	92	3	90
6	1	3	90	81	2	76
7	3	3	90	95	3	92
8	1.2	1.5	90	85	1	72
9[a]	1.2	3	90	-	0	87

Reaction conditions: Reactions time of 18 hours, (0.07 g with regards to Palladium). Conversions and yields determined by GC-FID as the average of two experiments with anisole as internal standard. [Note: Results reported in this table were generated by Mr Ian Strydom]

The immobilized catalysts **215a** and **215b** were then compared with commercially available unsupported tetrakis(triphenylphosphine)palladium (Sigma Aldrich, 216666) and polystyrene-supported (Sigma Aldrich, 511579) using the batch optimised conditions (Table 19).[‡] As shown in Table 20, catalyst **215a** performed comparably to the unsupported catalyst (87% vs 84%) and better than the commercially available polystyrene-supported tetrakis(triphenylphosphine)palladium (87% vs 79%). Although catalyst **215b** had a higher

[‡] From this section the experimental work reported conducted by Ms Valerie Ramaotsoa

© University of Pretoria

palladium loading (0.909 vs 0.460 mmol/g) it performed worse than **215a** (75% vs 87%). This is hypothesised to be due to the reduced surface area observed in **215b** as demonstrated by the SEM scans (Figure 22C).

Table 20: Catalyst comparison of Suzuki-Miyaura coupling reactions

Entry	Tetrakis(triphenylphosphine) palladium catalyst	Pd loading mmol/g	% Yield[a]
1	Commercial unsupported	-	84
2	Commercial PS- supported	0.500	79
3	Catalyst **215a**	0.460	87
4	Catalyst **215b**	0.909	75

Reaction conditions: **192** (1.2 eq), **216** (1.0 eq), base (3.0 eq), 5 mol % of **215a**, 90 °C, 18 hours, (0.07 g with regards to Palladium). [a] Isolated yield

6.3. Flow Synthesis

6.3.1. Synthesis of catalyst 215c

A PBR containing the finely ground solid-supported triphenylphosphine **146** was mounted into a Uniqsis FlowSyn SS column heating block and washed with dry degassed dichloromethane at 60 ˚C. Thereafter, the system was washed with degassed dimethyl sulfoxide for 30 minutes at 0.5 mL/min. A stock solution of palladium chloride in dimethyl sulfoxide (0.1 M) was then recycled across the PBR for 18 hours (0.5 mL/min, 150 °C) affording the pre-catalyst **215**, (Scheme 78, stage 1) with yellow colouration (Figure 29). The loaded bed was then washed with dimethyl sulfoxide to remove any unreacted $PdCl_2$ (failure to include the final dimethyl sulfoxide wash resulted in rapid blockage of the systems tubes). This was followed by recycling of hydrazine hydrate through the column for 6 hours using a flow rate of 0.5 mL/min at 0 °C (Scheme 78, stage 2) to give the desired catalyst **215c**, with a dark green colour (Figure 29). The catalyst was again characterised by FTIR and EDX, an improved loading of 0.689 mmol/g was noted (compared to the 0.460 mmol/g of the batch **215a**) with a Pd:P mol % ratio of 0.88 (unsupported tetrakis(triphenylphosphine)palladium requires 0.86). The catalyst **215c** was then validated under flow conditions by the reaction of 2-bromo-3-

© University of Pretoria

methoxynaphthalene **219** and phenyl boronic acid **192** using the batch optimized conditions (Table 19, entry 9).

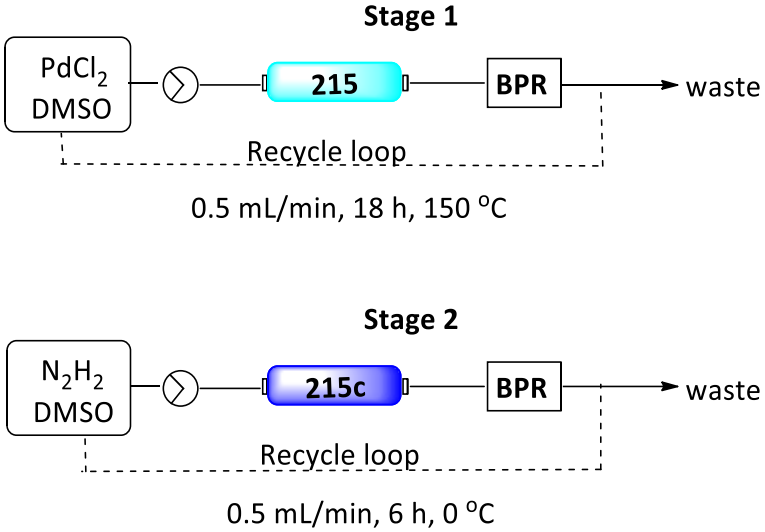

Scheme 78: Two stage flow-based preparation of supported catalyst **215c**

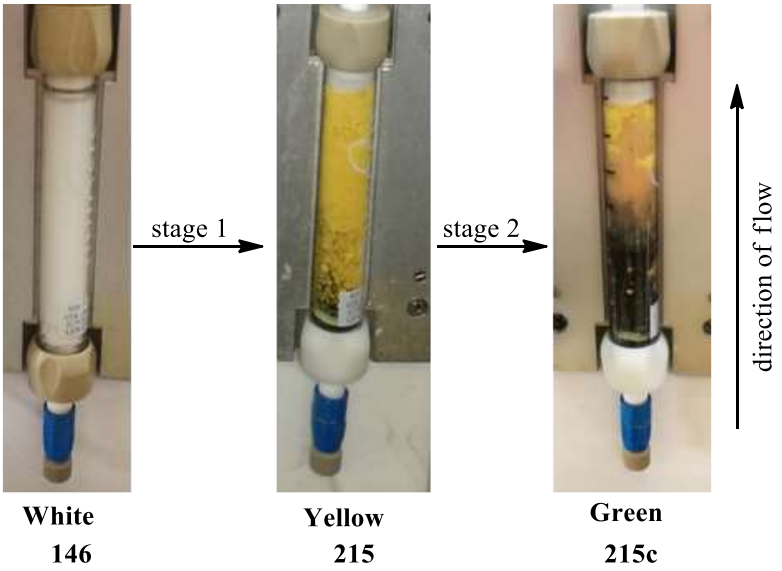

Figure 29: Observed colour changes during preparation of supported catalyst **215c**

The general flow set-up for Suzuki-Miyaura reactions (Scheme 79), was composed of a stock solution of aryl halide (1.0 eq) and boronic acid (1.2 eq) in tetrahydrofuran (1 M) reacting with a stock solution of base (3.0 eq) in water (3 M) at a T-piece mixer. Thereafter, the reaction stream was passed through a PBR containing **215c** (5 mol %) with a single pass at 0.183 mL/min and 90 ˚C, one hour residence time, followed by a BPR to afford the desired product.

© University of Pretoria

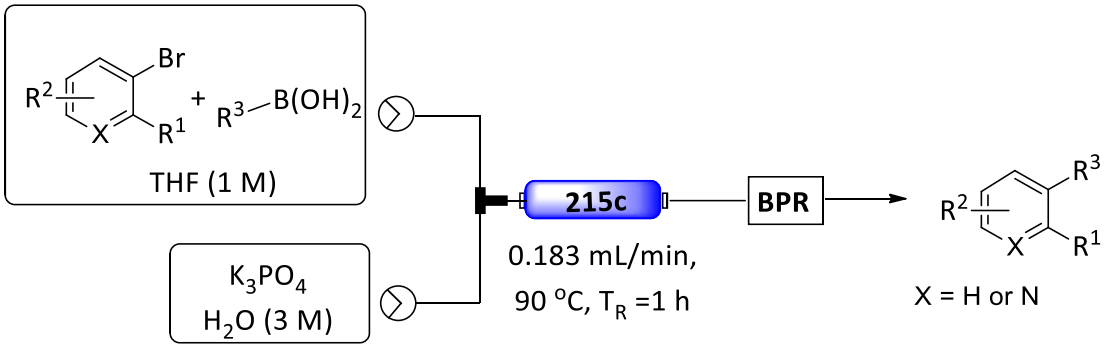

Scheme 79: General approach for Suzuki-Miyaura under flow conditions

6.3.2. Suzuki-Miyaura coupling reactions using catalyst 215a and 215c

The scope of the reaction was then screened under batch and flow conditions using 2-bromo-3-methoxynaphthalene **219** (Scheme 80, Table 21) and 3-bromopyridin-2-amine **221** (Scheme 81, Table 22) as the halide components to afford a variety of derivatives. The aryl halide 2-bromo-3-methoxynaphthalene was synthesized in two steps from naphthol using *N*-bromosuccinimide as a brominating reagent to yield bromonaphthol. This was then subjected to methylation using methyl iodide. Batch reactions were conducted by reacting aryl halide (1.0 eq) with the boronic acid (1.2 eq), potassium phosphate tribasic (3.0 eq) and catalyst **215a** (5 mol %) at 90 ˚C for 18 hours (as described in Table 19 entry 9). Flow reactions were conducted as described above, outlined in Scheme 79 with a residence time of 1 hour and a single pass through the PBR.

The coupling of aryl boronic acids (Table 21 and 18, entries 1-3) gave better results than those of alkyl and benzylic boronic acids (Table 21 and 22, entries 4-7). Under batch conditions, the use of commercial unsupported tetrakis(triphenylphosphine)palladium gave higher yields compared to the commercial polystyrene-supported tetrakis(triphenylphosphine)palladium and catalyst **215a**. Under flow conditions, the commercial unsupported tetrakis(triphenyl-phosphine)palladium was unstable to perform any reactions due to the sensitivity of the catalyst to oxygen, but both the commercial polystyrene-supported catalyst and **215c** performed comparably. The performance of immobilized tetrakis(triphenylphosphine)-palladium under flow conditions with one hour residence time (single pass of the PBR) afforded yields that were comparable to those achieved in eighteen hours under batch conditions.

© University of Pretoria

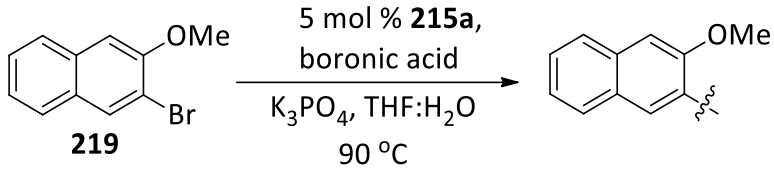

Scheme 80: Suzuki-Miyaura reactions using 2-bromo-3-methoxynaphthalene **219**

Table 21: Batch and flow Suzuki coupling reactions of 2-bromo-3-methoxynaphthalene using varying boronic acids

Entry	Boronic Acid	Product	% Yield[a]				
			Batch			Flow	
			$Pd(PPh_3)_4$	PS-$Pd(PPh_3)_4$	215a	PS-$Pd(PPh_3)_4$	215c
1	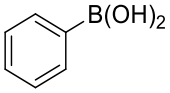	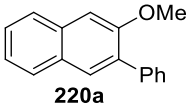 **220a**	84	79	76	63	65
2	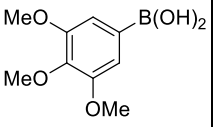	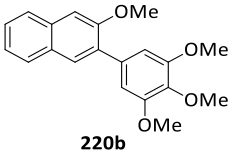 **220b**	91	44	35	65	63
3	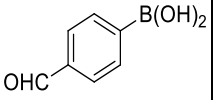	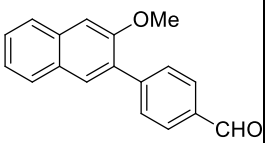 **220c**	70	31	29	56	54
4	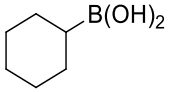	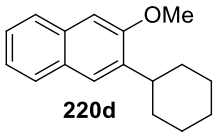 **220d**	NR	NR	NR	NR	NR
5	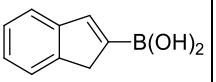	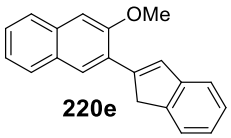 **220e**	NR	NR	NR	NR	NR
6	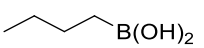	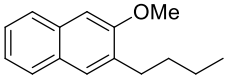 **220f**	20	10	8	21	18
7	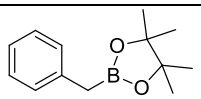	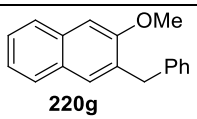 **220g**	NR	NR	NR	NR	NR

Reaction conditions: Boronic acid (1.2 eq), **219** (1.0 eq), base (3.0 eq), 5 mol % of **215a**, 90 °C.

[a] Isolated yield, NR indicates that no product formed.

© University of Pretoria

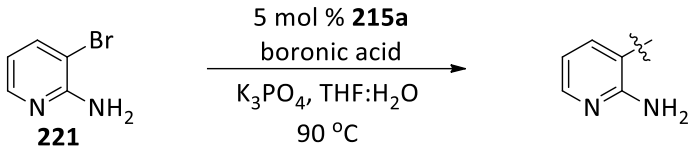

Scheme 81: Suzuki-Miyaura reactions using 3-bromopyridin-2-amine **221**

Table 22: Batch and flow Suzuki coupling reactions on 3-bromopyridin-2-amine using varying boronic acids

Entry	Boronic Acid	Product	% Yield			
			Batch			Flow
			$Pd(PPh_3)_4$	PS-$Pd(PPh_3)_4$	215a	215c
1	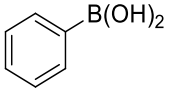	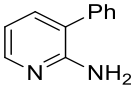 **222a**	88	37	56	58
2	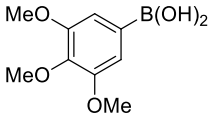	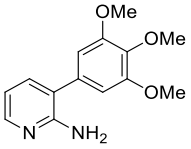 **222b**	90	58	68	71
3	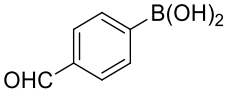	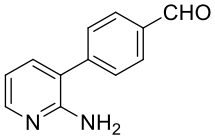 **222c**	88	58	67	65
4	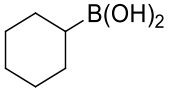	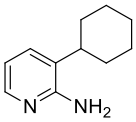 **222d**	NR	NR	NR	NR
5	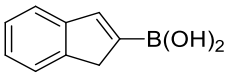	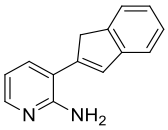 **222e**	24	18	7	21
6	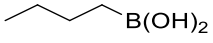	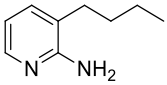 **222f**	NR	NR	NR	NR
7	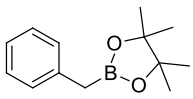	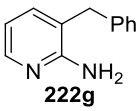 **222g**	75	15	10	20

Reaction conditions: Boronic acid (1.2 eq), **219** (1.0 eq), base (3.0 eq), 5 mol % of **215a**, 90 °C.

© University of Pretoria

Proton NMR was used to analyse of the products. As an example, in Figure 30, an aldehyde singlet at 10 ppm and four additional aromatic peaks were observed for **220c** (red spectrum). Two additional singlets integrating for nine protons were observed in the methoxy region together with two additional aromatic peaks for **220b** (green spectrum).

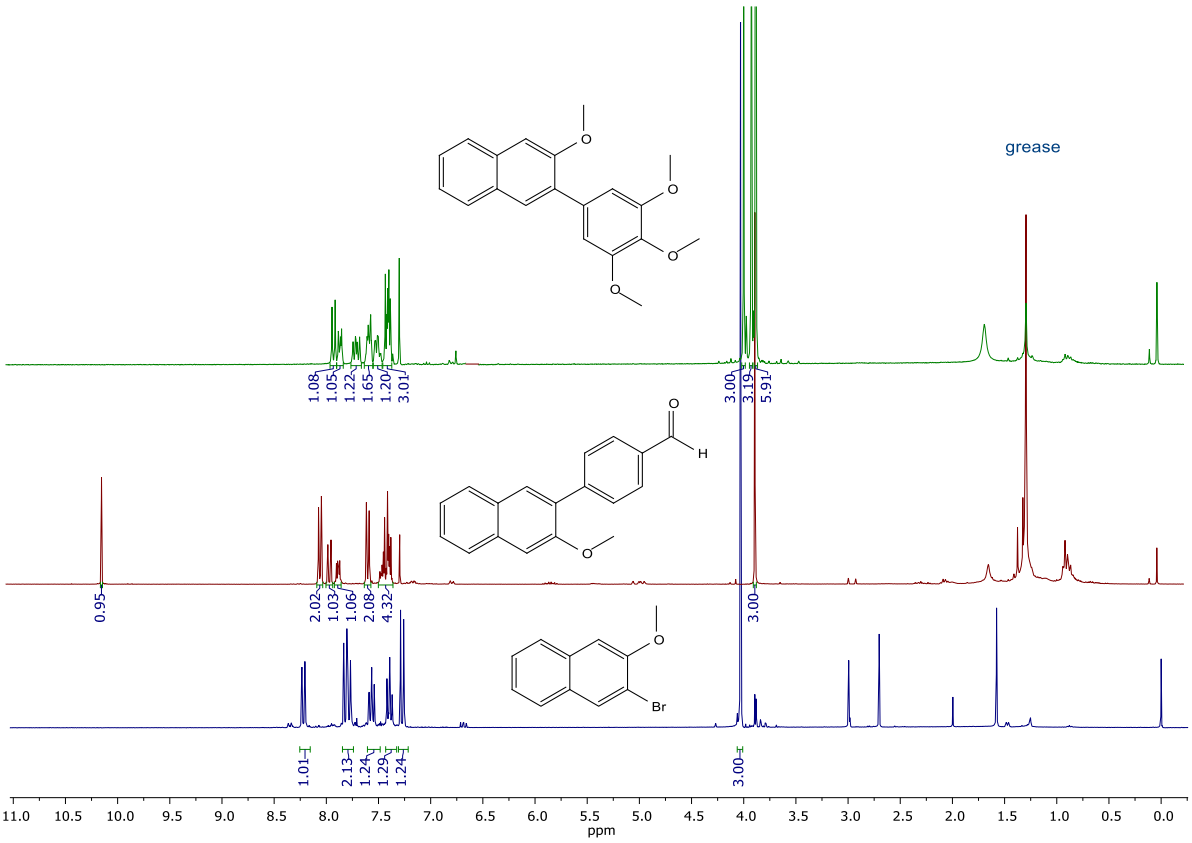

Figure 30: ^{1}H NMR spectra comparison of **220b** (green) and **220c** (red) against alkyl halide **219** (blue)

In Figure 31, a benzyl peak integrating for two protons between 3.5 and 4.0 ppm together with five additional peaks were observed for **222g** (red spectrum). Two methoxy singlets integrating for nine protons together with two new aromatic peaks were observed for **222b** (green spectrum).

© University of Pretoria

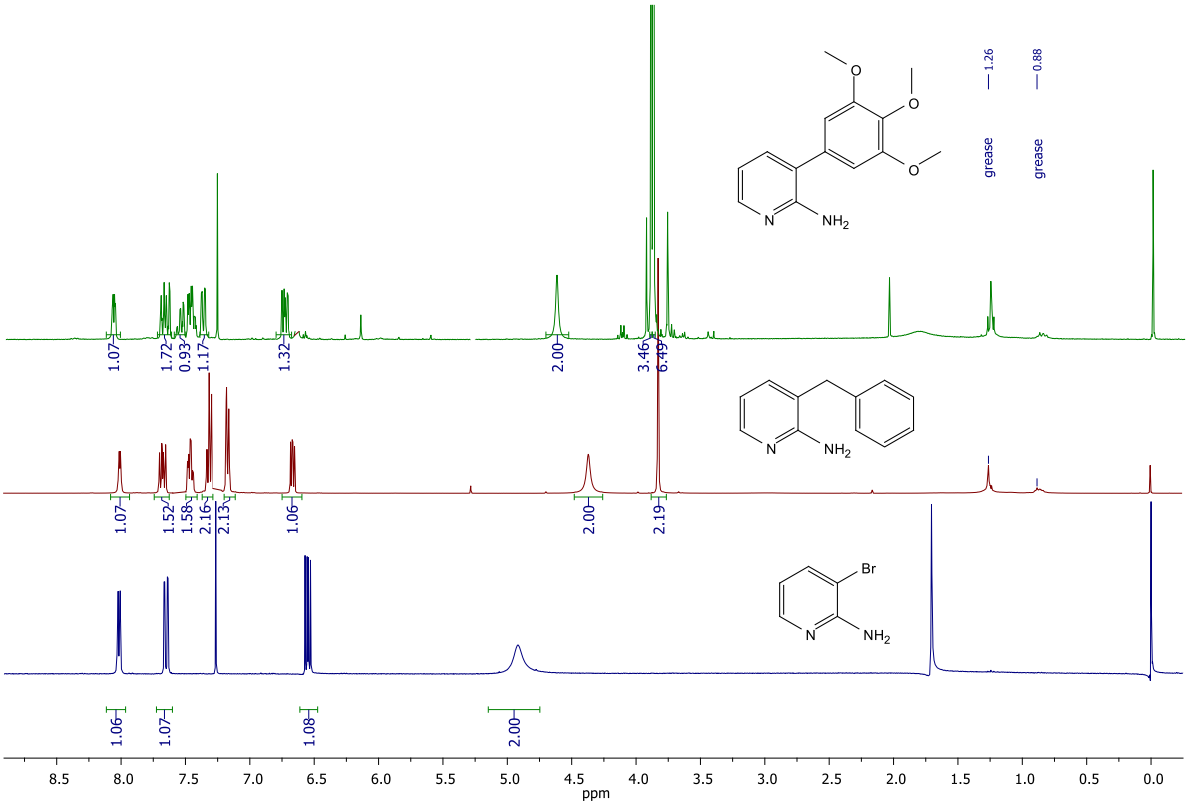

Figure 31: ^{1}H NMR spectra comparison of **222b** (green) and **222g** (red) against alkyl halide **221** (blue)

We were able to re-use the PBR of **215c** with only a small drop-off in yield between runs. Using the set-up shown in Scheme 82, phenylboronic acid **192**, 2-Bromo-3-methoxynaphthalene **219** and base was run three consecutive times through a single PBR to afforded yields of 65, 64 and 61% respectively of **220a**.

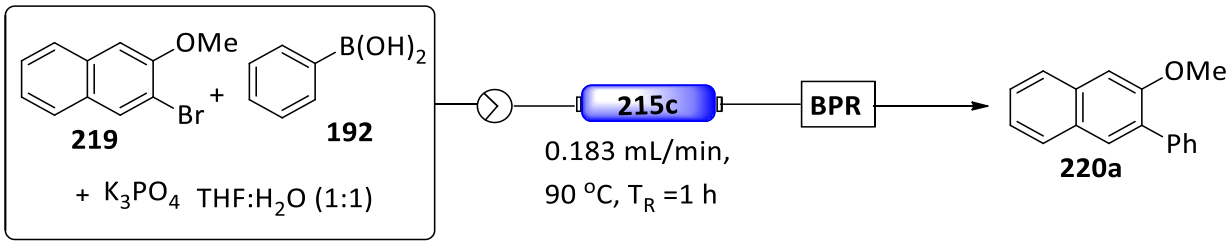

Scheme 82: Flow synthesis depicting multiple passes through 215c

A recycling study was conducted to see if the percentage conversion could be increased (Scheme 83).[§] The boronic acid **192**, aryl halide **219** and base were prepared as a single stock

[§]Note: Results for the recycling study were generated by Mr Ian Strydom and forms part of his PhD thesis, they are reported here for comparative analysis.

© University of Pretoria

solution in tetrahydrofuran:water (1:1). The stock solution was then pumped directly through the PBR housing catalyst **215c** before passing through a BPR with the outlet being fed back into the stock reagent reservoir creating a simple recycle loop. The reagent reservoir was then sampled every hour (Table 23) affording 99% conversion after three hours of reaction time (TON of 19.8 in 3 h, TOF of 1.83×10^{-3} s^{-1}).

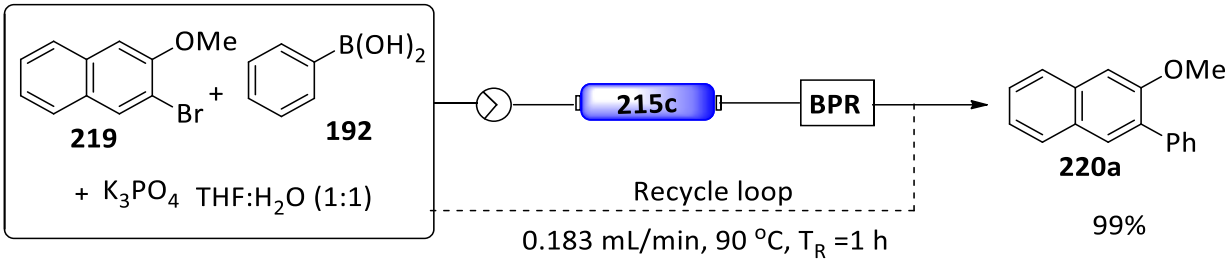

Scheme 83: General approach for flow recycling study

Table 23: Flow recycling study

Entry	Time (hours)	% Conversion
1	1	82
2	2	94
3	3	99

Reaction conditions: 192 (1.2 eq), **219** (1.0 eq), K_3PO4 (3.0 eq), **215c** (5 mol %), 90 ˚C. [Conversions determined by GC-FID as the average of two experiments and were performed by Mr Ian Strydom.]

6.4. Conclusion

In conclusion, we demonstrated the conversion of polymer-supported triphenylphosphine **146** to a polymer-supported tetrakis(triphenylphosphine)palladium(0) catalyst **215a**. The prepared catalyst **215a** offered an economical alternative to expensive commercial solid-supported versions of the catalyst (R422.25 vs R944) with comparable performance. Under flow conditions, preparation of catalyst **215c** was conveniently achieved by the sequential passage of the palladium source and the reducing agent across the PBR. Under these conditions, catalyst **215c** had a higher palladium loading (0.689 vs 0.460 mmol/g) and no detectable traces of Cl (as determined by EDX), the latter of which remain present in trace amounts when prepared under batch conditions.

The utility of catalyst **215a** and **215c** was demonstrated for Suzuki-Miyaura cross-coupling reactions under batch and flow conditions, with the flow translation requiring the use of a

© University of Pretoria

biphasic solvent system to ensure the solubilization of the inorganic base (potassium phosphate tribasic) and reaction salt by-products. Passage across a heated packed-bed reactor housing the catalyst **215c** afforded comparable yields to those obtained under batch conditions, but in a largely reduced reaction time (1 hour vs 18 hours) with only a single pass across the catalyst bed. Finally, it was demonstrated that multiple passes across the catalyst bed using a recycle loop could be used to improve the overall conversion, with 99% conversion observed after three passes (Table 23).

© University of Pretoria

Chapter 7

Overall conclusion and future work

7.1. Overall conclusion

A low-cost polystyrene-supported triphenylphosphine **201** was synthesized using Oshima's trialkylmagnesate reagent; Schlenk conditions had to be employed to prevent unwanted phosphorus oxidation of **201**. The crushed polymer-supported triphenylphosphine **146** was formed by precipitation polymerisation of diphenyl (4-vinylphenyl)phosphine and showed a phosphorus loading of 1.85 mmol/g for **146** versus 3.00 mmol/g for commercial polystyrene-supported triphenylphosphine **201a**.

The polymer-supported triphenylphosphine reagents were first demonstrated as reductants in ozonolysis reactions, converting alkenes into aldehydes using our newly developed in-house ozonolysis flow setup and gave moderate to high yields (52-70%). The reactions were setup as a batch-flow hybrid system whereby the ozonide was formed in flow, after which time the reduction stream flowed into a collection flask housing the reducing agent. Reactions were conducted at room temperature, as cooled temperatures favoured the formation of benzoic acid (Chapter 5, Figure 14). An overall flow rate of 1.0 mL/min was used as higher flow rates did not facilitate good conversion of the aldehydes. We have also reported that the polymer-supported reagent **146** showed an improvement relative to the commercial polystyrene reagent using four-fold less reagent.

Secondly, we demonstrated the conversion of polystyrene-supported triphenylphosphine **201a** and in-house polymer-supported triphenylphosphine **146** to Wittig benzyl phosphonium salts **208** and **209** with a phosphorous elemental loading of 0.817 mmol/g and 1.614 mmol/g respectively. At a temperature of 30 °C alkene products were formed when using solid-supported phosphonium salt **209** whereas products only resulted at 60 °C for the polystyrene support **208**. We demonstrated the use of the reagents in the Wittig reactions under batch and flow conditions which gave varying yields which were substrate dependant (Chapter 4, Table 14).

Lastly, we transformed reagent **146** into polymer-supported tetrakis(triphenyl-phosphine)palladium catalysts **215a** (batch) and **215c** (flow) with a palladium loading of 0.460 mmol/g and 0.689 mmol/g respectively. The prepared catalysts offered an economical

© University of Pretoria

alternative to the expensive commercial solid-supported catalyst (R422.25 vs R944) with a palladium loading of 0.500 mmol/g. Demonstration of its use in Suzuki-Miyaura coupling reactions under batch and flow conditions showed comparative results (Chapter 5, Table 21 and 22). Recycling the substrates across the catalysts in flow could be used to improve the overall conversion to 99% as shown in Table 23. Our in-house supported catalyst showed an advantage against the commercial supported catalyst

Overall, our in-house polymer-supported reagent (ozonolysis and Wittig) and catalyst (Suzuki-Miyaura) was an improvement to the commercially available polymer-supported counterparts. Although the unsupported reagents gave higher yields, much time was spent in removing the triphenylphosphine oxide in addition to other co-products. Flow synthesis in the Suzuki-Miyaura reactions showed to be an improvement to batch synthesis having the option of recycling the substrates across the packed column.

7.2. Future work

Current future work will look at the application of our three reagents to different pharmaceutical processes. For example, the antimalarial drug artemisinin **224** could be synthesized using our newly developed ozonolysis flow reactor system, Scheme 84. Compound **223** would react with dichloroacetic acid (DCA) in the presence of ozone and trifluoroacetic acid to give artemisinin.

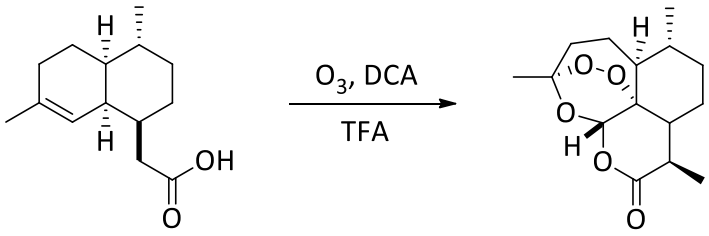

223 **224**
Artemisinin

Scheme 84: Known synthesis of artemisinin

A number of phosphonium salts can be produced for the Wittig reaction. For example, previtamin D **227** can be synthesized from aldehyde **225** and phosphonium salt **226**, Scheme 85.

© University of Pretoria

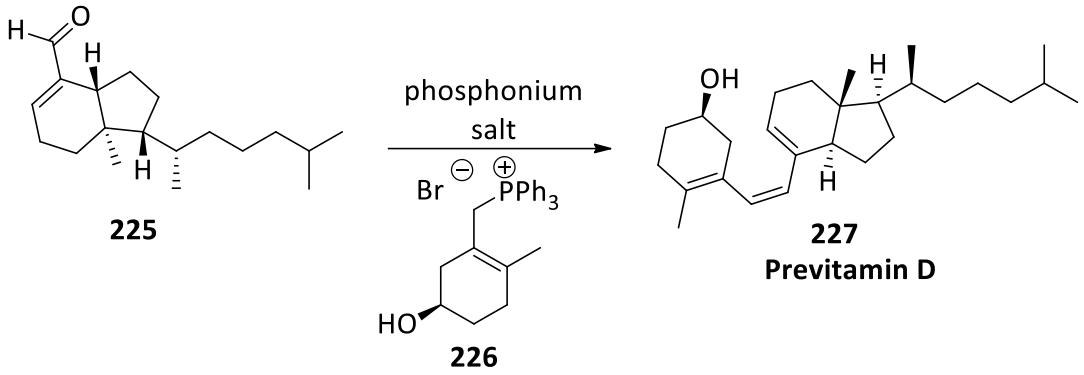

Scheme 85: Synthesis of previtamin D

The tetrakis(triphenylphosphine)palladium catalysts **215** may be used towards the synthesis of anti-cancer drug lapatinib **230**, Scheme 86. The bromo intermediate **228** could be reacted with the formyl boronic acid in the presence of a base to yield the Suzuki-Miyaura coupled intermediate **229**. Subsequent reactions could then lead to the formation of Lapatinib.

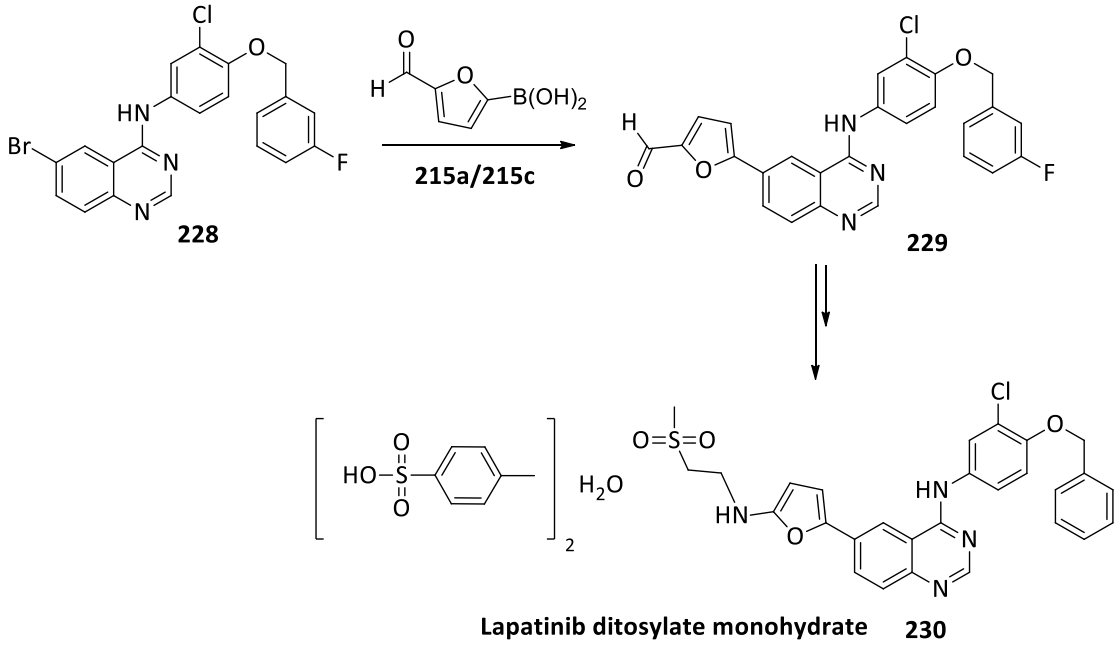

Scheme 86: Towards the synthesis of lapatinib ditosylate monohydrate

© University of Pretoria

Experimental

© University of Pretoria

Chapter 8

Experimental

8.1. General procedures

All reactions were carried out in oven-dried glassware with additional flame drying for Schlenk flasks. Dry solvents were distilled under nitrogen and degassed with argon before being used: acetonitrile from calcium hydride, tetrahydrofuran from sodium and benzophenone, and dichloromethane from phosphorous pentoxide. A 1.0 M solution of sodium ethoxide was prepared by dissolving sodium (0.05 mol) in ethanol (50 mL) and stored under argon. All reagents and other solvents were used without further purification from commercial sources. Polystyrene-supported triphenylphosphine was purchased from Sigma Aldrich. All known compounds afforded as solids were pure enough to proceed to the next step unless stated otherwise.

Titration: Anhydrous lithium chloride (10 mmol) was dried in an argon filled flask, under high-vacuum for 4 hours at 140 °C. After cooling to room temperature, anhydrous tetrahydrofuran (20 mL) was added and the mixture was stirred for 24 hours unto the lithium chloride was completely dissolved, resulting in a 0.5 M solution of lithium chloride. In a dry, argon filled round-bottomed flask fitted with a rubber septum was added iodine (254 mg, 1.0 mmol). To this was added the 0.5 M solution of lithium chloride (5 mL) and the mixture was stirred until the iodine was completely dissolved resulting in a brown solution. The mixture was then cooled to 0 °C and *n*-butyllithium was added dropwise until the brown colour of the solution disappeared.

Liquid Chromatography: Thin Layer Chromatography (TLC) analysis was carried out on aluminium sheets pre-coated with silica (Merck Silica Gel 60 F254), which was visualized by ultraviolet light and sprayed with potassium permanganate or a 2.5% solution of anisaldehyde in a mixture of sulfuric acid under heat. Column chromatography was carried out using silica gel (Fluorochem Silica Gel 60, 40-63 micron) as the stationary phase.

Melting Points (mp): Determined using a Stuart SMP10 melting point system. Dry samples were placed into glass capillary tubes and heated.

© University of Pretoria

Nuclear Magnetic Resonance Spectroscopy: Spectra were recorded in $CDCl_3$ solution unless otherwise stated using a Bruker Avance III (400 MHz), Varian Unity XR (300 and 400 MHz) or Varian Mercury (300 MHz) spectrometer for ^{1}H NMR and ^{31}P NMR, and a Bruker Ultrashield 400 Plus (101 MHz) or a Bruker Avance III (75 MHz) for ^{13}C NMR. Chemical shifts are reported relative to tetramethylsilane as the internal standard at 0.00 ppm for ^{1}H NMR, and relative to $CDCl_3$ at 77.36 ppm for ^{13}C NMR. Spectral features for ^{1}H NMR were recorded in the following order: chemical shift (δ_H, ppm); coupling constant(s) (J, Hz); multiplicity (s = singlet, d = doublet, t = triplet, p = pentet, q = quartet, m = multiplet, ppm = parts per million); number of protons; assignment. ^{13}C NMR and ^{31}P NMR spectral data is recorded in the form: chemical shift ($\delta_{C,}$ ppm); assignment.

Fourier-Transform Infrared Spectroscopy: Spectra were obtained on a Bruker Platinum-ATR spectrometer instrument as a neat sample. Spectral features are recorded as wavenumbers (cm^{-1}) and relative absorbance with respect to the most intense peak were noted as: w - weak (<40%), m - medium (40-75%), s - strong (>75%).

Scanning Electron Microscopy: Samples were prepared by placing a piece of double-sided conductive tape on a sample stub and sprinkling a small amount of sample on to it. The samples were all prepared on different stubs and then coated with carbon to render them conductive. The stubs were then placed onto a viewing stage. SEM and EDX data were processed using ZEISS Auriga SEM and an Oxford x-max detector. Software used for SEM analysis was SMART SEM version V05.04.05.00 and for EDX was Aztec 2.2 SP1.

Transmission Electron Microscopy: Samples were dispersed on enough ethanol to create a very lightly disperse solution. This was then sonicated for 30 minutes in an ultra-sonicator at room temperature. A carbon coated Cu grid was then dipped into the solution and left to dry at room temperature. Samples were then run using JEOL JEM 2100 instrument.

Powder X-Ray Diffraction: Samples were run on the Bruker D2 Phaser XRD machine and data was analysed using DiffractDW 1.3.0.1, 200 mg of each sample was placed on a low background sample holder and run at 2 seconds per 0.05 2 theta increments ranging from 5 to 60 2 theta.

© University of Pretoria

Brunauer-Emmett-Teller: Physisorption was performed by degassing the samples at 90 °C for 4 hours before nitrogen adsorption using Tristar II Micromeritics Instrument.

Particle Size Distribution:

Samples were measured on a Zetasizer nano series Malvern instrument, where 10 mg of the samples were put into a vial with 1 mL distilled water and vial was vortexed. Samples were then filtered into sample holder and run 3 times to get an average.

High Resolution Mass Spectrometry (HRMS): Performed on a Waters Synapt G2 instrument utilising either positive electrospray ionisation (ESI+) or positive electron ionisation (EI+) source equipped with a direct insertion probe. Limit: ± 5 parts per million.

Flow Equipment: Polymeric reagents were contained in glass 10 mL Omnifit™ columns and were connected to a Uniqsis FlowSyn SS flow system with standard Omnifit™ column end pieces, tubing connectors and PTFE tubing.

Gas Chromatography: Samples were run using a Shimadzu GC-2010 instrument with a FID detector. Stock solutions were made using 4-iodoanisole (1.000 g, 4.272 mmol) and anisole (0.4620 g, 4.272 mmol) dissolved in tetrahydrofuran in a 10 mL volumetric flask. A separate solution of phenylboronic acid (0.5210 g, 4.272 mmol) and K_3PO_4 (0.5904 g, 4.272 mmol) was made with water in a 10 mL volumetric flask. Catalytic runs were prepared with 1 mL of each solution pipetted into a Schlenk tube under a constant stream of argon. The Schlenk tube was sealed and lowered into an oil bath at 90 °C. After 18 hours, the tube was removed from the oil bath, and a 1.0 mL aliquot was transferred to an eppendorf tube. The tube was centrifuged for 5 min at 900 rpm. A 100 µL aliquot was dispensed directly into an MS vial, and diluted with 900 µL of dichloromethane.

© University of Pretoria

Table 24: GC-FID method

GC-FID method	
Column	INERTCAP5MS\NP, 30 m, 0.25 mm, 0.25 µm
Injector	Volume: 1 µL, Inlet temperature: 200 °C
Carrier Gas	Helium at 1.0 mL/min, Constant Flow
Oven Parameters	80 °C for 1 min, 5 °C/min ramp to 105 °C, 10 °C/min ramp to 135 °C, hold 0.5 min, 5 °C/min ramp to 190 °C, 20 °C/min to 250 °C
Detector	250 °C. Helium: 30 mL/min, Hydrogen 40 mL/min, Air: 400 mL/min. Sampling rate 40 milliseconds.

8.2. Synthesis and characterization of immobilized triphenylphosphine reagents

a. Batch synthesis of in-house polystyrene-supported triphenylphosphine (201)

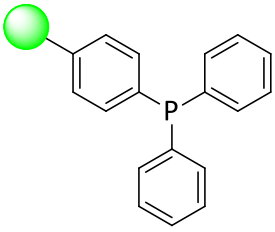

201

In a flame dried Schlenk flask under argon, was added dropwise 1.6 M *n*-butyllithium (3.44 mL, 5.0 mmol, 4.0 eq) or 2.5 M *n*-butyllithium (2.00 mL, 5.0 mmol, 4.0 eq) to a solution of 2.0 M *iso*propylmagnesium chloride (2.00 mL, 2.50 mmol, 2.0 eq) in dry tetrahydrofuran (0.2 M) at 0 °C. The resulting solution was stirred for 30 minutes to give a clear yellow solution of *i*-Pr(*n*-Bu)$_2$MgLi. In a separate Schlenk flask, dry 4-bromopolystyrene beads (500 mg, 1.25 mmol, 1.0 eq) were swollen in dry tetrahydrofuran (5.0 mL) for 1 hour at 0 °C under argon. The preformed *i*-Pr(*n*-Bu)$_2$MgLi was then added to the swollen beads and the resulting solution was shaken. After 3 hours chlorodiphenylphosphine (1.35 mL, 7.50 mmol, 6.0 eq) was added and the mixture was allowed to warm to room temperature. The beads were then filtered and washed with dry tetrahydrofuran (3 x 20 mL) and dried *in vacuo* to give flowing yellow beads.

^{31}P NMR (600 MHz, $CDCl_3$) -6.31 (s, 1P, P-Ph)

Attempted method 1

In a round bottomed flask under argon, was added 1.6 M *n*-butyllithium (3.44 mL, 5.0 mmol, 4.0 eq) or 2.5 M *n*-butyllithium (2.00 mL, 5.0 mmol, 4.0 eq) to a solution of 2.0 M *iso*propylmagnesium chloride (2.00 mL, 2.50 mmol, 2.0 eq) in tetrahydrofuran (0.2 M) at 0 °C. The resulting solution was stirred for 30 minutes to give a clear yellow solution of *i*-Pr(*n*-Bu)$_2$MgLi. In a separate flask, dry 4-bromopolystyrene beads (500 mg, 1.25 mmol, 1.0 eq) were swollen in dry tetrahydrofuran (5.0 mL) for 1 hour at 0 °C. The preformed

© University of Pretoria

i-Pr(*n*-Bu)$_2$MgLi was then added to the swollen beads and the resulting solution was stirred. After 3 hours chlorodiphenylphosphine (1.35 mL, 7.50 mmol, 6.0 eq) was added and the mixture was allowed to warm to room temperature for 2 or 18 hours. The beads were then filtered and washed with tetrahydrofuran (3 x 20 mL) and dried *in vacuo* to give free flowing yellow beads.

Attempted method 2

In a round bottomed flask, was swollen dry 4-bromopolystyrene beads (500 mg, 1.25 mmol, 1.0 eq) in dry tetrahydrofuran (5.0 mL) for 1 hour at 0 °C. To the flask was then added 1.6 M butyllithium (3.44 mL, 5.0 mmol, 4.0 eq) or 2.5 M butyllithium (2.00 mL, 5.0 mmol, 4.0 eq). After 3 hours, chlorodiphenylphosphine (1.35 mL, 7.50 mmol, 6.0 eq) was added and the mixture was allowed to warm to room temperature 2 or 18 hours. The beads were then filtered and washed with tetrahydrofuran (3 x 20 mL) and dried *in vacuo* to give flowing yellow beads.

Attempted method 3

In a round bottomed flask, was swollen dry 4-bromopolystyrene beads (500 mg, 1.25 mmol, 1.0 eq) in dry tetrahydrofuran (5.0 mL) for 1 hour at 0 °C. To the flask was then added 2.0 M *iso*propylmagnesium chloride (2.00 mL, 2.50 mmol, 2.0 eq) in dry tetrahydrofuran (0.2 M) at 0 °C. After 3 hours, chlorodiphenylphosphine (1.35 mL, 7.50 mmol, 6.0 eq) was added and the mixture was allowed to warm to room temperature 2 or 18 hours. The beads were then filtered and washed with tetrahydrofuran (3 x 20 mL) and dried *in vacuo* to give flowing yellow beads.

b. Batch synthesis of in-house polymer-supported triphenylphosphine (146)

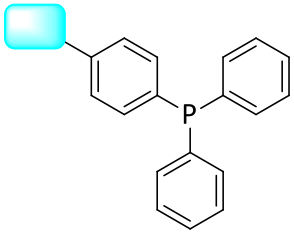

146

In a round bottomed flask was stirred a solution of diphenyl-(4-vinylphenyl)phosphine (1.67 g, 5.8 mmol, 2.6 eq), divinylbenzene (1.01 g, 7.7 mmol, 3.5 eq), styrene (0.23 g, 2.2 mmol, 1.0 eq) and 1-dodecanol (2.25 g, 12.1 mmol, 5.5 eq) at 50 °C. Upon complete dissolution, dibenzoyl peroxide (35.0 mg, 0.14 mmol, 0.9 mol %) was added and the mixture was stirred for 5 minutes at 50 °C. The mixture was then heated at 92 °C for 48 hours in a glass vial. The solid-supported reagent was then removed from the vial,

© University of Pretoria

crushed using a mortar and pestle and washed with hot dry dichloromethane (100 mL) by filtration to remove the dodecanol to give a white solid.

EDX: P = 1.850 mmol/g

Attempted method for flow synthesis of 146

In a round bottomed flask was stirred a solution of diphenyl(4-vinylphenyl)phosphine (1.67 g, 5.8 mmol, 2.6 eq), divinylbenzene (1.01 g, 7.7 mmol, 3.5 eq), styrene (0.23 g, 2.2 mmol, 1.0 eq) and 1-dodecanol (2.25 g, 12.1 mmol, 5.5 eq) at 50 °C. Upon complete dissolution, dibenzoyl peroxide (35.0 mg, 0.14 mmol, 0.9 mol %) was added and the mixture was stirred for 5 minutes at 50 °C. The mixture was then added to a 10 mL OmniFit™ glass column, ends closed and fitted to a Uniqsis FlowSyn reactor and heated at 92 °C for 48 hours. The ends were then fitted with tubing and dichloromethane was passed through the column at 60 °C at 1.0 mL/min.

8.3. Synthesis and characterization for batch ozonolysis reaction

In a 0.1 M solution of alkene (1.0 eq) in methanol:dichloromethane (10 mL) stained with Sudan Red dye was added ozone through a tube fitted with a Pasteur pipette. The solution was filled with ozone until the colour became colourless. Thereafter, triphenylphosphine (2.5 eq) was added to the solution. The reaction was then left overnight, the solvent was removed *in vacuo* and purified by column chromatography using 5% ethyl acetate/hexane as eluent.

8.4. Synthesis and characterization for flow ozonolysis reaction

a. General procedure 1: Ozonolysis reactions using commercial unsupported triphenylphosphine

A stock solution containing the alkene (1.0 eq) in methanol:dichloromethane (1:1) (0.1 M) was pumped at a flow rate of 0.5 mL/min and mixed with ozone in a 10 mL glass column at room temperature while the flow stream simultaneously passed through a 100 psi BPR. The stream was pumped out at flow rate of 0.5 mL/min and collected into a flask containing triphenylphosphine (2.5 eq). The reaction was then left overnight, the solvent was removed *in vacuo* and purified by column chromatography using 5% ethyl acetate/hexane as eluent.

Attempted method 1

A stock solution containing the alkene (1.0 eq) in methanol:dichloromethane (1:1) (0.1 M) was pumped at a flow rate of 0.5 mL/min and mixed with ozone in a 10 mL glass column at

© University of Pretoria

0 °C, -10 °C or -40 °C while the flow stream simultaneously passed through a 100 psi BPR. The stream was pumped out at flow rate of 0.5 mL/min and collected into a flask containing triphenylphosphine reagent (2.5 eq). The reaction was then left overnight, the solvent was removed in vacuo.

Attempted method 2

A stock solution containing the alkene (1.0 eq) in methanol:dichloromethane (1:1) (0.1 M) was pumped at a flow rate of 1.0 mL/min and mixed with ozone in a 10 mL glass column at room temperature while the flow stream simultaneously passed through a 100 psi BPR. The stream was pumped out at flow rate of 1.0 mL/min and collected into a flask containing triphenylphosphine reagent (2.5 eq). The reaction was then left overnight, the solvent was removed in vacuo.

b. General procedure 2: Ozonolysis reactions using commercial polystyrene-supported triphenylphosphine (201a)

A stock solution containing the alkene (1.0 eq) in methanol/dichloromethane (1:1) (0.1 M) was pumped at a flow rate of 0.5 mL/min and mixed with ozone in a 10 mL glass column at room temperature while the flow stream simultaneously passed through a 100 psi BPR at a flow rate of 0.5 mL/min and into a flask containing polystyrene-supported triphenylphosphine (3.0 mmol, 4-fold). The reaction was then left for 48 hours at room temperature, filtered then solvent removed *in vacuo* and purified by column chromatography using 5% ethyl acetate/hexane as eluent.

c. General procedure 3: Ozonolysis reactions using in-house polymer-supported triphenylphosphine (146)

A stock solution containing the alkene (1.0 eq) in methanol:dichloromethane (1:1) (0.1 M) was pumped at a flow rate of 0.5 mL/min and mixed with ozone in a 10 mL glass column at room temperature, while the flow stream simultaneously passed through a 100 psi BPR and collected into a flask containing in-house solid-supported triphenylphosphine (1.85 mmol, one-fold). The reaction was then left overnight at room temperature, filtered and the solvent removed *in vacuo.* The mixture was purified by column chromatography using 5% ethyl acetate/hexane as eluent.

© University of Pretoria

Table 8: Results of ozonolysis reactions

Entry	Alkene	Aldehyde	% Yield		
			PPh_3	201	146
1	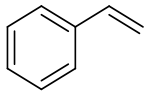 **143**	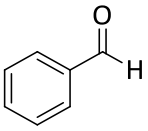 **143a**	76	67	70
2	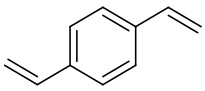 **142**	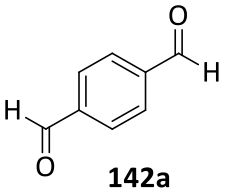 **142a**	74	67	69
3	**202**	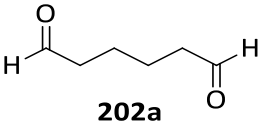 **202a**	73	66	68
4	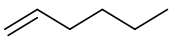 **203**	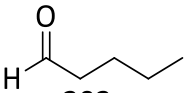 **203a**	65	55	58
5	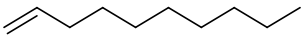 **204**	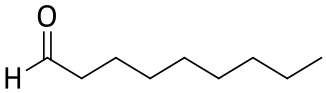 **204a**	63	52	55
6	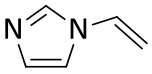 **205**	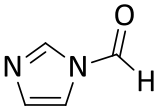 **205a**	68	62	64

Benzaldehyde (143a)

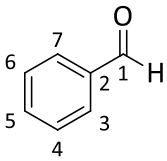
143a

Clear oil, **^{1}H NMR** (300 MHz, $CDCl_3$) δ 10.02 (s, 1H, H-1), 7.88 (m, 2H, H-3 and H-7), 7.72 – 7.58 (m, 1H, H-5), 7.57 – 7.42 (m, 2H, H-4 and H-6); **^{13}C NMR** (75 MHz, $CDCl_3$) δ 192.5 (C-1), 136.4 (C-2), 134.5 (C-5), 129.9 (C-4 and C-6), 129.0 (C-3 and C-7). The peaks were comparable to the values reported by Okuno and co-workers.[79]

© University of Pretoria

Terephthalaldehyde (142a)

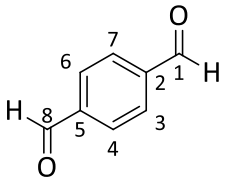

142a

White solid, **^{1}H NMR** (300 MHz, $CDCl_3$) δ 10.15 (s, 2H, H-1 and H-8), 8.07 (s, 4H, H-2 to H-7); **^{13}C NMR** (101 MHz, $CDCl_3$) δ 191.6 (C-1 and C-8), 140.1 (C-2 and C-5), 130.3 (C-3, C-4, C-6 and C-7); **mp:** 114-117 °C. The peaks were comparable to the values reported by Wu and co-workers.[80]

Hexanedial (202a)

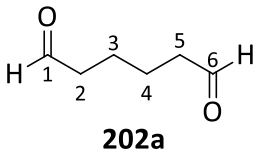

202a

Clear oil, **^{1}H NMR** (300 MHz, $CDCl_3$) δ 9.74 (s, 2H, H-1 and H-6). 1.56 (m, 4H, H-2 and H-5), 1.43 – 1.00 (m, 4H, H-3 and H-4); **^{13}C NMR** (101 MHz, $CDCl_3$) δ 202.3 (C-1 and C-6), 43.4 (C-2 and C-5), 21.7 (C-3 and C-4). The peaks were comparable to the values reported by Carrera and co-workers.[81]

Pentanal (203a)

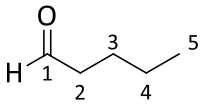

203a

Clear oil, **^{1}H NMR** (400 MHz, $CDCl_3$) δ 9.77 (s, 1H, H-1), 2.44 (m, 2H, H-2), 1.71 – 1.52 (p, *J* = 16 Hz and *J* = 8 Hz, 2H, H-3), 1.41 – 1.27 (m, 2H, H-4), 0.93 (t, *J* = 8 Hz, 3H, H-5); **^{13}C NMR** (101 MHz, $CDCl_3$) δ 203.0 (C-1), 43.6 (C-2), 24.1 (C-3), 22.3 (C-4), 13.8 (C-5). The peaks were comparable to the values reported by Matano and co-workers.[82]

Nonyl aldehyde (204a)

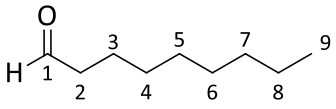

204a

Clear oil, **^{1}H NMR** (300 MHz, $CDCl_3$) δ 9.77 (s, 1H, H-1), 2.42 (m, 2H, H-2), 1.74 – 1.51 (m, 2H, H-3), 1.27 (m, 10H, H-4 to H-8), 0.96 – 0.72 (t, *J* = 6.0 Hz, 3H, H-9); **^{13}C NMR** (101 MHz, $CDCl_3$) δ 203.2 (C-1), 44.1 (C-2), 31.9 (C-7), 29.5 (C-6), 29.4 (C-5), 29.3 (C-4), 29.2 (C-3), 22.8 (C-8), 14.2 (C-9). The peaks were comparable to the values reported by Nicolaou and co-workers.[83]

Imidazole-1-carbaldehyde (205a)

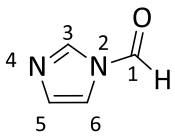

205a

Brown oil, **^{1}H NMR** (400 MHz, $CDCl_3$) δ 9.73 (s, 1H, H-1), 7.90 (s, 1H, H-3), 7.47 (s, 1H, H-6), 7.04 (s, 1H, H-5); **^{13}C NMR** (101 MHz, $CDCl_3$) δ 160.7 (C-1), 136.8 (C-3), 131.0 (C-5), 117.5 (C-6). The peaks were comparable to the values reported by Chen and co-workers.[84]

© University of Pretoria

8.5. Synthesis and characterization for batch Wittig reactions

a. Synthesis of benzyltriphenylphosphonium bromide (206)

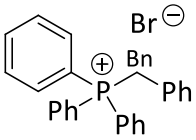

206

Triphenylphosphine (3.40 g, 12.9 mmol, 1.1 eq) was added to a solution of benzyl bromide (2.00 g, 11.7 mmol, 1.0 eq) in toluene (20 mL). The mixture was refluxed overnight to form a precipitate which was filtered and washed with toluene (2 x 20 mL) and hexane (2 x 20 mL), before being dried *in vacuo* to give the phosphonium salt (3.9 g with 78%) as a white solid.

^{1}H NMR (400 MHz, $CDCl_3$) 7.81 – 7.67 (m, 9H, Ar-H), 7.67 – 7.58 (m, 6H, Ar-H), 7.25 – 7.17 (m, 1H, Ar-H), 7.15 – 7.05 (m, 4H, Ar-H), 5.35 (d, *J* = 8.0 Hz, 2H, Bn); **^{13}C NMR** (101 MHz, $CDCl_3$) 135.1 (Ar), 135.1 (Ar), 134.4 (Ar), 134.3 (Ar), 131.5 (Ar), 131.5 (Ar), 130.3 (Ar), 130.1 (Ar), 128.9 (Ar), 128.8 (Ar), 128.5 (Ar), 128.4 (Ar), 127.2 (Ar), 127.1 (Ar), 118.2 (Ar), 117.4 (Ar), 30.9 (C-Bn); **^{31}P NMR** (300 MHz, $CDCl_3$) 23.19 (s, 1P, P-Ph); **mp:** 295-299 °C; **EDX:** P = 1.969 mmol/g and Br = 2.073 mmol/g. The peaks were comparable to the values reported by Smith and co-workers.[85]

b. Synthesis of polystyrene-supported benzyltriphenylphosphonium bromide (208)

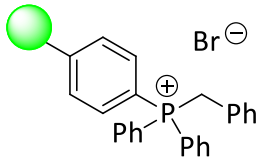

208

Benzyl bromide (0.72 mL, 6.02 mmol, 2.0 eq) was added dropwise with stirring to a suspension of commercial polystyrene-supported triphenylphosphine **201a** (1.004 g, 3.01 mmol, 1.0 eq) in dimethyl-formamide (15 mL). The mixture was stirred for 48 hours at 70 °C, cooled and filtered, before being washed with toluene (50 mL), dichloromethane (50 mL) and diethyl ether (50 mL). The crude product was then dried *in vacuo* to yield the phosphonium salt as brown beads.

^{31}P NMR (600 MHz, $CDCl_3$) 23.19 (s, P-Ph); **EDX:** P = 0.8179 mmol/g and Br = 0.3170 mmol/g.

c. Synthesis of in-house polymer-supported benzyltriphenylphosphonium bromide (209)

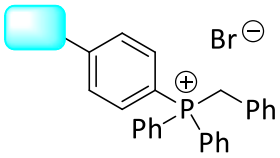

209

Benzyl bromide (0.72 mL, 6.02 mmol, 2.0 eq) was added dropwise with stirring to a suspension of in-house solid-supported triphenylphosphine **146** (1.004 g, 3.01 mmol, 1.0 eq) in toluene (15 mL). The mixture was stirred for 48 hours at 70 °C, cooled, filtered, washed with toluene (3 x 50 mL) and dried to yield the phosphonium salt as a white solid.

EDX: P = 1.614 mmol/g and Br = 1.042 mmol/g.

© University of Pretoria

d. General batch procedure 1: Wittig reactions using unsupported benzyl phosphonium salt (206)

To a flask containing 15 mL ethanol was added benzyltriphenylphosphonium bromide, **206**, (2.0 eq) and the aldehyde (1.0 eq). A solution of freshly prepared 1.0 M sodium ethoxide (3.0 eq) was added to the reaction mixture, which was then stirred for 30 minutes at room temperature before being quenched with ammonium chloride (10 mL). The mixture was then transferred to a separating funnel and the organic layer separated. The water layer was extracted with ethyl acetate (3 x 20 mL). The combined organic extracts were dried over magnesium sulfate, filtered and concentrated. The crude product was purified by column chromatography using 5% ethyl acetate/hexane as eluent to yield the desired alkene.

e. General batch procedure 2: Wittig reactions using polystyrene-supported benzyl phosphonium salt (208)

To a flask containing a suspension of polystyrene-supported phosphonium salt **208** (2.0 eq) in 15 mL ethanol was added the aldehyde (1.0 eq). A solution of freshly prepared 1 M sodium ethoxide (3.0 eq) was added to the reaction mixture, which was then stirred for 18 hours at room temperature before being quenched with ammonium chloride (10 mL). The mixture was filtered and washed with ethyl acetate (20 mL) and the organic layer separated. The water layer was extracted with ethyl acetate (3 x 10 mL). The combined organic extracts were dried over magnesium sulfate, filtered and concentrated. The crude product was then purified by column chromatography eluting 5% ethyl acetate/hexane to yield alkene.

f. General batch procedure 3: Wittig reactions using in-house polymer-supported benzyl phosphonium salt (209)

To a flask containing a suspension of polymer-supported phosphonium salt **209** (2.0 eq) in 15 mL ethanol was added the aldehyde (1.0 eq). A solution of freshly prepared 1 M sodium ethoxide (3.0 eq) was added to the reaction mixture which was then stirred for 18 hours at room temperature before being quenched with ammonium chloride (10 mL). The mixture was filtered and washed with ethyl acetate (20 mL) into a separating funnel and the organic layer separated. The water layer was extracted with ethyl acetate (3 x 10 mL). The combined organic extracts were dried over magnesium sulfate, filtered and concentrated. The crude product was then purified by column chromatography eluting 5% ethyl acetate/hexane to yield the desired alkene.

© University of Pretoria

8.6. Synthesis and characterization for flow Wittig reactions

a. Synthesis of polystyrene-supported benzyl phosphonium salt (208a)

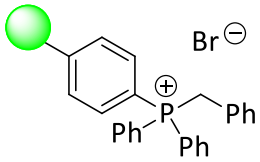

208a

A 10 mL glass OmnitFit™ column was loaded with commercial polystyrene-supported triphenylphosphine **201a** (1.000 g) which was then washed with dry toluene for 1 hour at 0.2 mL/min. Thereafter benzyl bromide (0.2 M) in toluene (50 mL) was recycled across the column for 24 hours at 0.2 mL/min, 70 °C. The polystyrene-supported reagent was then washed with toluene for 1 hour at 0.2 mL/min, 70 °C to remove any unloaded benzyl bromide to give the desired phosphonium salt at a white solid.

^{31}P NMR (300 MHz, $CDCl_3$) 23.19 (s, P-Ph); **EDX:** P = 0.935 mmol/g and Br = 0.422 mmol/g.

b. Synthesis of in-house polymer-supported benzyl phosphonium salt (209a)

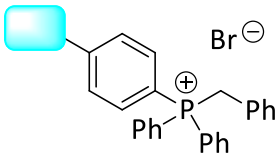

209a

A 10 mL glass OmnitFit™ column was loaded with ground, washed polymer-supported triphenylphosphine (1.003 g) which was then washed with dry toluene for 1 hour at 0.2 mL/min. Thereafter benzyl bromide (0.2 M) in toluene (50 mL) was recycled across the column for 24 hours at 0.2 mL/min, 70 °C. The solid-supported was then washed with toluene for 1 hour at 0.2 mL/min,70 °C to remove any unloaded benzyl bromide to give phosphonium salt as a white solid.

EDX: P = 1.012 mmol/g and Br = 1.002 mmol/g.

c. General flow procedure 1: Wittig reactions using unsupported benzyl phosphonium salt 206

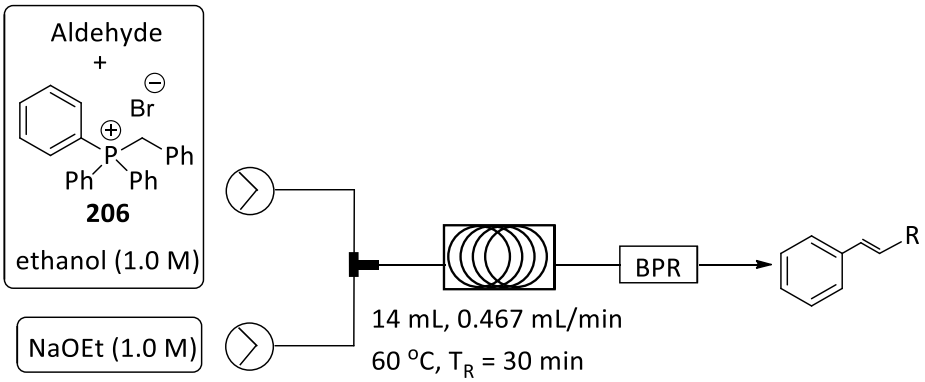

A stock solution containing the aldehyde (1.0 eq) and benzyl salt (2.0 eq) in ethanol (1.0 M) was mixed with a stock solution of sodium ethoxide (1.0 M, 3.0 eq) in a 1:3 ratio at a T-piece mixer. Thereafter the flow stream was passed through a 14 mL coil at 60 ˚C followed by a 100

© University of Pretoria

BPR at a flow rate of 0.467 mL/min (30 minutes residence time). A post-reaction wash with ethanol was performed at 1 mL/min for 30 minutes. The crude product was then quenched with ammonium chloride (10 mL), separated and the aqueous layers extracted with ethyl acetate (3 x 20 mL). The combined organic layers were dried over magnesium sulfate, filtered, evaporated *in vacuo* and purified by column chromatography using 5% ethyl acetate/hexane as eluent.

Attempted method 1

A stock solution containing the aldehyde (1.0 eq) and benzyl salt (2.0 eq) in dichloromethane (1.0 M) was mixed with a stock solution of 20% or 50% aqueous sodium hydroxide (3.0 eq) in a 1:3 ratio at a T-piece mixer. Thereafter the flow stream was passed through a 14 mL coil at 60 ˚C followed by a 100 BPR at a flow rate of 0.467 mL/min (30 minutes residence time). A post-reaction wash with dichloromethane was performed at 1 mL/min for 30 minutes. The crude product was then quenched with ammonium chloride (10 mL), separated and the aqueous layers extracted with dichloromethane (3 x 20 mL). The combined organic layers were dried over magnesium sulfate, filtered, evaporated *in vacuo* and purified by column chromatography using 5% ethyl acetate/hexane as eluent.

d. General flow procedure 2: Wittig reactions using polystyrene- or in-house polymer-supported benzyl phosphonium salt

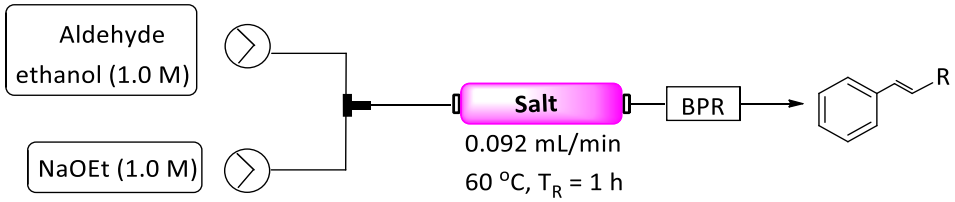

A 10 mL glass OmnitFit™ column packed with **208a** or **209a** (200 mg) was mounted in a Uniqsis FlowSyn SS reactor heating block and washed with ethanol for 5 minutes. A stock solution containing the aldehyde (1.0 M, 1.0 eq) in ethanol was mixed with a stock solution of base (1.0 M, 3.0 eq) in ethanol in a 1:3 ratio at a T-piece mixer. Thereafter the flow stream was passed through the glass OmniFit™ column housing **208a** or **209a** at 60 ˚C. A total flow rate of 0.092 mL/min (T_R = 1 hour) was used. A post-reaction wash with ethanol was performed at 0.5 mL/min for 1 hour. The crude product was then quenched with ammonium chloride (10 mL), separated and the aqueous layers extracted with ethyl acetate (3 x 20 mL).

© University of Pretoria

The combined organic layers were dried over magnesium sulfate, filtered, evaporated *in vacuo* and purified by column chromatography using 5% ethyl acetate/hexane as eluent.

Table 14: Batch vs flow comparison of Wittig reactions using commercial unsupported-, commercial polystyrene-supported- and in-house solid-supported benzyl salts.

Entry	Aldehyde	Alkene	% Yield					
			Batch			Flow		
			206	208	209	206	208a	209a
1	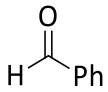 **143a**	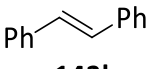 **143b**	97	40	43	95	50	51
2	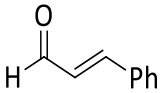 **210**	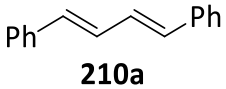 **210a**	88	32	44	82	28	49
3	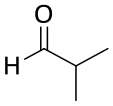 **211**	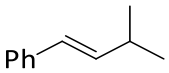 **211a**	96	38	23	84	42	25
4	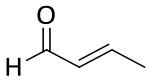 **212**	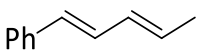 **212a**	98	42	24	91	40	27
5	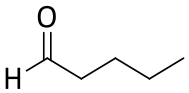 **213**	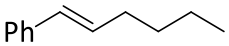 **213a**	98	35	20	83	51	22
6	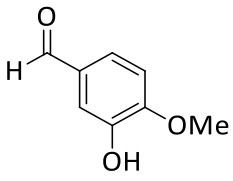 **214**	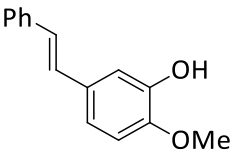 **214a**	83	40	24	61	35	27

© University of Pretoria

(*E*)-1,2-Diphenylethene (143b)

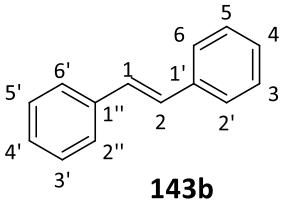

143b

White solid, **^{1}H NMR** (600 MHz, $CDCl_3$) 7.50 (d, *J* = 4.0 Hz, 2H, Ar-H), 7.34 (t, *J* = 2.7 Hz, 2H, Ar-H), 7.27 – 7.14 (m, 6H, Ar-H), 7.10 (s, 1H, H-1), 6.59 (s, 1H, H-2); **^{13}C NMR** (101 MHz, $CDCl_3$) δ 137.5 (C-1'), 137.4 (C-1''), 130.4 (Ar), 129.0 (Ar), 128.9 (Ar), 128.8 (Ar), 128.3 (Ar), 127.8 (C-2), 127.2 (C-1), 126.7 (C-1 and C-2); **mp:** 46-50 °C. The peaks were comparable to the values reported by Li and co-workers.[86]

(1*E*,3*E*)-1,4-Diphenylbuta-1,3-diene (210a)

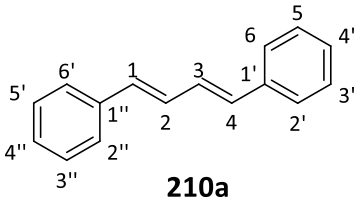

210a

White solid, **^{1}H NMR** (300 MHz, $CDCl_3$) δ 7.49 – 7.40 (m, 4H, Ar-H), 7.38 – 7.28 (m, 4H, Ar-H), 7.28 – 7.18 (m, 2H, Ar-H), 7.03 – 6.89 (m, 2H, H-1 and H-4), 6.74 – 6.60 (m, 2H, H-2 and H-3); **^{13}C NMR** (101 MHz, $CDCl_3$) δ 137.7 (C1' and C-1''), 133.2 (C-2 and C-3), 129.6 (C-1 and C-4), 129.0 (Ar), 127.9 (Ar), 126.7 (Ar); **mp:** 149 – 153 °C The peaks were comparable to the values reported by Blackwell and co-workers.[87]

(*E*)-(3-Methylbut-1-en-1-yl) benzene (211a)

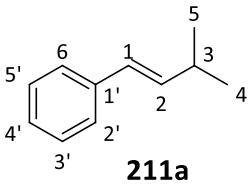

211a

Clear oil, **^{1}H NMR** (300 MHz, $CDCl_3$) δ 7.39 – 7.13 (m, 5H, Ar-H), 6.32 (m, 1H, H-1), 6.19 (m, 1H, H-2), 2.53 – 2.34 (m, 1H, H-3), 1.13 – 0.97 (m, 6H, H-4 and H-5) ; **^{13}C NMR** (101 MHz, $CDCl_3$) δ 142.5 (C-2), 136.5 (C-1'), 128.6 (Ar), 128.3 (Ar), 127.8 (Ar), 127.5 (C-1), 34.2 (C-3), 22.5 (C-4 and C-5). The peaks were to the values reported by Antonioletti and co-workers.[88]

(1*E*,3*E*)-Penta-1,3-dien-1-ylbenzene (212a)

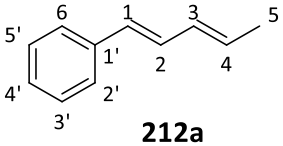

212a

Yellow oil, **^{1}H NMR** (300 MHz, $CDCl_3$) δ 7.43 – 7.10 (m, 5H, Ar-H), 6.87 – 6.51 (m, 1H, H-1), 6.34 – 6.11 (m, 2H, H-2 and H-3), 5.93 – 5.71 (m, 1H, H-4), 1.85 – 1.71 (m, 3H, H-5); **^{13}C NMR** (101 MHz, $CDCl_3$) δ 135.6 (C-1), 135.2 (C-1'), 131.7 (C-3), 130.7 (C-2 and C-4), 128.8 (Ar), 127.9 (Ar), 19.9 (C-5). The peaks were comparable to the values reported by Avery and co-workers.[89]

© University of Pretoria

(*E*)-Hex-1-en-1-ylbenzene (213a)

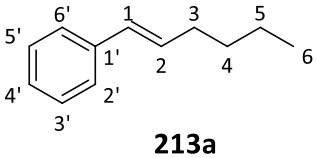

213a

Clear oil, **^{1}H NMR** (300 MHz, $CDCl_3$) δ 7.55 – 7.07 (m, 5H, Ar-H), 6.42 (m, 1H, H-1), 6.30 – 6.09 (m, 1H, H-2), 2.39 – 2.13 (m, 2H, H-3), 1.47 – 1.24 (m, 4H, H-4 and H-5), 0.98 – 0.77 (m, 3H, H-6) ; **^{13}C NMR** (101 MHz, $CDCl_3$) δ 136.7 (C-1'), 134.7 (C-2), 128.6 (Ar), 127.9 (C-1 and Ar), 37.9 (C-3), 26.4 (C-4), 22.9 (C-5), 14.3 (C-6). The peaks were comparable to the values reported by Kakiya and co-workers.[90]

(*E*)-2-Methoxy-5-styrylphenol (214a)

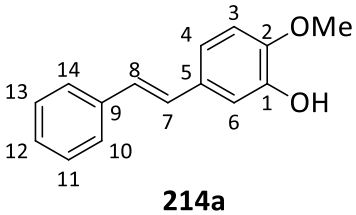

214a

White solid, **^{1}H NMR** (300 MHz, $CDCl_3$) δ 7.90 – 7.67 (m, 2H, Ar-H), 7.65 – 7.45 (m, 2H, Ar-H), 7.41 – 7.29 (m, 3H, Ar-H), 7.22 – 7.06 (m, 3H, H-3, H-7 and H-8), 4.91 (s, 1H, OH), 3.33 (s, 3H, OMe); **^{13}C NMR** (101 MHz, $CDCl_3$) δ 149.3 (C-2), 147.3 (C-1), 137.8 (C-9), 130.8 (C-5), 129.0 (C-7), 128.5 (C-8), 128.0 (Ar), 127.6 (Ar), 123.0 (Ar), 115.0 (Ar), 112.2 (Ar), 56.4 (OMe); **mp:** 149-153 °C. The peaks were comparable to the values reported by Gaukroger and co-workers.[91]

8.7. Synthesis and characterization for batch Suzuki-Miyaura coupling reaction

a. Synthesis of in-house polymer-supported tetrakis(triphenylphosphine)palladium (215a)

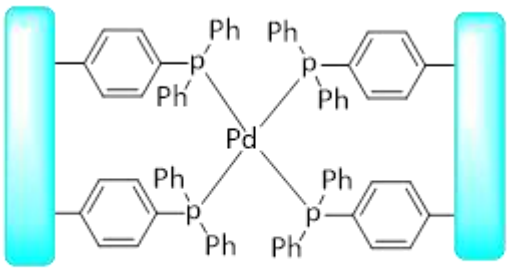

215a

To a suspension of in-house polymer-supported triphenylphosphine **146** (1.0051 g, 3.0 eq) in degassed dimethyl sulfoxide (20 mL) was added palladium chloride (245.8 mg, 1.0 eq) and the mixture was refluxed for 2 hours under argon. Thereafter the solution was cooled to 0 °C, hydrazine (0.25 mL, 2.0 eq) was added and the mixture was stirred for 1 hour. The immobilized catalyst was then filtered under argon and washed with degassed ethanol (50 mL) and degassed diethyl ether (50 mL) to yield **215a** as a green solid. **EDX**: Pd = 0.460 mmol/g.

© University of Pretoria

b. Synthesis of in-house polymer-supported tetrakis(triphenylphosphine)palladium (215b)

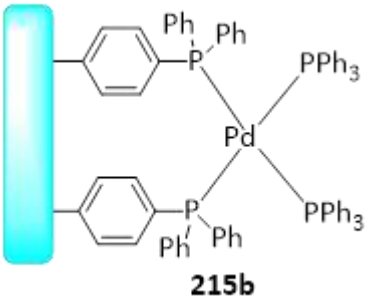

215b

To a suspension of solid-supported triphenylphosphine **146** (1.005 g) in degassed dimethyl sulfoxide (20 mL) was added palladium chloride (0.246 g, 1.0 eq) and the mixture was refluxed for 2 hours under argon. Thereafter triphenylphosphine (0.227 g, 2.0 eq) in degassed ethanol (5 mL) was added and the mixture was stirred for another 3 hours. The solution was then cooled to 0 °C, hydrazine hydrate (0.25 mL, 2.0 eq) was added and the mixture was stirred for 1 hour. The immobilized catalyst was then filtered under argon and washed with degassed ethanol (50 mL) followed by degassed diethyl ether (50 mL) to yield **215b** as a green solid.

EDX: Pd = 0.909 mmol/g.

c. General batch procedure 4: Suzuki-Miyaura coupling reactions using commercial unsupported tetrakis(triphenylphosphine)palladium

To a flame dried flask under argon was dissolved aryl halide (1.0 eq), boronic acid (1.2 eq) potassium phosphate tribasic (3.0 eq) and commercial tetrakis(triphenylphosphine)palladium (Sigma Aldrich, 216666) (0.05 eq) in dry degassed tetrahydrofuran (2.0 mL) and degassed water (2.0 mL) and the suspension mixture was refluxed overnight at 90 °C under argon. The crude mixture was then quenched with ammonium chloride (10 mL) and ethyl acetate (20mL) was added. The mixture was then transferred to a separating funnel and the layers separated, the aqueous layer was washed with ethyl acetate (3 x 10 mL), dried over magnesium sulfate, filtered, reduced *in vacuo* and purified using column chromatography with 5% ethyl acetate/hexane as eluent to yield the desired product.

Attempted method 1

To a flame dried flask under argon was dissolved aryl halide (1.0 eq), boronic acid (1.2 eq) potassium carbonate, triethylamine or potassium hydroxide (3.0 eq) and commercial tetrakis(triphenylphosphine)palladium (0.05 eq) in dry degassed tetrahydrofuran (2.0 mL) and degassed water (2.0 mL) and the suspension mixture was refluxed overnight at 90 °C under argon. The crude mixture was then quenched with ammonium chloride (10 mL) and ethyl acetate (20mL) was added. The mixture was then transferred to a separating funnel and the

© University of Pretoria

layers separated, the aqueous layer was washed with ethyl acetate (3 x 10 mL), dried over magnesium sulfate, filtered and reduced *in vacuo*.

Attempted method 2

To a flame dried flask under argon was dissolved aryl halide (1.0 eq), boronic acid (1.2 eq) potassium phosphate tribasic (3.0 eq) and commercial tetrakis(triphenylphosphine)palladium (0.05 eq) in dry degassed toluene, dioxane (2.0 mL) or dioxane and water mixture (2.0 mL) and the suspension mixture was refluxed overnight at 90 °C under argon. The crude mixture was then quenched with ammonium chloride (10 mL) and ethyl acetate (20mL) was added. The mixture was then transferred to a separating funnel and the layers separated, the aqueous layer was washed with ethyl acetate (3 x 10 mL), dried over magnesium sulfate, filtered and reduced *in vacuo*.

Attempted method 3

To a flame dried flask under argon was dissolved aryl halide (1.0 eq), boronic acid (1.2 eq) potassium phosphate tribasic (3.0 eq) and commercial tetrakis(triphenylphosphine)palladium (0.05 eq) in dry degassed tetrahydrofuran (2.0 mL) and the suspension mixture was refluxed overnight at 90 °C under argon. The crude mixture was then quenched with ammonium chloride (10 mL) and ethyl acetate (20mL) was added. The mixture was then transferred to a separating funnel and the layers separated, the aqueous layer was washed with ethyl acetate (3 x 10 mL), dried over magnesium sulfate, filtered and reduced *in vacuo*.

Attempted method 4

To a flame dried flask under argon was dissolved aryl halide (1.0 eq), boronic acid (1.2 eq) potassium phosphate tribasic (3.0 eq) and commercial tetrakis(triphenylphosphine)palladium (0.05 eq) in dry degassed tetrahydrofuran (2.0 mL) and degassed water (2.0 mL) and the suspension mixture was refluxed overnight at 70 °C or 80 °C under argon. The crude mixture was then quenched with ammonium chloride (10 mL) and ethyl acetate (20mL) was added. The mixture was then transferred to a separating funnel and the layers separated, the aqueous layer was washed with ethyl acetate (3 x 10 mL), dried over magnesium sulfate, filtered and reduced *in vacuo*.

© University of Pretoria

d. General batch procedure 5: Suzuki-Miyaura coupling reactions using commercial polystyrene-supported tetrakis(triphenylphosphine)palladium

To a flame dried flask under argon was added aryl halide (1.0 eq), boronic acid (1.2 eq) potassium phosphate tribasic (3.0 eq), polystyrene-supported tetrakis(triphenyl-phosphine)palladium (Sigma Aldrich, 511579) (0.05 eq), dry degassed tetrahydrofuran (2.0 mL) and degassed water (2.0 mL) and the suspension mixture was refluxed overnight at 90 °C under argon. The crude mixture was then quenched with ammonium chloride (10 mL) and ethyl acetate (20mL) was added. The mixture was filtered and then transferred to a separating funnel and layers separated, the aqueous layer was washed with ethyl acetate (3 x 10 mL), dried over magnesium sulfate, filtered, reduced *in vacuo* and purified using column chromatography using 5% ethyl acetate/hexane eluent to yield the desired product.

e. General batch procedure 6: Suzuki-Miyaura coupling reactions using in-house polymer-supported tetrakis(triphenylphosphine)palladium (215a)

To a flame dried flask under argon was added aryl halide (1.0 eq), boronic acid (1.2 eq) potassium phosphate tribasic (3.0 eq), **215a** (0.07 eq), dry degassed tetrahydrofuran (2.0 mL) and degassed water (2.0 mL) and the suspension mixture was refluxed for 18 hours at 90 °C under argon. The crude mixture was then quenched with ammonium chloride (10 mL) and diluted with ethyl acetate (20mL). The mixture was filtered to remove catalyst and the eluent transferred to a separating funnel and layers separated, aqueous layers washed with ethyl acetate (3 x 10 mL), dried over magnesium sulfate, filtered, reduced *in vacuo* and purified using column chromatography using 5% ethyl acetate/hexane eluent to yield the desired product.

8.8. Synthesis and characterization for flow Suzuki-Miyaura coupling reaction

a. Synthesis of in-house polymer-supported tetrakis(triphenylphosphine)palladium (215c)

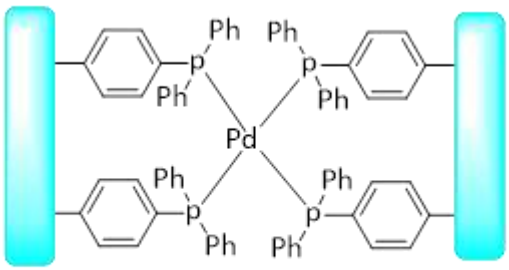

215c

A 10 mL OmniFit™ glass column was filled with ground and washed in-house polymer-supported triphenylphosphine **146** (1.0051 g). The column was mounted to a Uniqsis FlowSyn SS reactor heating block and washed with degassed dimethyl sulfoxide at 1.0 mL/min for 30 minutes followed by recycling of palladium chloride (1.38 mmol, 0.1 M) in degassed dimethyl sulfoxide (20 mL) for 18 hours

© University of Pretoria

at a flow rate of 0.5 mL/min at 150 °C, to give a yellow polymer-support. The polymer-support was then washed with dimethyl sulfoxide for 1 hour at 1.0 mL/min while cooling to room temperature to remove any unreacted palladium chloride. The column was then cooled to 0 °C and hydrazine (0.25 mL, 0.3 M) in dimethyl sulfoxide (10 mL) was recycled through the column at 0.5 mL/min for 6 hours. The polymer-support was then washed sequentially with degassed ethanol (50 mL) and degassed diethyl ether (50 mL) to give **215c** as a green solid.

EDX: Pd = 0.689 mmol/g.

b. General flow procedure 3: Suzuki-Miyaura coupling reactions using commercial polystyrene-supported tetrakis(triphenylphosphine)palladium

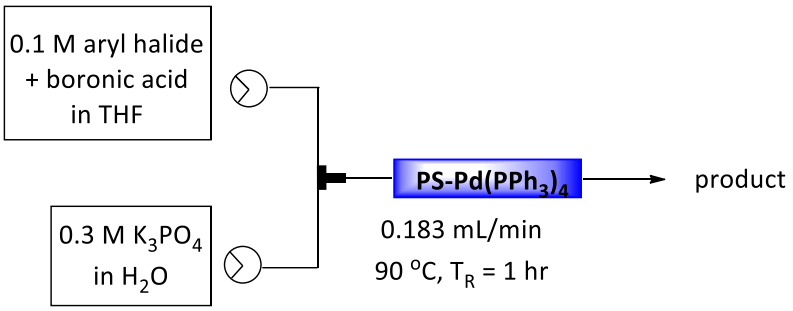

A 10 mL OmniFit™ glass column purged with argon was filled polystyrene-supported tetrakis(triphenylphosphine)palladium (Sigma Aldrich, 216666) (0.05 eq). The column was mounted to a Uniqsis FlowSyn SS reactor and washed with degassed mixture of tetrahydrofuran:water (1:1) mixture for 5 minutes. A stock solution containing the aryl halide (0.1 M, 1.0 eq) and the boronic acid (1.2 eq) in degassed tetrahydrofuran was mixed with a stock solution of potassium phosphate tribasic (0.3 M, 3.0 eq) in degassed water in a 1:1 ratio at a T-piece mixer. Thereafter the flow stream was passed through the glass OmniFit™ column housing the polystyrene-supported tetrakis(triphenylphosphine)palladium at 90 °C. A total flow rate of 0.183 mL/min (T_R = 1 h) was used. A post-reaction wash with tetrahydrofuran:water (1:1) mixture was performed at 0.5 mL/min for 1 hour. The crude mixture was then quenched with ammonium chloride (10 mL) and ethyl acetate (20mL) was added. The biphasic mixture was then separated, and the aqueous layers extracted with ethyl acetate (3 x 10 mL), dried over magnesium sulfate, filtered, reduced *in vacuo* and purified using column chromatography eluting 5% ethyl acetate/hexane mixture to yield product.

© University of Pretoria

c. General flow procedure 4: Suzuki-Miyaura coupling reactions using in-house polymer-supported tetrakis(triphenylphosphine)palladium (215c)

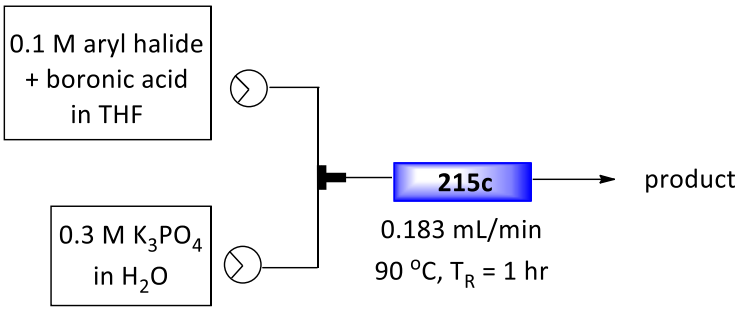

A 10 mL glass OmniFit™ column was purged with argon and packed with **215c** (0.07 eq). The column was mounted in a Uniqsis FlowSyn SS reactor heating block and washed with degassed tetrahydrofuran:water (1:1) mixture for 5 minutes. A stock solution containing the aryl halide (0.1 M, 1.0 eq) and the boronic acid (1.2 eq) in degassed tetrahydrofuran was mixed with a stock solution of potassium phosphate tribasic (0.3 M, 3.0 eq) in degassed water in a 1:1 ratio at a T-piece mixer. Thereafter the flow stream was passed through the glass OmniFit™ column housing **215c** at 90 °C. A total flow rate of 0.183 mL/min (T_R = 1 h) was used. A post-reaction wash with tetrahydrofuran:water (1:1) mixture was performed at 0.5 mL/min for one hour. The crude mixture was then quenched with ammonium chloride (10 mL) and ethyl acetate (20mL) was added. The biphasic mixture was then separated, and the aqueous layers extracted with ethyl acetate (3 × 10 mL). The combined organic layers were dried over magnesium sulfate, filtered, reduced *in vacuo* and purified by column chromatography using 5% ethyl acetate/hexane as eluent.

8.9. Synthesis of the 2-bromo-3-methoxynaphthalene (219) starting material for Suzuki-Miyaura coupling reactions

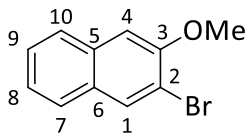

219

Naphthol (500 mg, 3.46 mmol, 1.0 eq) was dissolved in dry dichloromethane (10 mL) under argon and diisopropylamine (35.10 mg, 0.347 mmol, 0.1 eq) was added, followed by slow addition of *N*-bromosuccinimide (679.0 mg, 3.815 mmol, 1.1 eq). The reaction mixture was stirred at 40 °C overnight. The crude mixture was then reduced *in vacuo* and purified using column chromatography eluting 10-20% ethyl acetate/hexane mixtures to yield bromonaphthol as a brown solid (86 %).

© University of Pretoria

A solution of bromonaphthol (1.50 g, 6.75 mmol, 1.0 eq), potassium hydroxide (758 mg, 13.51 mmol, 2.0 eq) and methyl iodide (2.52 mL, 40.54 mmol, 6.0 eq) in dry acetonitrile (40 mL) was stirred at room temperature overnight under argon. The mixture was then washed with water (20 mL), extracted with dichloromethane (3 x 30 mL), dried over magnesium sulfate, filtered, concentrated *in vacuo* and purified by column chromatography eluting 10% ethyl acetate /hexane mixture to give 94% of **219** as a brown solid.

^{1}H NMR (300 MHz, $CDCl_3$) δ 8.57 – 6.97 (m, 6H, Ar-H), 3.96 (s, 3H, OMe); **^{13}C NMR** (101 MHz, $CDCl_3$) δ 153.9 (C-3), 133.2 (Ar), 129.9 (Ar), 129.1 (Ar), 128.2 (Ar), 127.9 (Ar), 126.2 (Ar), 124.4 (Ar), 113.7 (C-2), 108.8 (Ar), 57.1 (OMe); **mp:** 68-71 °C. The peaks were comparable to the values reported by Nishinaga and co-workers.[92]

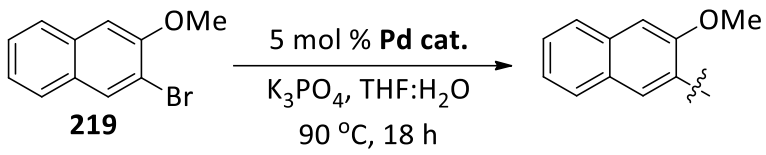

Table 25: Selected batch and flow Suzuki-Miyaura coupling reactions on 2-bromo-3-methoxynaphthalene using varying boronic acids

Entry	Boronic Acid	Product	% Yield[a]				
			Batch			Flow	
			Pd-$(PPh_3)_4$	PS-Pd$(PPh_3)_4$	215a	PS-Pd$(PPh_3)_4$	215c
1	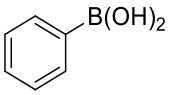	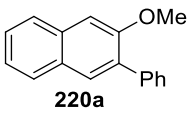 **220a**	84	79	76	63	65
2	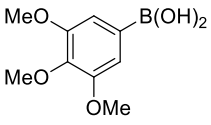	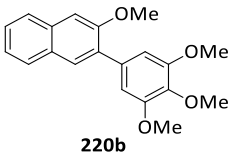 **220b**	91	44	35	65	63
3	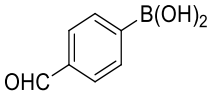	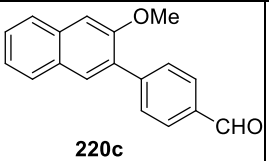 **220c**	70	31	29	56	54
4	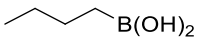	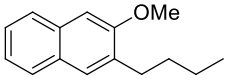 **220f**	20	10	8	21	18

© University of Pretoria

2-Methoxy-3-phenylnaphthalene (220a)

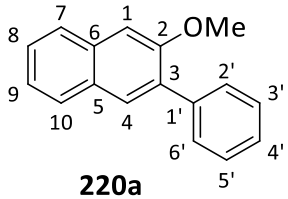

220a

White solid, **^{1}H NMR** (300 MHz, $CDCl_3$) δ 7.84 – 7.69 (m, 2H, Ar-H), 7.47 – 7.18 (m, 9H, Ar-H), 3.74 (s, 3H, OMe); **^{13}C NMR** (101 MHz, $CDCl_3$) δ 154.1 (C-2), 136.8 (C-1'), 133.9 (C-6), 131.3 (Ar), 129.4 (C-5), 129.4 (Ar), 128.5 (Ar), 128.2 (Ar), 127.4 (Ar), 126.6 (Ar), 125.7 (Ar), 125.6 (Ar), 123.9 (Ar), 114.2 (Ar), 57.1 (OMe); **mp:** 57-61 °C. The peaks were comparable to the values reported by Lukeman and co-workers.[93]

2-Methoxy-3-(3',4',5'-trimethoxyphenyl)naphthalene (220b)

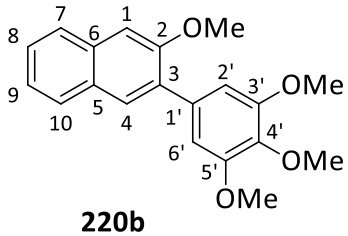

220b

Brown solid, **HRMS** (ESI): *m/z* 325.1438 $[M+H]^+$, $C_{20}H_{20}O_4$ requires 324.1362; **FTIR** vmax/cm^{-1} 2930 (m, C-H), 1582 (s, C=C), 1236 (s, C-O); **^{1}H NMR** (300 MHz, $CDCl_3$) δ 7.89 (d, *J* = 9.0 Hz, 1H, Ar-H), 7.86 – 7.79 (m, 1H, Ar-H), 7.73 – 7.62 (m, 1H, Ar-H), 7.60 – 7.51 (m, 1H, Ar-H), 7.49 – 7.43 (m, 1H, Ar-H), 7.42 – 7.33 (m, 3H, Ar-H), 3.96 (s, 3H, OMe), 3.89 (s, 3H, OMe), 3.84 (s, 6H, 2 x OMe); **^{13}C NMR** (101 MHz, $CDCl_3$) δ 153.9 (C-2), 153.3 (C-2' and C-3'), 137.1 (C-4'), 133.9 (C-5'), 129.4 (C-1'), 128.9 (Ar), 128.7 (Ar), 128.1 (C-3), 126.7 (Ar), 125.6 (Ar), 123.9 (Ar), 114.0 (Ar), 108.2 (Ar), 61.2 (OMe), 57.1 (OMe), 56.3 (2 x OMe); **mp:** 104-106 °C.

4-(3'-Methoxynaphthalen-2'-yl) benzaldehyde (220c)

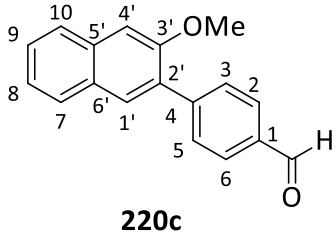

220c

Yellow oil, **HRMS** (ESI): *m/z* 301.1954 $[M+K]^+$, $C_{18}H_{18}O_2$ requires 262.0994; **FTIR** vmax/cm^{-1} 2928 (m, C-H), 1695 (s, C=O), 1598 (s, C=C), 1252 (s, C-O); **^{1}H NMR** (300 MHz, $CDCl_3$) δ 10.11 (s, 1H, CHO), 8.05 – 7.99 (d, *J* = 8.4 Hz, 2H, Ar-H), 7.93 (d, *J* = 4.2 Hz, 1H, Ar-H), 7.88 – 7.82 (m, 1H, Ar-H), 7.56 (d, *J* = 7.8 Hz, 2H, Ar-H), 7.46 – 7.32 (m, 4H, Ar-H), 3.85 (s, 3H, OMe); **^{13}C NMR** (101 MHz, $CDCl_3$) δ 192.5 (CHO), 153.9 (C-3'), 143.8 (C-4), 135.5 (Ar), 133.2 (Ar), 132.2 (Ar), 130.2 (Ar), 129.9 (Ar), 129.2 (Ar), 128.4 (Ar), 127.1 (Ar), 124.9 (Ar), 124.0 (Ar), 124.0 (Ar), 113.7 (Ar), 56.8 (OMe).

2-Butyl-3-methoxynaphthalene (220f)

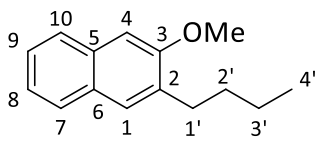

220f

Yellow oil, **HRMS** (ESI): *m/z* 215.1448 $[M+H]^+$, $C_{15}H_{18}O$ requires 214.1358; **FTIR** vmax/cm^{-1} 2923 (m, C-H), 1590 (m, C=C), 1341 (m, C-O); **^{1}H NMR** (300 MHz, $CDCl_3$) δ 7.96 (d, *J* = 8.7 Hz, 1H, Ar-H),

© University of Pretoria

7.82 – 7.67 (m, 2H, Ar-H), 7.51 – 7.42 (m, 1H, Ar-H), 7.39 – 7.27 (m, 2H, Ar-H), 3.94 (s, 3H, OMe), 1.67 – 1.53 (m, 4H, H-1' and H-2'), 1.52 – 1.41 (m, 2H, H-3'), 0.97 (t, *J* = 14.4 Hz, 3H, H-4'); **^{13}C NMR** (101 MHz, $CDCl_3$) δ 154.6 (C-3), 133.3 (C-5), 129.6 (Ar), 128.8 (Ar), 127.6 (Ar), 126.4 (Ar), 124.8 (Ar), 123.7 (Ar), 123.4 (Ar), 113.9 (Ar), 57.0 (OMe), 32.7 (C-1'), 30.1 (C-2'), 23.4 (C-C3'), 14.4 (C-4').

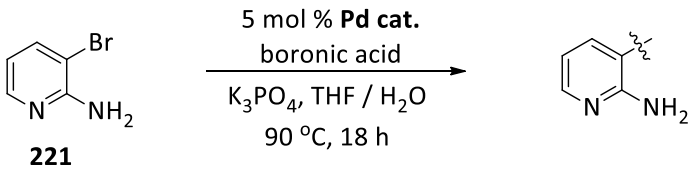

221

Table 26: Selected batch Suzuki coupling reactions on 3-bromopyridin-2-amine using varying boronic acids

Entry	Boronic Acid	Product	% Yield				
			Batch			Flow	
			$Pd(PPh_3)_4$	PS-$Pd(PPh_3)_4$	215a	PS-$Pd(PPh_3)_4$	215c
1	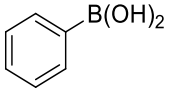	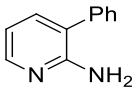 **222a**	88	37	56	-	58
2	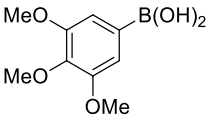	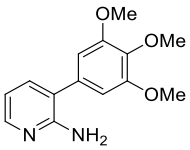 **222b**	90	58	68	-	71
3	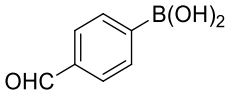	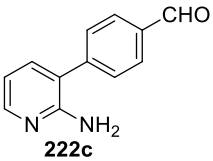 **222c**	88	58	67	-	65
4	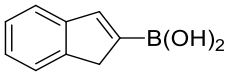	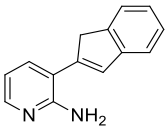 **222e**	24	18	7	-	21
5	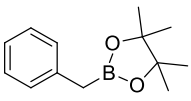	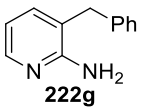 **222g**	75	15	10	-	20

© University of Pretoria

3-Phenyl-2-aminopyridine (222a)

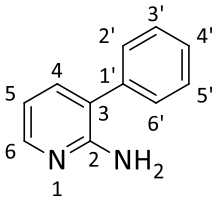

222a

Brown oil, **^{1}H NMR** (400 MHz, $CDCl_3$) δ 8.08 (d, *J* = 6.0, Hz, 1H, Ar-H), 7.51 – 7.42 (m, 2H, Ar-H), 7.41 – 7.33 (m, 2H, Ar-H), 7.43 -7.38 (m, 2H, Ar-H) 6.81 – 6.72 (m, 1H, Ar-H), 4.56 (s, 2H, NH_2); **^{13}C NMR** (400 MHz, $CDCl_3$) δ 155.8 (C-2), 147.0 (C-6), 138.9 (Ar), 133.9 (Ar), 129.9 (Ar), 129.5 (Ar), 129.0 (Ar), 123.1 (C-3), 114.4 (C-5). The peaks were comparable to the values reported by Li and co-workers.[94]

3-(3',4',5'-Trimethoxyphenyl)-2-aminopyridine (222b)

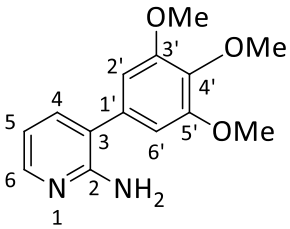

222b

Orange solid, **HRMS** (ESI): *m/z* 261.1170 $[M+H]^+$, $C_{14}H_{12}N_2O_3$ requires 260.1161; **FTIR** vmax/cm^{-1} 3452 (m, N-H), 1575 (m, C=N), 1121 (m, C-O); **^{1}H NMR** (300 MHz, $CDCl_3$) δ 8.07 (d, *J* = 6.6, Hz, 1H, Ar-H), 7.71 – 7.61 (m, 1H, Ar-H), 7.58 – 7.51 (m, 1H, Ar-H), 7.40 – 7.33 (m, 1H, Ar-H), 6.79 – 6.69 (m, 1H, Ar-H), 4.63 (s, 2H, NH_2), 3.89 (s, 3H, OMe), 3.88 (s, 6H, 2 x OMe); **^{13}C NMR** (101 MHz, $CDCl_3$) δ 156.2 (C-2), 154.0 (C-3' and C-4'), 147.6 (C-5'), 137.9 (Ar), 134.0 (Ar), 132.3 (Ar), 122.2 (Ar), 114.6 (Ar), 106.0 (Ar), 61.2 (OMe), 56.5 (2 x OMe); **mp:** 160-162 °C.

4-(2'-Aminopyridin-3'-yl) benzaldehyde (222c)

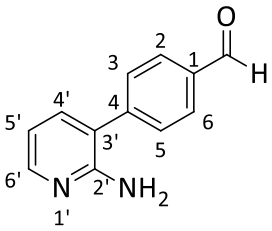

222c

Yellow solid, **HRMS** (ESI): *m/z* 199.0873 $[M+H]^+$, $C_{12}H_{10}N_2O$ requires 198.0793; **FTIR** vmax/cm^{-1} 3336 (m, N-H), 1694 (s, C=O), 1598 (s, C=N); **^{1}H NMR** (400 MHz, $CDCl_3$) δ 10.06 (s, 1H, CHO), 8.18 – 8.06 (m, 1H, Ar-H), 7.61 – 7.50 (m, 1H, Ar-H), 7.48 – 7.43 (m, 3H, Ar-H), 7.40 – 7.32 (m, 1H, Ar-H), 6.84 – 6.74 (m, 1H, Ar-H), 4.73 (s, 2H, NH_2); **^{13}C NMR** (101 MHz, $CDCl_3$) δ 191.9 (CHO), 155.8 (NH_2), 148.4 (C-6'), 144.8 (Ar), 138.3 (Ar), 135.8 (Ar), 133.1 (Ar), 130.7 (Ar), 129.6 (Ar), 128.9 (Ar), 128.8 (Ar), 116.5 (C-3'), 114.9 (Ar); **mp:** 155-160 °C.

© University of Pretoria

3-(Indenyl)-2-aminopyridine (222e)

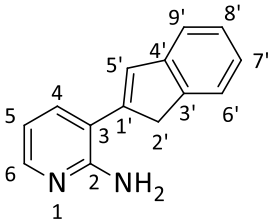

222e

Red oil, **HRMS** (ESI): *m/z* 209.1080 $[M+H]^+$, $C_{14}H_{12}N_2$ requires 208.1000; **FTIR** vmax/cm^{-1} 2920 (s, N-H), 1707 (m, C=C), 1456 (s, C=N); **^{1}H NMR** (400 MHz, $CDCl_3$) δ 8.08 – 8.07 (m, 1H, H-6), 7.72 – 7.62 (m, 2H, Ar-H), 7.59 – 7.51 (m, 2H, Ar-H), 7.50 – 7.42 (m, 3H, Ar-H), 6.78 – 6.71 (m, 1H, Ar-H), 6.68 – 6.60 (m, 1H, H-5'), 4.65 (s, 2H, NH_2); **^{13}C NMR** (101 MHz, $CDCl_3$) δ 156.6 (NH_2), 147.6 (C-6), 144.5 (Ar), 143.7 (Ar), 140.7 (C-1'), 132.5 (Ar), 132.4 (Ar), 126.7 (Ar), 125.7 (Ar), 124.5 (Ar), 120.9 (Ar), 115.3 (C-3), 114.2 (C-3), 38.9 (C-2').

3-Benzyl-2-aminopyridine (222f)

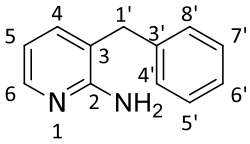

222f

Brown oil, **^{1}H NMR** (400 MHz, $CDCl_3$) δ 8.00 (d, *J* = 6.0 Hz, 1H, H-6), 7.75 – 7.62 (m, 1H, Ar-H), 7.47 – 7.43 (m, 1H, Ar-H), 7.36 – 7.28 (m, 2H, Ar-H), 7.18 – 7.12 (m, 2H), 6.72 – 6.63 (m, 1H, Ar-H), 4.36 (s, 2H, NH_2), 3.82 (s, 2H, H-1'); **^{13}C NMR** (101 MHz, $CDCl_3$) δ 157.4 (NH_2), 146.7 (C-6), 138.4 (Ar), 132.4 (Ar), 129.1 (Ar), 128.9 (Ar),127.1 (Ar), 119.7 (C-3), 114.8 (Ar), 37.9 (C-1'). The peaks were comparable to the values reported by Andres and co-workers.[95]

© University of Pretoria

References

© University of Pretoria

Chapter 9

References

1 R. B. Merrifield, *J. Am. Chem. Soc.*, 1963, **14**, 2149–2154.

2 S. sun Wang and R. B. Merrifield, *J. Am. Chem. Soc.*, 1969, **91**, 6488–6491.

3 D. C. Sherrington, *J. Polym. Sci.*, 2001, **39**, 2364–2377.

4 S. V. Ley and I. R. Baxendale, *J. Chem. Soc. Perkin Trans. 1*, 2000, **85**, 3815–4195.

5 H. Mahdavi and J. Amani, *Tetrahedron Lett.*, 2008, **49**, 2204–2207.

6 G. L. Thomas, C. Böhner, M. Ladlow and D. R. Spring, *Tetrahedron*, 2005, **61**, 12153–12159.

7 D. E. Bergbreiter, B. Chen and T. J. Lynch, *J. Org. Chem.*, 1983, **48**, 4179–4186.

8 S. V. Ley, I. R. Baxendale, R. N. Bream, P. S. Jackson, A. G. Leach, D. A. Longbottom, M. Nesi, J. S. Scott, R. I. Storer and S. J. Taylor, *J. Chem. Soc. Perkin Trans. 1*, 2000, 3815–4195.

9 I. R. Baxendale, A. L. Lee and S. V. Ley, *J. Chem. Soc. Perkin 1*, 2002, **2**, 1850–1857.

10 C. E. Humphrey, M. A. M. Easson, J. P. Tierney and N. J. Turner, *Org. Lett.*, 2003, **5**, 849–852.

11 F. Gendre, M. Yang and P. Diaz, *Org. Lett.*, 2005, **7**, 2719–2722.

12 Understanding SynPhase Lanterns - http://www.mimotopes.com/knowledgeBaseListing.asp?cid=26,34,57, (accessed 21 May 2020).

13 P. Ploypradith, P. Cheryklin, N. Niyomtham, D. R. Bertoni and S. Ruchirawat, *Org. Lett.*, 2007, **9**, 2637–2640.

14 R. Mello, A. Alcalde-Aragonés, M. E. G. Núñez and G. Asensio, *J. Org. Chem.*, 2012, **77**, 6409–6413.

© University of Pretoria

15 N. Jung, S. Grässle, D. S. Lütjohann and S. Bräse, *Org. Lett.*, 2014, **16**, 1036–1039.

16 M. H. Nguyen and A. B. Smith, *Org. Lett.*, 2014, **16**, 2070–2073.

17 A. B. Smith, A. T. Hoye, D. Martinez-Solorio, W. S. Kim and R. Tong, *J. Am. Chem. Soc.*, 2012, **134**, 4533–4536.

18 P. K. Maity, S. Faisal, A. Rolfe, D. Stoianova and P. R. Hanson, *J. Org. Chem.*, 2015, **80**, 9942–9950.

19 S. Gräßle, S. Vanderheiden, P. Hodapp, B. Bulat, M. Nieger, N. Jung and S. Bräse, *Org. Lett.*, 2016, **18**, 3598–3601.

20 I. Protasova, B. Bulat and N. Jung, *Org. Lett.*, 2017, **19**, 34–37.

21 I. Chorendorff and J. W. Niemantsverdriet, *Concepts of Modern Catalysis and Kinetics*, 2003.

22 D. J. Cole-Hamilton, *Science (80)*, 2003, 299, 1702–1706.

23 N. Kann, *Molecules*, 2010, **15**, 6306–6331.

24 B. Clapham, T. S. Reger and K. D. Janda, *Tetrahedron*, 2001, **57**, 4637–4662.

25 N. E. Leadbeater and M. Marco, *Chem. Rev.*, 2002, **102**, 3217–3274.

26 L. Mafu, B. Zeelie and P. Watts, *Beilstein J. Org. Chem.*, 2016, **12**, 2046–2054.

27 J. M. Andre, J. Losada, A. Maestro, P. Rodr and R. Pedrosa, *J. Org. Chem.*, 2017, **82**, 8444–8454.

28 S. Watanabe, N. Nakaya, J. Akai, K. Kanaori, T. Harada, N. Nakaya, J. Akai, K. Kanaori and T. Harada, *Org. Lett.*, 2018, **20**, 2737–2740.

29 D. Webb and T. F. Jamison, *Chem. Sci.*, 2010, **1**, 675–680.

30 I. R. Baxendale and S. V. Ley, in *New Avenues to Efficient Chemical Synthesis*, Springer Berlin Heidelberg, 2007, pp. 151–185.

31 C. D. Scott, R. Labes, M. Depardieu, C. Battilocchio, M. G. Davidson, S. L. Ley, C. C.

© University of Pretoria

Wilson and K. Robertson, *React. Chem. Eng.*, 2018, **3**, 631–634.

32 M. Baumann and I. R. Baxendale, *Beilstein J. Org. Chem.*, 2015, **11**, 1194–1219.

33 R. Porta, M. Benaglia and A. Puglisi, *Org. Process Res. Dev.*, 2016, **20**, 1–25.

34 L. Malet-Sanz and F. Susanne, *J. Med. Chem.*, 2012, **55**, 4062–4098.

35 Uniqsis Ltd - The FlowSyn system, http://www.uniqsis.com/paFlowSystem.aspx, (accessed 10 July 2019).

36 Asia - Award-Winning Lab Scale Flow Chemistry by Syrris, https://syrris.com/product/asia-flow-chemistry/, (accessed 10 July 2019).

37 Flow Chemistry method development: Labtrix, https://www.chemtrix.com/products/labtrix-s1, (accessed 10 July 2019).

38 R-Series flow chemistry system - Vapourtec, https://www.vapourtec.com/products/r-series-flow-chemistry-system-overview/, (accessed 10 July 2019).

39 H-Cube® Pro - ThalesNano, https://thalesnano.com/products-and-services/h-cube-pro/, (accessed 12 July 2019).

40 KeyChem Series (Flow reactor systems) | YMC CO., LTD., http://www.ymc.co.jp/en/nanotech/keychem/, (accessed 10 July 2019).

41 W. Thamas, *Microreactors in Organic Synthesis and Catalysis*, Wiley-VCH Verlag GmbH & Co. KGaA, Weinheim, Germany, 2008.

42 J. C. Pastre, D. L. Browne and S. V. Ley, *Chem. Society Rev.*, 2013, **42**, 8849–8869.

43 M. Baumann and I. R. Baxendale, *Beilstein J. Org. Chem.*, 2015, **11**, 1194–1219.

44 M. Baumann, I. R. Baxendale, S. V Ley, C. D. Smith and G. K. Tranmer, *Org. Lett.*, 2006, **8**, 5231–5234.

45 I. R. Baxendale, J. Deeley, C. M. Griffiths-jones, S. V. Ley, S. Saaby and G. K. Tranmer, *Chem. Commun.*, 2006, 2566–2568.

46 L. J. Martin, A. L. Marzinzik, S. V. Ley and I. R. Baxendale, *Org. Lett.*, 2011, **13**, 320–

© University of Pretoria

323.

47 M. D. Hopkin, I. R. Baxendale and S. V. Ley, *Chem. Commun.*, 2010, **46**, 2450–2452.

48 J. Zak, D. Ron, E. Riva, H. P. Harding, B. C. S. Cross and I. R. Baxendale, *Chem. - A Eur. J.*, 2012, **18**, 9901–9910.

49 J. C. Pastre, J. C. Pastre, D. L. Browne and S. V. Ley, *Chem. Scociety Rev.*, 2013, **42**, 8849–8869.

50 E. Chiurchiù, Y. Patehebieke, S. Gabrielli, R. Ballini and A. Palmieri, *Adv. Synth. Catal.*, 2019, **361**, 2042–2047.

51 D. Zhao and K. Ding, *ACS Catal.*, 2013, **3**, 928–944.

52 A. R. Bogdan, B. P. Mason, K. T. Sylvester and D. T. McQuade, *Angew. Chem. - Int. Ed.*, 2007, **46**, 1698–1701.

53 R. Munirathinam, J. Huskens and W. Verboom, *Adv. Synth. Catal.*, 2015, **357**, 1093–1123.

54 C. Csajagi, B. Borcsek, K. Niesz, I. Kovacs, Z. Szekelyhidi, Z. Bajko, L. Urge and F. Darva, *Org. Lett.*, 2008, **10**, 1589–1592.

55 C. Ayats, A. H. Henseler and M. A. Perica, *Catalysts*, 2014, **4**, 3027–3033.

56 M. Gliński, U. Ulkowska and E. Iwanek, *J. Chem. Ed.*, 2016, **93**, 1623–1625.

57 P. Llanes, C. Rodr, S. Sayalero and M. A. Perica, *Org. Lett.*, 2016, **18**, 6292–6295.

58 H. Xie, L. Zu, H. Li, J. Wang and W. Wang, *J. Am. Chem. Soc.*, 2007, **129**, 10886.

59 B. E. C. Peters, F. Svec and J. M. J. Fréchet, *Adv. Mater.*, 1999, 1169–1181.

60 M. Kubín, P. Špaček and R. Chromeček, *Collect. Czechoslov. Chem. Commun.*, 1967, **32**, 3881–3887.

61 F. Svec and J. M. J. Fréchet, *Anal. Chem.*, 1992, **64**, 820–822.

62 F. Svec and C. G. Huber, *Anal. Chem.*, 2006, 2101–2107.

© University of Pretoria

63 F. Roohi, M. Antonietti and M. M. Titirici, *J. Chromatogr. A*, 2008, **1203**, 160–167.

64 M. R. Buchmeiser, *Polymer*, 2007, **48**, 2187–2198.

65 C. F. Poole, in *The Essence of Chromatography*, Elsiever, Amsterdam, 2003, pp. 267–429.

66 H. Lange, M. J. Capener, A. X. Jones, C. J. Smith, N. Nikbin, I. R. Baxendale and S. V. Ley, *Synlett*, 2011, 869–873.

67 C. J. Smith, C. D. Smith, N. Nikbin, S. V. Ley and I. R. Baxendale, *Org. Biomol. Chem.*, 2011, **9**, 1927–1937.

68 K. Matyjaszewski and S. G. Gaynoy, in *Applied Polymer Science: 21st Century*, Elsiever, Amsterdam, 2000, pp. 929–977.

69 K. A. Roper, H. Lange, A. Polyzos, M. B. Berry, I. R. Baxendale and S. V. Ley, *Beilstein J. Org. Chem.*, 2011, **7**, 1648–1655.

70 K. A. Roper, M. B. Berry and S. V. Ley, *Beilstein J. Org. Chem.*, 2013, **9**, 1781–1790.

71 S. Newton, C. F. Carter, C. M. Pearson, L. De C. Alves, H. Lange, P. Thansandote and S. V. Ley, *Angew. Chem. - Int. Ed.*, 2014, **53**, 4915–4920.

72 K. J. Barlow, G. Moad, X. Hao, T. C. Hughes, O. E. Hutt, A. Polyzos, K. A. Turner and G. Moad, *Polym. Chem.*, 2014, **5**, 722–732.

73 K. J. Barlow, V. Bernabeu, X. Hao, T. C. Hughes, O. E. Hutt, A. Polyzos, K. A. Turner and G. Moad, *React. Funct. Polym.*, 2015, **96**, 89–96.

74 C. Gimbert, M. Lumbierres, C. Marchi, M. Moreno-Mañas, R. M. Sebastián and A. Vallriber *Tetrahedron*, 2005, **61**, 8598–8605.

75 P. W. Tang, *Org. sytheses*, 2012, **89**, 432–437.

76 X. Li, M. Zhou, M. Turson, S. Lin, P. Jiang and X. Dong, *Analyst*, 2013, **138**, 3066.

77 M. V. Rojo, L. Guetzoyan and I. R. Baxendale, *Org. Biomol. Chem.*, 2015, **13**, 1768–1777.

© University of Pretoria

78 F. G. Adly and A. Ghanem, *Tetrahedron Lett.*, 2016, **57**, 852–857.

79 J. Kula, *J. Chem. Heal. Saf.*, 1999, **6**, 21–22.

80 M. Irfan, T. N. Glasnov and C. O. Kappe, *Org. Lett.*, 2011, **13**, 984–987.

81 C. Battilocchio, I. R. Baxendale, M. Biava, M. O. Kitching and S. V. Ley, *Org. Process Res. Dev.*, 2012, **16**, 798–810.

82 S. Edvinsson, S. Johansson and A. Larsson, *Tetrahedron Lett.*, 2012, **53**, 6819–6821.

83 M. O. Brien, I. R. Baxendale and S. V. Ley, *Org. Lett.*, 2010, **12**, 1596–1598.

84 J. Westman, *Org. Lett.*, 2001, **3**, 3745–3747.

85 N. Miyaura and A. Suzuki, *Chem. Rev.*, 1995, **95**, 2457–2483.

86 I. Fenger and C. Le Drian, *Tetrahedron Lett.*, 1998, **39**, 4287–4290.

87 V. Pandarus, R. Ciriminna, F. Béland, G. Gingras, M. Drobot, O. Jina and M. Pagliaro, *Tetrahedron Lett.*, 2013, **54**, 1129–1132.

88 N. E. Leadbeater and M. Marco, *Chem. Rev.*, 2002, **102**, 3217–3274.

89 G. L. Thomas, M. Ladlow and D. R. Spring, *Org. Biomol. Chem.*, 2004, **2**, 1679.

90 K. Inoue and S. Oshima, *Angew. Chem. Int. Ed. Engl.*, 2000, **39**, 2481–2483.

91 S. Xu, T. Toyama, J. Nakamura and H. Arimoto, *Tetrahedron Lett.*, 2010, **51**, 4534–4537.

92 B. E. Maryanofl, A. B. Reitz, M. S. Mutter, R. R. Inners and H. R. Almond, *J. Am. Chem. Soc.*, 1985, **107**, 1068–1070.

93 J. Clayden, N. Greeves, S. Warren and P. Wothers, in *Organic Chemistry*, Oxford Univerity Press, 2001, p. 817.

94 R. Robiette, J. Richardson, V. K. Aggarwal and J. N. Harvey, *J. Am. Chem. Soc.*, 2006, **128**, 2394–2409.

© University of Pretoria

95 Y. Okuno, Y. Kitagawa, S. Kamiya, A. Hasegawa, T. Kawashima, K. Otani, S. Aoki, J. Kanno, S. Isomura and Y. Sato, *J. Org. Chem*., 2018, **7**, 1071-1074.

96 S. Wu, L. Chen, B. Yin and Y. Li, *Chem. Comm*., 2015, **51**, 9884-9887.

97 I. Carrera, M. C. Brovetto, J. Ramos and G. A. Seoane, *Tetrahedron. Lett*., 2009, **50**, 5399-5402.

98 Y. Matano, T. Suzuki, T. Shinokura and H. Imahori, *Tetrahedron. Lett*., 2007, **48**, 2885-2888.

99 K. C. Nicolaou, V. A. Adsool and C. R. H. Hale, *Org. Lett.,* 2010, **12**, 1552-1555.

100 Z. Chen, R. Fu, W. Chai, H. Zheng, L. Sun, Q. Lu and R. Yuan, *Tetrahedron*, 2014, **70**, 2237-2245.

101 A. Smith and K. D. Moeller, *Org. Lett.,* 2013, **15**, 5818-5821.

102 Z-J. Li, L. Cai, R-F. Mei, J-W. Dong, S-Q. Li, X-Q. Yang, H. Zhou, T-P. Yin and Z-T. Ding, *Tetrahedron*, 2015, **56**, 7197-7200.

103 D. T. Blackwell, R. J. D. G. Warren and R. S. David, *Synlett*, 2011, **15**, 2144-2144.

104 R. Antonioletti, F. Bonadies, A. Ciammaichella and A. Viglianti, *Tetrahedron*, 2008, **64**, 4644-4648.

105 T. D. Avery, D. K. Taylor and E. R. T. Tiekink, *J. Org. Chem*., 2000, **65**, 5531-5546.

106 H. Kakiya, H. Shinokubo and K. Oshima, *Tetrahedron*, 2001, **57**, 10063-10069.

107 K. Gaukroger, J. A. Hadfield, N. J. Lawrence, S. Nolan and A. T. McGown, *Org. Biomol. Chem.*, 2003, **1**, 3033-3037.

108 S. Nishinaga, Y. Sawanaka, R. Toyama, T. Ishida, H. Mori and Y. Nishihara, *Chem. Lett*., 2018, **47**, 1409-1411.

109 M. Lukeman, H. Simon, P. Wan and Y-H. Wang, *J. Org. Chem*., 2015, **80**, 11281-11293.

© University of Pretoria

110 Z. Li, C. Gelbaum, J.S. Fisk, B. Holden, A. Jaganathan, G. T. Whiteker, P. Pollet and C. L. Liotta, *J. Org. Chem.,* 2016, **81**, 8520-8529.

111 J. I. Andres, J. M. Alonso, J. Fernández, L. Iturrino, P. Martínez, T. F.Meert and V. K. Sipido*, Bio. Med. Chem. Lett*., 2002, **12**, 3573-3577.

© University of Pretoria

Appendix

© University of Pretoria

Chapter 10

Appendices

10.1. Appendix A: Supporting information

10.1.1. Synthesis of solid-supported triphenylphosphine 201

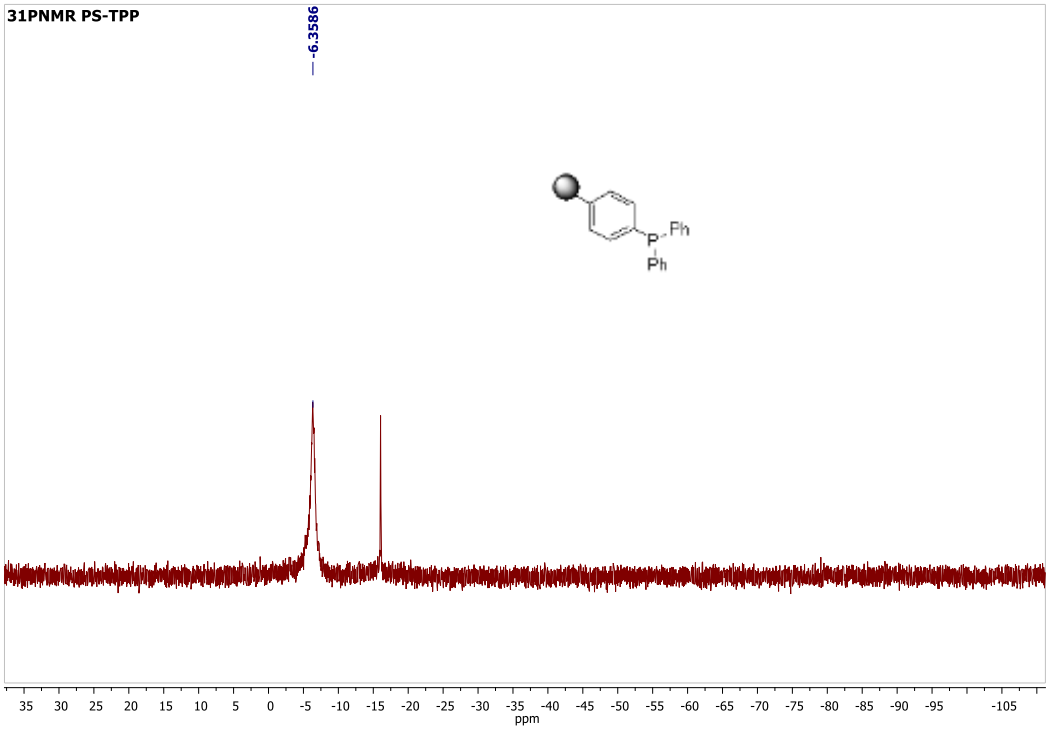

Figure 32: ^{31}P NMR spectra of polystyrene-supported triphenylphosphine **201**

© University of Pretoria

10.1.2. Ozonolysis selected examples from model study

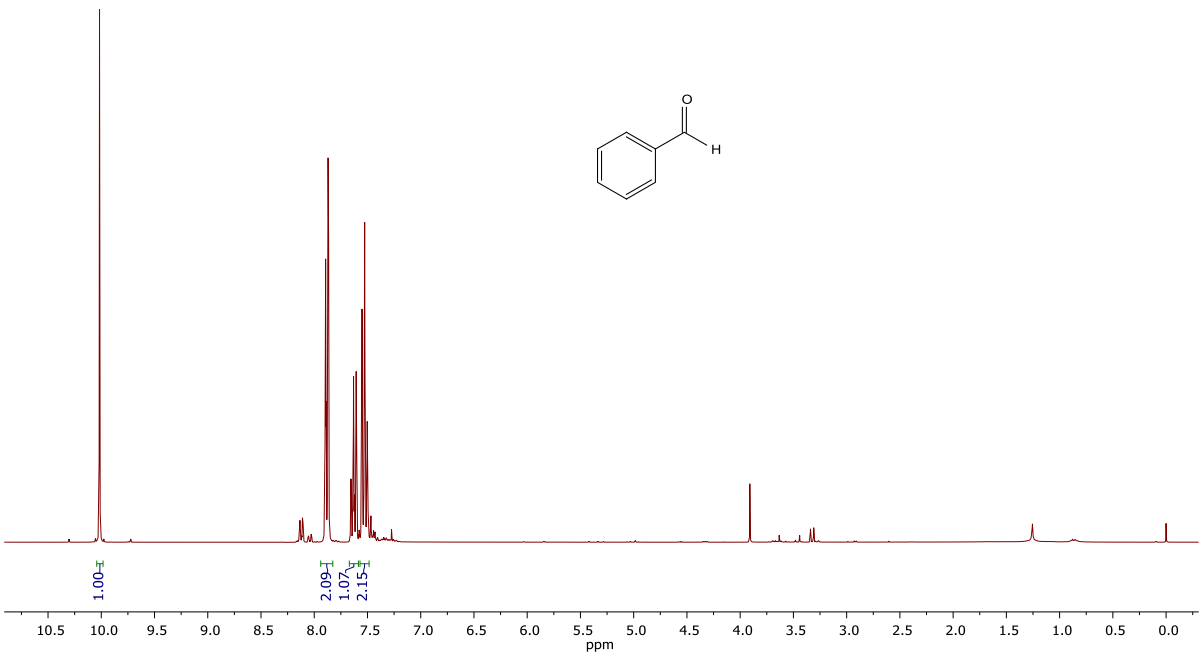

Figure 33: ^{1}H NMR of benzaldehyde **143a**

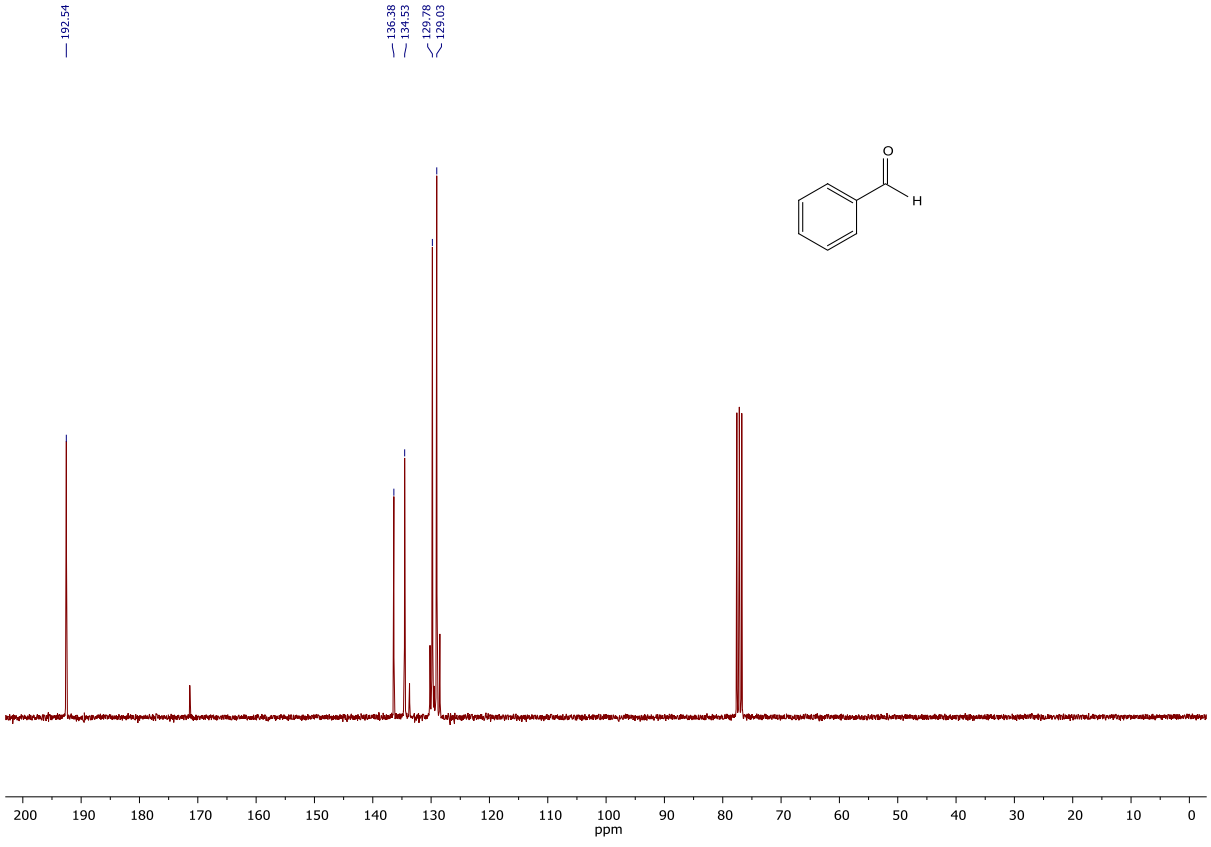

Figure 34: ^{13}C NMR of benzaldehyde **143a**

© University of Pretoria

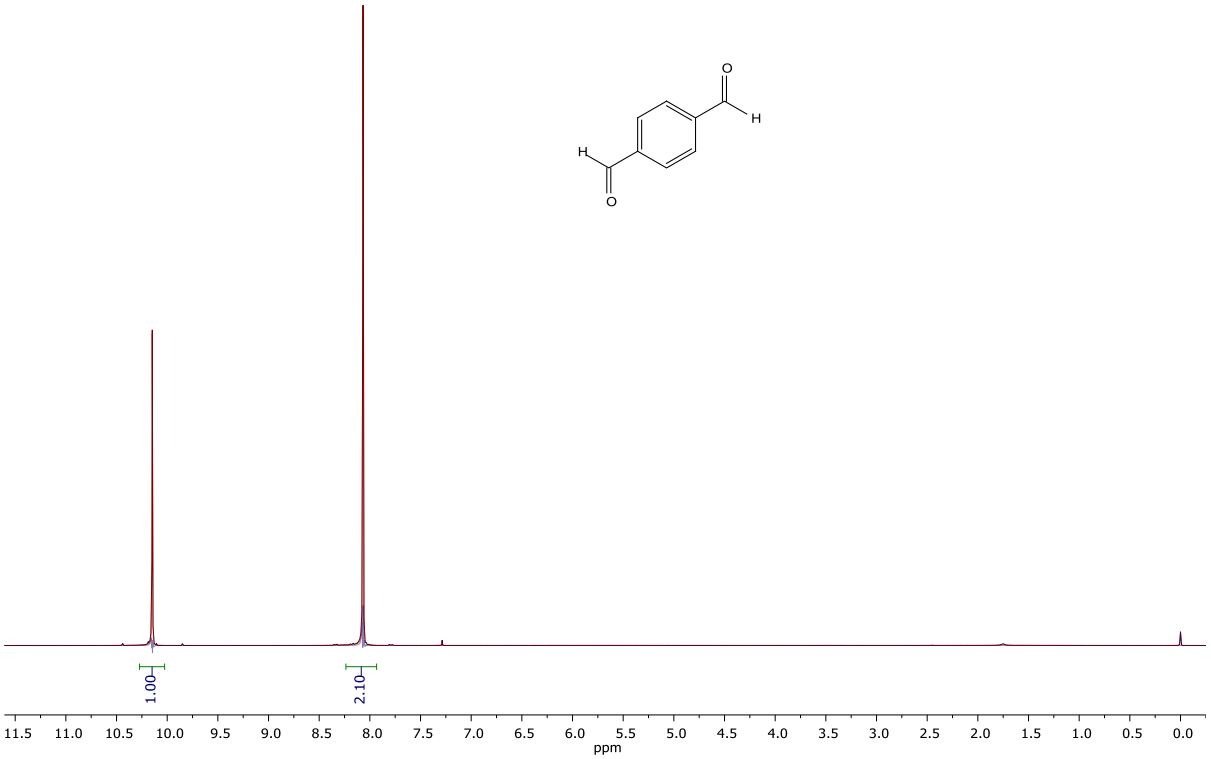

Figure 35: ^{1}H NMR of terephthalaldehyde **142a**

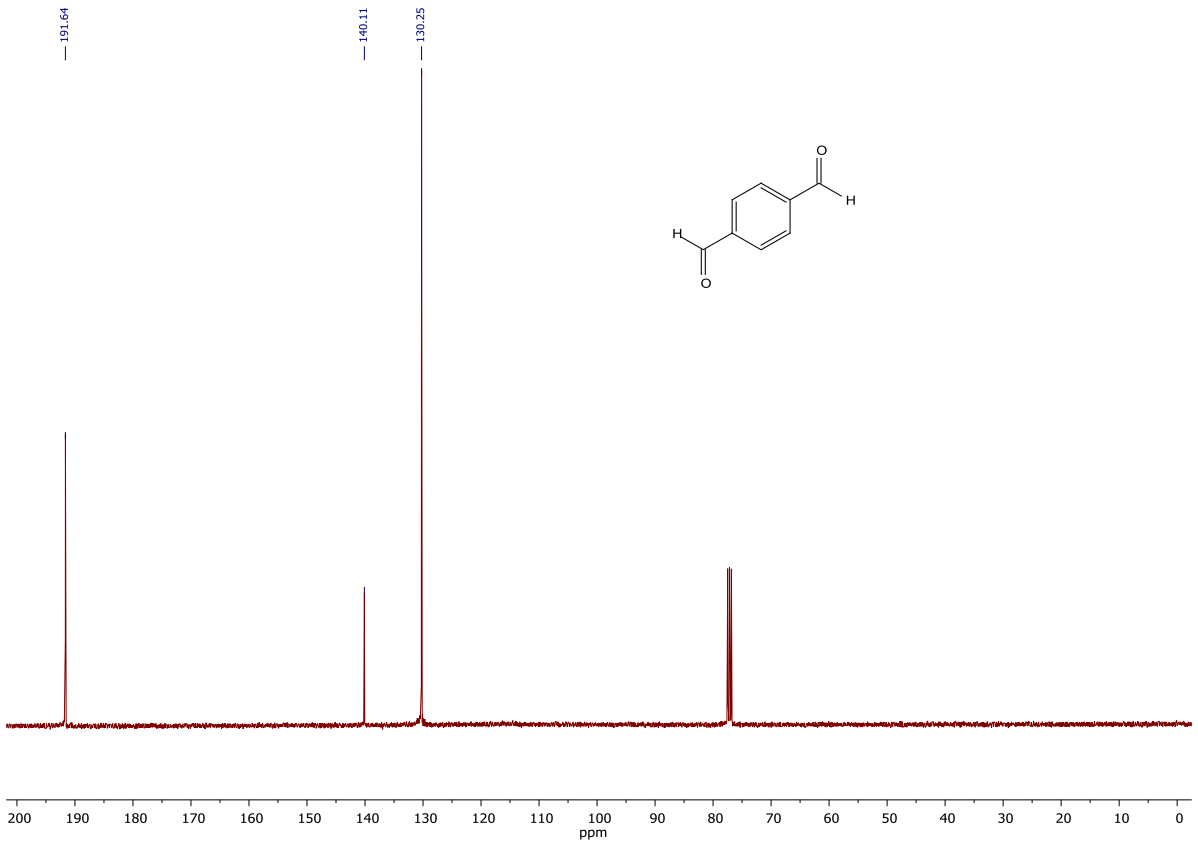

Figure 36: ^{13}C NMR of terephthalaldehyde **142a**

© University of Pretoria

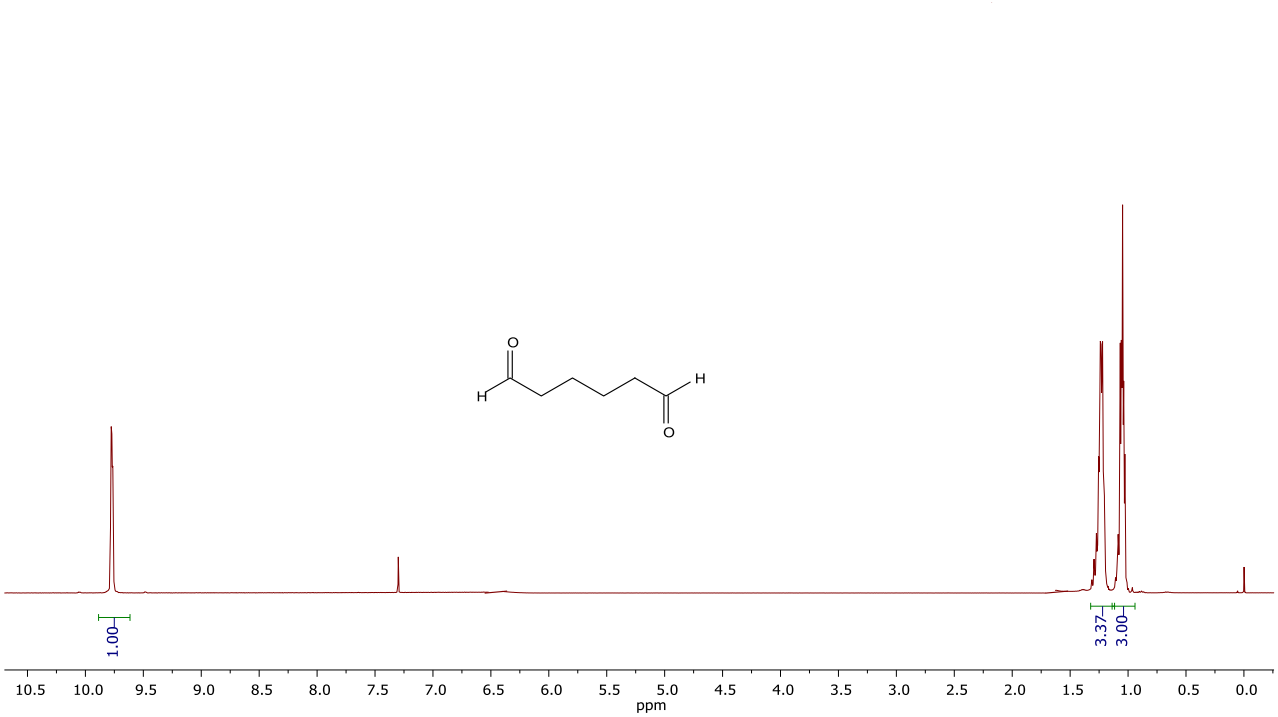

Figure 37: ^{1}H NMR of hexanedial **202a**

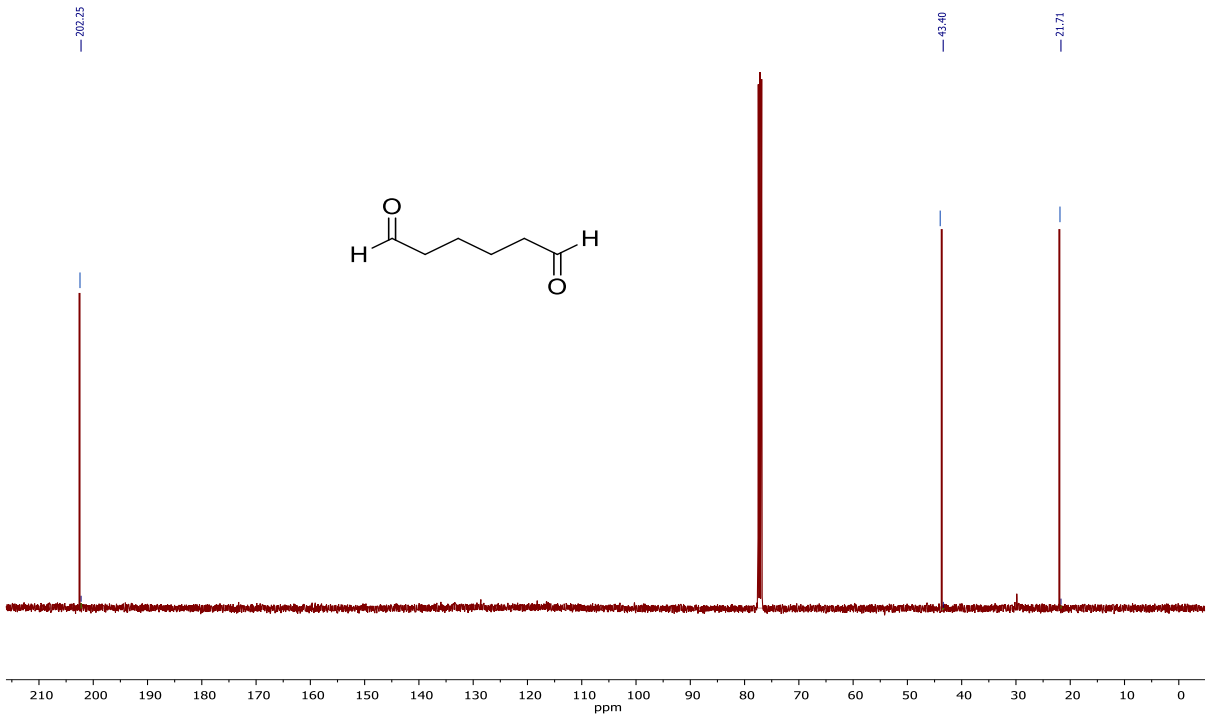

Figure 38: ^{13}C NMR of hexanedial **202a**

© University of Pretoria

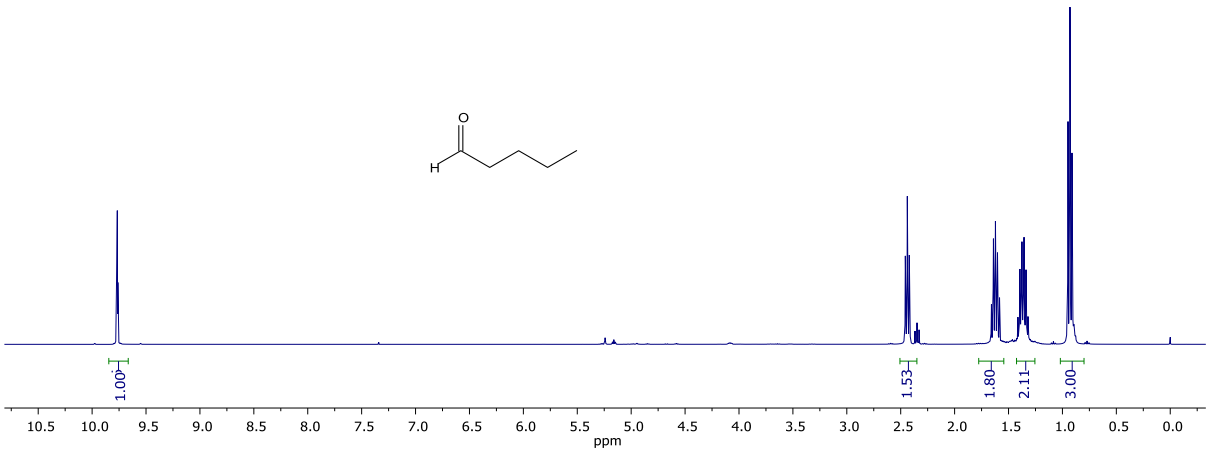

Figure 39: ^{1}H NMR of pentanal **203a**

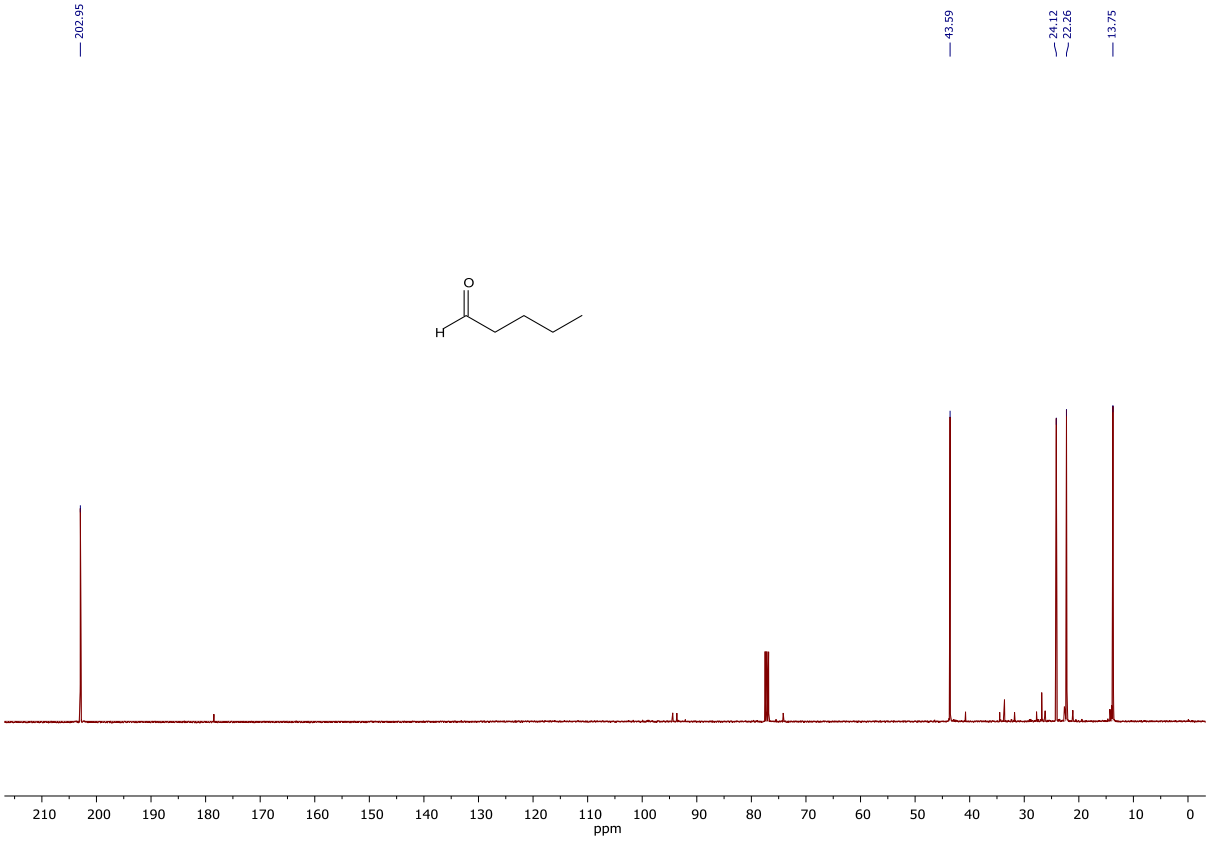

Figure 40: ^{13}C NMR of pentanal **203a**

© University of Pretoria

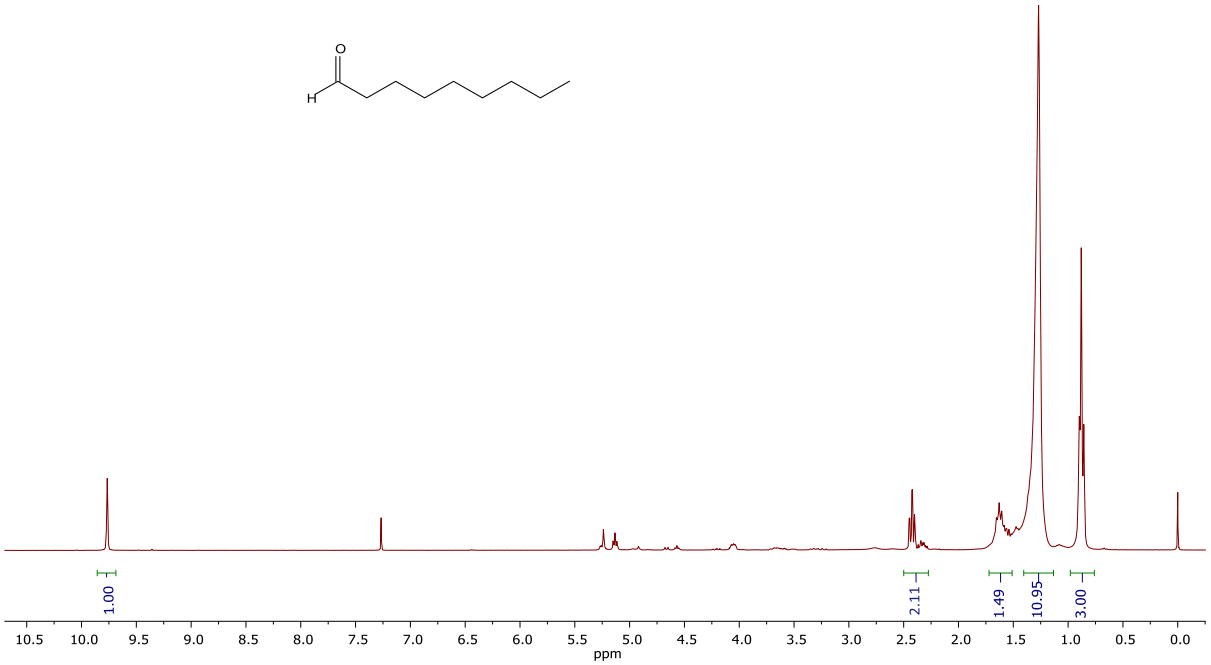

Figure 41: ^{1}H NMR of nonyl aldehyde **204a**

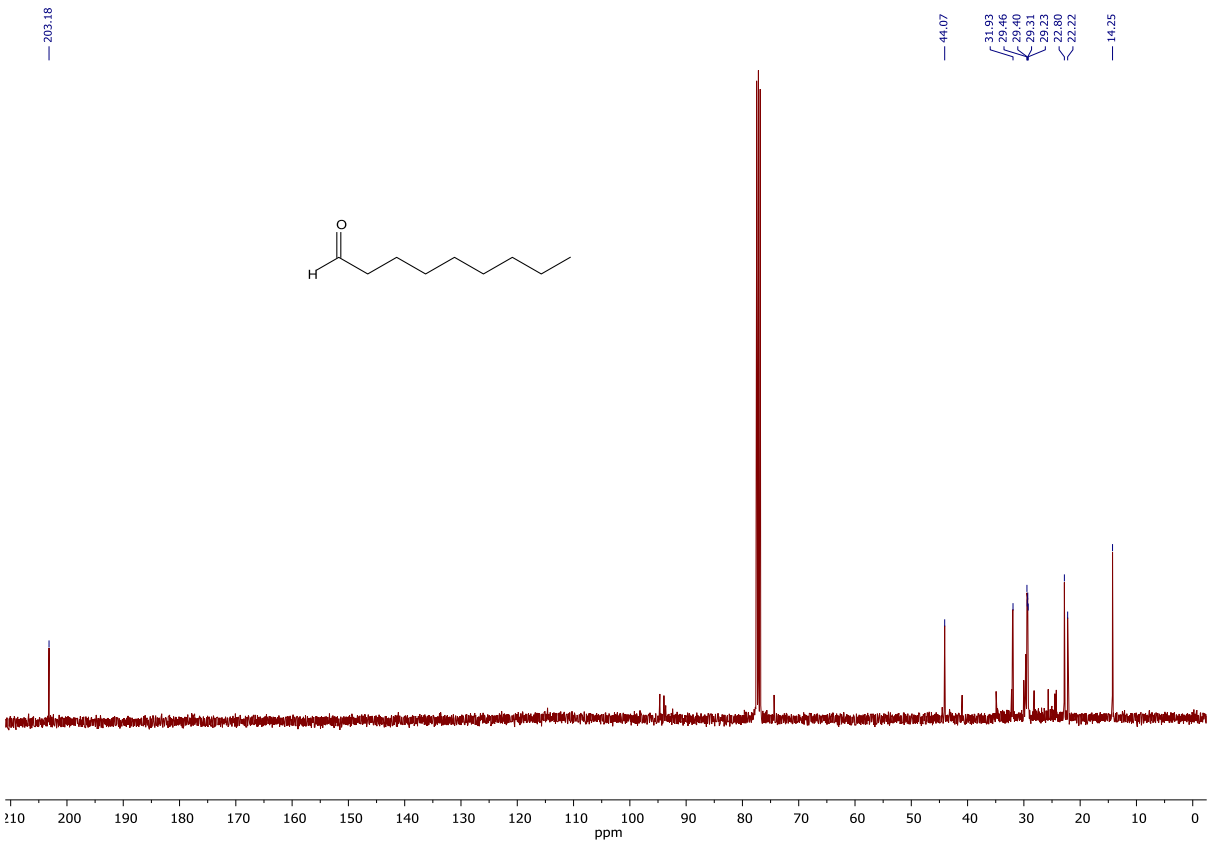

Figure 42: ^{13}C NMR of nonyl aldehyde **204a**

© University of Pretoria

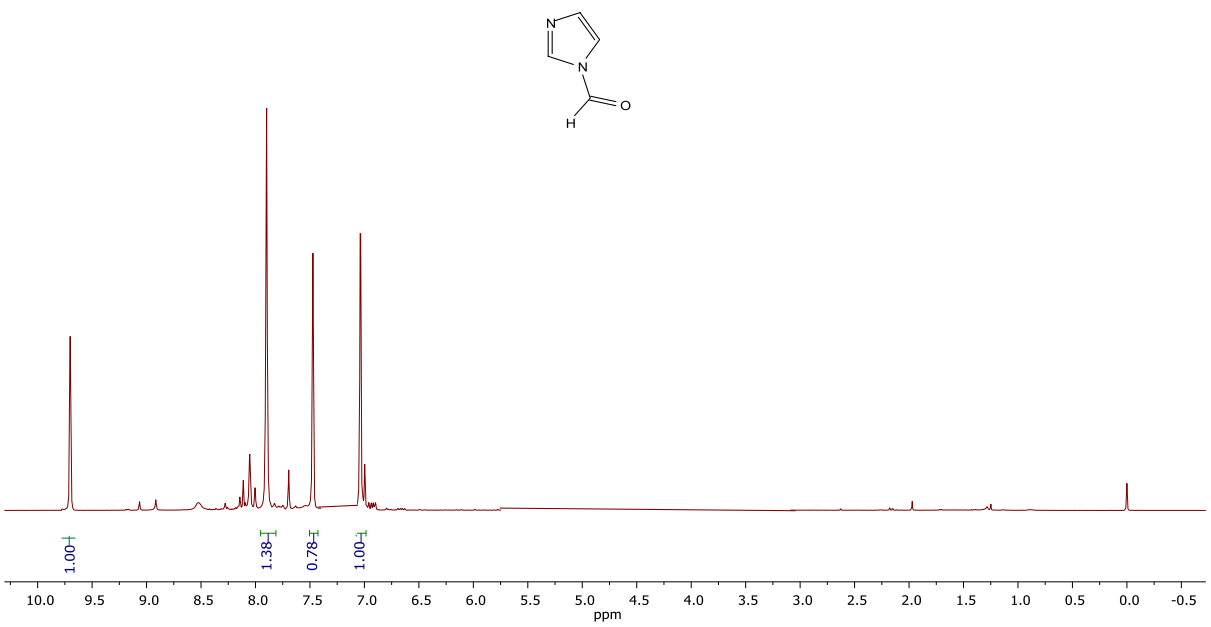

Figure 43: ^{1}H NMR of imidazole-1-carbaldehyde **205a**

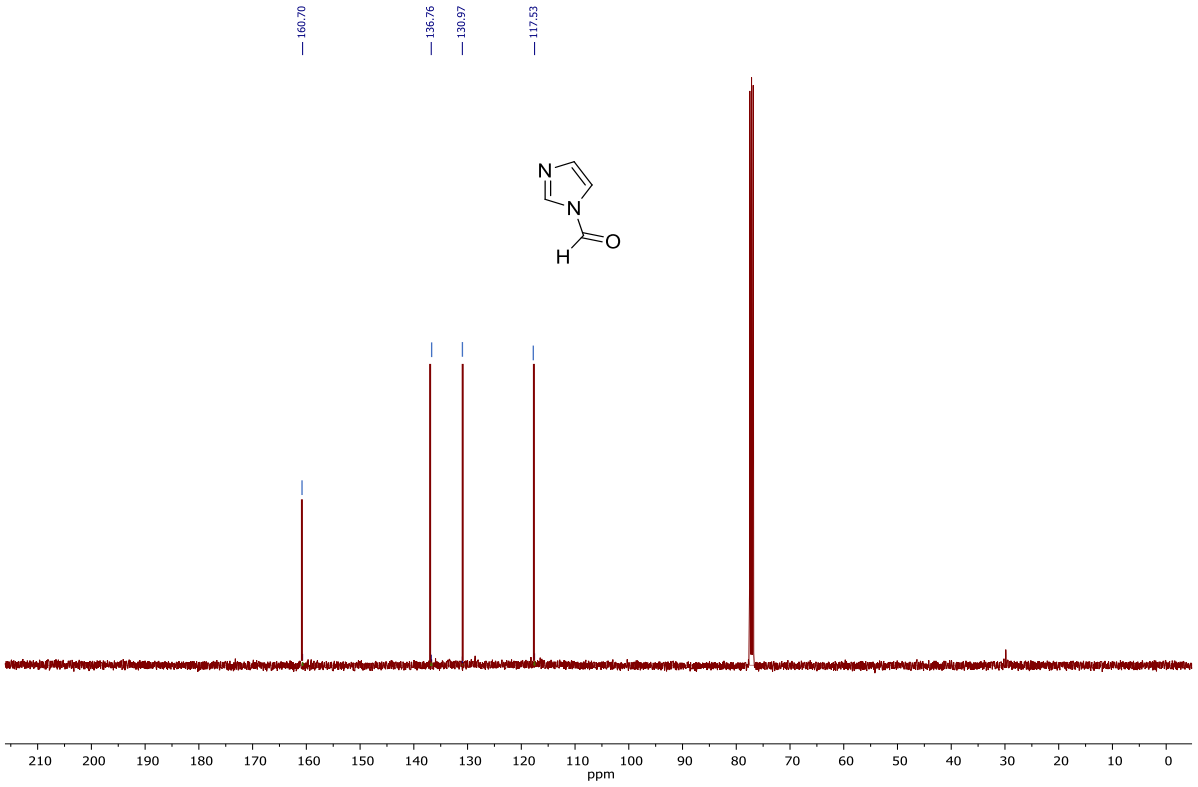

Figure 44: ^{13}C NMR of imidazole-1-carbaldehyde **205a**

© University of Pretoria

10.1.3. Wittig selected examples from model study

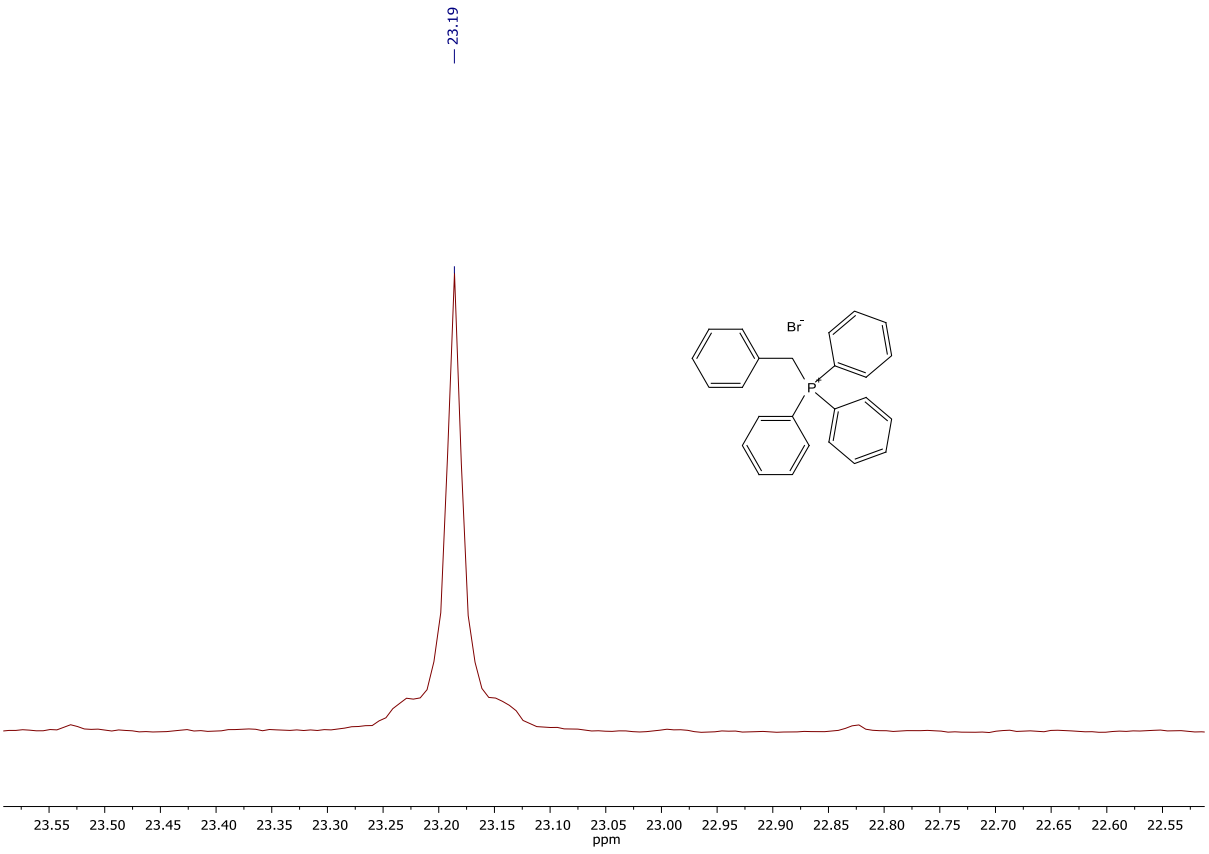

Figure 45: ^{31}P NMR of polystyrene-supported benzyl ylide **206**

© University of Pretoria

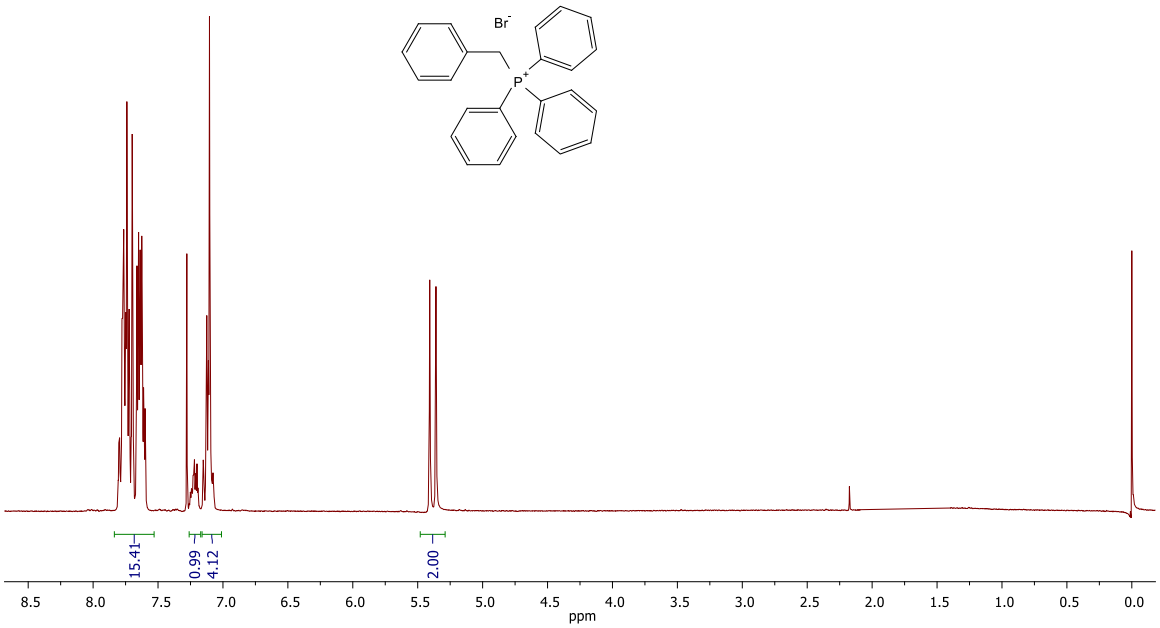

Figure 46: ^{1}H NMR of benzyltriphenylphosphonium bromide **206**

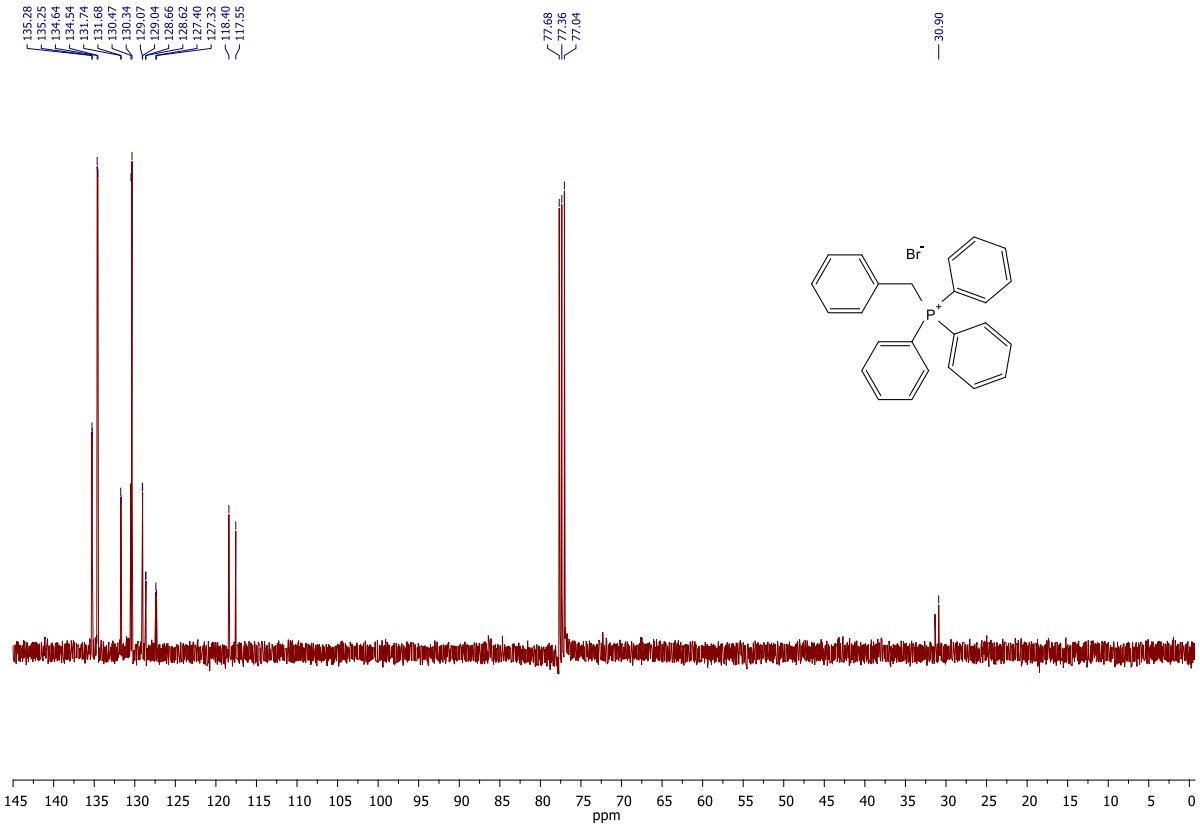

Figure 47: ^{13}C NMR of benzyltriphenylphosphonium bromide **206**

© University of Pretoria

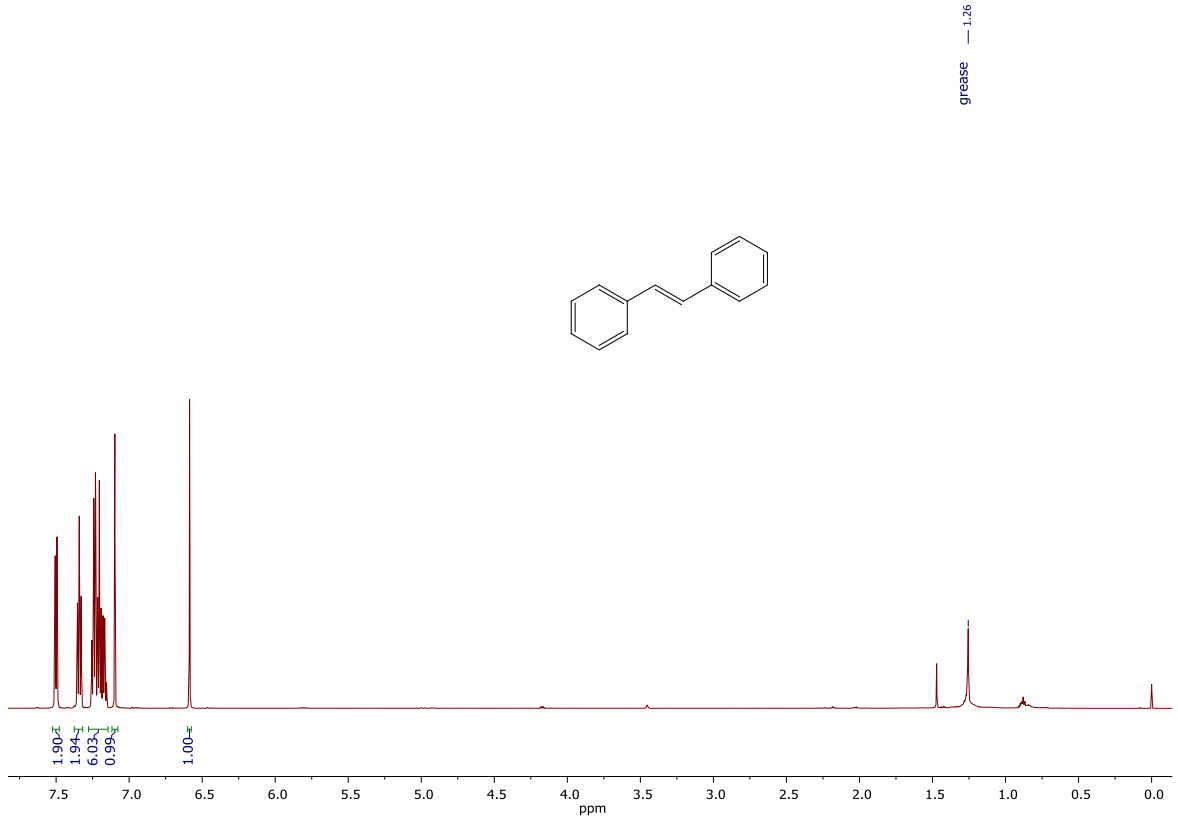

Figure 48: ^{1}H NMR of (*E*)-1,2-diphenylethene **143b**

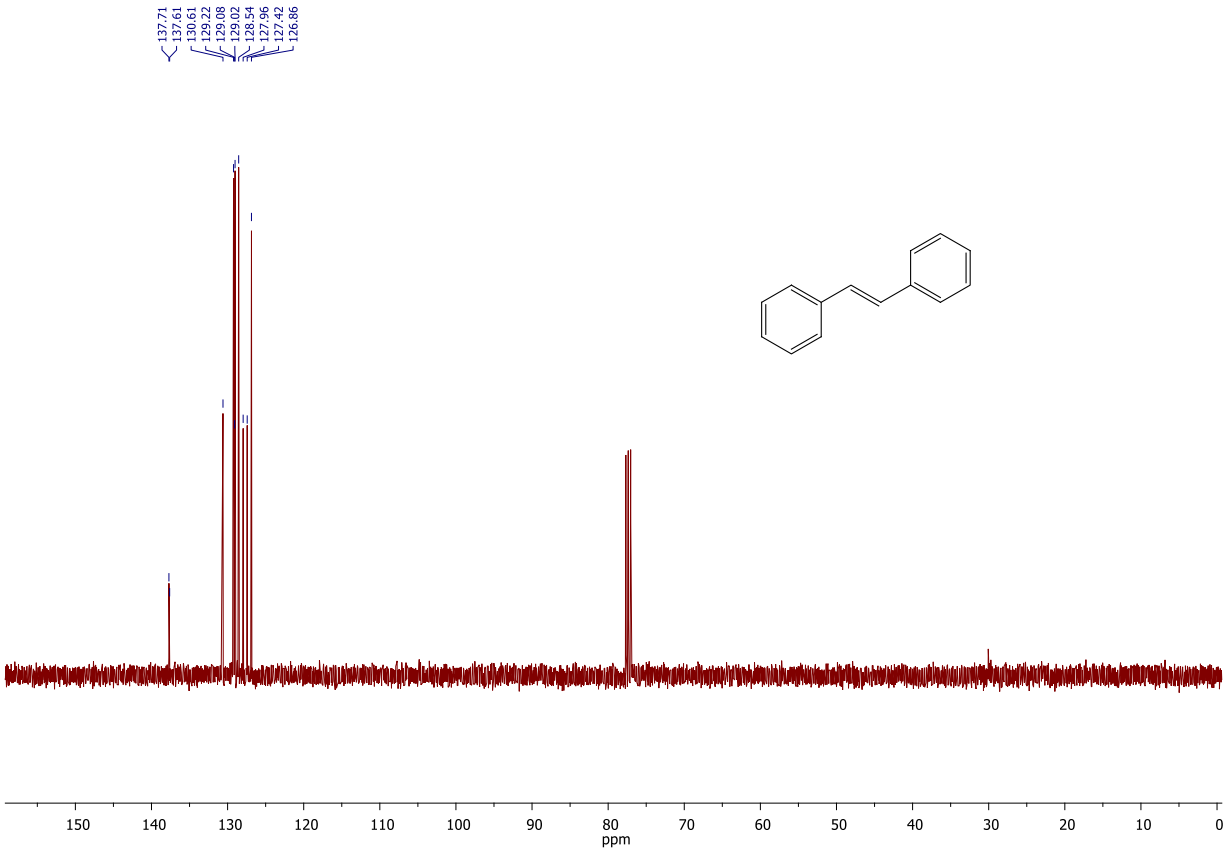

Figure 49: ^{13}C NMR of (*E*)-1,2-diphenylethene **143b**

© University of Pretoria

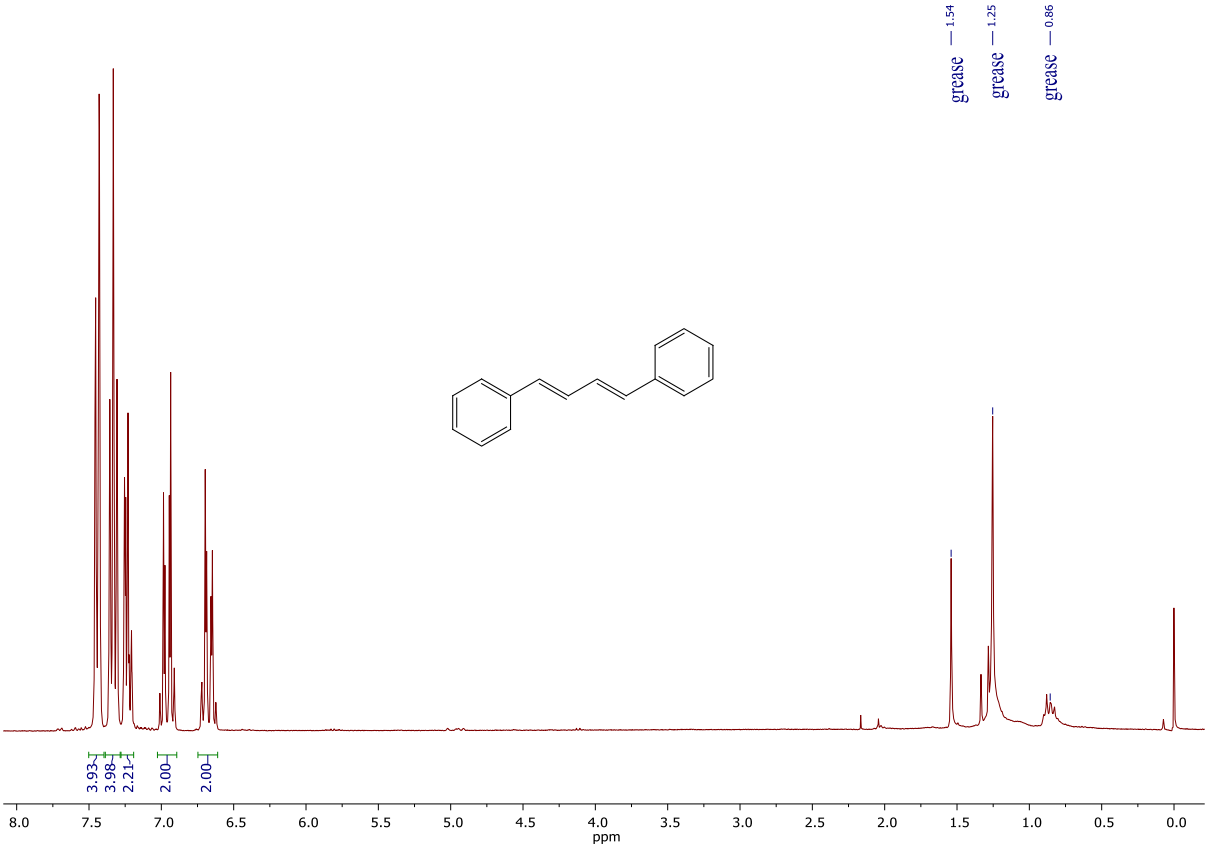

Figure 50: ^{1}H NMR of (1*E*,3*E*)-1,4-diphenylbuta-1,3-diene **210a**

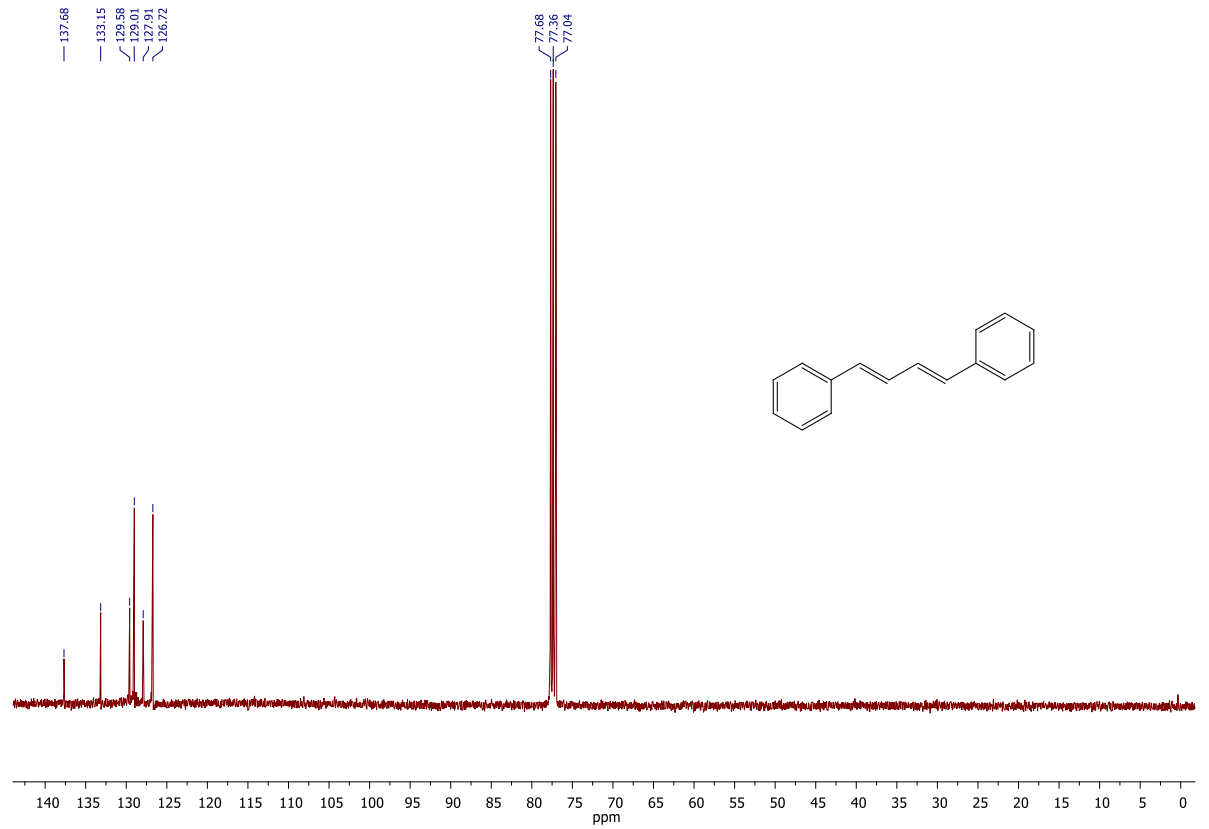

Figure 51: ^{13}C NMR of (1*E*,3*E*)-1,4-diphenylbuta-1,3-diene **210a**

© University of Pretoria

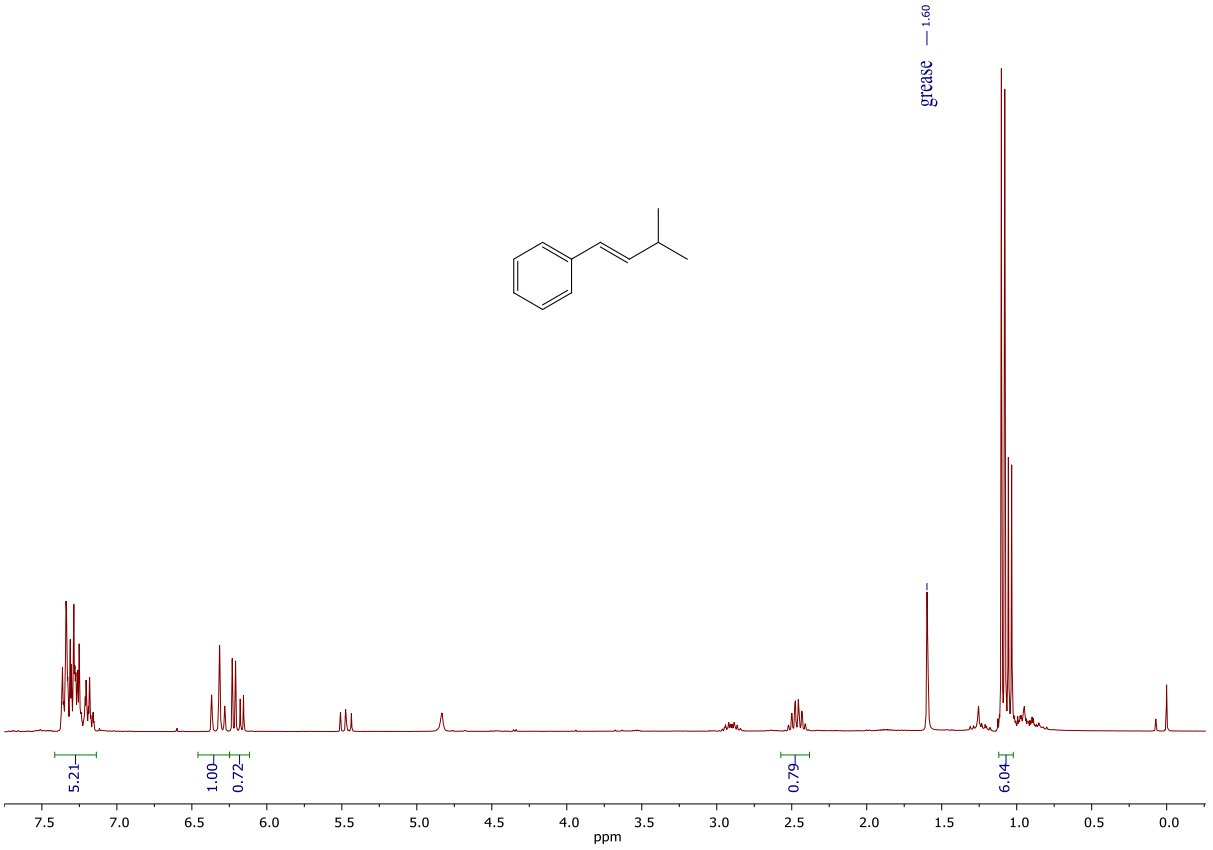

Figure 52: ^{1}H NMR of (*E*)-(3-methylbut-1-en-1-yl)benzene **211a**

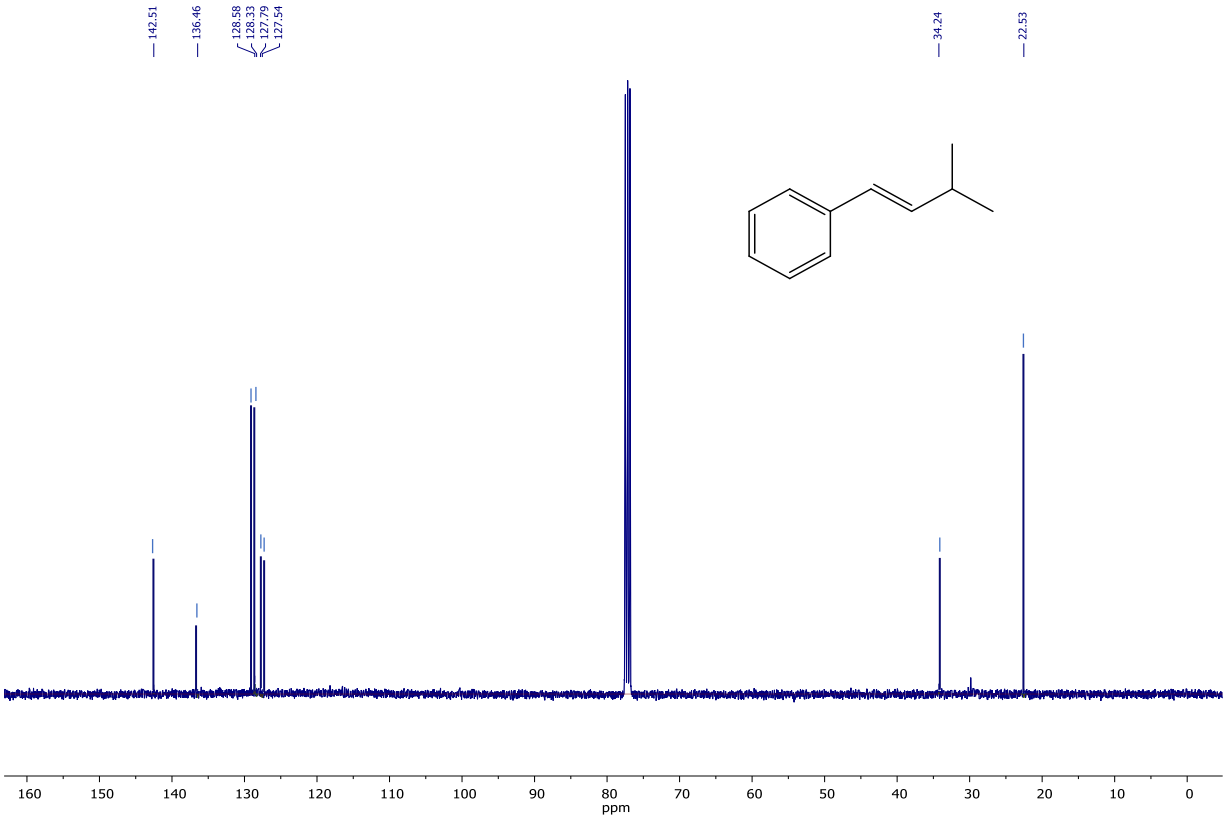

Figure 53: ^{13}C NMR of (*E*)-(3-methylbut-1-en-1-yl)benzene **211a**

© University of Pretoria

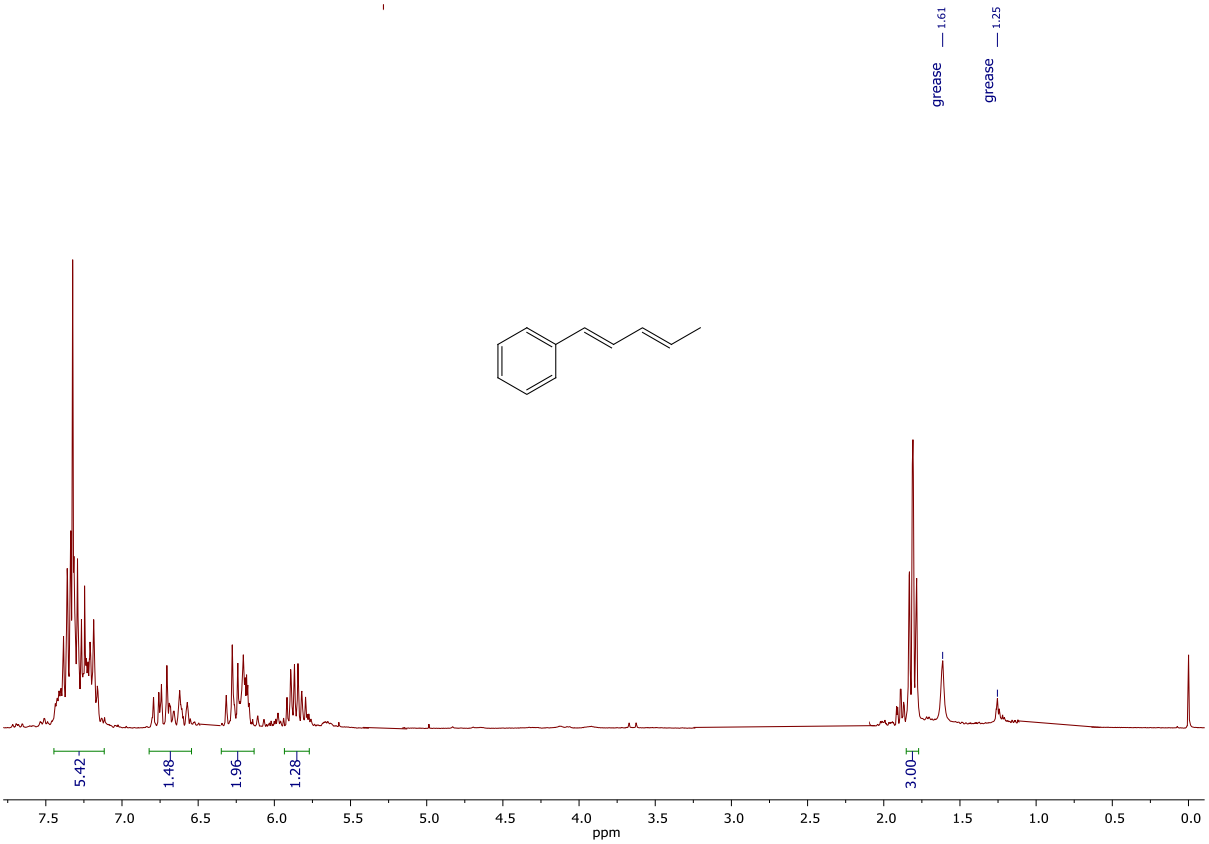

Figure 54: ^{1}H NMR of (1*E*,3*E*)-penta-1,3-dien-1-ylbenzene **212a**

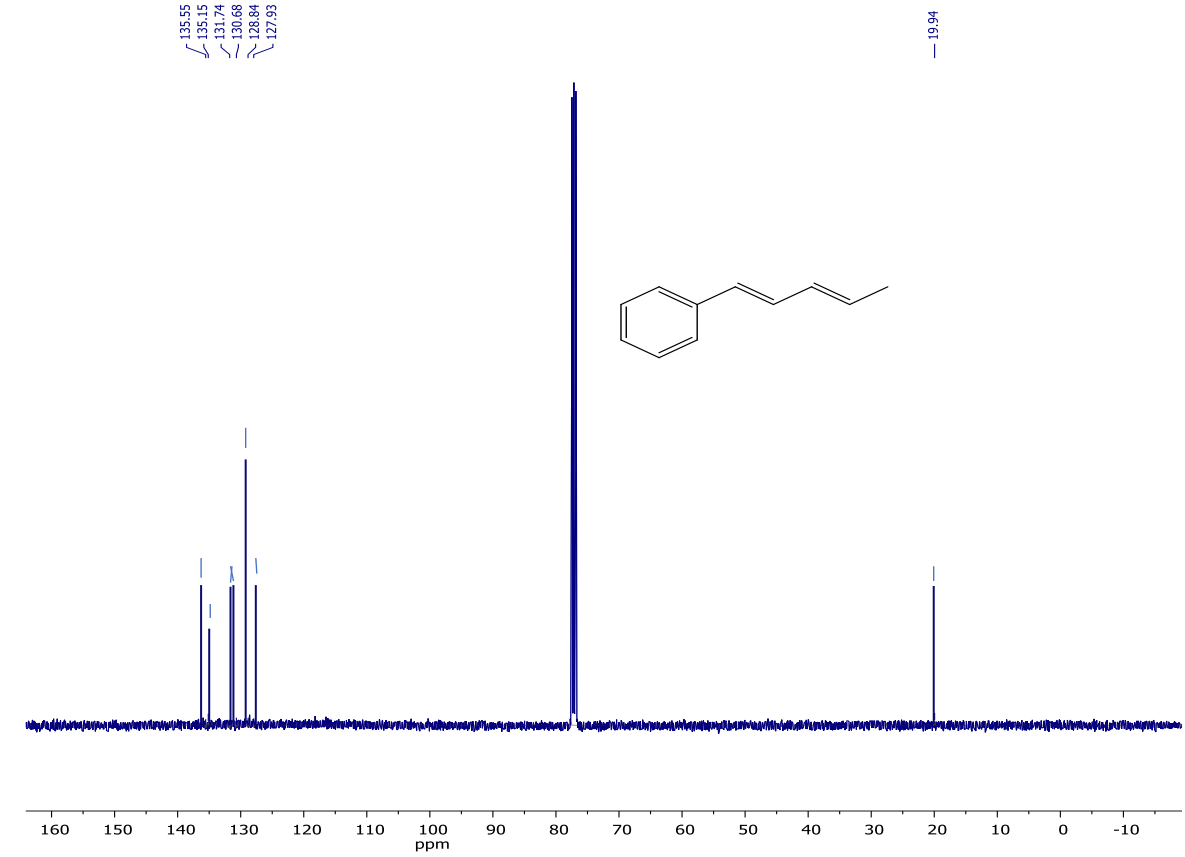

Figure 55: ^{13}C NMR of (1*E*,3*E*)-penta-1,3-dien-1-ylbenzene **212a**

© University of Pretoria

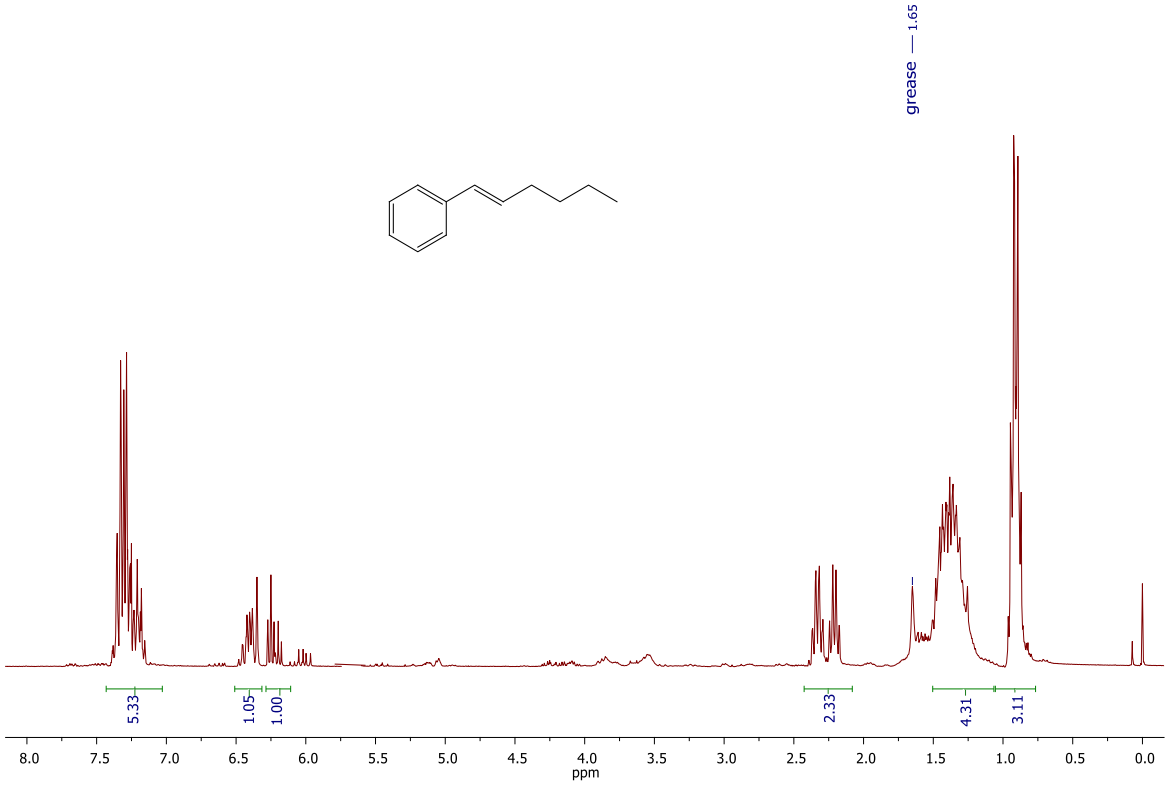

Figure 56: ^{1}H NMR of (*E*)-hex-1-en-1-ylbenzene **213a**

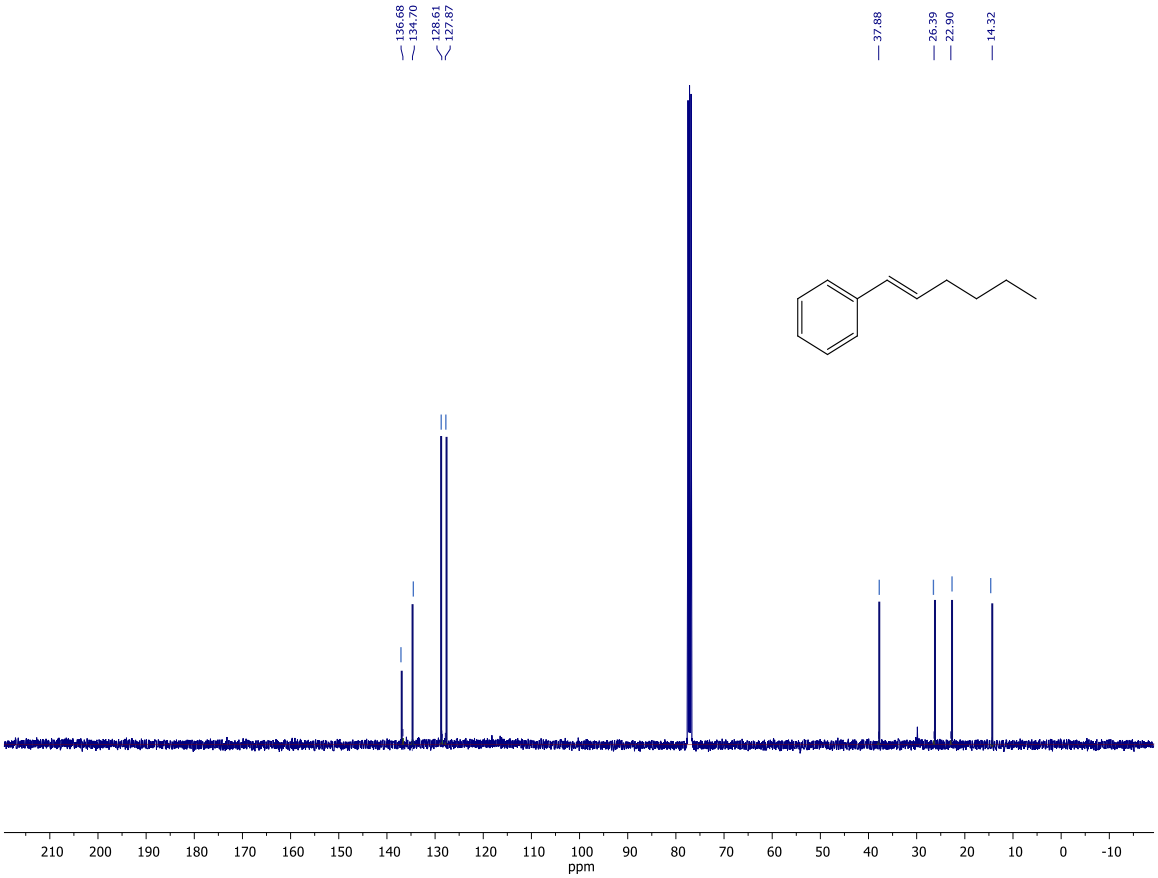

Figure 57: ^{13}C NMR of (*E*)-hex-1-en-1-ylbenzene **213a**

© University of Pretoria

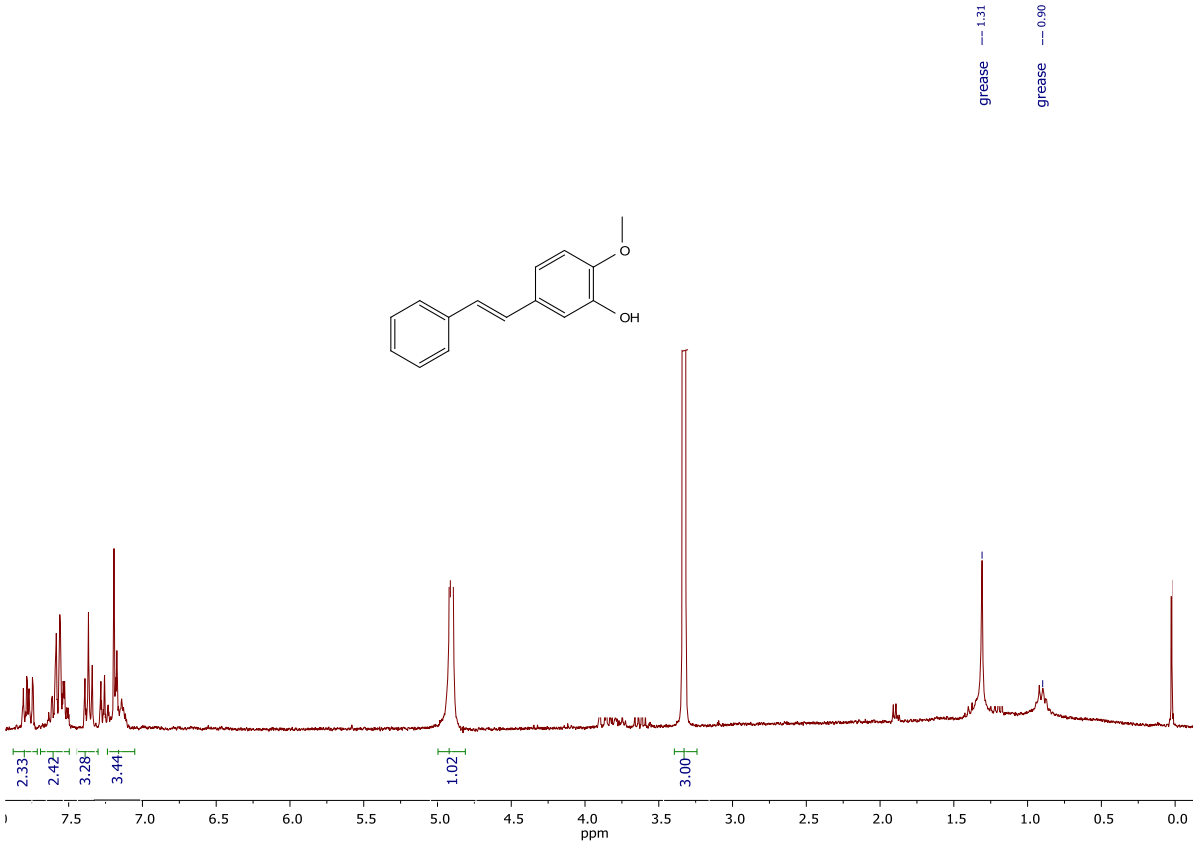

Figure 58: ^{1}H NMR of (*E*)-2-methoxy-5-styrylphenol **214a**

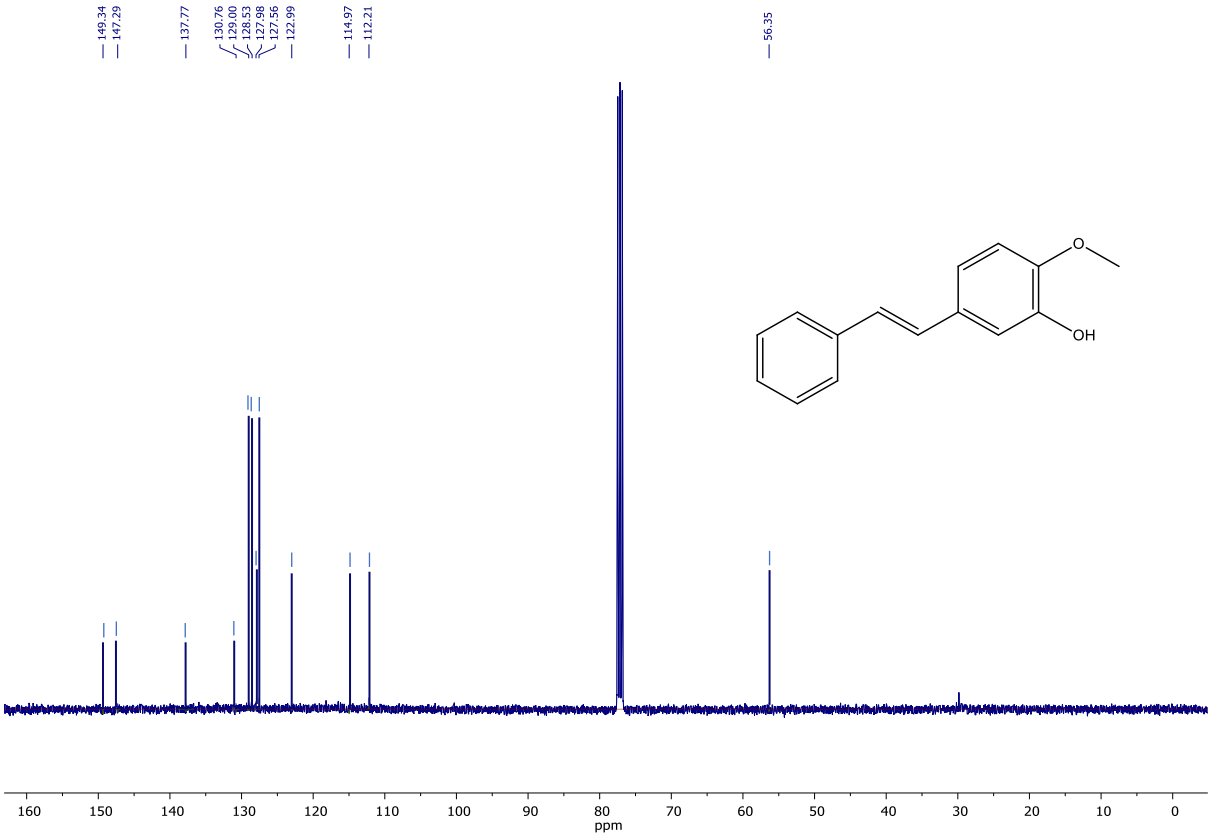

Figure 59: ^{13}C NMR of (*E*)-2-methoxy-5-styrylphenol **214a**

© University of Pretoria

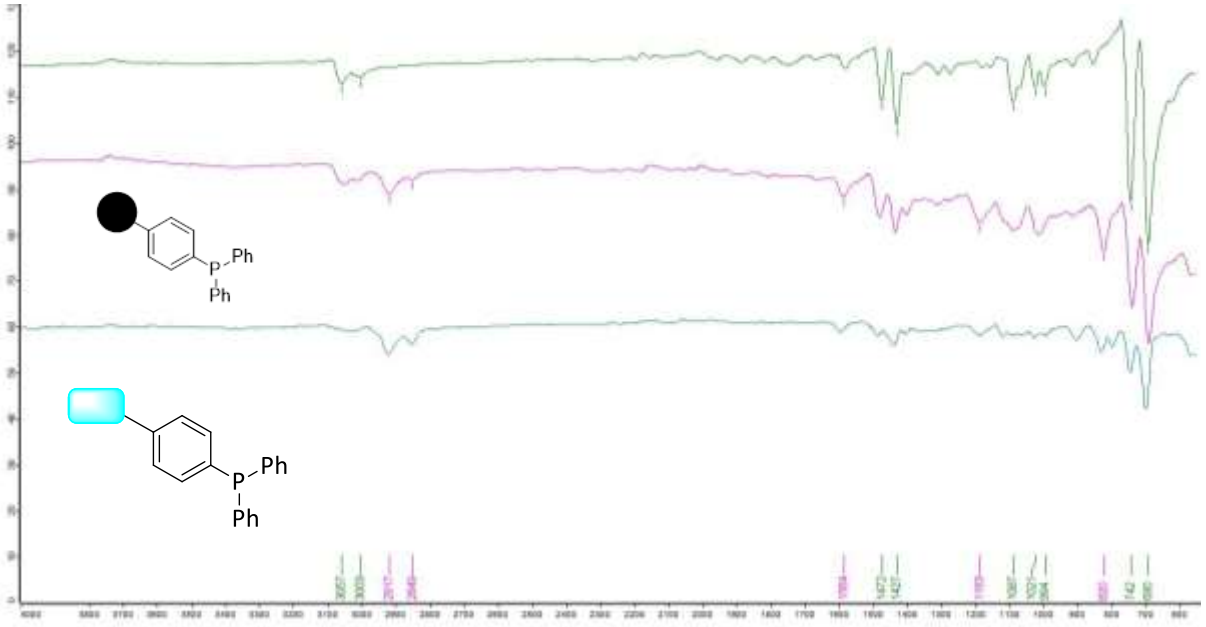

Figure 60: FTIR spectra comparison of unsupported- (top), polystyrene-supported- (middle) and solid-supported triphenylphosphine (bottom).

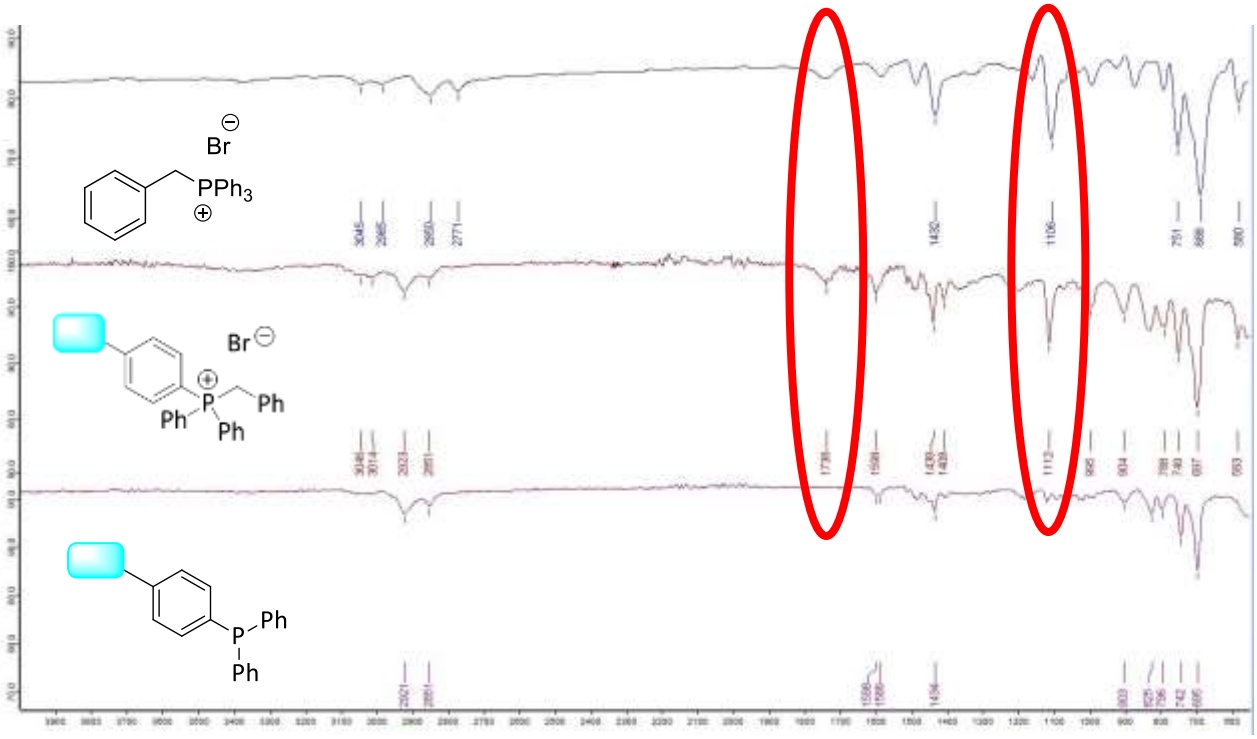

Figure 61: FTIR spectra comparison of unsupported benzyl phosphonium salt, solid-supported phosphonium salt and solid-supported triphenylphosphine

© University of Pretoria

10.1.4. Suzuki-Miyaura selected examples from model study

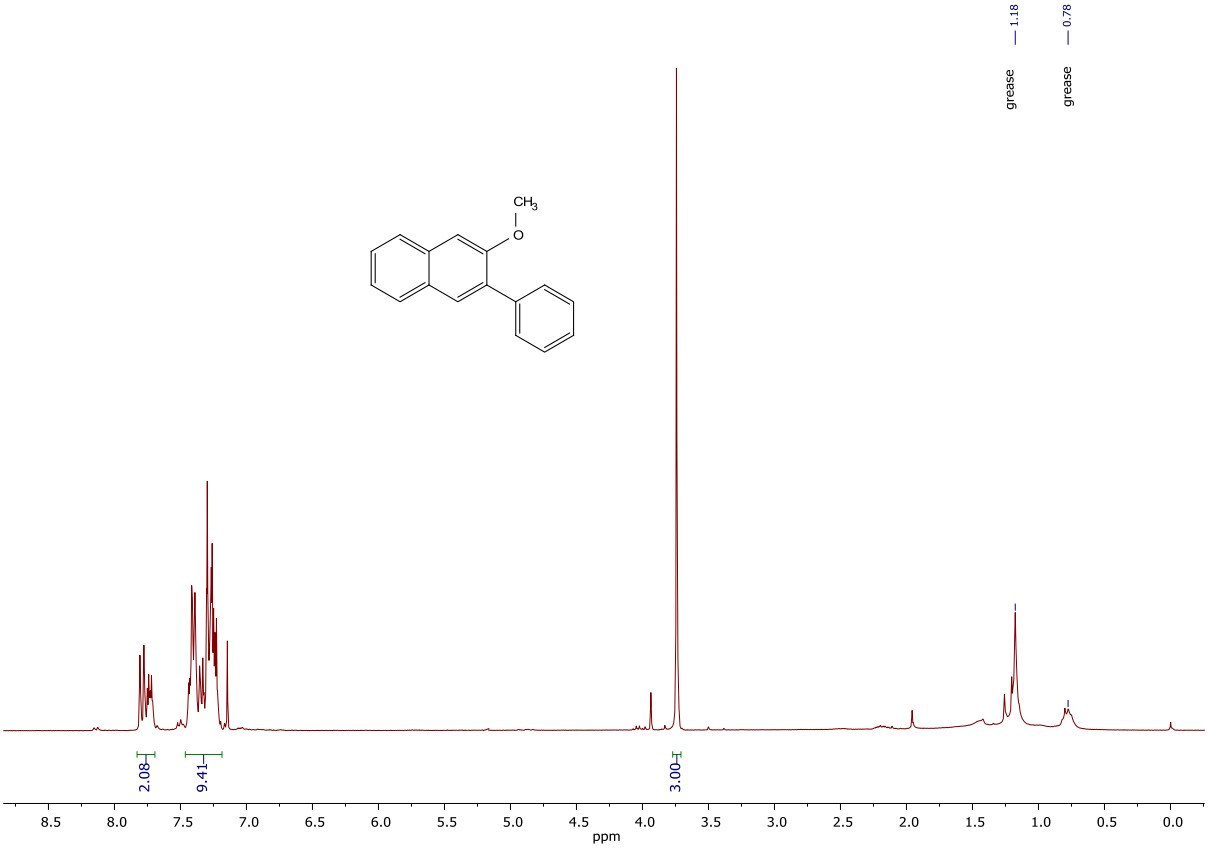

Figure 62: ^{1}H NMR of 2-methoxy-3-phenylnaphthalene **220a**

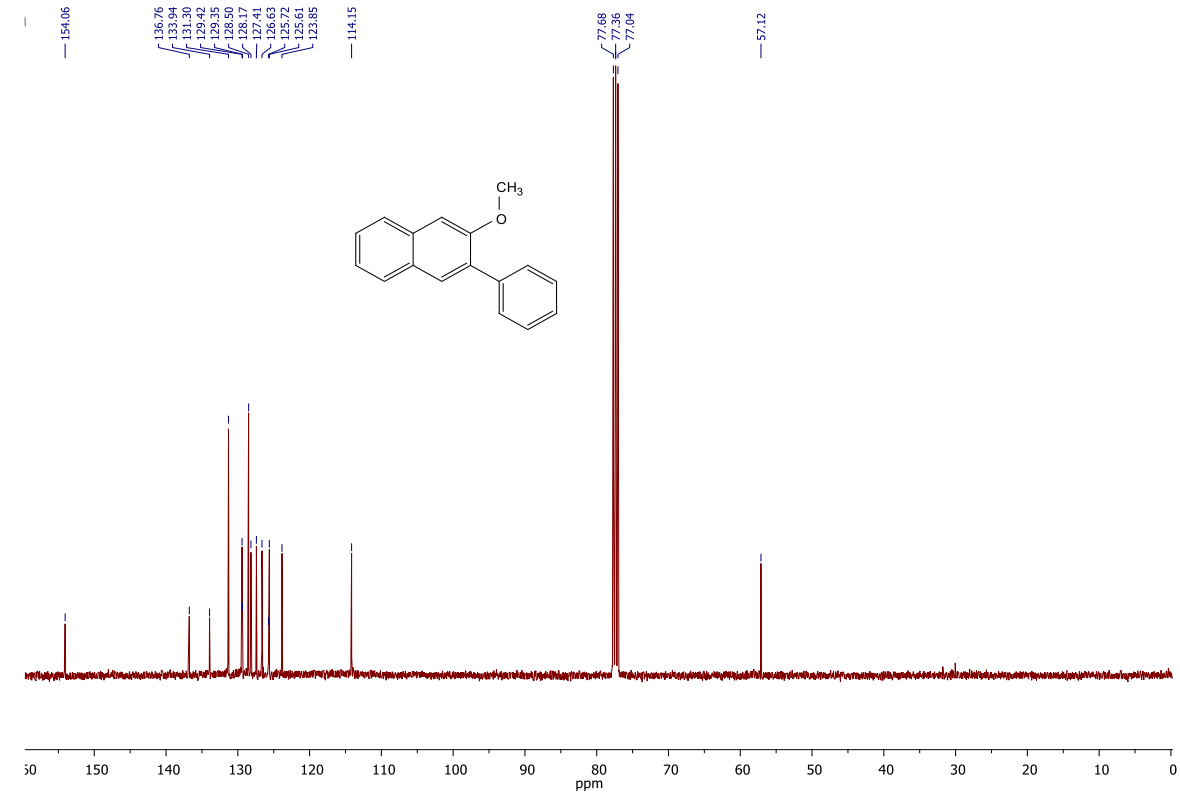

Figure 63: ^{13}C NMR of 2-methoxy-3-phenylnaphthalene **220a**

© University of Pretoria

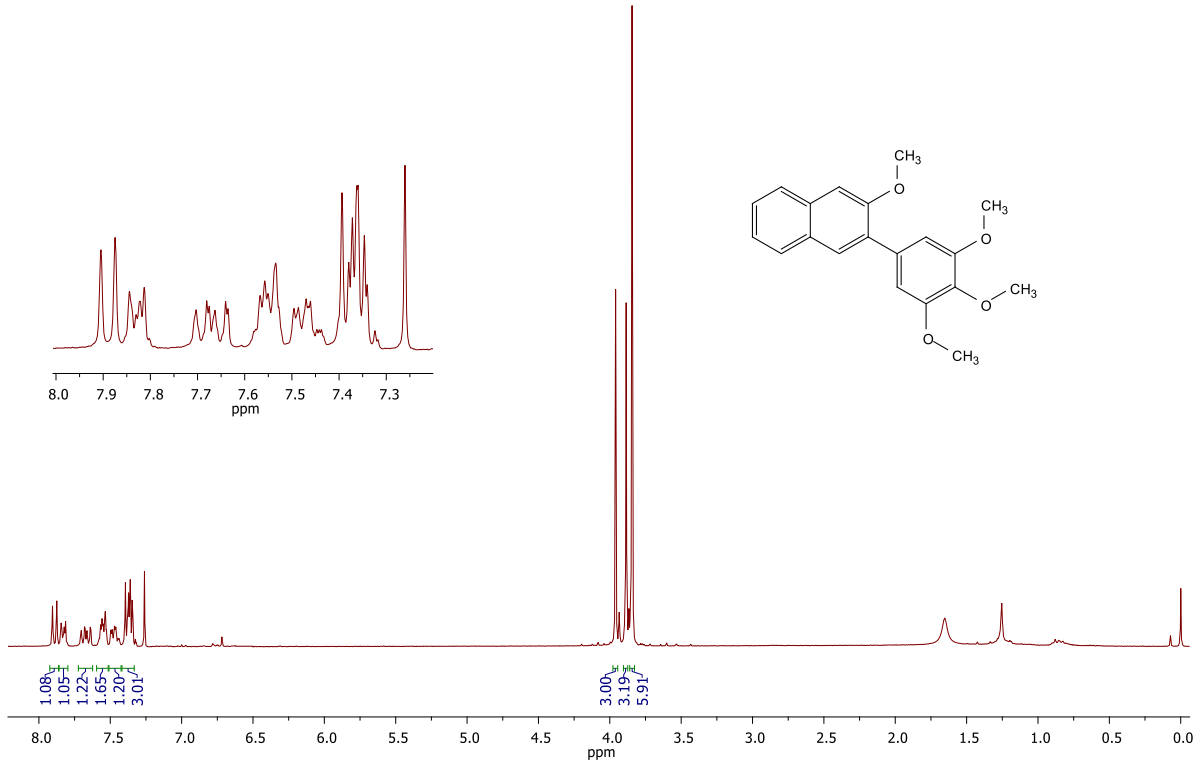

Figure 64: ^{1}H NMR of 2-methoxy-3-(3,4,5-trimethoxyphenyl)naphthalene **220b**

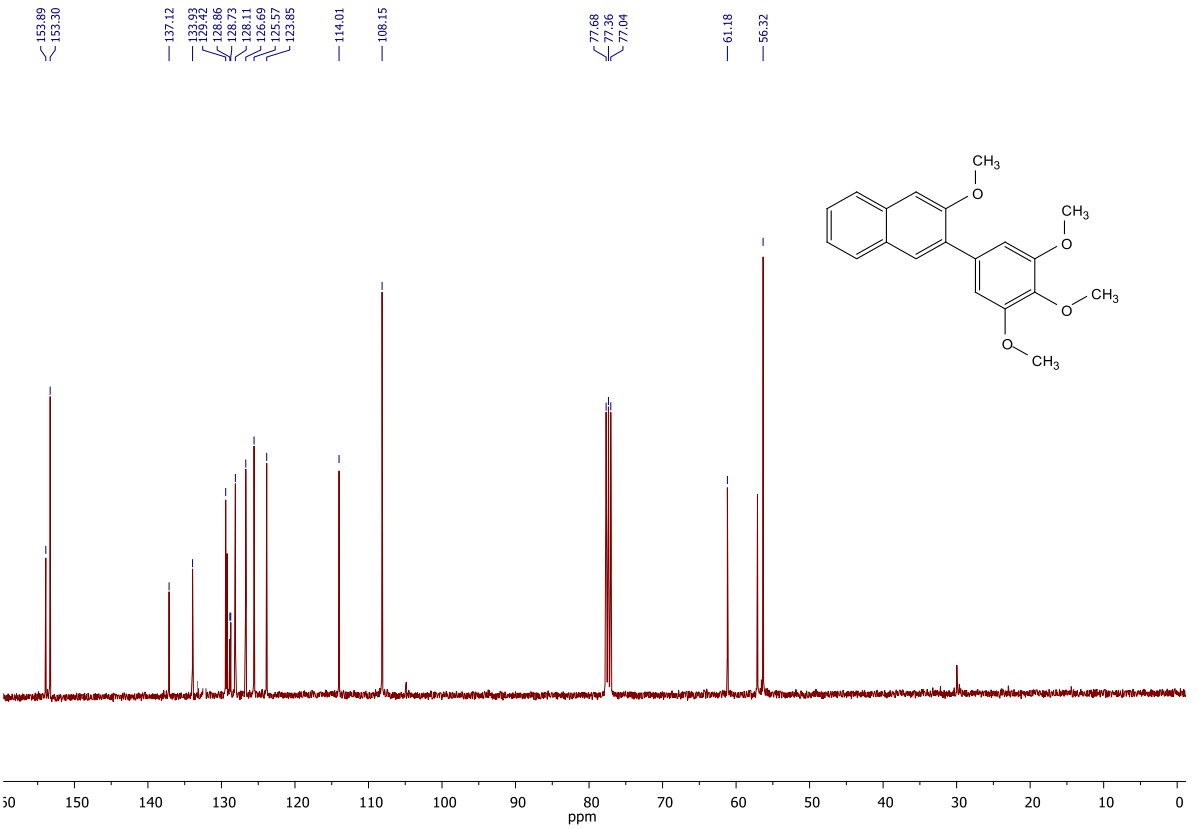

Figure 65: ^{13}C NMR of 2-methoxy-3-(3,4,5-trimethoxyphenyl)naphthalene **220b**

© University of Pretoria

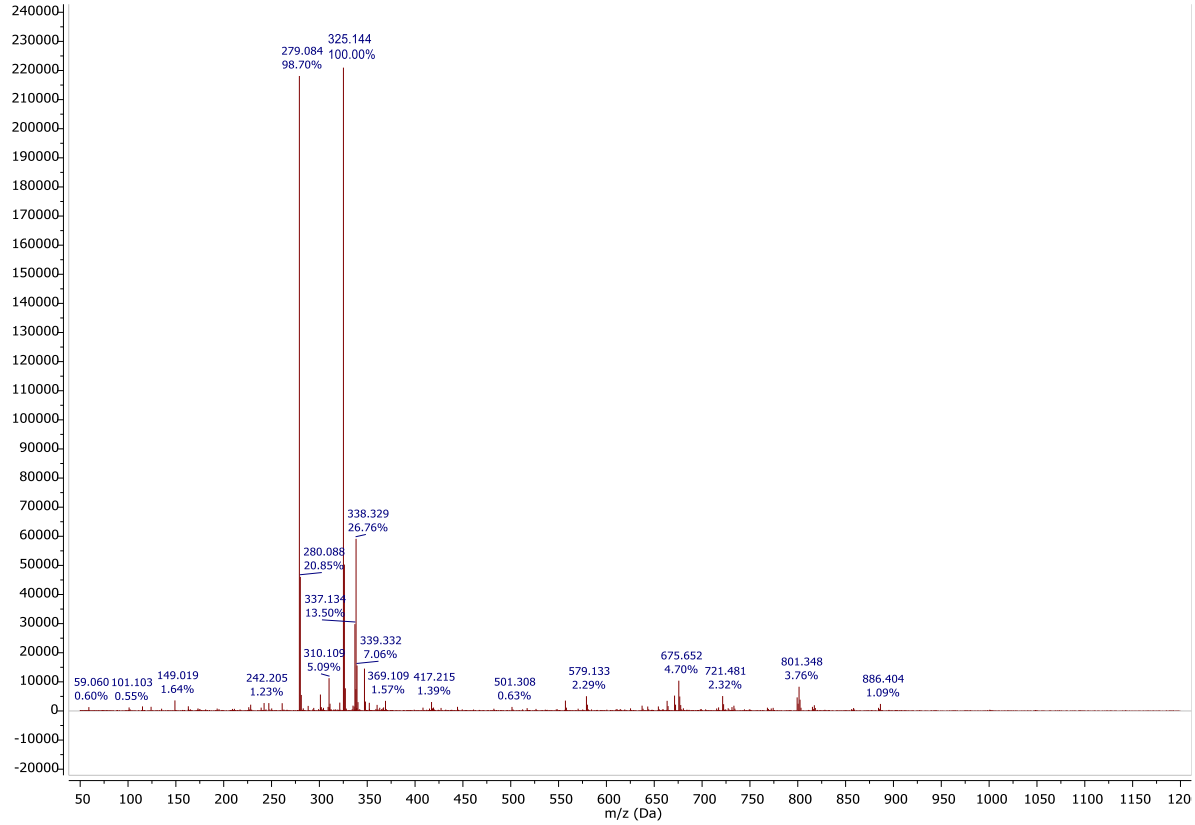

Figure 66: HRMS of 2-methoxy-3-(3,4,5-trimethoxyphenyl)naphthalene **220b**

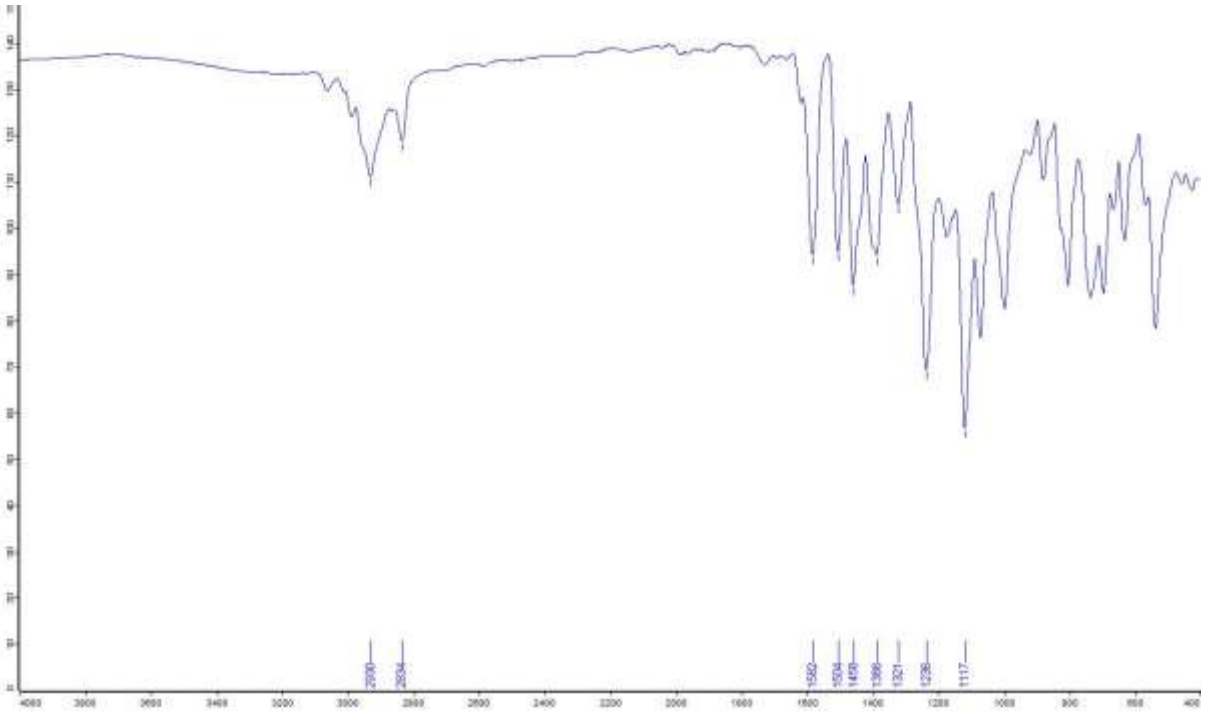

Figure 67: FTIR spectrum of 2-methoxy-3-(3,4,5-trimethoxyphenyl)naphthalene **220b**

© University of Pretoria

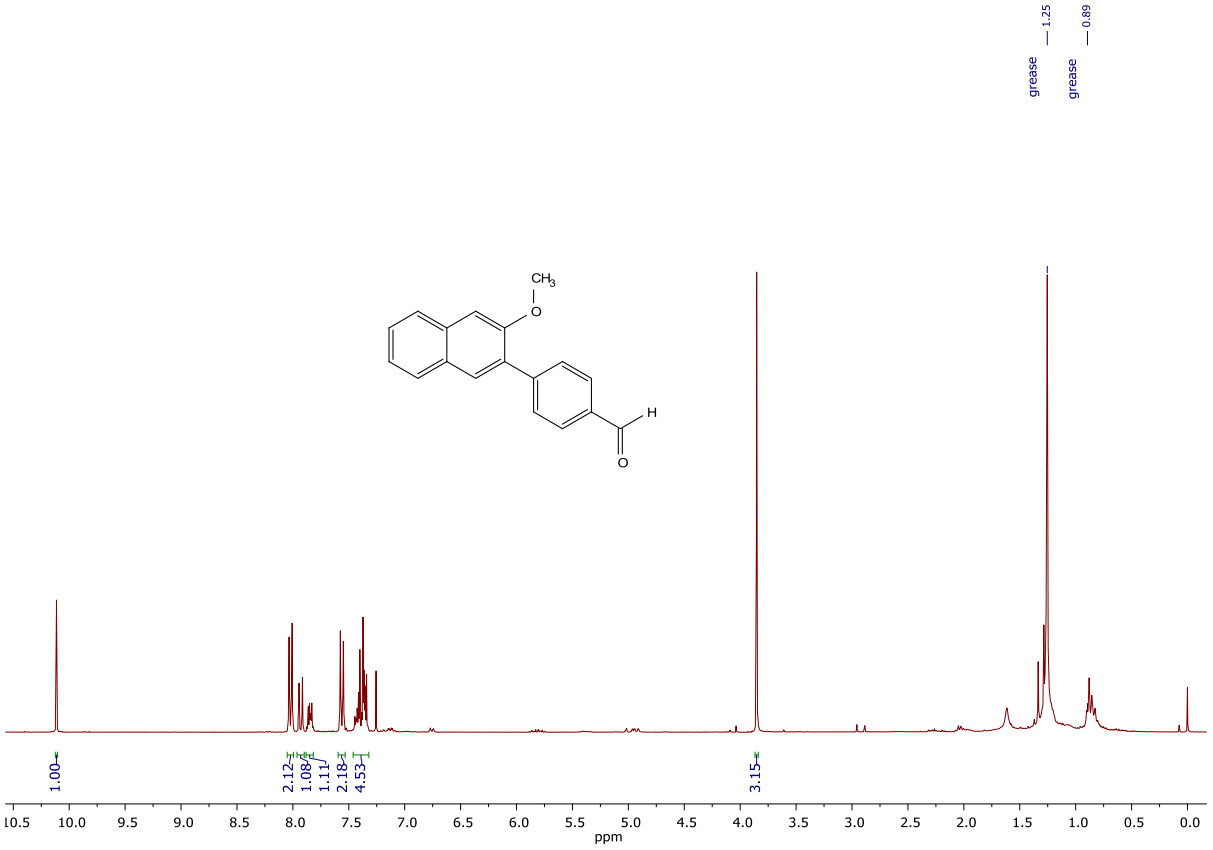

Figure 68: ^{1}H NMR of 4-(3-methoxynaphthalen-2-yl)benzaldehyde **220c**

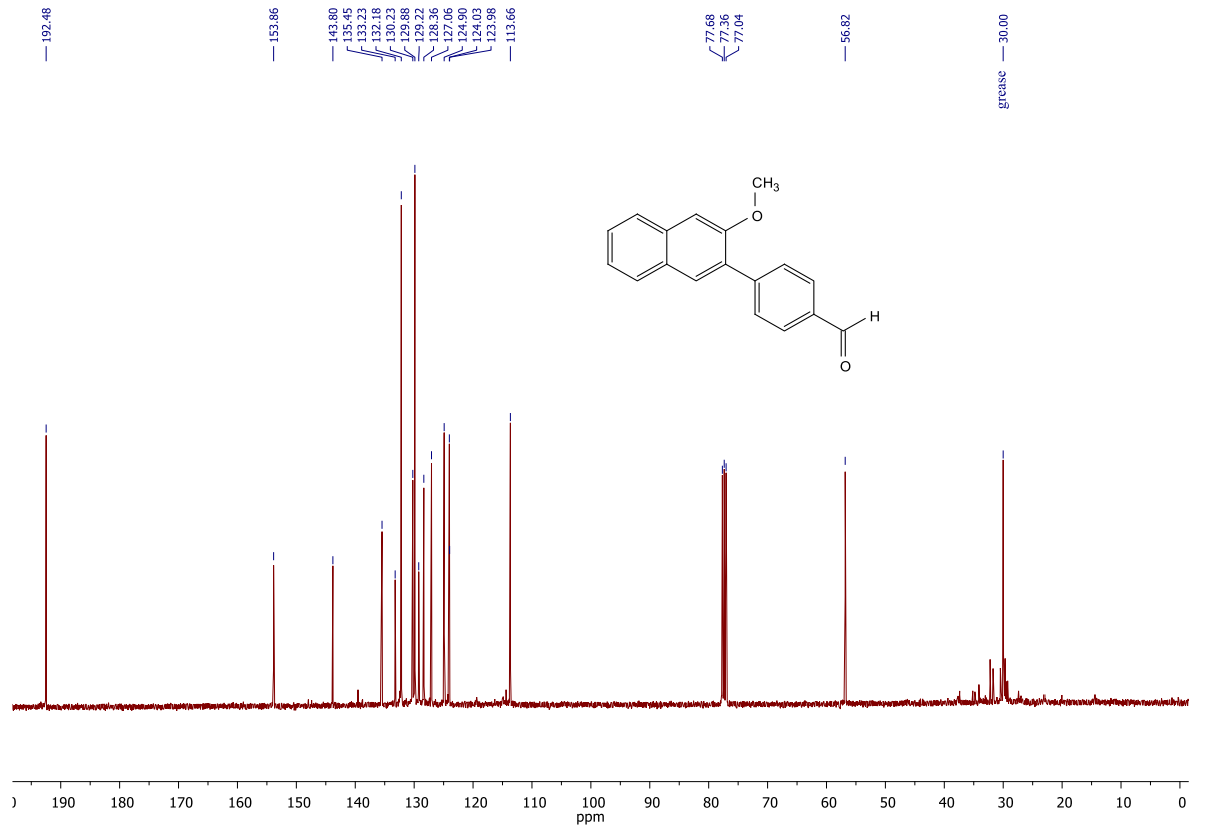

Figure 69: ^{13}C NMR of 4-(3-methoxynaphthalen-2-yl)benzaldehyde **220c**

© University of Pretoria

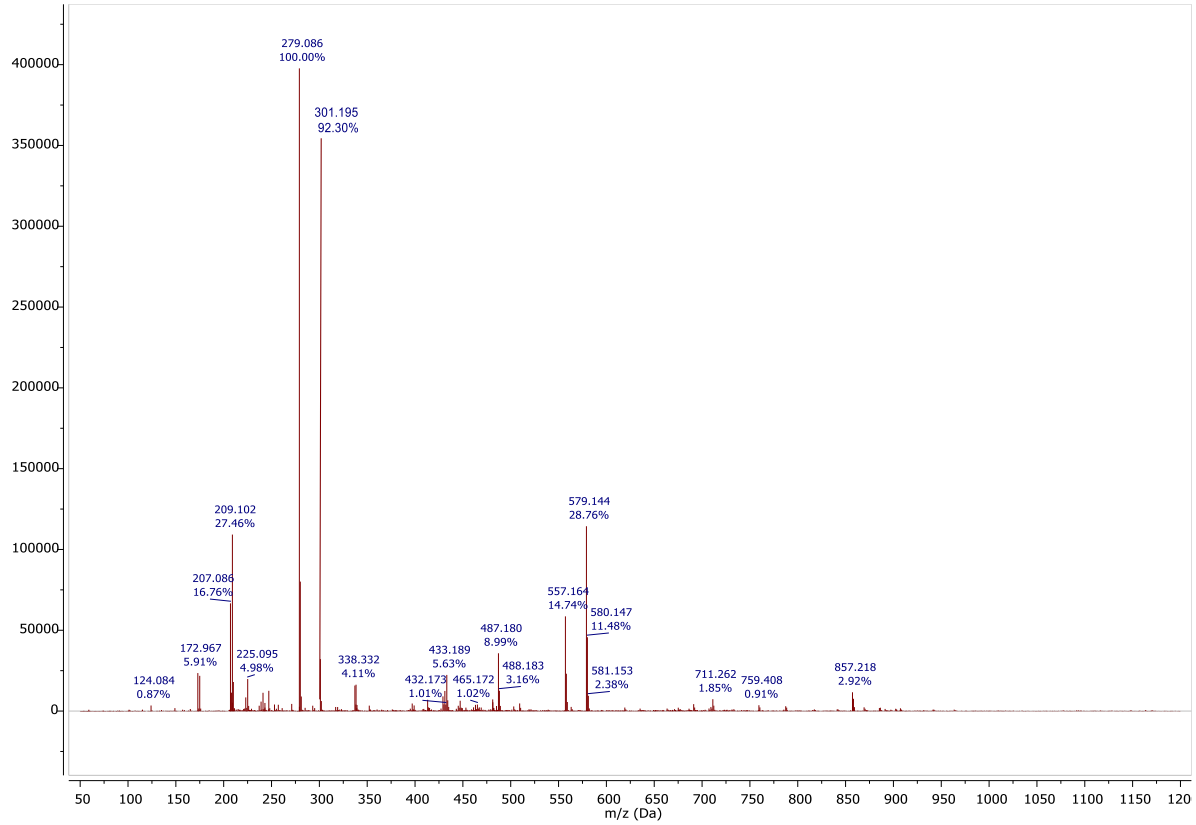

Figure 70: HRMS of 4-(3-methoxynaphthalen-2-yl)benzaldehyde **220c**

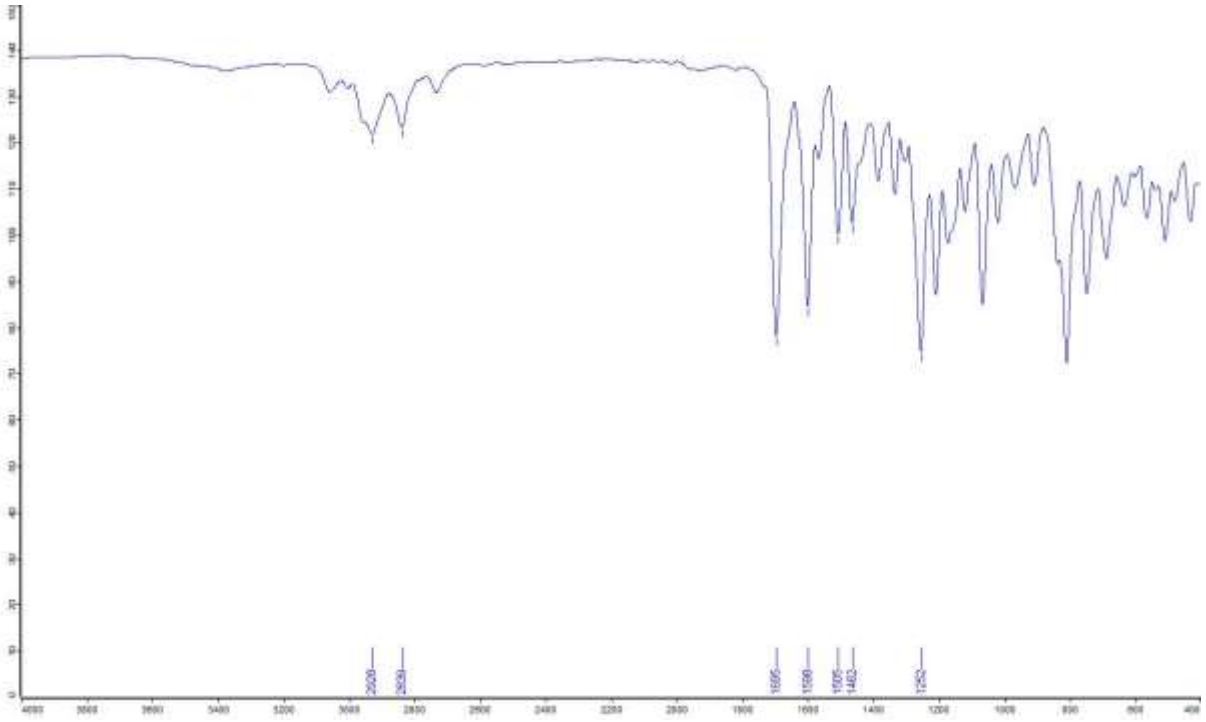

Figure 71: FTIR spectrum of 4-(3-methoxynaphthalen-2-yl)benzaldehyde **220c**

© University of Pretoria

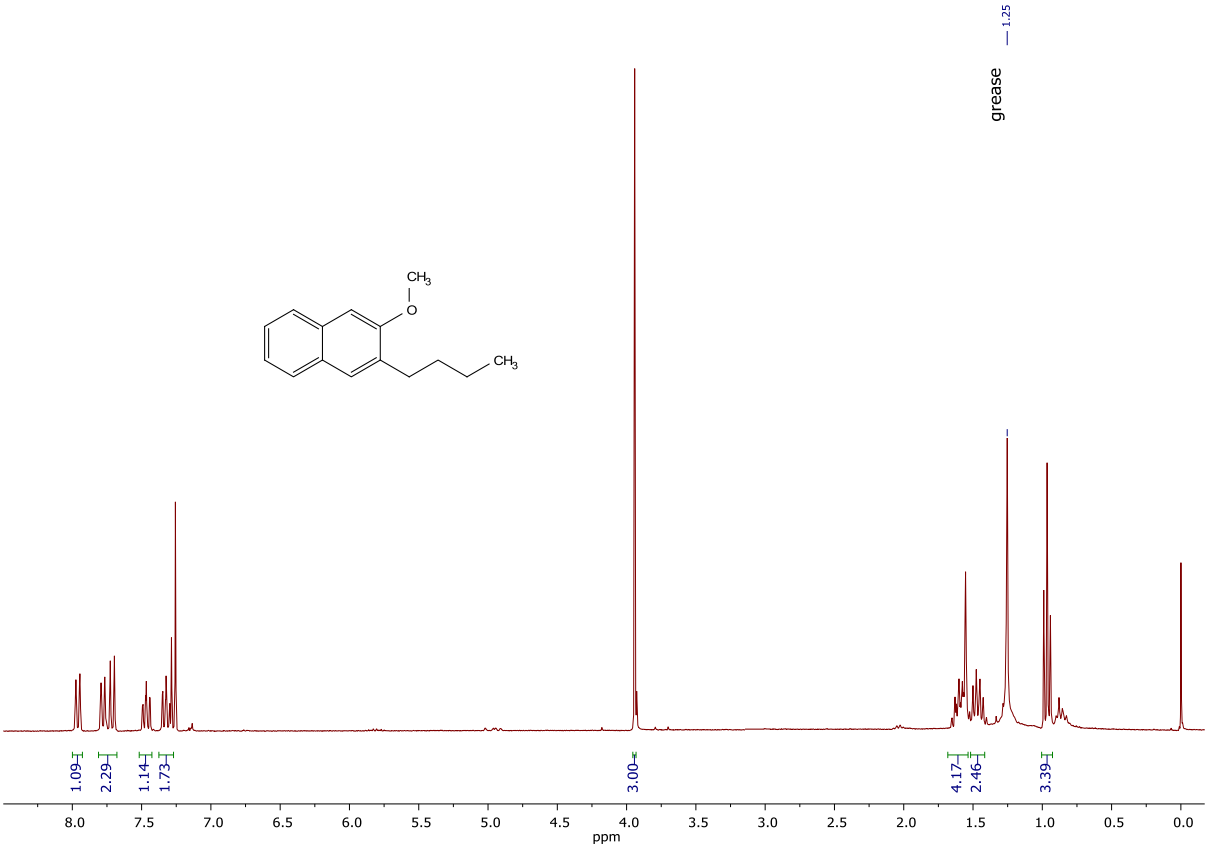

Figure 72: ^{1}H NMR of 2-butyl-3-methoxynaphthalene **220f**

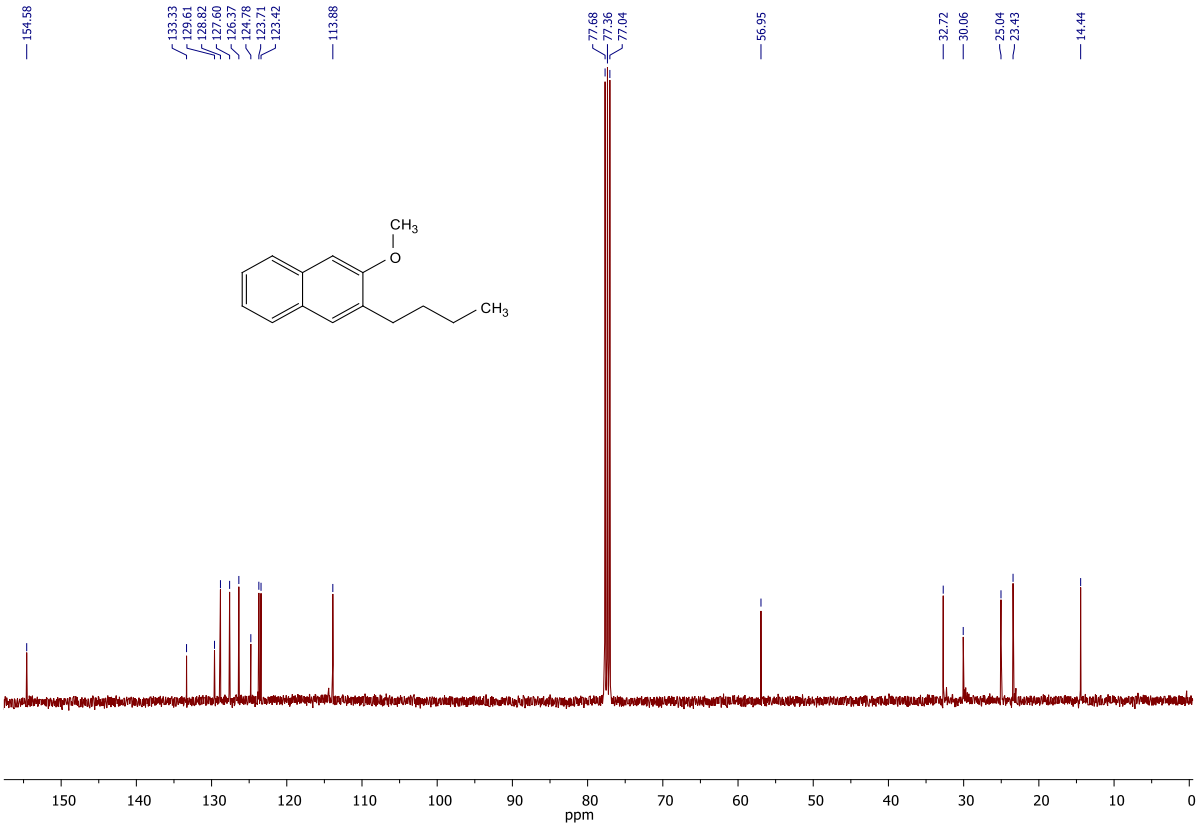

Figure 73: ^{13}C NMR of 2-butyl-3-methoxynaphthalene **220f**

© University of Pretoria

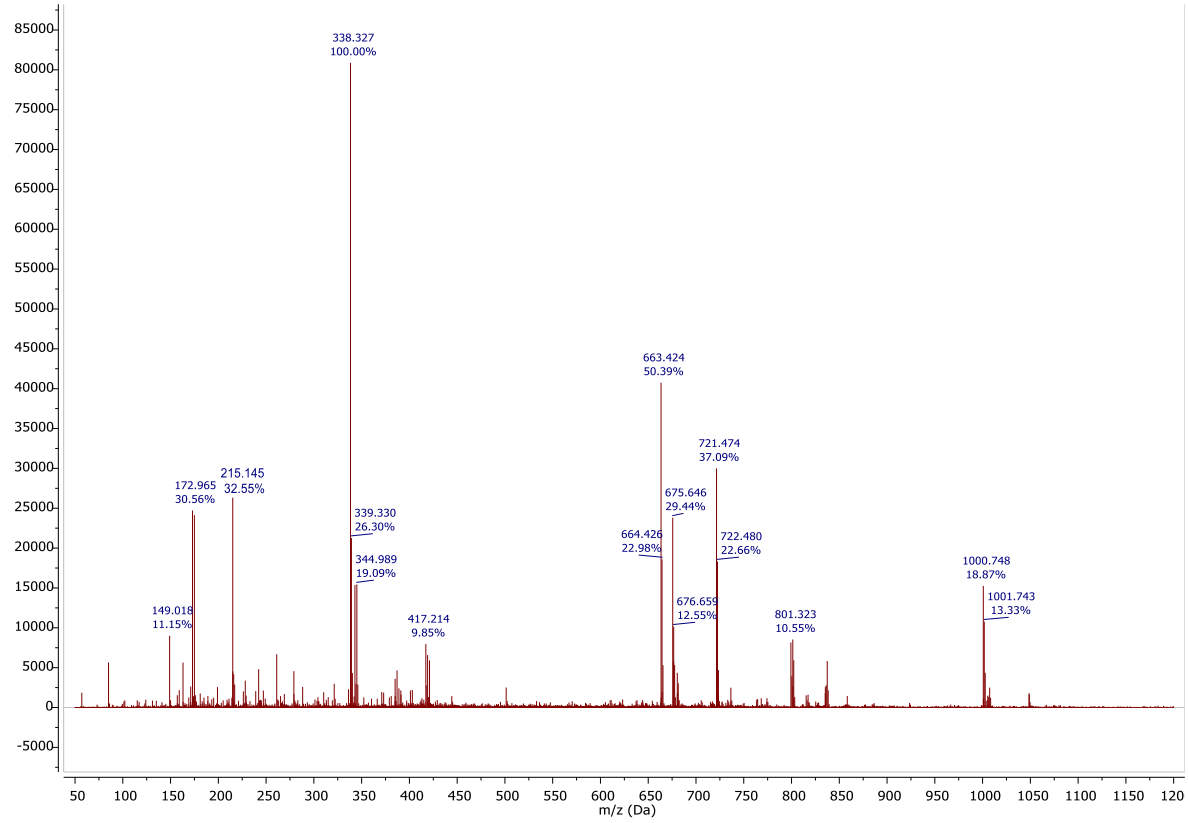

Figure 74: HRMS of 2-butyl-3-methoxynaphthalene **220f**

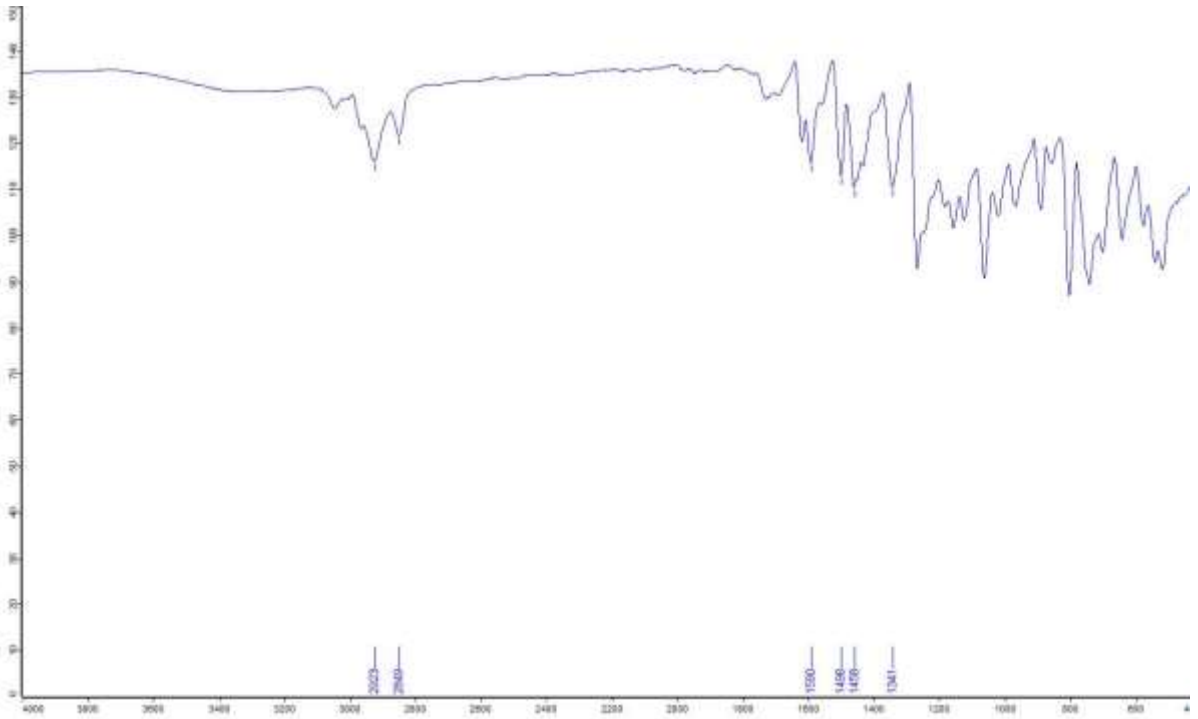

Figure 75: FTIR spectrum of 2-butyl-3-methoxynaphthalene **220f**

© University of Pretoria

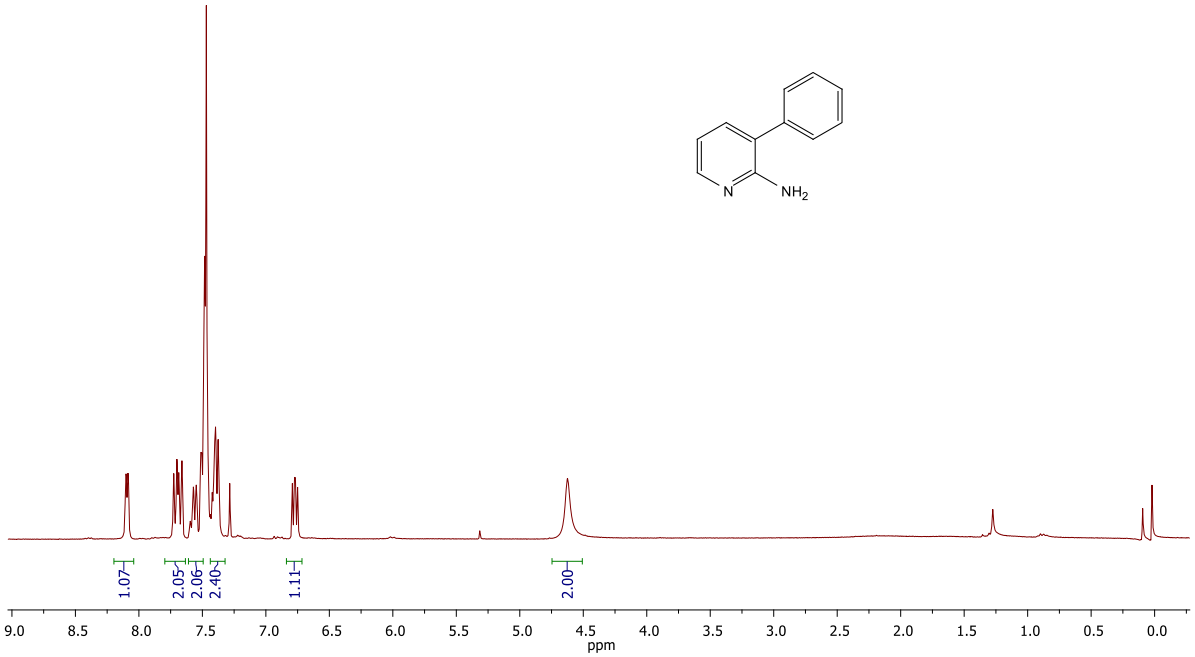

Figure 76: ^{1}H NMR of 3-phenylpyridin-2-amine **222a**

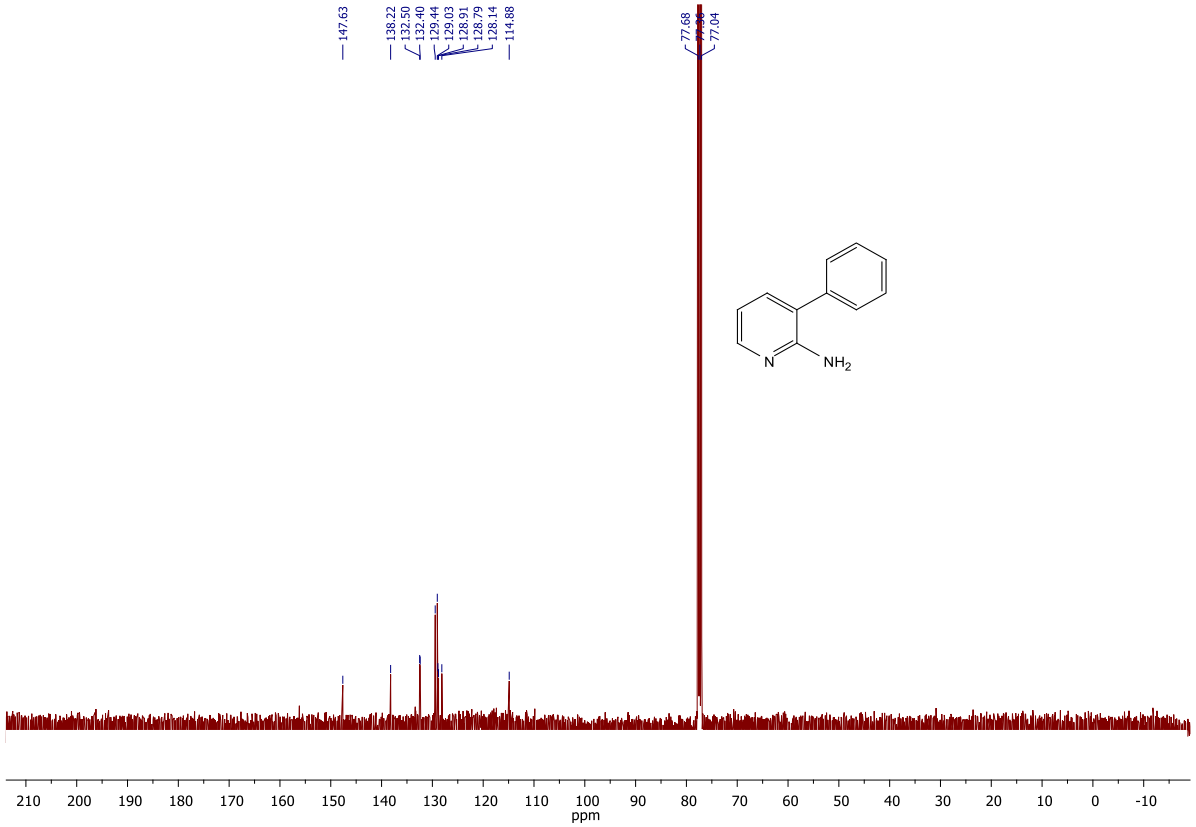

Figure 77: ^{13}C NMR of 3-phenylpyridin-2-amine **222a**

© University of Pretoria

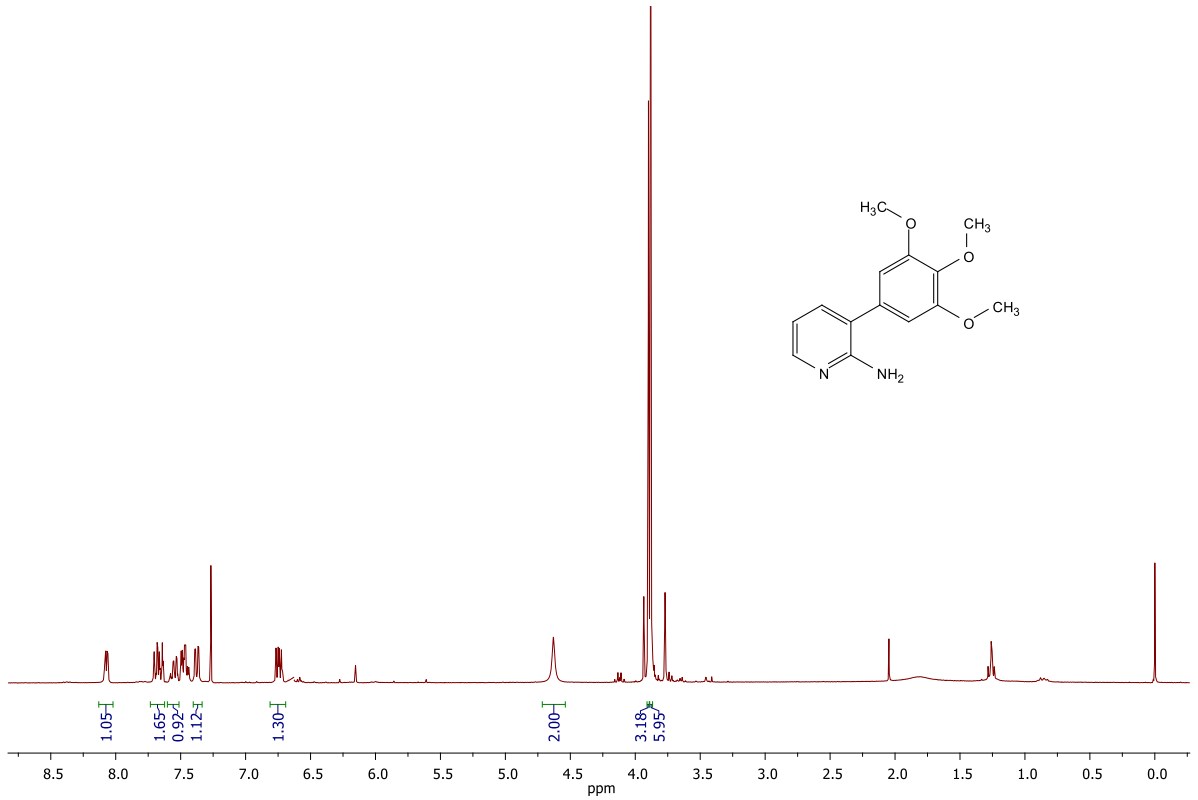

Figure 78: ^{1}H NMR of 3-(3,4,5-trimethoxyphenyl)pyridin-2-amine **222b**

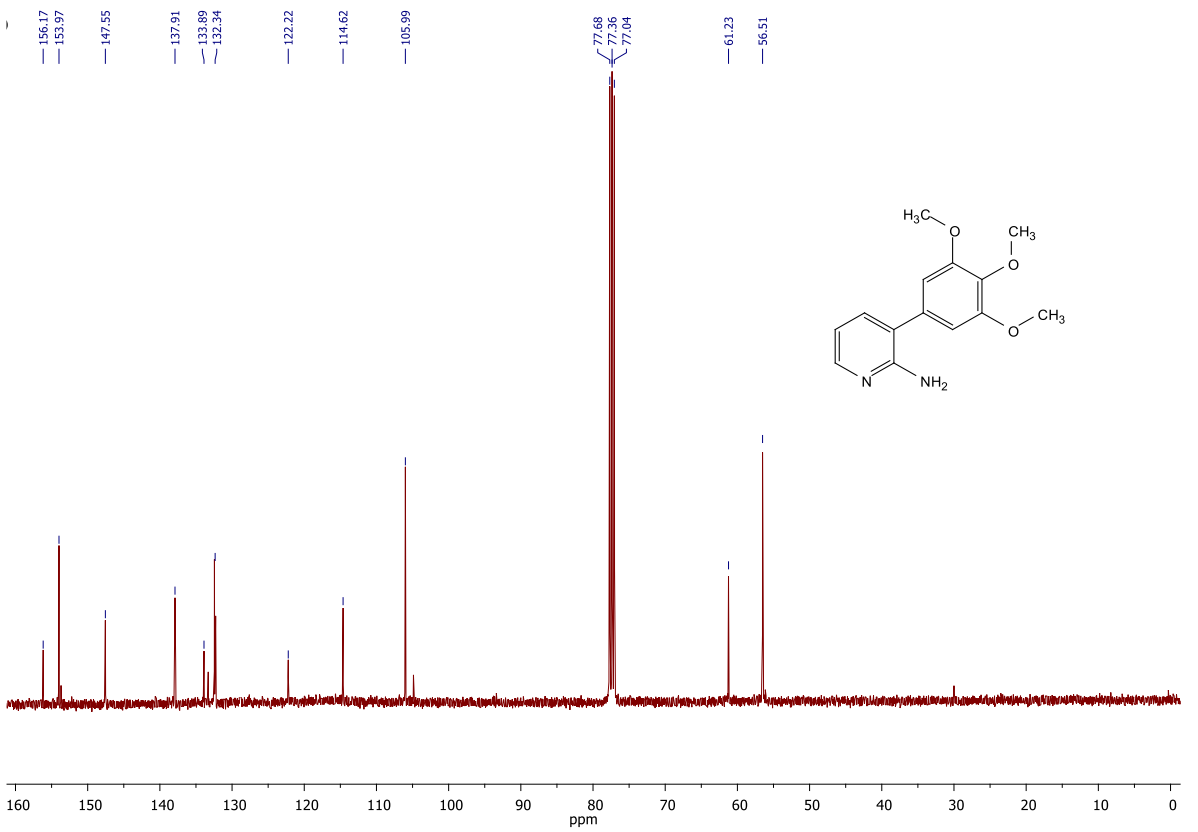

Figure 79: ^{13}C NMR of 3-(3,4,5-trimethoxyphenyl)pyridin-2-amine **222b**

© University of Pretoria

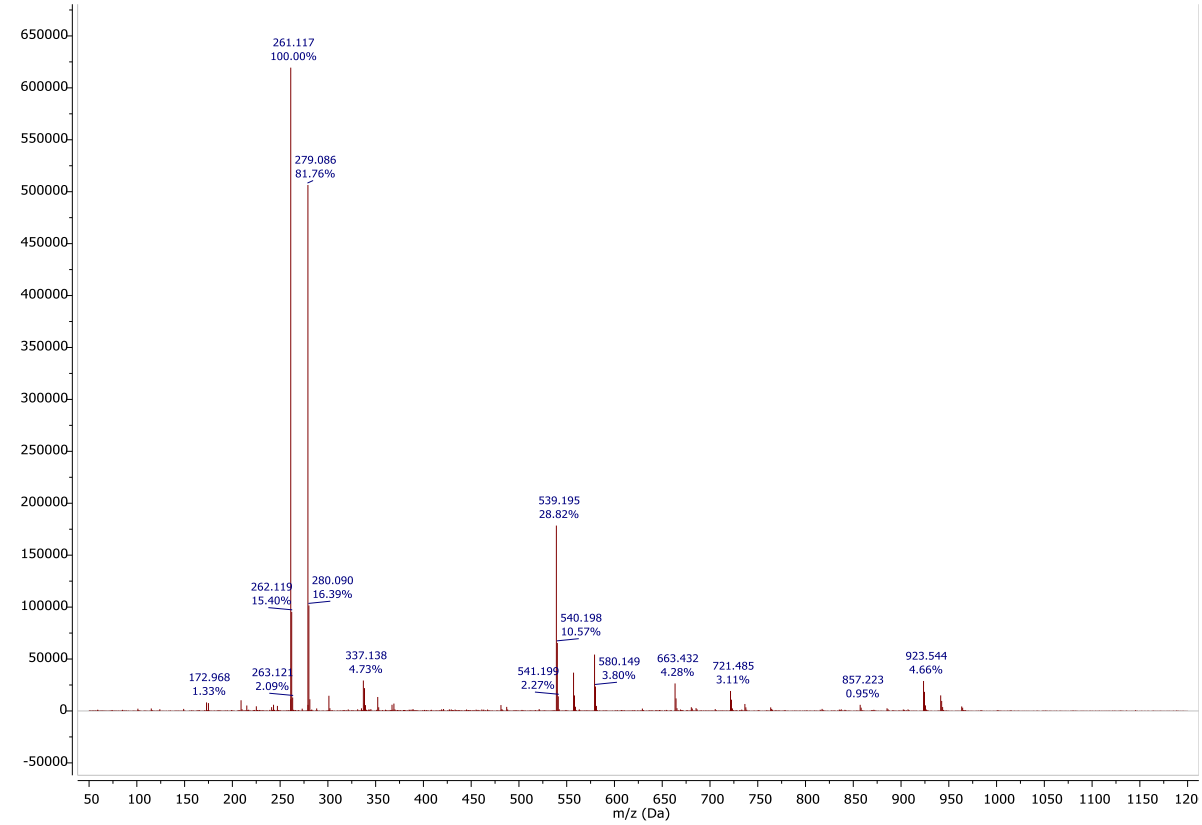

Figure 80: HRMS of 3-(3,4,5-trimethoxyphenyl)pyridin-2-amine **222b**

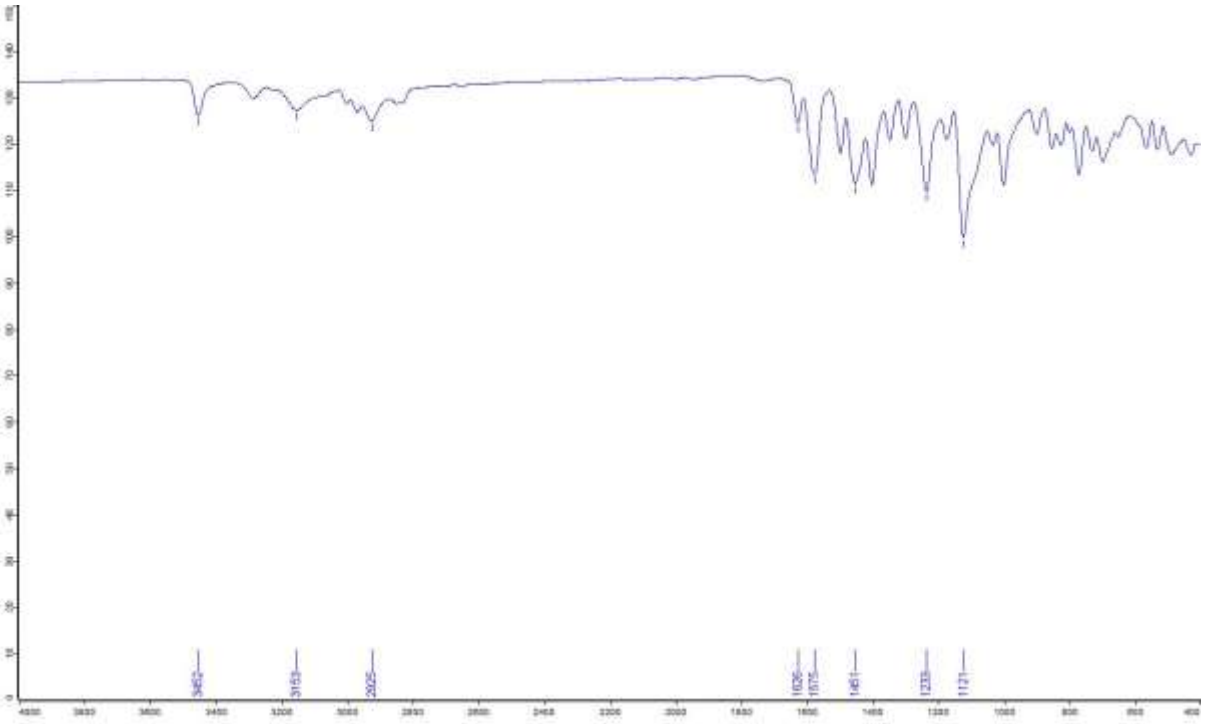

Figure 81: FTIR spectrum of 3-(3,4,5-trimethoxyphenyl)pyridin-2-amine **222b**

© University of Pretoria

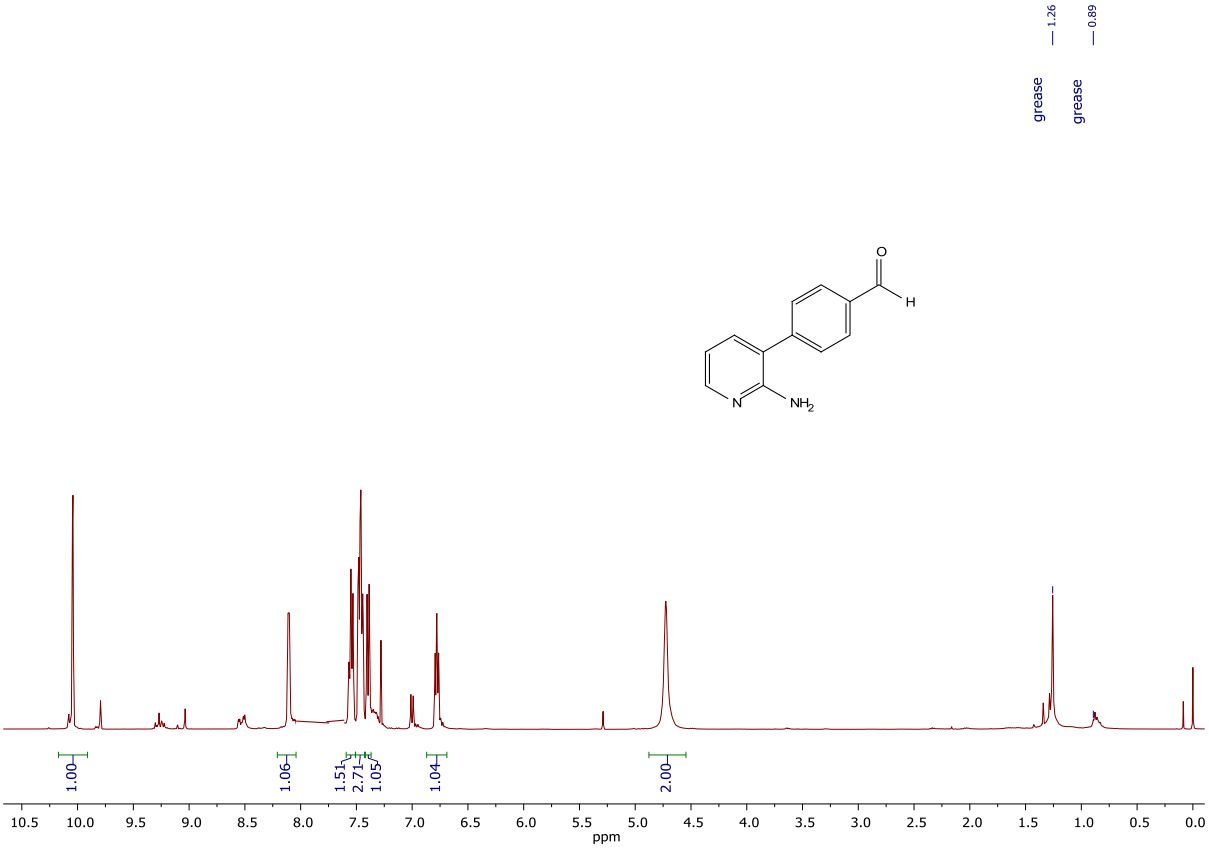

Figure 82: ^{1}H NMR of 4-(2-aminopyridin-3-yl)benzaldehyde **222c**

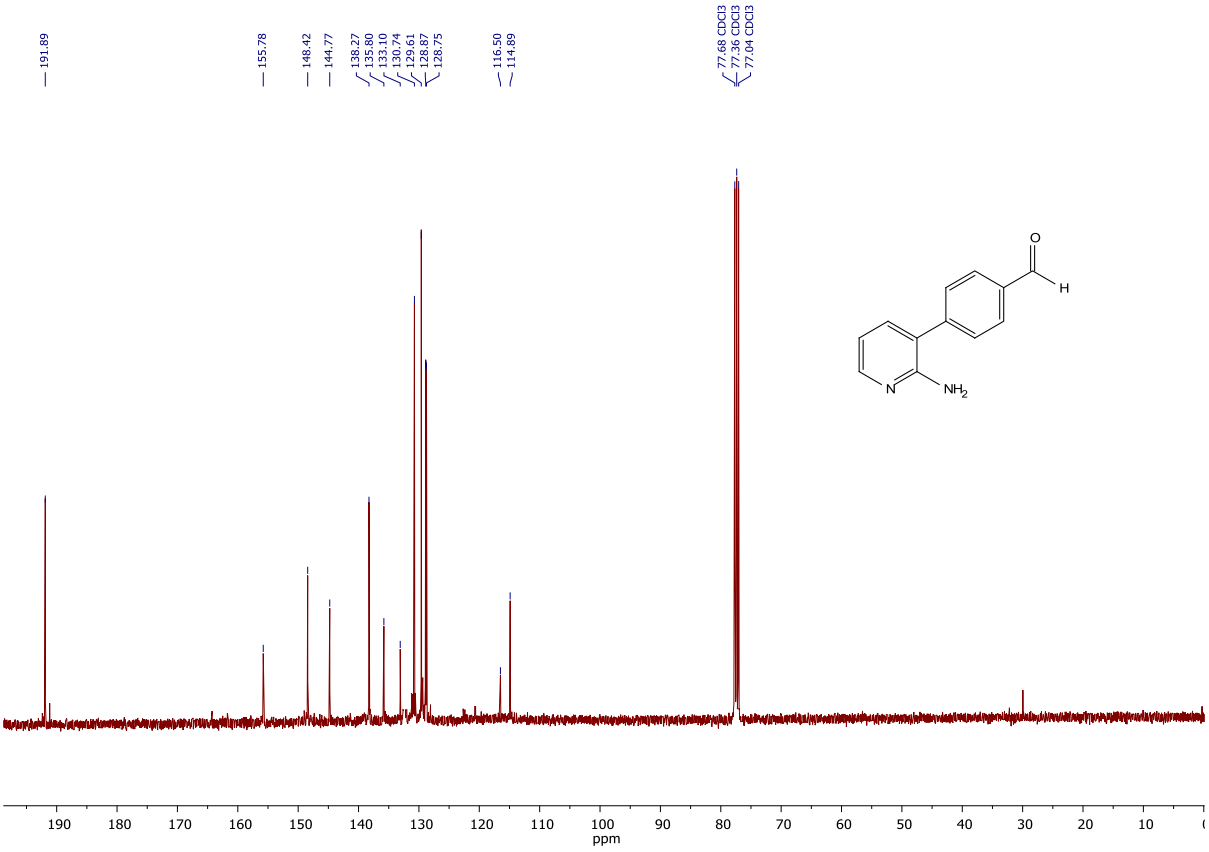

Figure 83: ^{13}C NMR of 4-(2-aminopyridin-3-yl)benzaldehyde **222c**

© University of Pretoria

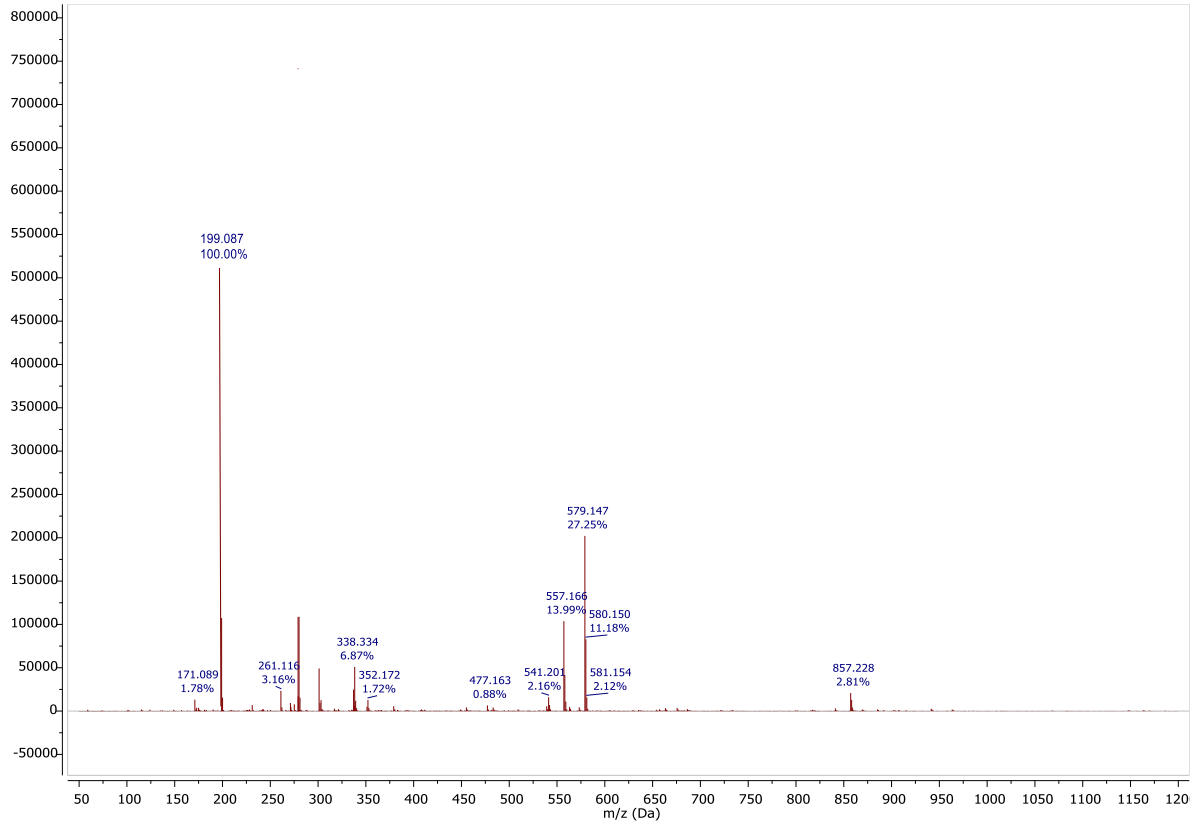

Figure 84: HRMS of 4-(2-aminopyridin-3-yl)benzaldehyde **222c**

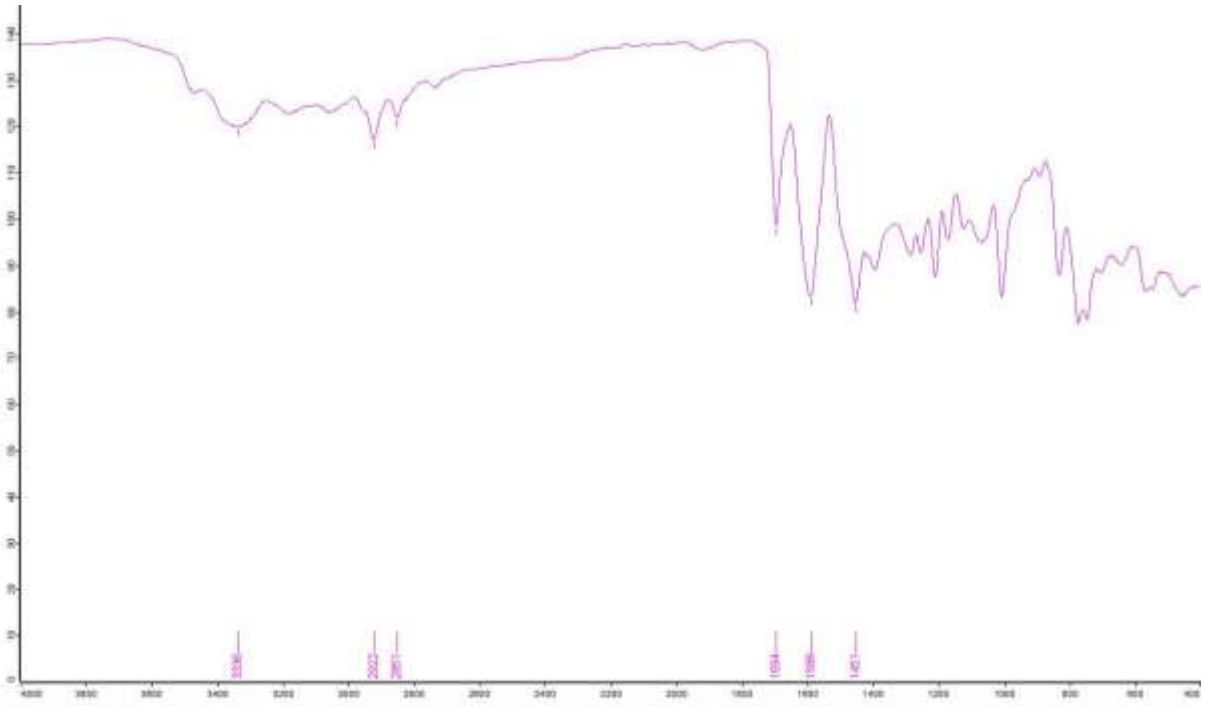

Figure 85: FTIR spectrum of 4-(2-aminopyridin-3-yl)benzaldehyde **222c**

© University of Pretoria

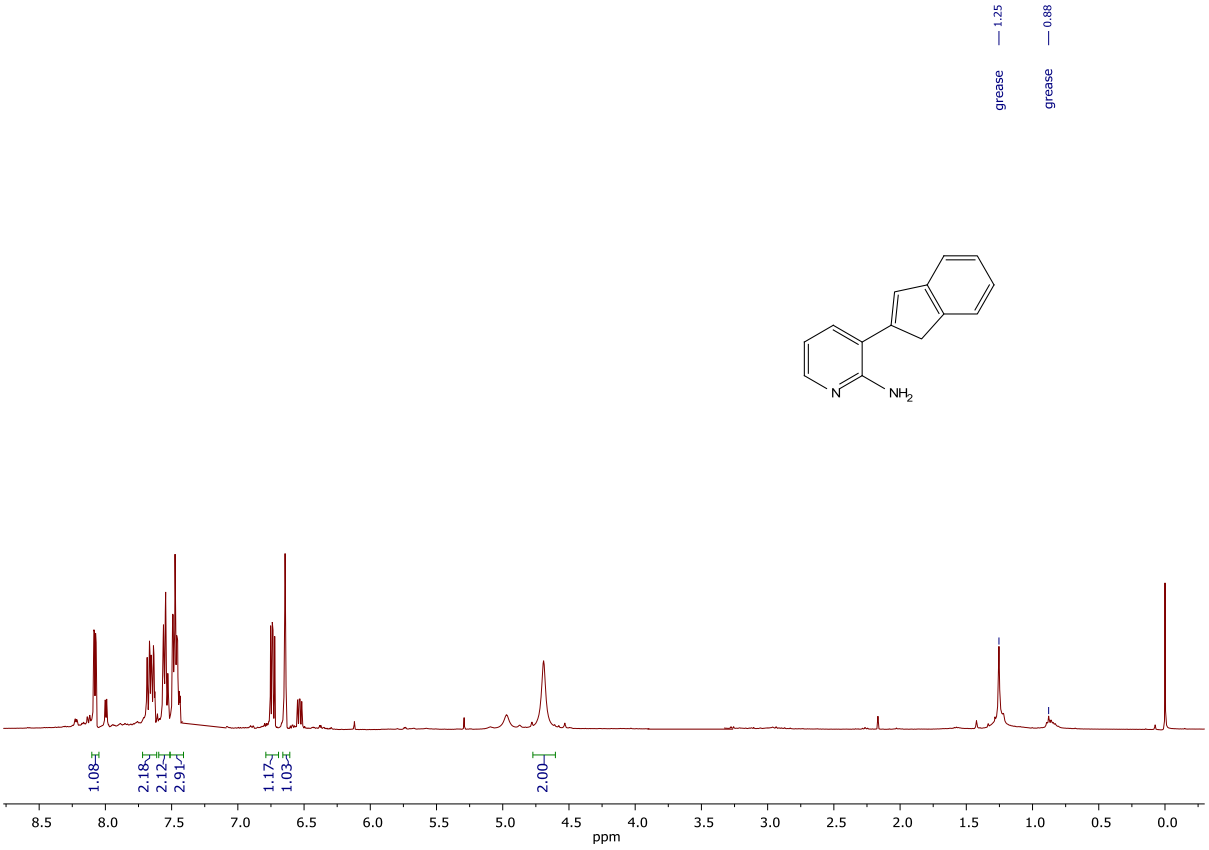

Figure 86: ^{1}H NMR of 3-(1*H*-inden-2-yl)pyridin-2-amine **222e**

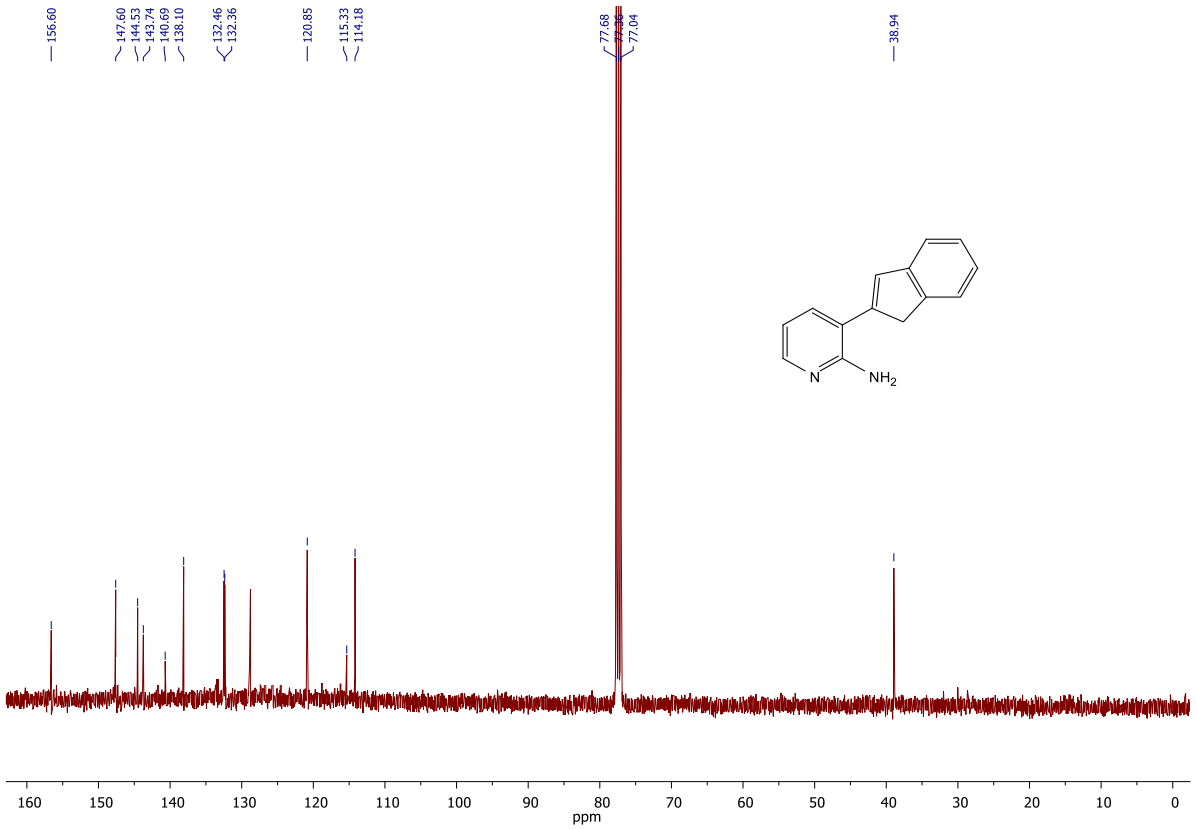

Figure 87: ^{13}C NMR of 3-(1*H*-inden-2-yl)pyridin-2-amine **222e**

© University of Pretoria

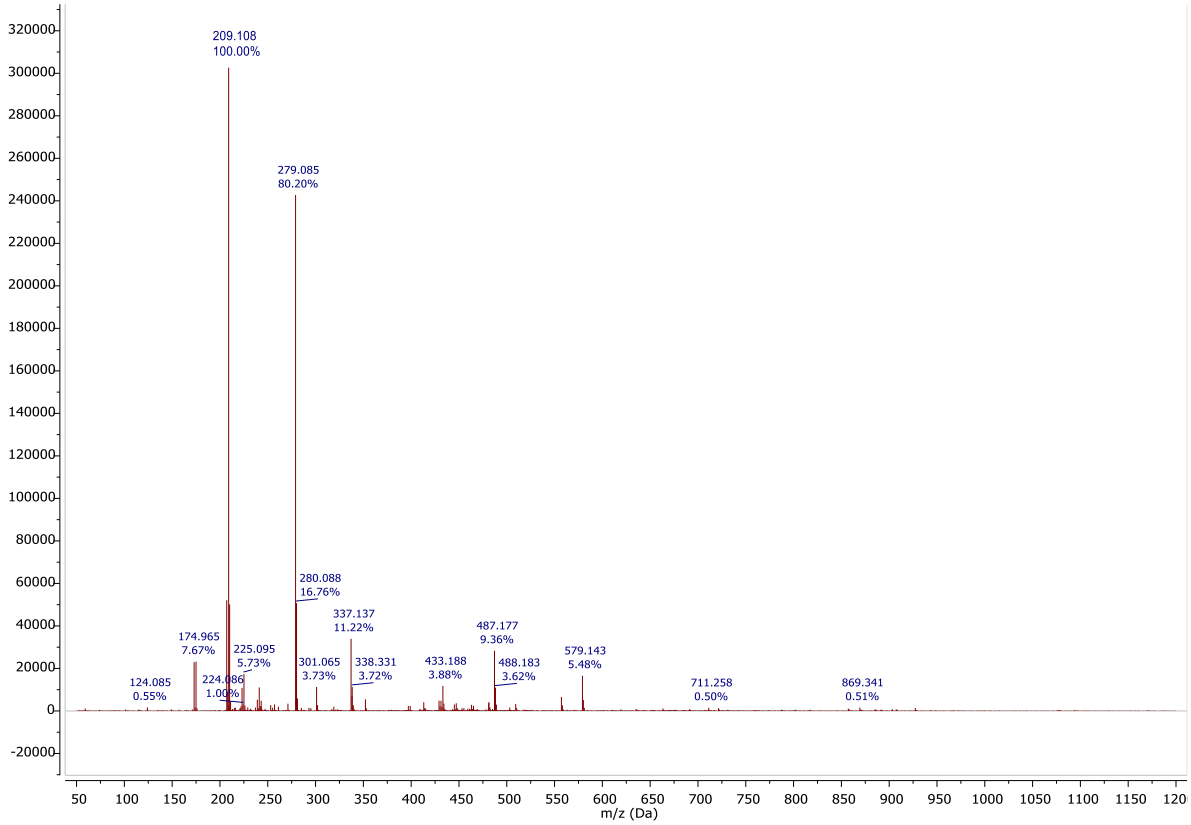

Figure 88: HRMS of 3-(1H-inden-2-yl)pyridin-2-amine, **222e**

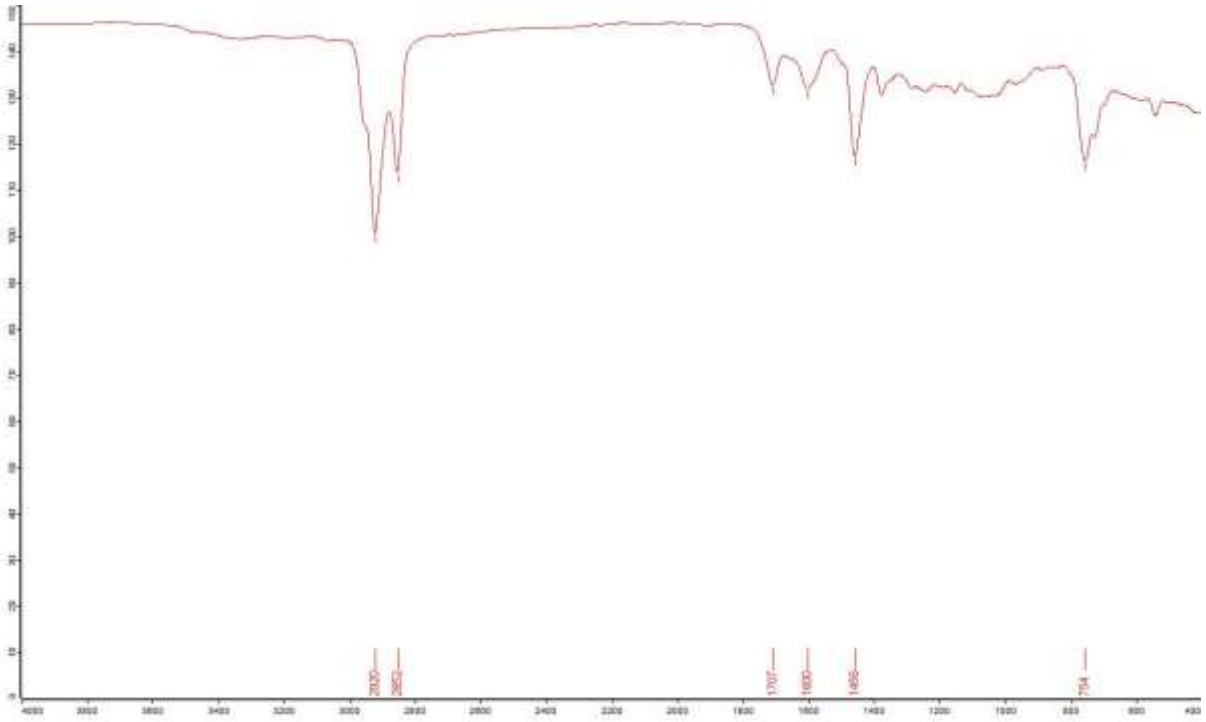

Figure 89: FTIR spectrum of 3-(1H-inden-2-yl)pyridin-2-amine **222e**

© University of Pretoria

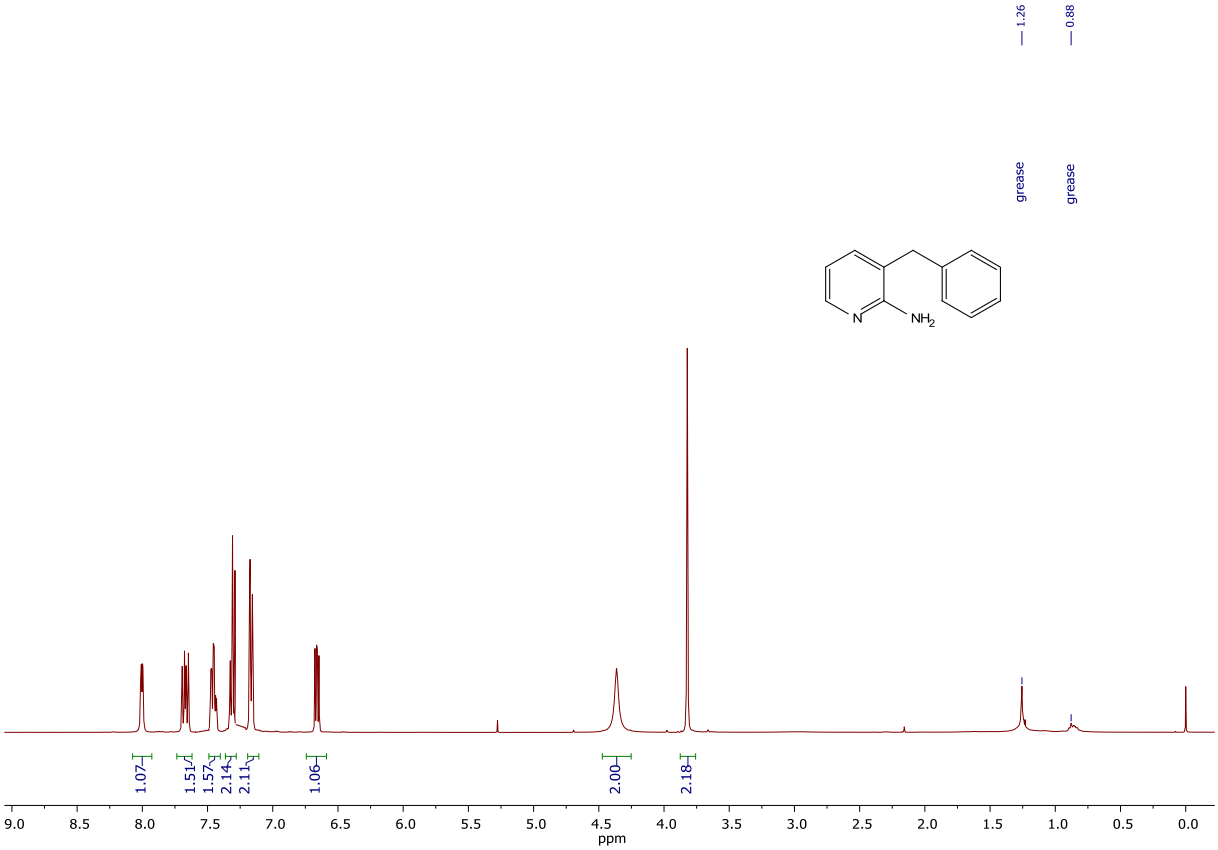

Figure 90: ^{1}H NMR of 3-benzylpyridin-2-amine **222g**

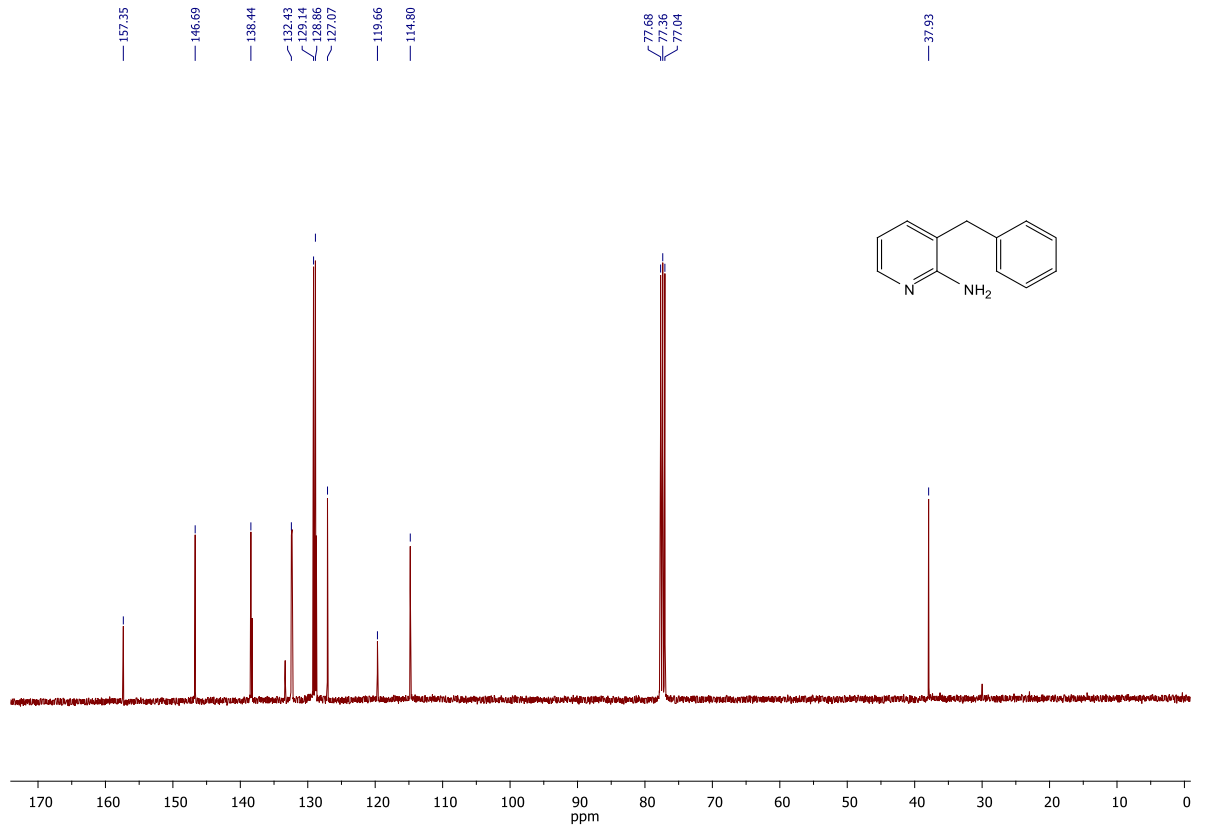

Figure 91: ^{13}C NMR of 3-benzylpyridin-2-amine **222g**

© University of Pretoria

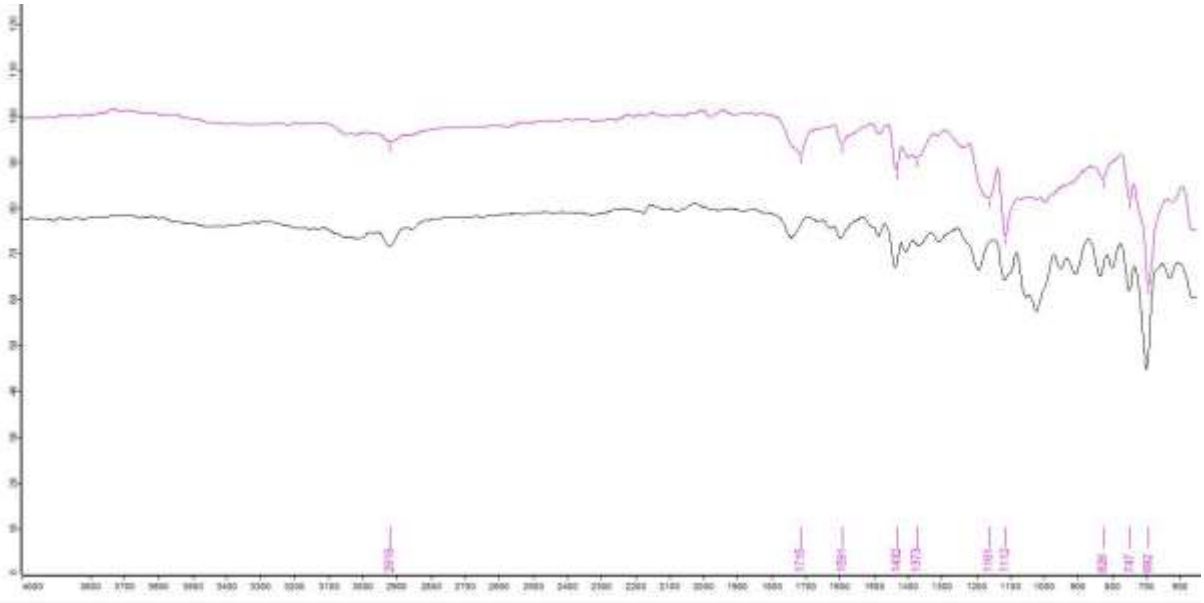

Figure 92: FTIR spectra comparison of commercial polystyrene-supported tetrakis(triphenylphosphine)palladium (top) (Sigma Aldrich, 216666) vs in-house solid-supported tetrakis(triphenylphosphine)palladium **215a** (bottom).

© University of Pretoria